Adsorption of Novel Block Copolymers for Steric Stabilization and Flocculation of Colloidal Particles in Aqueous Environments

Jody L. Krsmanovic

Dissertation submitted to the Faculty of the
Virginia Polytechnic Institute and State University in partial
fulfillment of the requirements for the degree of
Doctor of Philosophy
in
Chemical Engineering

Dr. Richey M. Davis, Chairman
Kevin E. VanCott
Aaron S. Goldstein
William A. Ducker
Alan R. Esker

January 15, 2003
Blacksburg, Virginia

Keywords: Polymer, Adsorption, Alumina, Silica, Polypeptide

Adsorption of Novel Block Copolymers for Steric Stabilization and Flocculation of Colloidal Particles in Aqueous Environments

Jody Lynn Krsmanovic

(ABSTRACT)

The adsorption of several homopolymer polypeptides on α-Al_2O_3 and SiO_2 particles and surfaces was investigated to identify possible anchor and tail blocks for brush-forming block copolypeptides. Poly-L-(glutamic acid) (GLU) and poly-L-(aspartic acid) (ASP) were found to adsorb on positively charged and nearly neutral Al_2O_3, while the GLU did not adsorb on negatively charged SiO_2. Poly-L-proline (PRO) adsorbed only slightly on the alumina, but showed high affinity adsorption on silica. These results are useful in designing a brush forming block copolymer with the GLU acting as the anchor block and the PRO as the tail block. An important finding in this work is that these unstructured polypeptides, or proteins that only have primary and secondary structure, have adsorption behavior that is similar to that of synthetic polymers.

The complexation between a random copolymer of two amino acids, glutamic acid and tyrosine, and poly(ethylene oxide) (PEO) was studied using an in-situ adsorption experiment. It was shown that the adsorption of the random copolymer greatly increased the adsorption of PEO. The results strongly suggest that the conformation of the copolymer on the surface was controlled by the ionic strength, and the conformation of the adsorbed PEO was controlled by the PEO molecular weight. Both of these factors affected the molar complexation ratio between the PEO and the tyrosine repeat units.

The adsorption of two novel triblock copolymers, with PEO tails and anionic hydrophobic center blocks, was studied on alumina and silica surfaces. On silica the

adsorption was due to the PEO tails, resulting in low adsorbed amounts. The adsorption was much greater on alumina, indicating either brush formation on the surface or the adsorption of micelles, which are present in solution. The effect of adsorbed polymer on the steric stabilization of alumina particles was studied using sedimentation and electrophoretic mobility experiments. These results do not show conclusively that the triblock copolymer adsorption led to particle stabilization. It is possible that better colloid stabilization of the alumina may be realized by changing the triblock composition to get greater extension and higher packing of the PEO tails.

Table of Contents

List of Figures

List of Tables

1 Introduction

1.1 Motivation

The interactions between polymers and particles in aqueous suspensions are important for a number of different applications, including paints, coatings, filled adhesives, structural ceramics, personal care products, pharmaceuticals, and in the paper making industry. In all of these cases, controlling the state of aggregation of the particles, whether stabilized of flocculated, is crucial.

The adsorption of long chain polymers on surfaces is very different from small molecules due to the connectivity and flexibility of the chain. More specifically, homopolymers can take on three conformations at an interface: trains, loops and tails. Copolymers consisting of two or more monomers can have different molecular architectures. They can be a series of blocks, each made up of one monomer, as a random mixture of the two, or as an alternating copolymer of the two monomers. The adsorption of copolymers leads to even more possibilities for the adsorbed conformation on a surface. Brush formation is possible for diblocks, triblocks and graft (comb) copolymers.

For an adsorbing diblock copolymer, one block may preferentially adsorb over the other. The adsorbed block, or the anchor, will have a higher affinity for the surface. The other block, or the tail, will not adsorb and thus will form tails in the solution. If one block has just a slightly higher segmental adsorption energy, $\chi_s kT$, than the other block than that block will preferentially absorb over the other.[1]

Polymer adsorption on particles can have a significant effect on the colloidal stability. Figure 1.1 shows the effect of polymer adsorption on colloidal stability at different

[1] Fleer, G.J; Cohen Stuart, M.A.; Scheutjens, J.M.H.M.; Cosgrove, T.; Vincent, B. *Polymers at Interfaces*, Chapman and Hall: London, 1993.

polymer concentrations. It is evident from this picture that this is a complicated issue, that demands the understanding of the adsorbed polymer conformation and the interactions between particles. Some particles, such as polymer colloids in water, are relatively easy to stabilize, due to relatively weak van der Waals forces. Others, particles like metal oxides in water, exhibit stronger van der Waals forces and can be difficult to stabilize, especially at high solids volume fraction.

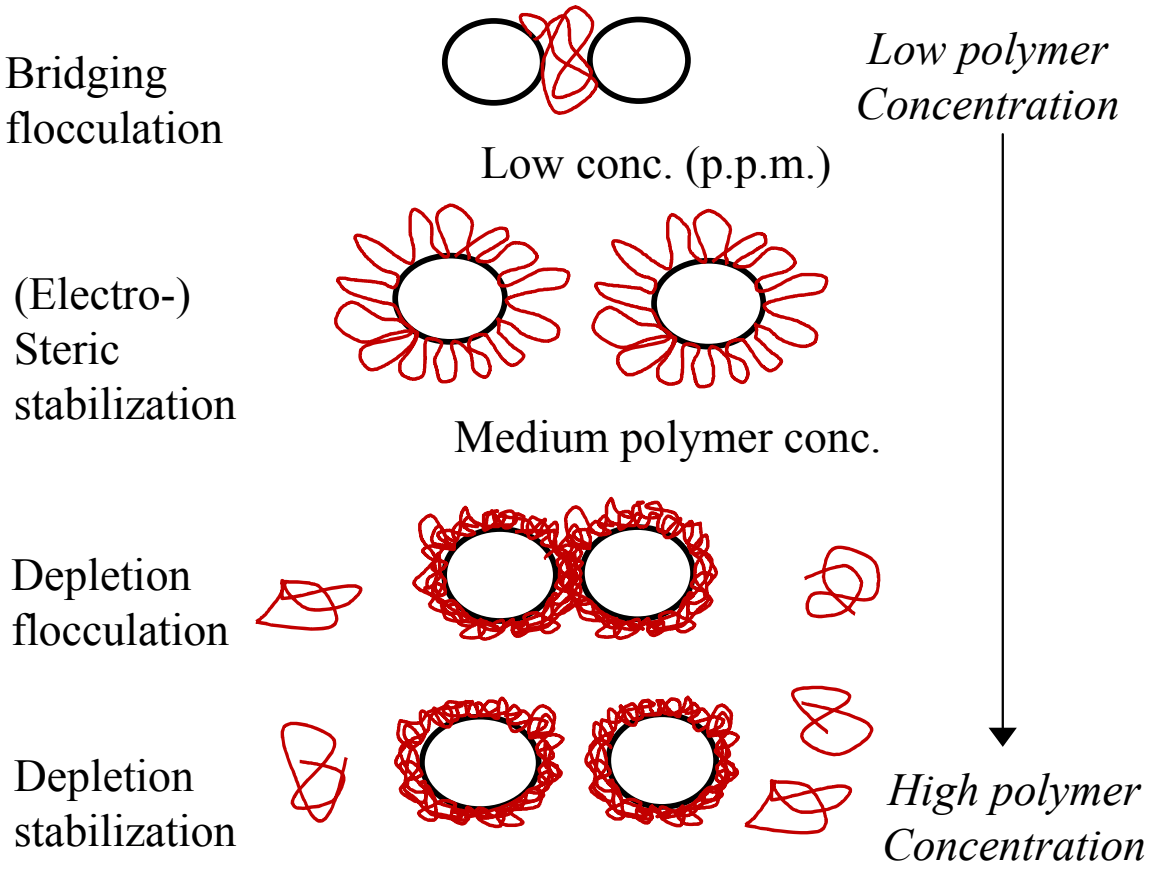

Figure 1.1: Effect of adsorbed polymer on the stabilization and flocculation of colloidal particles. Adapted from Reference 2.

The rheology of colloidal dispersions is strongly affected by the particle-particle and particle-fluid interactions that affect colloidal stability. There are many factors which can affect these interactions, including the liquid phase viscosity, pH, ionic strength, particle

[2] Hunter Foundations of Colloid Science

size, particle volume fraction, and the presence of any soluble polymers or surfactants. In order for a colloidal dispersion to be processable, the rheology must be controlled so that the flow behavior can be predicted in a given flow geometry. The stability of the colloidal dispersion is crucial and can change the rheology dramatically, greatly affecting the processability. For example, when a suspension becomes colloidally unstable, the viscosity can increase by several orders of magnitude and a yield stress can develop.[3]

Throughout this research the principal focus has been on studying the adsorption of polymers made from amino acid monomers on metal oxide surfaces from aqueous media. This approach is the first step to understanding how these simple proteins interact and adsorb on non-biological surfaces. There is great potential for synthetic proteins for applications where the control of surface activity is important, because there is a wide range of possible protein chemistries. The results of this work can be used by future researchers to synthesize monodisperse, well-defined proteins from genetically engineered *E. coli* that have the desired features for a specific system. A second focus of this work was to study the solution and interfacial behavior of a novel triblock copolymer developed by Professor Judy Riffle in the Chemistry Department at Virginia Tech.

1.2 Specific Research Objectives

1. Adsorption of simple polypeptides on metal oxide surfaces - The adsorption of homopolymer poly(amino acids) on alumina is studied with the goal of finding potential amino acids for tail and anchor blocks for brush forming block copolymers.

[3] Buscall, B.; Corner, T.; Stageman, J.F. *Polymer Colloids*, Elsevier Science Publishing Co., Inc.: London, 1985.

2. Effect of surface chemistry on polypeptide adsorption - Different polymer chemistries are studied on alumina and silica with the goal of understanding the role that polypeptide structure plays on the adsorption onto two metal oxides – SiO_2 and Al_2O_3 – chosen for their very different surface chemistries.

3. Stimulation of a non-adsorbing polymer by adsorption of a polypeptide - The effect of an adsorbing copolymer polypeptide on the subsequent adsorption of poly(ethylene oxide) (PEO) on alumina is studied.

4. Adsorption of a novel triblock copolymer on metal oxide surfaces - The adsorption of novel triblock copolymers with PEO tails and an anionic hydrophobic center block is studied on alumina and silica in order to understand the polymer-surface interactions and the potential for using these polymers as brush forming steric stabilizers.

1.3 Outline of Chapters

Chapter 2 is a detailed review of the relevant literature. This chapter is divided into three main sections. The first part discusses the adsorption of homopolymers, copolymers and biological polymers at the solid-liquid interface. Adsorbed amounts and the conformation of the adsorbed polymers are be reviewed with respect to the effect of polymer composition, molecular weight and solution properties. There is also a brief review of the relevant surface techniques used to measure the adsorption of polymers and proteins. The second section discusses colloidal stability, with a detailed review of the relevant theory. The important experimental work is also reviewed with respect to the effect of electrostatic interactions, polymer adsorption, and non-adsorbed polymer on the colloidal stability. The final section deals with the rheology of colloidal suspensions. Again, the effect of electrostatic interactions and polymer adsorption on the colloidal stability are discussed in terms of the resulting rheological behavior.

The objective of **Chapter 3** is to find a combination of polypeptides that would serve as anchor and tail blocks for diblock and triblock copolymers designed to form brushes at the interface between Al_2O_3 and water. This is done by measuring the adsorption of selected homopolymers of amino acids from both pure solutions and from mixtures and by characterizing their solution properties (i.e. size and solubility). Relatively little work has been reported on the adsorption of synthetic, unstructured polypeptides,[4,5] and none has been reported with the aim to define candidate anchor and tail blocks for a designed copolymer. The focus is on pH 7, which is below the IEP of Al_2O_3 and where Al_2O_3 is positively charged, and pH 9 which is near the IEP. Three poly(amino acids) are studied, poly-L-proline (PRO), poly-L-(glutamic acid) (GLU), and poly-L-(aspartic acid) (ASP).

Chapter 4 examines the effect of varying the substrate surface chemistry from a Lewis base (e.g. Al_2O_3) to a Lewis acid (e.g. SiO_2) on the adsorption of polypeptides. This type of study is important because a wide range of surface chemistries are encountered in colloid applications. The effect of hydroxylation of a nonionic, soluble polypepetide on the solution properties and adsorption behavior is also studied. This is important for understanding polypeptide adsorption because there are several hydroxylated nonionic amino acids (e.g. threonine and serine) that might be included in future copolymers. The effect of salt concentration and different salt types on adsorption are also examined. This has both scientific and practical benefits, in that it is often difficult to control the background electrolyte in a processing situation and mixtures of salts are thus often encountered. In this chapter the adsorption from a NaCl solution will be compared to that from a NaCl/$CaCl_2$ solution. Of particular interest is the possible association between the charged GLU and the divalent Ca^{2+} ions. Prior work has shown that multivalent ions can reduce the intermolecular repulsions between polyelectrolyte chains to an extent that can

[4] Blaakmeer, J.; Cohen Stuart, M.A.; Fleer, G.J., 'The Adsorption of Polyampholytes on Negatively and Positively Charged Polystyrene Latex', *Journal of Colloid and Interface Science*, **1990**, *140*, 314-325.

[5] Killmann, E.; Reiner, M., 'Adsorption of Poly-L-Lysine and Poly-L-(glutamic acid) on Silica Surfaces', *Tenside, Surface, Detergent* **1996**, *33*, 220-227.

not be explained by the Debye-Huckel model alone.[6,7] It has also been shown that the Ca^{2+} ions will specifically adsorb on the silica surface.[8] Thus the Ca^{2+} ions may act as a bridging unit between the GLU and the SiO_2 surface that facilitates adsorption.

The focus of this work is on homopolymers and copolymer that do not exhibit any tertiary or quaternary structure. Four poly(amino acids) were studied - (PRO), poly-L-hydroxyproline (HPRO), (GLU), and a copolymer consisting of the trimer proline-glycine-proline (PGP). The adsorption of aqueous solutions of poly(amino acids) on Al_2O_3 and water and SiO_2 were measured. All adsorption experiments were done at pH 7, which is below the IEP of Al_2O_3[9] and therefore the Al_2O_3 was positively charged, but above the IEP of SiO_2.

HPRO was studied to determine what effect, if any, the pendent hydroxyl group had on adsorption. A copolymer consisting of the trimer PRO-GLY-PRO was also studied to determine the effect on adsorption of adding other monomers into the PRO chain. In nature, long chains of only amino acids are not common, and thus other amino acids are needed to create the long chain needed for the buoy block.

---

[6] Mahltig, B.; Walter, H.; Harrats, C.; Muller-Buschbaum, P.; Jerome, R.; Stamm, M. 'Adsorption of Polyampholyte Copolymers at the Solid/Liquid Interface: The Influence of pH and Salt on the Adsorption Behaviour', *Physical Chemistry Chemical Physics* **1999**, *1*, 3853-3856.

[7] Zhang, Y.; Tirrell, M.; Mays, J.W. 'Effects of Ionic Strength and Counterion Valency on Adsorption of Hydrophobically Modified Polyelectrolytes', *Macromolecules* **1996**, *29*, 7299-7301.

[8] Meagher, L. 'Direct Measurement of Forces Between Silica Surfaces in Aqueous $CaCl_2$ Solutions Using an Atomic Force Microscope', *Journal of Colloid and Interface Science* **1992**, *152*, 293-295.

[9] Cesareno, J.; Aksay, I.A.; ' Processing of Highly Concentrated Aqueous α-Alumina Suspensions Stabilized with Polyelectrolytes', *Journal of the American Ceramic Society* **1988**, *71*, 1062-1067.

Chapter 5 focuses on the adsorption of polypeptides on surfaces that are smooth and well-defined enough for atomic force microscopy (AFM) studies. This type of experiment would rigorously test a brush-forming block copolymer by measurement of the surface forces generated by the attached chains. It is also desirable to study the effect of salt concentration and different salt types on adsorption. The goal of this chapter is to study the adsorption of two poly(amino acids), (GLU) and (PRO) on two surfaces, silicon dioxide and aluminum oxide using in-situ ellipsometry. Two ionic strengths were studied, 0.01 M and 0.1 M NaNO3, both at pH 6.

In **Chapter 6**, the effect of copolymer cofactors containing glutamic acid (GLU) and tyrosine (TYR) on the stimulation of the adsorption of PEO on aluminum oxide were studied using in-situ ellipsometry. Two random copolymers were used, which contain different ratios of GLU:TYR, namely 4:1 and 1:1, to study the effect of composition. There has also been little work to study the effect of molecular weight of the PEO on complexation with the cofactors and thus, two different molecular weight PEO samples were used to probe the interactions between the ethylene oxide repeat units and TYR repeat units. Finally, the effect of ionic strength on cofactor and PEO adsorption was studied.

Chapter 7 concerns a novel triblock system consisting of PEO tails and a negatively charged, hydrophobic center block. The solubility and micellization of the copolymers in aqueous solutions was characterized using dynamic light scattering and surface tension measurements. The adsorption behavior of two different triblocks on silica and alumina was measured in-situ, using ellipsometry, to determine the usefulness of these types of copolymers as stabilizers for these surfaces. The adsorption was studied as a function of ionic strength. In addition, sedimentation and zeta potential measurements were made using nanometer scaled alumina particles.

It is expected that on silica the PEO tails will adsorb, which has been well documented,[10] while the negatively charged center block will have little association with the negatively charged substrate. On the alumina surfaces, it is expected that the oppositely charged center block will adsorb, while PEO has been previously found to be non-adsorbing.[10,11] It is possible that the PEO tails will for a brush layer, or that there could be micelle adsorption on the surface. The addition of salt is expected to reduce the charge repulsion between two [12]center blocks and lead to greater micellization.

Chapter 8 is a summary of the main conclusions from this work and recommendations for future work.

[10] Mathur, S.; Moudgil, B.M. 'Adsorption Mechanism(s) of Poly(ethylene oxide) on Oxide Surfaces', *Journal of Colloid and Interface Science* **1997**, *196*, 92.

[11] Gibson, F.W. *Stabilization of Submicron Metal Oxide Particles in Aqueous Media*, Virginia Tech, 1998.

2 Literature Review

This literature review will cover the main principles relevant to this work. The first section is a discussion on how polymers adsorb, and what conformation they have due to adsorption. This is essential for understanding how a polypeptide block copolymer will adsorb, in order to design a brush former. The second section will focus on the effect that adsorbed polymers have on the colloidal stability of a suspension. Again, this is directly related to the polypeptide work to show what kind of brush layer is required for effective steric stabilization. The final section will discuss how the colloidal stability then effects the macroscopic properties, such as the rheology and sedimentation of a suspension. This will illustrate how to effectively monitor the stability of a colloidal dispersion in the laboratory. The literature cited here will be a guide to help in the design of the polypeptide diblock copolymer, and to help quantify the steric stabilization imparted by the copolymer.

2.1 Effect of Adsorption of Polymers

There have been many studies on the adsorption of polymers on surfaces, and this review by no means encompasses all of this work. The most useful work that illustrates how different types of polymers adsorb will be covered with respect to the present work in this proposal. The first section will discuss some theoretical and experimental results for the adsorption of neutral and charged homopolymers. Specifically, the nature of adsorption and the relevant quantities that characterize adsorption will be explained. This will act as a prelude to the block copolymer adsorption section, which will discuss the relevant aspects of adsorption, to help in the design of the polypeptide diblock. Next, a very brief description of protein adsorption will follow. This section is relevant to the polypeptide work of this proposal, and some of the important issues that arise with protein adsorption will be discussed. The final section is an overview of several techniques which are used

to probe the adsorption on surfaces. The emphasis is on ellipsometry, which will be used in this work.

2.1.1 Homopolymers – Trains, Tails and Loops

The simplest case of polymer adsorption is that of homopolymers, but even this is a nontrivial phenomenon to model. The adsorption process consists of three main steps: diffusion of the molecule to the surface, attachment to the surface, and any reconfiguration of the molecule on the surface. For small molecules only the first two of these processes are significant, but for a macromolecule all three are important.

Long chain polymers also adsorb in a manner very different from small molecules due to the length and flexibility of the chain. More specifically, homopolymers can take on three conformations at an interface: trains, loops and tails. Trains are the series of segments which are adsorbed onto the surface. Loops have only their two ends attached, with the middle forming a loop into the solution. The tails are the nonadsorbing chain ends, which can extend far into solution. Figure 2.1 shows a schematic of these three conformations.

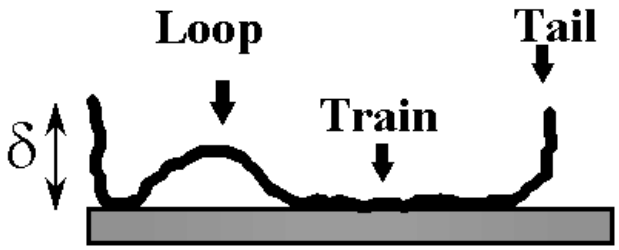

Figure 2.1: Schematic of an adsorbed homopolymer with trains, loops and tails.

There are several properties which can be measured or estimated to characterize polymer adsorption. The adsorbed amount, Γ, quantifies the total mass of polymer adsorbed to the surface per surface area of adsorbent, usually given in mg/m^2. The fraction of loops, trains and tails can also be determined, as function of distance from the surface, to help give a more accurate description of how the polymer is adsorbing. The bound fraction gives a value for the amount of polymer actually in contact with the surface compared to

the total adsorbed amount. This is basically a determination of the fraction of segments in trains. Only one segment needs to be attached in order for the chain to be counted in the adsorbed amount. Another important value is the layer thickness, δ, of the polymer on the surface, which is a weighted average based on the segment distribution function. The kinetics of adsorption will also be discussed, which will determine whether the polymer diffusion to the surface or the adsorption onto the surface is the rate limiting step. An understanding of polymer desorption and competitive adsorption is important when studying polymer adsorption. It is crucial to understand how all of these values are affected by different experimental variables, such as degree of polymerization, solvent quality and the polydispersity of the polymer.

2.1.1.1 Uncharged Homopolymers

2.1.1.1.1 Theoretical Background

The adsorption of polymers is affected by several key parameters, as described by Scheutjens et al.[1]: χ_s, the segmental adsorption energy parameter, χ, the Flory polymer-solvent interaction parameter, the molecular weight of the polymer, and ϕ^b, the bulk polymer concentration. The energy of adsorption per segment can be defined as:

$$\chi_s kT = \left(u_1^a - u_2^a\right) \qquad \text{Equation 2.1}$$

where, $u_1{}^a$ is the adsorption energy of the solvent on the surface and $u_2{}^a$ is the adsorption energy of the polymer on the surface. Both quantities need to be negative in order for adsorption to occur. Thus, adsorption involves competition between the polymer and the solvent for the surface, and no adsorption will occur if χ_s is less than zero, i.e. if $u_2{}^a < u_1{}^a$.

Due to the large number of configurations possible for an adsorbed molecule on a surface, adsorption models are very complex. One of the most successful modeling approaches employs a lattice model, such as the Scheutjens and Fleer self-consistent-field lattice model.[1] In these types of models, space is discretised into z lattice layers as shown

[1] Fleer, G.J.; Cohen Stuart, M.A.; Scheutjens, J.M.H.M.; Cosgrove, T.; Vincent, B. "Polymers at Interfaces"; Chapman and Hall: London, 1993.

in Figure 2.2, with a step length *l*, where z = *l* is the adsorbed layer on the surface and layers 2*l*, 3*l*, ... go outward from the surface. This simplification of the actual structure of an adsorbed layer is related to Flory's lattice theory for polymer solutions. This model greatly reduces the number of possible configurations and allows for computations to be done.

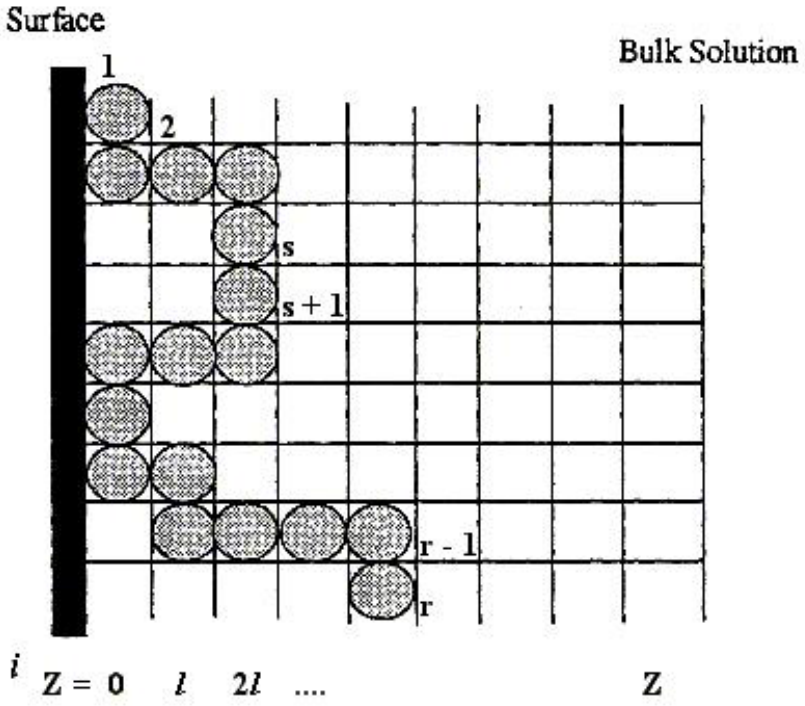

Figure 2.2: Configuration of a polymer in a discretised lattice, where z = *l* is in contact with the surface and z = z is the bulk solution.

The mean-field approach employs a weighting factor, $G_i(z)$, to the probability of finding a polymer segment of species *i* in a lattice site, which takes into accounts the average excluded volume and the energetic interactions:

$$G_i(z) = e^{-u_i(z)/kT} \qquad \text{Equation 2.2}$$

where $u_i(z)$ is the potential energy with respect to the bulk. For polymer adsorbing from a melt, or with no solvent interactions, the potential energy can be separated into two parts:

$$u_i(z) = u'(z) + u_i^{\text{int}}(z) \qquad \text{Equation 2.3}$$

an entropic portion, u'(z), which is independent of the polymer, and an interaction part, $u_i^{int}(z)$, which takes into account χ_s, χ, and ϕ^b. The potential energy is set so that for $z \leq 0$, $u_i(z) = \infty$ and so $G_i(z) = 0$, because polymer can not be below the surface, and for large z $u_i(\infty) = u'(\infty) = u_i^{int}(\infty) = 0$ and $G_i(z) = 1$.

For the adsorption of polymers from solvents a more complex pair of equations defines the potential energy, which takes into account polymer-solvent interactions and excluded volume:

$$u_1(z) = u'(z) + u_1^a \delta(z-l) + \chi kT\left\{\langle\phi_2(z)\rangle - \phi_2^b\right\} \qquad \text{Equation 2.4}$$

$$u_2(z) = u'(z) + u_2^a \delta(z-l) + \chi kT\left\{\langle\phi_1(z)\rangle - \phi_1^b\right\} \qquad \text{Equation 2.5}$$

where δ is the Kronecker delta function and $\langle\phi_2(z)\rangle$ is the average concentration of the polymer in layer z and $\langle\phi_1(z)\rangle$ is the average concentration of the solvent in layer z, and ϕ_1^b and ϕ_2^b are the volume fraction of solvent and polymer in the bulk, respectively.

The analysis of the polymer segments in the lattice starts with the end segment of a polymer with *s* segments. Assuming a monodisperse polymer, so that all of the chains have the same number of segments, the probability of finding an end segment in layer z of a longer chain with *s*+1 segments gives the recurrence relation:

$$G_i(z;s+1) = G_i(z)\{\lambda_1 G_i(z-l;s) + \lambda_0 G_i(z;s) + \lambda_1 G_i(z+l;s)\} \qquad \text{Equation 2.6}$$

with the initial condition $G_i(z,1) = G_i(z)$, which is the probability of finding the first segment in layer z. The parameter λ_0 is the fraction of neighboring segments in the same layer, and λ_1 is the fraction in the adjacent layers, and are related by $\lambda_0 = 1\text{-}2\lambda_1$. The end point distribution can be reduced to:

$$G_i(z;s+1) = G_i(z)\langle G_i(z;s)\rangle \qquad \text{Equation 2.7}$$

where $\langle G_i(z;s)\rangle$ is an average of neighbors over the three layers.

The concentration of the middle segments can be determined using the composition law, which states that the probability of finding segment *s*, of a chain that is r_i segments long,

where r_i is proportional to the degree of polymerization, is found from the joint probabilities that both the sequence 1, 2, ... *s* and the sequence *s*, ... r_i-1, r_i end in layer z. The volume fraction of segments *s* in layer z is then defined by:

$$\phi_i(z;s) = \frac{C_i}{G_i(z)} G_i(z;s) G_i(z; r_i - s + 1) \qquad \text{Equation 2.8}$$

where C_i is a normalization constant and is given by $C_i = \phi_i^b / r_i$. The total volume fraction is then calculated from:

$$\phi_i(z) = \sum_{S=1}^{r_i} \phi_i(z;s) \qquad \text{Equation 2.9}$$

The final equation needed to form a self-consistent set of equations is the definition of a full occupancy of any layer in the lattice:

$$\sum \phi_i(z) = 1 \qquad \text{Equation 2.10}$$

Now the system can be solved numerically.

The results from the above equations will give the volume fraction of chains in each layer. Then, the conformation of the adsorbed polymer, i.e. the fraction of these chains in loops, trains and tails, can be calculated. The first step is to break the weighting factor into two parts, G_i^a, for chains which have at least one segment adsorbed onto the surface and, G_i^f, for the free chains which are not adsorbed but are in the lattice:

$$G_i(z;s) = G_i^a(z;s) + G_i^f(z;s) \qquad \text{Equation 2.11}$$

These two parts can be reduced using the requirement for the free segments that z = *l* is forbidden, or there are no free segment in the first layer on the surface, thus:

$$G_i^f(l;s) = 0 \qquad (z \neq l) \qquad \text{Equation 2.12}$$

$$G_i^f(z;s+1) = G_i(z)\langle G_i^f(z;s)\rangle \qquad (z/l = 2, 3, ...) \qquad \text{Equation 2.13}$$

$$G_i^a(l;s) = G_i(l;s) \qquad (z \neq l) \qquad \text{Equation 2.14}$$

$$G_i^a(z;s+1) = G_i(z)\langle G_i^a(z;s)\rangle \qquad (z/l = 2, 3, ...) \qquad \text{Equation 2.15}$$

A similar analysis for the volume fraction of segments results in:

$$\phi_i(z) = \phi_i^a(z) + \phi_i^f(z) \qquad \text{Equation 2.16}$$

$$\phi_i^f(z) = \frac{C_i}{G_i(z)} \sum_{S=1}^{r_i} G_i^f(z;s) G_i^f(z; r_i - s + 1) \qquad \text{Equation 2.17}$$

Using the above equation the volume fraction of loops, trains, tails, and free chains can be calculated. The volume fraction of trains can easily be simplified using the fact that all of the segments that are in layer *l* are trains (the first layer), and the loops, tails and free chains contribute to all other layers, thus:

$$\phi_i(l) = \phi_{tr,i}(l) \qquad (z = l) \qquad \text{Equation 2.18}$$

$$\phi_i(z) = \phi_{lp,i}(z) + \phi_{tl,i}(z) + \phi_i^f(z) \quad (z/l = 2, 3,...) \quad \text{Equation 2.19}$$

In order to determine the volume fraction of trains, loops and tails, the expression for the contribution of segments *s* to the volume fraction, $\phi_i(z,s)$, needs to be expanded in terms of $G_i^a(z;s)$ and $G_i^f(z;s)$;

$$\phi(z,s) = \frac{C_i}{G_i(z)} \left\{ \begin{array}{l} G_i^a(z;s) G_i^a(z; r_i - s + 1) + G_i^a(z;s) G_i^f(z; r_i - s + 1) + \\ G_i^f(z;s) G_i^a(z; r_i - s + 1) + G_i^f(z;s) G_i^f(z; r_i - s + 1) \end{array} \right\} \qquad \text{Equation 2.20}$$

The last term in Equation 2.20 is the volume fraction of the free chains, since there are no adsorbed segments. For z > l, the first term in Equation 2.20 refers to the loops, where both ends are adsorbed, and the volume fraction of loops is:

$$\phi_{lp,i}(z) = \frac{C_i}{G_i(z)} \sum_{S=1}^{r_i} G_i^a(z;s) G_i^a(z; r_i - s + 1) \qquad \text{Equation 2.21}$$

For tails only one end is adsorbed and the second term in Equation 2.20 refers to tails at the chain ends, and the third term to tails at the beginning of the chain. The volume fraction of tails is then reduced to:

$$\phi_{tl,i}(z) = \frac{2C_i}{G_i(z)} \sum_{S=1}^{r_i} G_i^a(z;s) G_i^f(z; r_i - s + 1) \qquad \text{Equation 2.22}$$

where, the factor of two is added because the tails have the same probability at both chain ends.

The number of trains, loops and tails per adsorbed chain can also be calculated. First, the fraction of chain ends for adsorbed chains on the surface need to be determined, which would directly lead to the number of tails. The number of tails per adsorbed chain are:

$$n_{tl,i} = 2\left[1 - \frac{G_i^a(l; r_i)}{G_i^a(r_i)}\right] \qquad \text{Equation 2.23}$$

where, the factor of two is again added for the equal probability of both chain ends and the second term is the fraction of chain ends which are adsorbed onto the surface, and:

$$G_i^a(r_i) = \sum_{z/l=1}^{Z} G_i^a(z; r_i) \qquad \text{Equation 2.24}$$

where, Z is the number of layers parallel to the surface in the lattice.

In order to calculate the number of loops per adsorbed chain, the last segment in a loop is set to be *s* (at z = 2*l*), which is connected to the adsorbed segment *s*+1 (at z = *l*). Then the weight of all chains with *s* as their last segment of a loop is:

$$G_i^a(2l; s)\lambda_1 G_i^a(l; r_i - s) \qquad \text{Equation 2.25}$$

where, the λ_1 accounts for the bond perpendicular to the surface between *s* and *s*+1. Thus, the number of loops per adsorbed chain is:

$$n_{lp,i} = \frac{\lambda_1}{G_i^a(r_i)} \sum_{S=2}^{r_i-1} G_i^a(2l; s) G_i^a(l; r_i - s) \qquad \text{Equation 2.26}$$

where, the summation goes from *s* = 2 to *s* = r_i-1 because neither segment *s* = 1 or *s* = r_i can be in the loop, they must be adsorbed. The loop is bound by trains at both ends and so the number of trains per adsorbed chain can easily be calculated:

$$n_{tr,i} = n_{lp,i} + 1 \qquad \text{Equation 2.27}$$

The size distribution of the trains, loops and tails can also be calculated. Using a similar analysis for the tails as for the loops above, the weight of chains where *s* is the last segment in the tail is:

$$G_i^f(2l;s)\lambda_1 G_i^a(l;r_i-s) \qquad \text{Equation 2.28}$$

where again, the first segment in the tail is *s* (at z = 2*l*) and it is connected to the adsorbed segment *s* +1 (at z = *l*). Then the number of tails that are s segments long per adsorbed chain are:

$$n_{tl,i}(s)=\frac{2\lambda_1}{G_i^a(r_i)}G_i^f(2l;s)G_i^a(l;r_i-s) \qquad \text{Equation 2.29}$$

The determination of the size distribution of the trains needs more analysis. First, a train, which is *s* segments long, is made up of segments t+1, t+2, ..., t+*s*. Then, the summation over all t is taken of the weight of all chains with trains of length *s*:

$$n_{tr,i}(s)=\frac{(\lambda_1)^2(\lambda_0)^2[G_i(l)]^s}{G_i^a(r_i)}\sum_{t=0}^{r_i-s}G_i(2l;t)G_i(2l;r_i-s-t) \qquad \text{Equation 2.30}$$

where, $G_i(2l;0) = 1/\lambda_1$.

The size distribution of tails is determined by first defining the tail end segment distribution function, $G^t_i(z;s)$, which takes the weight of chains with tails that are *s* segments long and end at layer z:

$$G_i^t(l;s)=0 \qquad (z = l) \quad \text{Equation 2.31}$$

$$G_i^t(z;s+1)=G_i(z)\langle G_i^t(z;s)\rangle \qquad (z/l = 2, 3,...) \quad \text{Equation 2.32}$$

Thus, the number of loops of *s* segments per adsorbed chain are determined from the $G_i^t(2l;s)$:

$$n_{lp,i}(s)=\frac{(\lambda_1)^2 G_i^t(2l;s)}{G_i^a(r_i)}\sum_{t=1}^{r_i-s-1}G_i(l;t)G_i(l;r_i-s-t) \qquad \text{Equation 2.33}$$

From the terms defined so far it is easy to calculate the fraction of segments in the trains, loops and tails. The fraction of segments in the tails is calculated from the summation over the total number of segments that contain $sn_{tl,i}(s)$ segments:

$$\nu_{tl,i} = \frac{1}{r_i}\sum_{S=1}^{r_i-1} s n_{tl,i}(s) \qquad \text{Equation 2.34}$$

The fraction of segments in trains is determined by dividing the volume fraction of trains by the total adsorbed amount per surface site:

$$\nu_{tr,i} = \frac{\phi_i(l)}{\theta_i^a} \qquad \text{Equation 2.35}$$

$$\theta_i^a = \sum_{z/l=0}^{Z} \phi_i^a(z) \qquad \text{Equation 2.36}$$

The fraction of segments in the loops follows easily from the other two:

$$\nu_{lp,i} = 1 - \nu_{tl,i} - \nu_{tr,i} \qquad \text{Equation 2.37}$$

The length of the tails, trains, and loops is also easy to calculate, since there are $r_i\nu_{tl,i}$ tail segments in $n_{tl,i}$ tails, and similarly for the trains and loops:

$$l_{tl,i} = r_i\nu_{tl,i} \Big/ n_{tl,i} \qquad \text{Equation 2.38}$$

$$l_{tr,i} = r_i\nu_{tr,i} \Big/ n_{tr,i} \qquad \text{Equation 2.39}$$

$$l_{lp,i} = r_i\nu_{lp,i} \Big/ n_{lp,i} \qquad \text{Equation 2.40}$$

2.1.1.1.2 Review of Literature

2.1.1.1.2.1 Adsorbed Amount

The general trends for uncharged homopolymer adsorption have been summarized in a number of sources, most notably in "Polymers at Interfaces"[1]. The adsorbed amount for adsorption from a poor solvent shows a strong dependence on the molecular weight of the polymer, while that from a good solvent has a much weaker effect. This feature is evident in the theoretical calculations illustrated in Figure 2.3, where polymers at the theat-state show a linear relationship between adsorbed amount, given in terms of equivalent monolayers and equal to θ_i^a from theory described above, and the degree of polymerization, while the polymer in a good solvent has a much weaker dependence. In the dilute and semidilute regime the adsorbed amount forms a pseudo-plateau when

plotted against equilibrium concentration, Figure 2.4, which is nearly flat, and is indicative of high affinity adsorption. The term Γ^{ex} is the concentration of polymer in the interfacial region which is in excess of the bulk concentration, and Γ^{a} is the total polymer that is in contact with the surface. For dilute polymer solutions Γ^{ex} is equal to Γ^{a}, and will be defined as just Γ. The adsorption is also dependent on the adsorption energy parameter, as shown in Figure 2.5, especially just above the critical adsorption energy, χ_{sc}, where there is a rapid increase in adsorption.

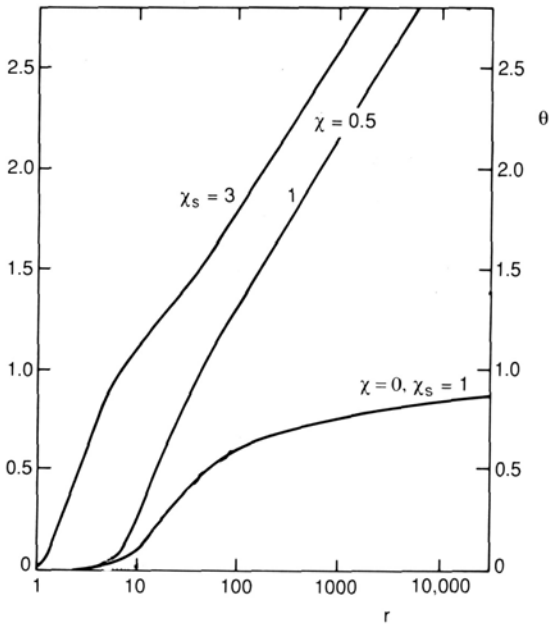

Figure 2.3: Adsorbed amount, θ_2^{a}, as a function of chain length, r. Theoretical curves obtained with SF theory for $\phi^{b} = 10^{-3}$ (the bulk polymer concentration), and various values of χ_s and χ, as indicated. Modified from reference 1.

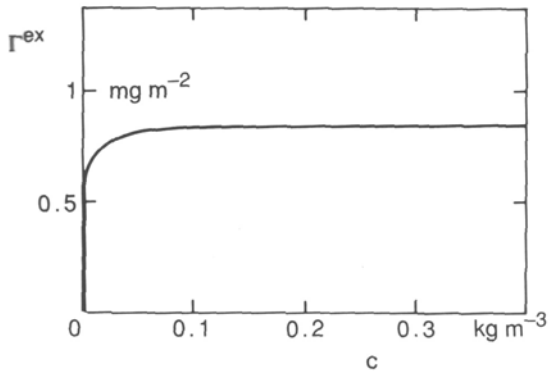

Figure 2.4: A typical high-affinity polymer adsorption isotherm[1].

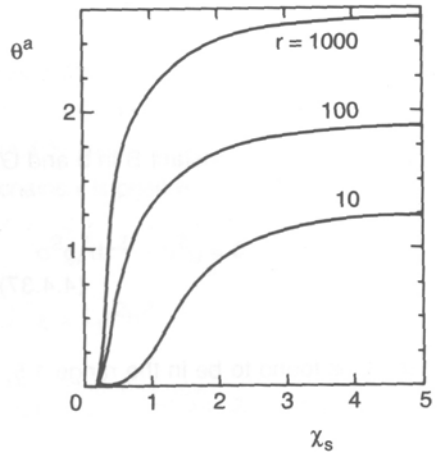

Figure 2.5: Adsorbed amount θ_2^a as a function of the χ_s parameter for three chain lengths, as calculated from the SF model. Parameters: $\chi = 0.5$, $\phi^b = 10^{-3}$, hexagonal lattice[1].

An early experimental paper on homopolymer adsorption discusses the results of poly(vinylpyrrolidone) (PVP) on nonporous silica from two different solvents, water and 1,4-dioxane[2]. In this study a number of variables were examined to determine their effect on the adsorbed amount, determined by the depletion method. Two fundamental results were concluded from this work. The first result was that a higher molecular weight sample will adsorb more slowly than a low molecular weight polymer. This seems

[2] Cohen Stuart, M.A.; Fleer, G.J.; Bijsterbosch, B.H. *Journal of Colloid and Interface Science* **1982**, *90*, 310.

intuitive since the diffusion rate of the larger chain to the surface is expected to be slower than that of a smaller chain. Secondly, when the solvent quality is decreased, by using a poorer solvent, the adsorbed amount increases, as illustrated in Figure 2.3. Again, this can be understood because the polymer will have a stronger affinity for a surface in a poorer solvent and thus adsorb more strongly. In the case of PVP, the authors concluded that there is hydrogen bonding between the carbonyl groups on the polymer and –OH groups on the surface, resulting in strong adsorption.

In general homopolymers adsorb in a manner such that the adsorbed amount increases sharply with increasing polymer concentration, until it reaches a plateau value. For a monodisperse polymer this transition would be very sharp, see Figure 2.4, but for polydisperse polymers the curve is more rounded.[1,3] The differences lie in the fact that polydisperse polymers are really mixtures of the same polymer at different molecular weights. Thus, the rounded curve of the experimental isotherms has been determined to be caused by preferential adsorption of long chains over shorter chains, due to a lower solubility of the longer chains. At low polymer concentrations all of the polymer can adsorb, but as the concentration increases the surface becomes saturated and this is when the longer chains in solution start to displace the shorter chains on the surface. This causes the curvature in the adsorption isotherm as each molecular weight polymer is selectively displaced with high molecular weight analogs. For a very polydisperse system the plateau will in actuality be a pseudo-plateau since there is continuous displacement even at high concentrations.

The adsorption and desorption of polystyrene (PS) on porous silica has been studied with respect to the effect of pore size and compared to results on nonporous silica.[4] Cyclohexane was used as the solvent and dioxane as the displacer for the desorption experiments. Different molecular weights of PS were adsorbed on silica with different pore sizes. The results showed that for low molecular weight polymers ($<4.4 \times 10^4$

[3] Cohen Stuart, M.A.; Scheutjens, J.M.H.M.; Fleer, G.J. *Journal of Polymer Science: Polymer Physics Edition* **1980**, *18*, 559.

[4] (Kawaguchi, M.; Arai, T. *Macromolecules* **1991**, *24*, 889.

g/mol), when the pore size became greater than six times the radius of gyration of the polymer, there was no further change in the maximum adsorbed amount, which was greater than for the small pore size silica. For larger molecular weights (>3.5 X 10^5 g/mol) there was an increase in the adsorption plateau with increasing pore size, and the nonporous silica had the greatest adsorption. The shape of the adsorption isotherms of the porous samples was different from the nonporous material, with the former having a more rounded shape than the latter. Since the polymers are fairly monodisperse, the round shape is attributed to the adsorption on the porous silica not being of the high-affinity type, like the nonporous silica. All of the work done on the current project will involve nonporous particles and surfaces.

2.1.1.1.2.2 Layer Thickness

The layer thickness can be measured using several different analytical techniques. Figure 2.6 shows the differences in the layer thickness when measured by ellipsometry (δ_{ell}), small angle neutron scattering (SANS) (δ_{rms}), or a hydrodynamic technique (DLS or streaming potential) (δ_h). It has been hypothesized that δ_{ell} and δ_{rms} are sensitive to the length of the loops, while δ_h is most sensitive to the length of the tails, which would explain why δ_h is so much greater than the other two. The most interesting of these is the hydrodynamic layer thickness, which shows a strong dependence on adsorbed amount, as shown in Figure 2.7. At low θ, the surface is covered mostly by trains and δ_h is small. As θ increases, the surface becomes more crowded and tails start to form, thus increasing δ_h. It has been determined from both experimental and theoretical work[1], that unlike the adsorbed amount, the layer thickness does not show a strong dependence with solvent quality or the segmental adsorption energy. When either the polymer concentration or the degree of polymerization of the polymer is increased the layer thickness will also increase. Figure 2.8 shows some theoretical calculations of how the contribution from tails quickly becomes the dominate part of the layer thickness.

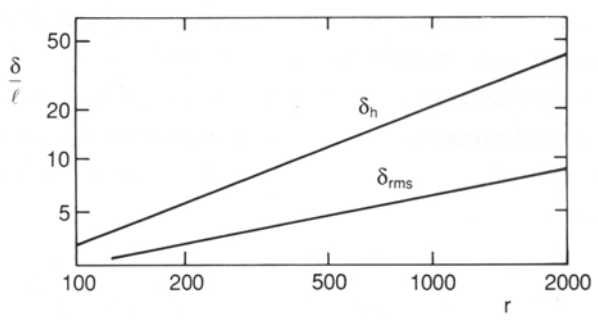

Figure 2.6: Chain length dependence of the hydrodynamic layer thickness, δ_h, and the rms thickness δ_{rms}. Theoretical calculations obtained from the SF theory; parameters: $\chi_s = 1$, $\chi = 0.4$, $\phi^b = 10^{-3}$, or a hexagonal lattice[1].

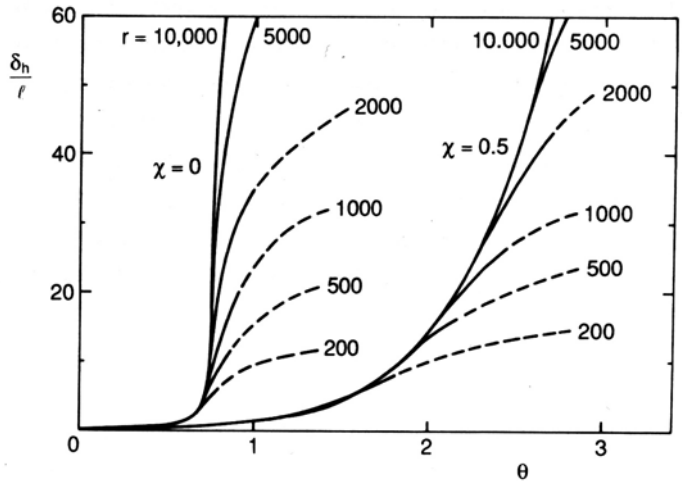

Figure 2.7: Theoretical hydrodynamic layer thickness, δ_h, as a function of coverage θ_2[a] for various chain lengths and two solvencies, as indicated. Along each curve the solution concentration varies; the curve are dashed for $\phi^b > \phi_{ov}$[1].

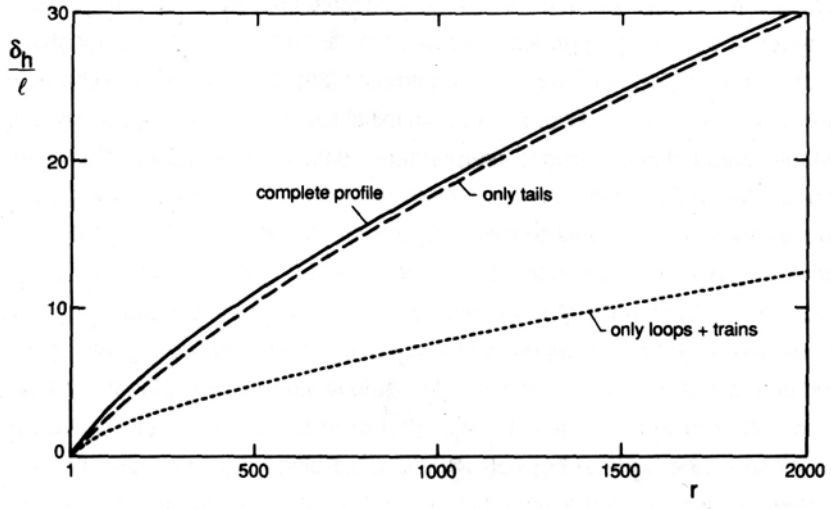

Figure 2.8: Theoretical hydrodynamic layer thickness as a function of chain length. For $\chi_s = 1$, gives δ_h as computed from the complete volume fraction profile (solid curve), from the loops and trains only (dotted curve), and from the tails only (dashed curve)[1].

Another early paper discusses the adsorption of PVP in water, but this time the adsorbent was a glass capillary[5], in which the hydrodynamic layer thickness, δ_h, was measured using streaming potential measurements. The polymer was injected into the capillary in a series of pulses, so that not only could the layer thickness be studied, but also the relaxation of the thickness after each pulse.

The results showed that as the amount of polymer on the wall builds, the layer thickness increases and the rate of relaxation decreases. This agrees well with work discussed in the next section, in that as the adsorbed amount increases the bound fraction decreases, thus the loops and tails increase, and the layer thickness is governed by the tails. Also, as the surface becomes more crowded the chains are not able to relax as quickly. One exception to these findings was that at high molecular weights the layer thickness was smaller that at lower molecular weights. It is believed that this was due to the diffusion-controlled adsorption at high molecular weights, created by the limited time allowed for the polymer to contact with the surface.

[5] Cohen Stuart, M.A. and Tamai, H. *Macromolecules* **1988**, *21*, 1863.

In other work, the adsorption of poly(ethylene oxide) (PEO) on polystyrene latex[6] was discussed. The authors use dynamic light scattering (DLS) to measure the hydrodynamic layer thickness, and the depletion method to calculate the adsorption isotherms. The experimental results were compared to theoretical computations from the Scheutjens and Fleer model, discussed in the theoretical background. The general qualitative trends were in good agreement between the experimental and theoretical results. They both showed the expected trend that as the molecular weight was increased the adsorbed amount also increased. An interesting result was that for short chains the hydrodynamic layer thickness was less than two times the radius of gyration of the polymer in the bulk. As the molecular weight was increased the two gradually become closer until they cross, so at high molecular weights the hydrodynamic layer thickness is greater than twice the radius of gyration. This again shows that at higher molecular weights the adsorbed polymer has a higher fraction of longer tails. It is interesting to note that a block copolymer that forms a brush on a surface can have a layer thickness well in excess of twice the radius of gyration.

2.1.1.1.2.3 Bound Fraction

For the fraction of trains or bound polymer, in Figure 2.9, there is little effect of the polymer molecular weight. After an initial adsorption increase, the fraction of trains decreases as the polymer concentration increases, indicating the development of tails. Similar effects of solvent quality and segmental adsorption energy are seen on the bound polymer fraction as was discussed for the adsorbed amount.

---

[6] Cohen Stuart, M.A.; Waajen, F.H.W.H.; Cosgrove, T.; Vincent, B.; Crowley, T.L. *Macromolecules* **1984**, *17*, 1825.

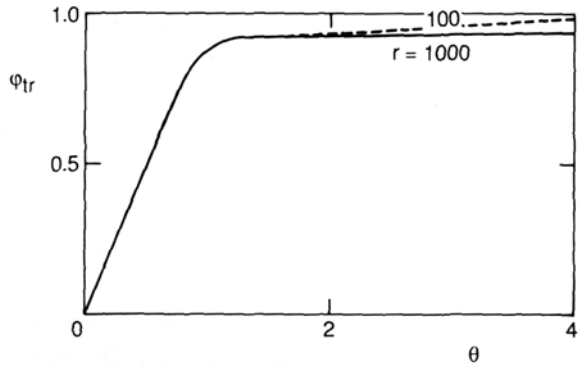

Figure 2.9: Volume fraction of segments in trains as a function of coverage as calculated from the SF theory. The theoretical plot was calculated for two chain lengths (indicated), $\chi_s = 3$, $\chi = 0.5$, $\phi^b = 10^{-3}$, hexagonal lattice[1].

The system of PVP on nonporous silica from water and 1,4-dioxane was used to measure the fraction of bound segments or segments in trains, (p)[7]. Both infrared spectroscopy (IR) and microcalorimetry were used to probe the adsorption, and results were compared to previous studies of PVP on silica from water which used nuclear magnetic resonance (NMR) and electron paramagnetic resonance (EPR). An important comment on how the bound fraction is related to the polymer structure is made here. Namely, at a large p the molecule is highly flattened on the surface, where as for a small p the molecule will more resemble its random coil configuration. Also, the bound fraction for a few long chains adsorbed on the surface can be equivalent to that from the adsorption of many short chains.

All of the analytical techniques showed the same trend, that at a low adsorbed amount there was a high bound fraction, but as the adsorbed amount increased the bound fraction decreased, as shown in Figure 2.10. The IR results gave a value for p about half that measured with all three of the other techniques. The authors believe this is due to the fact that IR only detects the hydrogen bonds between the surface and the polymer, thus excluding other bonding sources, and giving inaccurate results. The recommended

[7] Cohen Stuart, M.A.; Fleer, G.J.; Bijsterbosch, B.H. *Journal of Colloid and Interface Science* **1982**, *90*, 321.

methods for determining bound fraction are NMR and EPR, because the microcalorimetry technique is only good for low molecular weight polymers.

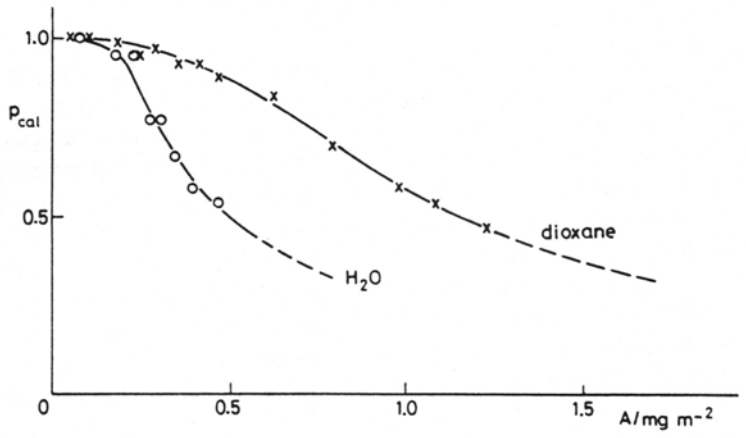

Figure 2.10: Bound fraction from calorimetry as a function of adsrobed amount A, for PVP in water and dioxane[7].

2.1.1.1.2.4 Kinetics of Adsorption

The kinetics of the adsorption of polymers has three main contributions: the rate of mass transfer of the polymer to the surface, the rate of attachment of the polymer to the surface, and any rearrangement of the polymer molecule that takes place after adsorption onto the surface. This makes studying the kinetics of adsorption challenging, because it is difficult to isolate and investigate these contributions individually.

The streaming potential technique was used to study the adsorption of (PEO) in water on a glass capillary[8]. This work studied the mass-transfer limited case for polymer adsorption. The authors found that the rate of adsorption is controlled by the rate of mass transfer toward the surface, meaning that the rate of attachment was greater than the mass transfer to the surface. Conversely, the rate of desorption was controlled by the rate of mass transfer away from the surface. It was determined that as more polymer was desorbed by the addition of solvent, the rate of desorption dropped off dramatically.

[8] Dijt, J.C.; Cohen Stuart, M.A.; Fleer, G.J. *Macromolecules* **1992**, *25*, 5416.

Thus, desorption by dilution is practically impossible to observe experimentally, because as the solution is diluted the concentration of adsorbent at the surface is also reduced, and thus any desorbed polymer can not be detected. The layer thickness measurements were compared to those from DLS and were in good agreement. This confirms what was earlier stated, that both the streaming potential and the DLS experiments measure the hydrodynamic layer thickness.

The kinetics of adsorption have been studied for PEO on silica in water using a stagnation point flow reflectometry apparatus[9]. This allows for a well defined hydrodynamic flow condition, so that it can be determined if the adsorption is mass-transfer or interfacial limited. The flux, *J*, of particles toward the surface has been calculated by Dijt[10] to be:

[9] Dijt, J.C.; Cohen Stuart, M.A.; Hofman, J.E.; Fleer, G.J. *Colloids and Surfaces* **1990**, *51*, 141.

[10] Dijt, J.C.; "Kinetics of Polymer Adsorption, Desorption, and Exchange, **1993**, thesis.

$$J = \frac{Dc_p}{a} Sh \qquad \text{Equation 2.41}$$

where, D is the diffusion coefficient, c_p is the bulk polymer concentration, a is the radius of the particles, and Sh is the Sherwood number given by the following equation in the limit of very small Peclet numbers, Pe:

$$Sh = 0.616 Pe^{1/3} \qquad \text{Equation 2.42}$$

$$Pe = \frac{2a^3 \upsilon \alpha \,\mathrm{Re}}{R^3 D} \qquad \text{Equation 2.43}$$

where ν is the kinematic viscosity, α is the dimensionless streaming intensity parameter, R is the raius of the inlet tube, and Re is the Reynolds number, given by:

$$\mathrm{Re} = \frac{UR}{\upsilon} \qquad \text{Equation 2.44}$$

where U is the mean fluid velocity at the end of the inlet tube. Thus, for mass transfer limited adsorption, the initial rate is proportional to the polymer concentration in the bulk.

The results showed that the adsorption was mass-transfer limited until the surface approached saturation, when the interfacial interactions, attachment and rearrangement rates, became the limiting factor. The adsorbed amount was found to increase strongly with molecular weight for small chains, but the dependence decreased as the molecular weight increased. This is the general trend found for polymer adsorption from good solvents. The authors also found that with the addition of pure solvent, there is no desorption for the polymers with molecular weights greater than 10^5 g/mole, and as the molecular weight decreases the desorbed amount increases.

Another group studied the adsorption of fluorescein isothicyanate (FITC) tagged PEO on silica using total internal reflection fluorescence (TIRF)[11]. This allows for a very accurate description of the adsorption kinetics to be made. The authors found that in dilute solution the adsorption rate was proportional to the polymer solution concentration, as shown above. This suggests that the adsorption kinetics are transport-limited, or that

[11] Rebar, V.A.; Santore, M.M. *Macromolecules* **1996**, *29*, 6273.

the rate of the diffusion of the polymer to the surface was the slower than the adsorption and rearrangement processes at the surface. Above a concentration of 50 ppm the rate was dominated by the diffusion of polymer clusters to the surface.

2.1.1.1.2.5 Desorption, Displacers, and Competitive Adsorption

As discussed above, it is difficult experimentally to desorb a polymer from a surface by dilution, due to thermodynamic and kinetic restrictions, but desorption can be accomplished more readily by the use of displacers. Both monomeric and polymeric displacers can be used to remove a polymer from a surface. Displacement occurs if the displacer has a higher affinity for the surface than the adsorbed polymer, or for polymeric displacers, if the displacer has a longer chain length, as discussed above in reference to polydispersity. Although the chain length aspect will play a role in displacement, the surface affinity, χ_s, is the more important factor during displacement. The kinetics of the displacement by polymeric molecules is also much slower than by monomeric displacers due to transport limitations.

The crucial experimental quantity measured during displacement is the critical displacer concentration, ϕ_{cr}. As shown in Figure 2.11, as the concentration of displacer is increased, the effective adsorption energy parameter, χ_s^{eff}, drops. At the ϕ_{cr} the $\chi_s^{eff} = \chi_{sc}$, and all of the polymer is desorbed from the surface. Also, notice that the higher the χ_{sDO} for the displacer, the lower the value of ϕ_{cr}.

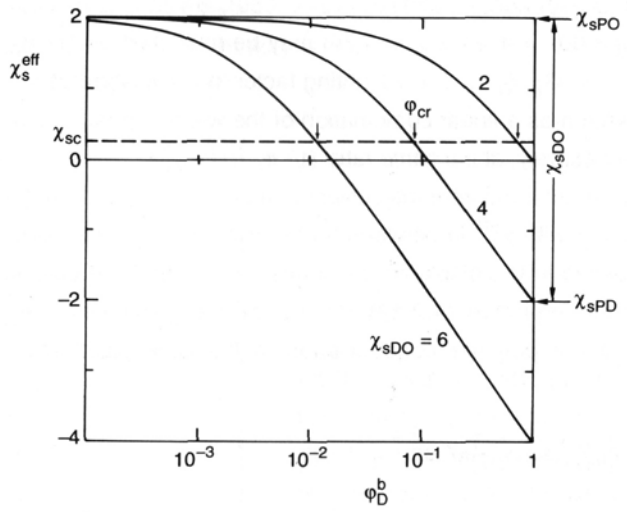

Figure 2.11: The effective adsorption energy parameter, χ_s^{eff} as a function of the displacer volume fraction ϕ_D^b for three values of the displacer adsorption energy parameter χ_{sDO}[1].

The question of desorption has also been discussed in reference to the reversibility of polymer adsorption. Many early workers believed that because polymers do not desorb when diluted with pure solvent that the adsorption is irreversible. It is now thought that this is incorrect, and the lack of desorption is thermodynamically driven because the equilibrium is strongly in favor of polymer adsorption on the surface over the polymer in solution[3]. Also, desorption will only occur at the critical polymer concentration, which is usually very small, smaller than can be detected analytically.

An early paper discusses the desorption of PVP on silica in water and 1,4-dioxane, analogous to the worked mentioned above[12]. Low molecular weight solvents were used to displace the polymer, in order to study the desorption. This desorption occurs because the displacer effectively lowers the adsorption energy of the polymer. As mentioned above, the PVP has a high affinity for the silica in both solvents, and there is strong adsorption. Due to this, the displacers chosen were all completely miscible in both water

[12] Cohen Stuart, M.A.; Fleer, G.J.; Scheutjens, J.M.H.M. *Journal of Colloid and Interface Science* **1984**, *97*, 515.

and dioxane and were proton-acceptors, thus having a strong affinity for the surface. As more displacer was added to the adsorbed polymer system the polymer began to desorb, until the critical displacer concentration was reached at which point all of the polymer was desorbed. From the critical displacer concentration and the adsorption isotherms for the displacers the polymer segmental adsorption energy can be calculated.

The resulting order of displacer strength was the same in both solvents, which indicates that the adsorption/desorption is dominated by polymer/surface and displacer/surface interactions. There was stronger displacement in water and this is believed to be due to some ionic effects, which are not present in the dioxane. The calculated segmental adsorption energy of 4kT, confirms that there is indeed strong adsorption between the PVP and the silica.

The adsorption of PS on silica from carbon tetrachloride and cyclohexane was studied using adsorption thin layer chromatography (ATLC)[13]. In particular, the desorption that occurs when a low molecular weight solvent is added to the adsorbed polymer system was measured using the ATLC and bulk adsorption techniques. The ATLC desorption curves gave a much steeper drop in adsorbed polymer amount with increasing displacer concentration compared with the bulk desorption experiments. This sharper drop from the ATLC curves allows for greater ease in determining the critical desorption point. Several displacers were used in this study and the effective adsorption energy that were calculated agreed well with the expected results. The ATLC has one negative attribute, in that it does not work for solvents that have poor chromatographic developing characteristics for the thin layer, such as water.

Displacers have also been used to quantify the segmental adsorption energy of poly(2-ethyl-2-oxazoline) (PEOX) on silica[14]. The PEOX was adsorbed on silica from both

[13] van der Beek, G.P.; Cohen Stuart, M.A.; Fleer, G.J.; Hofman, J.E. *Langmuir* **1989**, *5*, 1180.

[14] Chen, C.H.; Wilson, J.E.; Davis, R.M.; Chen, W.; Riffle, J.S. *Macromolecules* **1994**, *27*, 6376.

water and ethanol, and then subsequently desorbed using five different proton accepting small molecules. The resulting χ_s^{PO} values, 3.2 in ethanol and 5.1 in water, were larger than expected based on the previous mentioned work for different polymers and showed strong adsorption. The difference in the values for the two solvents was attributed to specific solvent effects between the water and the PEOX.

The desorption of PVP and PEO on silica in water has also been studied[15]. The method used to quantify the adsorption, H-NMR, was highly effective because it differentiates between the adsorbed trains and the nonadsorbing loops and tails. In this study a base was used to displace the PEO, because as the pH is increased the PEO will desorb due to adsorbing electrolyte. The results showed that as polymer was desorbed the number of trains decreased, while the number of tails and the total adsorbed amount remained fairly constant until pH 10.5, where they too drop off very quickly. This makes sense because only one adsorbed segment is needed per chain to keep the length of the tails and the adsorbed amount at a high value.

An earlier paper discussed the competitive adsorption of PEO and PS on nonporous silica from carbon tetrachloride[16]. Both polymers had very narrow molecular weight distributions. IR was used to determine the supernatant concentrations of the PEO while UV-spectroscopy in dioxane was used to measure the PS concentration. Two effects were studied, adding both polymers to the silica at the same time, and adding the PS first and then adding the PEO. In both cases there was eventually complete displacement of the PS by the PEO. The reason for this is that the PEO has a much stronger adsorption energy for silica, compared to the PS. The rate at which PEO desorbs PS in the second type of experiment was dependent on the fraction of PS segments that were adsorbed onto the surface and the molecular weight of both the PS and the PEO.

---

[15] van der Beek, G.P.; Cohen Stuart, M.A.; Cosgrove, T. *Langmuir* **1991**, *7*, 327.

[16] Kawaguchi, M.; Sakai, A.; Takahashi, A. *Macromolecules* **1986**, *19*, 2952.

2.1.1.2 Charged Homopolymers

The presence of charged groups on polymers adds to the richness of the adsorption phenomena. Now, along with the solvent quality and surface adsorption energy, the ionic strength and pH also become important factors. There are four different systems where electrostatics play a significant role in adsorption: neutral polymers on charged surface, charged polymers on uncharged surface, polymer and surface with the same charge, and both with opposite charges.

Charged molecules in solution exhibit an electric field, which will attract or repel ions. The strength of this field will be reduced or screened by small ions. The characteristic length that describes the decay in the electric field with distance is the Debye length κ^{-1}, which is defined as:

$$\kappa^2 = \frac{2e^2 \sum_{i=1}^{N} n_i z_i^2}{\varepsilon kT} \qquad \text{Equation 2.45}$$

where, n_i is the number concentration of counterion *i* in the equilibrium salt solution, z_i is their valence, ε is the dielectric permittivity of the solvent medium, *e* is the elementary charge and kT is the thermal energy.

The ionic strength has a strong effect on the level of adsorption and on how polyelectolytes adsorb. In the limit of low ionic strength electrostatic effects dominate adsorption, and the sign of the polymer and surface charge will determine the amount of adsorption. At high ionic strength, non-electrostatic effects such as hydrogen bonding and dipole interactions become more important because the electrostatics are screened by the high salt concentration. If the ionic strength increases too high the solvent quality may drop and increase adsorption, and further increase may cause polymer precipitation.

2.1.1.2.1 Adsorption of Homopolymers onto Charged Surfaces

The adsorption of an uncharged polymer onto a charged surface is only significantly affected when the surface charge density is large, for a Stern potential of >50 mV.[1] Any counter-ions in the solution can have a significant affect on adsorption because they can

compete with the polymer for surface sites. Examples of this type of adsorption have been discussed above, and Figure 2.12 shows the effect that the surface charge density had on PEO adsorption onto silica in water.

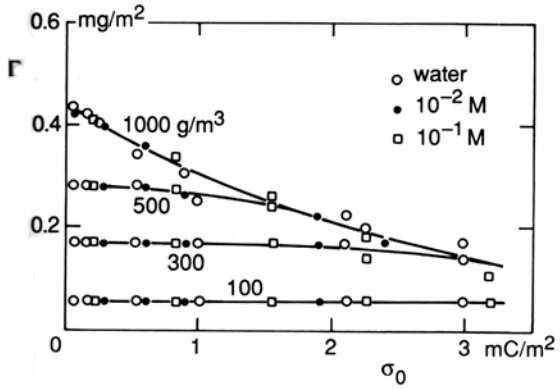

Figure 2.12: Adsorbed amount of PEO from aqueous solution onto silica, as a function of surface charge density, σ_o. Modified from reference 1.

2.1.1.2.2 Adsorption of Polyelectrolytes onto Uncharged Surfaces

For polyelectrolytes on uncharged surfaces the only important electrostatic effects are those from the mutual repulsion between the adsorbed chain segments. When the ionic strength is low there is little adsorption due to the unfavorable restrictions of having many charged segments close to each other at the surface. The chains lie very flat on the surface, with few loops and tails present, and little effect of molecular weight on the adsorption. At high salt concentrations these effects become negligible and the adsorption more closely resembles that for uncharged polymers, as shown in Figure 2.13. The solubility is also reduced by increasing the salt concentration, which would increase adsorption. For weak polyelectrolytes such as polyacids, the adsorption is strongly controlled by the pH of the system. At low pH, below the pK_a of the acid, the polymer is uncharged and adsorbs like a typical homopolymer. When the pH surpasses the pK_a electrostatics become important and adsorption is hindered. Thus, at a lower pH there is greater adsorption for polyacids on uncharged surfaces.

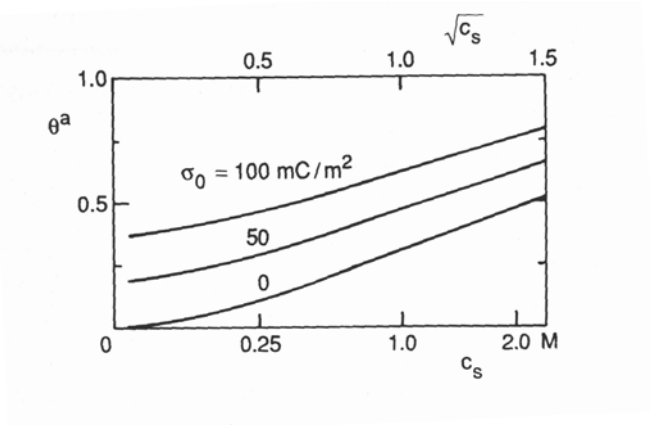

Figure 2.13: Adsorbed amount of a strong polyelectrolyte as a function of the salt concentration on an uncharged surface ($\sigma_o = 0$) and on two positively charged surfaces. Note that the abscissa scale is not linear in c_s but in $\sqrt{c_s}$. Parameters: r = 500, $\phi^b = 10^{-4}$, $\chi_s = 1$, $\chi = 0.5$, $l = 0.6$ nm, hexagonal lattice[1].

The adsorption of negatively charged polystyrene sulfonate (PSS) onto single crystals of polyoxymethylene (POM) has been studied in water[17]. The results showed a low-affinity type isotherm with low adsorbed amounts. This is characteristic of adsorption on an uncharged, low-energy surface. The adsorbed amount was found to increase dramatically with increasing molecular weight and ionic strength. This latter trend was due to screening of the intermolecular and intramolecular repulsive forces of the PSS, which allowed more PSS to adsorb onto the surface.

2.1.1.2.3 Adsorption of Polyelectrolytes onto Surfaces with the Same Charge

When the charge on the surface and the charge of the polymer are the same sign there is relatively little adsorption at low ionic strengths. This is due to a decrease in the effective surface adsorption energy, caused by repulsive interactions of the charges on the surface and on the polymer. As the salt concentrations increases, and the electrostatic effects are screened, the polyelectrolyte resembles more closely an uncharged polymer and the adsorption increases, as shown in Figure 2.14.

[17] Papenhuijezen, J.; Fleer, G.J.; Bijsterbosch, B.H. *Journal of Colloid and Interface Science* **1985**, *104*, 530.

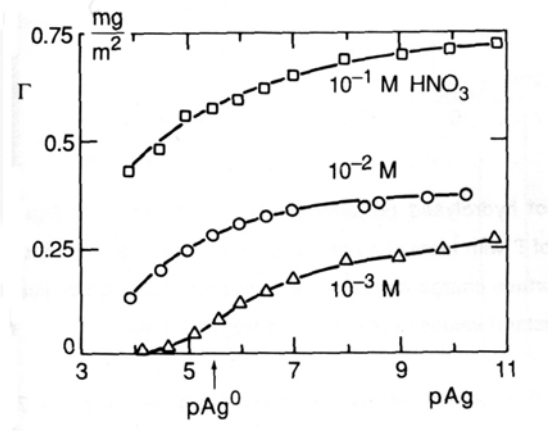

Figure 2.14: The adsorbed amount of positively charged poly-L-lysine (250 K) on AgI as a function of pAg, at three different HNO_3 concentrations. The surface is positively charge for $pAg < pAg^0$. Modified from reference 1.

2.1.1.2.4 Adsorption of Polyelectrolytes onto Surfaces with an Opposite Charge

For the adsorption of a polymer on a surface which have opposite charges there are two different factors which can effect adsorption. The first is a purely electrostatic contribution, when the segmental adsorption energy is zero. For this case, the adsorption is higher at low salt concentrations, where the polymer is attracted to the surface by electrostatic forces. An interesting caveat is that the polymer adsorbs in a very extended coil conformation because of mutual repulsion of the segments, which results in a very small adsorbed layer thickness. At higher ionic strengths these effects are screened by the salt and desorption occurs by an ion-exchange process.

When the surface and polymer have opposite charges the adsorption can also be affected by a specific affinity for one another. This type of adsorption is highly controlled by the effect that the charges have on changing the effective surface adsorption energy and the effective solvent quality, as shown in Figure 2.15. These two factors have opposing effects on the polymer adsorption: an increase in the effective surface adsorption energy promotes adsorption, while an increase in the effective solvent quality decreases adsorption. For both of these situations the adsorption resembles that of an uncharged polymer at high ionic strengths, as discussed above. At low salt concentrations the adsorption is dependent on the specific system: polymer, solvent and adsorbent. For the

weak polyelectrolytes again, the pH becomes a significant factor. At low pH, below the pK_a of the acid, the adsorbed amount is low because the salt ions compete with the uncharged polymer for surface sites, and the adsorbed polymer consists of a large number of loops and tails. At higher pH, above the pK_a, the charged polymer can better compete for the surface sites and adsorption increases, as do the number of trains, as the polymer lies in a very flat conformation on the surface.

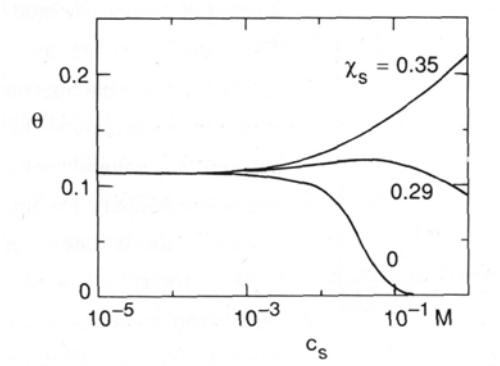

Figure 2.15: SCF calculation (for a polyelectrolyte adsorbing on an oppositely charged wall) of the adsorbed amount as a function of salt concentration. Three different χ_s values were used, as indicated in the figure. Polymer charge density $\alpha = 0.2$, surface charge density $\sigma_o = 0.01$ C/m^2, r = 100, $\chi = 0.5$, $\phi^b = 10^{-3}$, $l = 0.6$ nm, hexagonal lattice. Modified from reference 1.

The adsorption of sodium poly(methacrylic acid) (PMAA-Na) on α-Al_2O_3 has been studied as a function of pH and polymer concentration[18]. Potentiometric titration was used to determine the fraction of dissociated or ionized carboxylic acid groups and the surface charge on the alumina, prior to the adsorption experiments. As the pH increased, the fraction of dissociated groups, which become dissociated on the polymer, increased and thus the negative charge increased. At pH > IEP (above 8.7) the net charge on the alumina was negative. Based on these two important observations, the adsorption experiments were carried out in a pH range from 3.5-8.7, where the polymer charge was negative and the net surface charge was positive, and thus where there should be an electrostatic attraction between the polymer and the surface. At high pH the adsorbed

[18] Cesarano, J.; Aksay, I.A.; Bleier, A. *Journal of the American Ceramic Society* **1988**, *71*, 250.

amount was small and it was believed that loops are suppressed because the large charge on the polymer caused inter-particle repulsion. At lower pH, the adsorbed amount increases and the number of loops was believed to increase, because the charge on the polymer was reduced.

The adsorption of two salts of poly acrylic acid, sodium and ammonium, were measured on α-Al_2O_3 in water[19]. The adsorption was measured in the bulk and by using diffuse reflectance infrared Fourier transform (DRIFT), which can probe the adsorbent for surface variations caused by polymer adsorption. Two important factors arise from this system when the pH is varied. First, at low pH, the polyacrylate was less ionized and it adopted a coil configuration, similar to an uncharged polymer, but at high pH the polymer became charged and it took on a more rod-like shape. The second factor is the charge on the alumina surface. As discussed above, at low pH the net charge is positive, but at a higher pH, above the pzc (8.7), the net surface charge becomes negative. Thus, there are three different regimes of interest: low pH, where the surface has a positive charge and the polymer is uncharged; mid-range pH, where the surface is still positive but the polymer becomes negatively charged; and high pH where both the polymer and the surface both have a net negative charge. At low pH, the adsorption is similar to homopolymer adsorption and the polymer takes on a coiled conformation with enhanced loop formation. As the pH is increased, but still less than the IEP, there is stronger adsorption, due to electrostatics, but the polymer adopts a more rigid conformation on the surface due to the repulsive interactions. At pH > IEP there is still some adsorption on the positive surface sites, but it is greatly reduced. This work shows how important the solution conditions are in determining not only the amount of adsorption, but also the conformation of the adsorbed polymer.

The adsorption of a monodisperse, strongly anionic polyelectrolyte, poly(styrene sulphonate) (PSS) was studied on both positively and negatively charged poly(styrene

[19] Lee, D.H.; Condrate, R.A.; Reed, J.S. *Journal of Material Science* **1996**, *31*, 471.

latex (PSL) in water[20]. Both small angle neutron scattering (SANS) and DLS were used to characterize the adsorption and to construct an accurate description of the polymer conformation on the surface. For both the positive and negative surfaces, there was little adsorption at low ionic strength. This was due to the repulsion between chain segments and resulted in very flat adsorbed layers. For the positively charged latex, as the magnitude of the surface charge density increased, the adsorbed amount decreased. This was due to a higher segmental adsorption energy, from the electrostatic interactions between the surface with the polymer, and again resulted in a flat adsorbed polymer layer. This was different from neutral homopolymers, the adsorbed amount increased with increasing adsorption energy. Although neither the positive nor negative surfaces showed a significant increase in adsorbed amount with molecular weight, the thickness of the adsorbed layer did increase, possible due to the formation of loops.

The same group measured the bound fraction of PSS using NMR on positively charged PSL in water[21]. This is a very powerful technique to measure the bound fraction because the dispersion medium is actually used to probe the adsorbed amount, and there are no chemical labels required. When the polymer adsorbs, it prevents the interaction of water with the surface, and the relaxation of water is the quantity that is measured. There were expected to be strong hydrophobic interactions between the polystyrene backbone and the polystyrene surface, which would facilitate adsorption. The results showed that the polymer did exhibit a very flat conformation on the surface, regardless of the charge on the surface. Also, it was believed that the polymer actually occupied the space between the charged surface sites, due to the before mentioned hydrophobic interactions. It was found that as the adsorbed amount increased the bound fraction decreased significantly, indicating the formation of loops and tails.

This section has shown that strong electrostatic attractions can occur for the adsorption of a polyelectrolyte on an oppositely charged surface. Based on this, the first generation

[20] Cosgrove, T; Obey, T.M.; Vincent, B. *Journal of Colloid and Interface Science* **1986**, *111*, 409.

[21] Cosgrove, T.; Obey, T.M.; Taylor, M. *Colloids and Surfaces* **1992**, *64*, 311.

diblock polypeptide will have an adsorbing anchor block that is charged. This will help to ensure good adsorption of the copolymer, and thus brush formation.

2.1.2 Block Copolymers – Trains and Tails

The next case to be discussed is block copolymers. There are three main ways that a copolymer made from two different monomers can be arranged: as a series of blocks, each made up of one monomer, as a random mixture of the two, or as an alternating copolymer of the two monomers. The adsorption of these types of copolymers will be the focus of this discussion. Block copolymers are frequently used for both the stabilization and the flocculation of colloid particles.

For an adsorbing diblock copolymer, typically one block will preferentially adsorb over the other. The adsorbed block, or the anchor, will have a high affinity for the surface. The other block, or the tail, will not adsorb and thus will form tails into the solution. If one block has just a slightly higher segmental adsorption energy than the other than that block will completely preferentially absorb over the other.

A block copolymer in a solvent can take on one of two conformations. First, if the solvent is a good solvent for both blocks, then the anchor block will be swollen on the surface. If the solvent is good solvent for one block, but a non-solvent for the other, than above a critical polymer concentration the polymers will form micelles in solution. Usually, the polymer in the micelle core will adsorb on the surface due to solubility, but the adsorption mechanism will be much more complicated due to the presence of micelles.

Figure 2.16: Schematic of block copolymer adsorption with and adsorbed anchor and an extended tail with a thickness δ.

2.1.2.1 Uncharged Diblock Copolymers

Numerous experimental and theoretical adsorption studies have been done on uncharged block copolymers in organic solvents, primarily because until recently these were the systems most easily synthesized in well-controlled compositions, or narrow molecular weight distributions for both blocks. The general trends for these types of polymers are well known and well documented. The adsorption of block copolymers can be divided into two categories, from a nonselective solvent and from a selective solvent. A nonselective solvent is one in which both blocks are soluble and micellization does not occur. A selective solvent is one in which one block is soluble and the other is not, and thus micelles will form.

The SCF lattice theory from Scheutjens and Fleer, described above for homopolymer adsorption, can be extended for block copolymers by introducing new weighting factors for each type of monomer[1]. Calculations have been done to illustrate the trends for block copolymer adsorption. An alternative method for predicting adsorption behavior is given by the scaling theory of Marques and Joanny (MJ)[22,23]. Although their results are not as quantitative as those from the SCF lattice theory, they do nonetheless make very useful predictions for block copolymer adsorption.

2.1.2.1.1 Nonselective Solvent

[22] Marques, C.M.; Joanny, J.F. *Macromolecules* **1989**, *22*, 1454.

[23] Marques, C.M.; Joanny, J.F.; Leibler, L. *Macromolecules* **1988**, *21*, 1051.

The MJ theory for block copolymer adsorption from a nonselective solvent starts by introducing an asymmetry ratio β, which is defined by:

$$\beta = \left(\frac{R_B}{R_A}\right) = \left(\frac{N_B}{N_A}\right)^{3/5} \qquad \text{Equation 2.46}$$

where, R_B and R_A are the radius of gyration of the tail block and anchor block respectively, and N_B and N_A are the degrees of polymerization for each block. This relation assumes that the size of the monomer in each block are similar. The nonselective solvent adsorption theory works on the assumption that the anchor block is strongly attracted to the surface, while the tail block is strongly repulsive, and thus there is only adsorption of the anchor block.

In a nonselective solvent there are two regimes that have been predicted from both the Scheujtens and Fleer lattice model and the Marques and Joanny scaling theory. The buoy regime occurs when the tail block has a higher molecular weight than the anchor block and $\beta > N_A^{0.5}$. For this case the adsorbed amount for the anchor block layer is below saturation and breaks into individual chains, with a thickness on the order of the monomer size, as illustrated in Figure 2.17. The repulsive forces between tail blocks are strong, forcing the tails to become extended. When the anchor block molecular weight becomes larger, the copolymer enters the anchor regime of adsorption, $\beta < N_A^{0.5}$. The surface is saturated with anchor groups, which form a fluffy swollen layer on the surface as shown in Figure 2.18, and any further increase in the anchor block molecular weight causes the adsorbed amount and the number of tails on the surface to decrease. The transition from the buoy regime to the anchor regime, at $\beta = N_A^{0.5}$, corresponds to a mole fraction of anchor blocks, X_A near 0.05, for long chains, where X_A is given by:

$$X_A = \frac{N_A}{(N_A + N_B)}$$ Equation 2.47

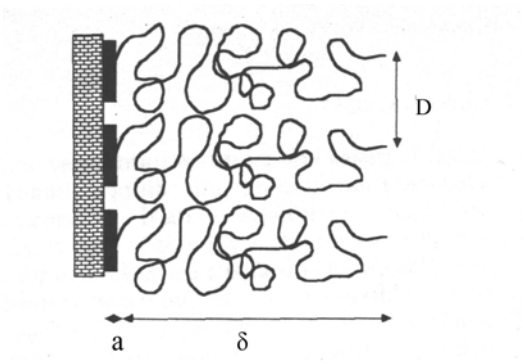

Figure 2.17: Schematic of block copolymer chains adsorbed in the buoy regime, $\beta > N_A^{0.5}$. Note the discontinuity of the adsorbed block layer[22].

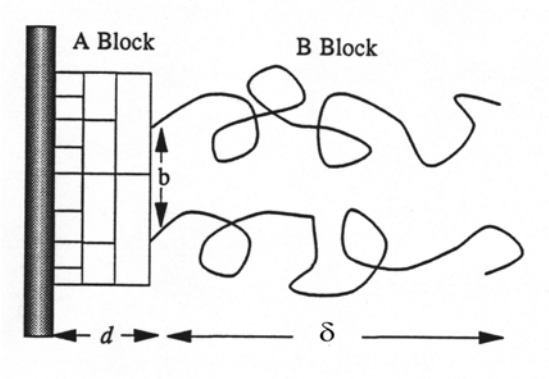

Figure 2.18: Schematic of block copolymer chains adsorbed in the anchor regime, $\beta < N_A^{0.5}$. Note the thick, continuous adsorbed block layer[22].

The number of adsorbed chains per unit area on the surface, σ, is given by the MJ theory for the two regimes:

$$\sigma \propto N_A^{-1}$$ for the Anchor Regime $\beta < N_A^{0.5}$ Equation 2.48

$$\sigma \propto \beta^{-2}$$ for the Buoy Regime $\beta > N_A^{0.5}$ Equation 2.49

The thickness of the anchor block in the buoy regime is just the monomer size, *a*, while in the anchor regime it is given by the following expression:

$$d \propto \frac{N_A^{0.5}}{\beta} \qquad \text{for } \beta < N_A^{0.5} \qquad \text{Equation 2.50}$$

Finally, the thickness of the brush is determined for each regime using the Alexander-de Gennes expression[24] for grafted chains:

$$\delta \propto N_B \sigma^{1/3} \qquad \text{Equation 2.51}$$

$$\delta \propto N_B N_A^{-1/3} \qquad \text{for } \beta < N_A^{0.5} \qquad \text{Equation 2.52}$$

$$\delta \propto N_B^{3/5} N_A^{2/5} \qquad \text{for } \beta > N_A^{0.5} \qquad \text{Equation 2.53}$$

The adsorbed amount for a block copolymer in a non-selective solvent shows a sharp increase for small anchor blocks, which peaks at the transition between anchor and buoy regime, as discussed above. As the anchor block molecular weight increases further, while holding the molecular weight of the tail block fixed, the adsorbed amount gradually decreases. The trends for layer thickness are similar, except, that the thickness drops more quickly in the anchor regime. This shows the sensitivity of the layer thickness to the extension of the tails. The volume fraction profiles for block copolymers show that the anchor block consists of mainly trains and loops, and the tail block forms the tails. As the solvent quality decreases the tail density becomes more crowded and less extended.

This review will focus on model block copolymer systems, where the molecular weight distribution for both blocks is well-controlled and typically near one. Extensive work has been done on the polystyrene – poly(ethylene oxide) block copolymer in toluene and xylene, both of which are good solvents for both blocks[25]. This is thus an example of adsorption from a non-selective solvent. For the adsorption of this copolymer on mica, the PEO forms the anchor block due to hydrogen bonding, while the PS is the tail block. These researchers used a surface force apparatus developed by Israchalvilli, which

[24] A) de Gennes, P.G. *Macromolecules* **1982**, *15*, 492. B) Alexander, S. *J. Phys.* (Paris) **1977**, *38*, 983.

[25] Taunton, H.J.; Torakcioglu, C.; Fetters, L.J.; Klein, J. *Macromolecules* **1990**, *23*, 571.

measures the forces between two cylinders brought into proximity. In this work the diblock copolymer adsorption was compared to that of homopolymer PS and end-functionalized PS, both having a similar degree of polymerization as the PS block in the diblock. Some of the key differences in the block copolymer to the non-adsorbing PS is that an attractive force is found for the PS due to depletion flocculation which does not occur for the block copolymer. Secondly, the surface-to-surface separation at the onset of force for the diblock is (12-14)*Rg of the PS block which is roughly twice that found for adsorbing homopolymers. These two observations show that the PEO end of the diblock is adsorbing and the PS block is forming an extended brush, which is not in contact with the mica surface. The authors found little difference in the adsorption of the end-functionalized polymer to that of the diblock, except for the density of surface coverage. This shows that the diblock is essentially an end-functionalized polymer, except that the adsorbing group takes up more area on the surface.

The PEO-PS block copolymer has also been used in a similar experiment using toluene as the solvent and mica as the substrate.[26] A similar force-distance apparatus was used to determine the polymer layer thickness. The lengths of both blocks were varied to determine the effect that each has on the brush layer thickness. For the least symmetric polymers, with a very long tail block and a short anchor block, the layer thickness increased with increasing PS molecular weight, while it decreased with increasing PEO molecular weight. This is reasonable because, as the anchor block molecular weight increases, it takes up more space on the mica surface and thus the tail population is less dense and is not fully extended. For a more symmetric polymer it was found that the anchor block begins to contribute more to the layer thickness because the anchor block forms a fluffy layer due to the solvency. The workers were unable to differentiate the molecular weight effects caused by PS and PEO blocks on the anchor layer thickness and the total layer thickness. Certainly for practical brush application it is desirable to use a very asymmetric brush at the composition predicted by the Marques and Joanny and the Scheujtens and Fleer theories, $X_A \sim 0.05$.

[26] Guzonas, D.; Boils, D.; Hair, M.L. *Macromolecules* **1991**, *24*, 3383.

The adsorption of the PEO-PS diblock copolymer on silica from toluene has also been studied[27]. The authors first used DLS to check for micelles, and found none. Ellipsometry was used to follow the adsorption over time and surface force measurements were done using mica as discussed above. For dilute polymer solutions, the adsorption was transport-limited, or the diffusion to the surface is the rate limiting step in adsorption, which is governed by Fickian diffusion. For more concentrated solutions there is an overshoot seen in the adsorption as a function of time. Several triblock copolymers of PEO-PS-PEO were also studied, the details of which will be discussed later. There were significant differences in the adsorption behavior of the diblocks compared to the triblocks, which shows that chain architecture can dictate adsorbed chain conformation.

2.1.2.1.2 Selective Solvents

Similar effects on the conformation are seen for a block copolymer in a selective solvent, as for the non-selective solvent, except that the anchor block forms a melt on the surface in order to minimize contact with the solvent. This was called the van der Waals brush regime by Marques and Joanny[23]. This occurs when the asymmetric ratio, β, is greater than zero, where for the selective solvent case:

$$\beta = \frac{R_{FB}}{R_{GA}} = \frac{N_B^{3/5}}{N_A^{1/2}} \qquad \text{Equation 2.54}$$

where R_{FB} is the radius of gyration for the tail block using the Flory approximation, and R_{GA} is the characteristic radius of the tail block at the wall.

There is the possibility of micelle formation for these types of systems due to the incompatibility of the anchor block and the solvent. It is expected that the adsorption for copolymer systems above the critical micelle concentration (cmc) will be different for

[27] Dorgan, J.R.; Stamm, M.; Torakcioglu, C.; Jerome, R.; Fetters, L,J. *Macromolecules* **1993**, *26*, 5321.

those below it, but for most systems the cmc is very low, often below experimentally accessible concentrations.

2.1.2.1.2.1 Equilibrium

Work has been done on the system poly(vinyl-2-pyridine) – PS in toluene and cyclohexane on mica using the surface force apparatus[28]. For PS, both solvents are good solvents, whereas for PVP, both are poor solvents. This is thus an example of adsorption from a selective solvent, where the PVP is the anchor block and the PS is the tail block. Similar to the non-selective solvent case there is an onset of force at around 10*Rg of the PS block, far larger than for homopolymer adsorption. The authors conclude that the forces generated were due to the osmotic pressure between the PS chains in the brush layer and that the situation closely resembled that of a terminally attached polymer.

Work has also been done on a PVP- PIB (polyisobutylene) diblock copolymer in comparison to the PVP – PS copolymer[29]. The adsorption was performed in toluene onto mica in the Israchalvilli surface forces apparatus described above. One particularly interesting aspect of this work is that the authors adsorbed the polymer onto the mica, rinsed with toluene and then replaced one of the mica sheets in the apparatus with another adsorbed polymer sheet. In this manner, they were able to study how different adsorbed polymer layers interact with one another. Specifically, the chemical differences that occur when one tail block is PIB and the other is PS, the molecular weight differences from varying the tail block length, and the structural differences that occur when the anchor block molecular weight is varied and there is a different number of chains per unit area were all studied. The authors concluded that the brush layer was nearly impenetrable by chains attached to another surface, even when the surface density was fairly low, due to differences in the chemical nature of PS and PIB.

---

[28] Hadziioannou, G.; Patel, S.; Granick, S.; Tirrell, M. *Journal of the American Chemical Society* **1986**, *108*, 2869.

[29] Watanabe, H.; Tirrell, M. *Macromolecules* **1993**, *26*, 6455.

The diblock copolymer PEO-PS has also been studied in water at room temperature[30]. For this system the PEO is in a good solvent, while the PS in a non-solvent. The adsorption was characterized by four independent methods. Scanning angle reflectometry (SAR) was used to determine the adsorbed amount on methylated silica and polystyrene flat surfaces. Hydrodynamic and streaming potential measurements were used to determine the layer thickness of the adsorbed polymer on the pore walls of track-etched polycarbonate membranes. Finally, total internal reflection microscopy (TIRM) was used with methylated glass slide and polystyrene surfaces to determine chain conformation. All of the diblocks used in these experiments had very long PEO segments, while having short PS segments. This does not seem like an appropriate choice of polymer since the PEO is the adsorbing polymer and it is in a good solvent. Thus, it was no surprise that all of the experiments showed trends that more resembled homopolymer adsorption than diblock adsorption. This type of behavior was labeled as 'kinetic trapping' by the authors. Essentially, the long PEO chains are kinetically restricted from desorbing from the surface to form a brush layer because too many monomers are interacting with the surface, making desorption kinetically unfavorable, even if brush formation is thermodynamically favorable.

2.1.2.1.2.2 Kinetics

In another study the adsorption of PEO-PS block copolymer onto glass and sapphire from cyclopentane was investigated[31]. A modified Mach-Zehnder interferometer was used to obtain the adsorbed amount, layer thickness and change in the refractive index. Two block copolymers of differing molecular weights were used, but both had a very long PS (tail) block and a shorter PEO (anchor) block. The results showed that at low adsorption levels the adsorbed polymer resembles a mushroom on the surface, and as the surface becomes more concentrated the tails begin to extend into solution and form a brush. The layer thickness was 3.5 times larger and the average area per adsorbed chain, determined from the surface density, and was 5 times larger than the hydrodynamic radius from DLS,

[30] Pagac, E.S.; Prieve, D.C.; Solomentsev, Y.; Tilton, R.D. *Langmuir* **1997**, *13*, 2993.

[31] Munch, M.R.; Gast, A.P. *Macromolecules* **1990**, *23*, 2313.

which depicts a highly compact adsorbed layer with tightly packed anchor blocks. It was also shown that when the tail block molecular weight increased, the surface density decreased, but the layer thickness increased.

The adsorption of the PVP-PS block copolymer on silver from toluene was also studied, where the PVP was insoluble and the PS was soluble. The kinetics of adsorption probed by using surface plasma resonance (SPR)[32]. SPR is an optical technique induced by the electromagnetic surface waves propagating along the interface between a metal and a dielectric medium, and will be discussed further in Section 2.1.5.2. The adsorbed polymer causes a shift in the reflectance minimum due to its higher index of refraction compared to the solvent. A model developed by the authors described the adsorbed PVP as a dense layer with a given thickness and the PS tails as a second layer with a uniform concentration. This agreed with the interpretation for selective solvent adsorption that the adsorbed polymer forms a dense, tightly compressed layer, while the tail block extends into solution. There are two different modes that the kinetics of adsorption can be studied using SPR, at a fixed angle over time (fast kinetics) or by scanning over a range of angles (slow kinetics, but more reliable parameters).

The authors varied the molecular weight of the anchor and tail blocks independently to determine how each one affects adsorption. These polymers form micelles in toluene, and solutions were studied above and below the cmc. It was found that the highest adsorption rate occurred above the cmc for the low molecular weight PVP polymer and that below the cmc the rate was independent of the copolymer. Decreasing the anchor block molecular weight led to a higher surface density, σ, and thus a higher layer thickness, as discussed above, but for the high molecular weight PS sample the surface density was no longer determined by the PVP block size due to the large PS blocks. The authors attribute the very fast initial adsorption rate above the cmc to micelle adsorption, and the small continued adsorption at long times to that of unimer adsorption.

[32] Tassin, J.F.; Siemens, R.L.; Tang, W.T.; Hadziioannou, G.; Swalen, J.D.; Smith, B.A. *Journal of Physical Chemistry* **1989**, *93*, 2106.

The kinetics of adsorption have been studied for a diblock copolymer in a selective solvent, with interest on the differences induced by micelles in solution. A PEO –PS block copolymer was adsorbed onto a sapphire, Al_2O_3, surface from cyclopentane, which is a good solvent for PS and a non-solvent for PEO[33]. For this system the PEO will be the anchor block, and the PS does not adsorb onto sapphire. A total internal reflection interferometer was used to measure the adsorbed amount as a function of time. Several observations were made in comparison to adsorption with a homopolymer of similar molecular weight. First, the block copolymer adsorption was much faster and that the adsorbed amount was an order of magnitude higher. These differences can be explained by comparing the adsorbed polymer conformations for the two. The homopolymer would have many surface-polymer encounters before finally adsorbing on the surface, whereas the block copolymer adsorption is driven by the insolubility of the anchor block and adsorbs more quickly. Also, the homopolymer adsorbs in loops, tails, and trains, while the block copolymer has only trains and tails, thus achieving a higher density on the surface and a considerably higher adsorbed amount.

For the PEO-PS block copolymer adsorption measurements were taken above and below the cmc to compare how micelles affect adsorption kinetics. Below the cmc, the polymer adsorbs in a very homogeneous manner and the packing density on the surface is high. Above the cmc the adsorption is more rapid because of the attachment of micelles on the surface, but the value of the rate constant is smaller and the adsorbed amount is lower than for the non-micelle case. These differences were attributed to the fact that the PS can not adsorb and thus the micelle must rearrange so that the PEO can adsorb on the surface, which is a rate-limiting step. The lower adsorbed amount is caused by the micelles adsorbing in a patchy manner on the surface and thus good packing is not achieved.

[33] Munch, M.R.; Gast, A.P. *Journal of the Chemical Society Faraday Transactions* **1990**, *86*, 1341.

The PEO-PS diblock copolymer system was also studied in cyclopentane on silica glass[34]. Dynamic scanning angle reflectometry was used to monitor the adsorption kinetics of the polymer. The solutions tested were above the cmc and thus micelles were present. The results showed an overshoot in the adsorption as a function of time, above the cmc. This is attributed to rearrangement of the micelle with polymer adsorption, and specifically, that polymer adsorption is faster than the time needed for the chain to find its optimal conformation.

Based on the work done on diblock copolymers several key characteristics can be mentioned which will facilitate brush formation, and colloidal stabilization. First, the anchor block should have a high affinity for the surface, and have a mole fraction for optimal brush formation, $X_A = 0.05$, based on the MJ scaling theory. The anchor block may be either soluble or insoluble, but a soluble anchor would be beneficial for avoiding the formation of micelles, and thus a shorter time would be required for brush formation. The tail block must be soluble in the solvent, in order to get good extension of the brush layer. The length of the tail block must be long enough to impart a repulsive force that overcomes the attractions of the colloidal particles, as will be discussed in Section 2.2.

2.1.2.2 Triblock Copolymers

The adsorption behavior of three commonly used stabilizers, Pluronics™, Meroxapols™, and Ucons™ have been studied on polystyrene latex (PSL) in water[35]. The Pluronics polymer is a triblock, consisting of two PEO blocks surrounding a PPO block in the middle, while the Meroxapols has the PEO block in between two PPO blocks. The structure of the Ucons is debated. It has been reported to be similar to that of Pluronics, except that the two PEO blocks have different molecular weights, or it is a random copolymer of PEO and PPO. DLS was used to determine the hydrodynamic layer thickness of the adsorbed polymers. The Pluronics had a very thick layer with the PEO chains extending into solution, as expected because the PPO adsorbs on PSL due to poor

[34] Leermakers, F.A.M.; Gast, A.P. *Macromolecules* **1991**, *24*, 718.

[35] Baker, J.A.; Berg, J.C. *Langmuir* **1988**, *4*, 1055.

solubility in water. The Meroxapols and the Ucons showed similar trends in layer thickness, but was about half the value obtained for the Pluronics. For the Meroxapols this is expected because the PPO blocks will be adsorbed on the surface and the PEO will be trapped in between the two, in loops and trains. The authors hypothesize that the Ucons are random copolymers because of their small layer thickness compared to the Pluronics.

The adsorption of Pluronics has also been studied on hydrophilic silica in water[36]. An interesting effect here is that PEO adsorbs on this surface, while PPO does not. The adsorption was characterized using the solution depletion method, ellipsometry, and DLS. The experimental results were compared to the adsorption behavior of PEO and PPO homopolymers, and model calculations. The results showed very low adsorbed amounts for the copolymer, similar to values obtained for the homopolymer PEO, and the layer thickness was also very small. As discussed earlier, PEO will desorb from silica when the pH is increased, and this phenomena occurred for this system also. This confirms that the two PEO blocks are adsorbing on the surface, while the PPO is caught at both ends, and so does not extend out far into the solution. A final observation was that upon micellization the adsorbed amounts increased while the layer thickness remained small. This dependence on micelles was not seen on hydrophobic surfaces, which have high values of adsorbed amounts and layer thicknesses.

2.1.2.3 Charged Block Copolymers

Block copolymers have also been designed that have one or more charged blocks. In polar solvents, such as water and isopropanol, there is now the addition of electrostatic forces contributing to adsorption and possibly stabilization. One possible advantage for a charged block copolymer would be using the charged block as the anchor, because there would be strong attractive forces contributing to adsorption. If an uncharged tail block were used, then the resulting block copolymer could be an effective steric stabilizer.

---

[36] Malmsten, M.; Linse, P.; Cosgrove, T. *Macromolecules* **1992**, *25*, 2474.

2.1.2.3.1 Charged Anchor-Uncharged Tail

One example of this class of copolymer is the diblock consisting of dimethyl amino methacrylate (DMAEM) and n-butyl methacrylate (BMA) in 2-propanol[37]. Both of the blocks are soluble in the solvent, but only the positively charged DMAEM will adsorb on silica. The solution depletion method with thermal gravimetric analysis and DLS were used to characterize the adsorption of the block copolymers on nearly monodisperse silica particles. A series of copolymers were studied over a range of molecular weights of the anchor and tail blocks. The results showed that when keeping a constant total number of repeat units, but increasing the mole fraction of anchor units, there was a maximum in the layer thickness. This maximum occurred at about 5 mole % anchor groups which is slightly less than the value predicted by the self-consistent field theory using a lattice model of 10-15 mole %, but the same value as predicted by the MJ theory. The differences from the SCF theory were attributed to polydispersity, which is not accounted for in the theory.

Another group of researchers studied poly(vinyloxy-4-butyric acid) (PVOBA) as the anchor block and PVME as the tail to adsorb onto α-Fe_2O_3 in water[38]. The solution depletion method was used along with DLS in order to determine the adsorbed amount and the hydrodynamic layer thickness. ζ-potential measurements were also take to determine the electrophoretic mobility of Fe_2O_3 particles (diameter of 65-70 nm) with adsorbed copolymer. Concurrently, the adsorption behavior of both of the homopolymers were also studied. The PVOBA adsorbed reasonably well, comparable to typical polyelectrolyte results, while the PVME adsorbed very little on the substrate. It was found that as the tail block molecular weight was increased the adsorbed amount and the layer thickness increased, until surface density began to decrease, which limited the extent of stretching and thus thickness. The maximum adsorbed amount and layer thickness was at 6.5 %mole anchor block, very close to the value determined by the MJ

[37] Wu, D.T.; Yokoyama, A.; Setterquist, R.L. *Polymer Journal* **1991**, *23*, 709.

[38] de Laat, A.W.M.; Schoo, H.F.M. *Journal of Colloid and Interface Science* **1997**, *191*, 416.

theory. In general the adsorption values were low for a block copolymer, due to the electrostatic repulsion between anchor blocks. At low salt concentrations it was found that all polymers containing PVOBA, including the homopolymer, stabilized the particles in suspension. This was due to electrostatic stabilization from the anchor block. At high ionic strength, where $\kappa^{-1} < \delta$ and electrostatic effects are screened, stability was found to be insensitive to further increases in ionic strength, which implied steric stabilization. Only those block copolymers with long (greater than 400 repeat units) tail blocks stabilized the suspension.

The diblock copolymer of dihydroxypropyl methacrylate (HMA), which is neutral, and dimethylaminoethyl methacrylate (AMA), which is positive, was studied in water on TiO_2 and SiO_2.[39] The adsorption was measured using reflectometry with a stagnation point flow cell at various ionic strengths, pH, and block length ratio. The copolymer was synthesized via anionic polymerization, and was considered to be fairly monodisperse. The adsorption was complicated because not only was the AMA charge a function of pH, but the charge on the surface was also a function of pH. Both blocks in the copolymer can adsorb on the surface, but the AMA will more strongly adsorb, at pH > IEP of the oxide, due to electrostatic attraction. The adsorption was a complicated function of pH and ionic strength, with both charge compensation and charge screening affecting the results. The adsorbed amount increased with decreasing AMA anchor block, until a maximum was reached at around 10% AMA. At low Γ it is believed that both blocks adsorbed on the surface in a flat conformation. As the adsorption was increased, the HMA forms more loops and tails, while the AMA stays on the surface.

The adsorption of a block copolymer consisting of PSS and PVP on a positively charged modified PSL has been studied in water[40]. DLS was used to measure the hydrodynamic layer thickness, and the adsorbed amount was measured using the solution depletion method with radio-actively labeled PVP employed to detect the polymer in solution. The

[39] Hoogeveen, N.G.; Cohen Stuart, M.A.; Fleer, G.J. *Faraday Discussions* **1994**, *98*, 161.

[40] Ouali, L.; Pefferkorn, E. *Macromolecules* **1996**, *29*, 686.

adsorption of the PSS on the charged surface was promoted by hydrophobic effects and the electrostatic attraction. Thick layers of adsorbed polymer were found in a range of pH from 2.5-3.8. One unexpected result was that the layer thickness increased with increasing ionic strength, which would lead to screening of the electrostatic attraction between the surface and the PSS, possibly due to poor solubility at high salt concentrations.

2.1.3 Random Copolymers

Random or statistical copolymers presents another way to incorporate the characteristics of two different polymers into one. The adsorption of random copolymers is particularly interesting, if one segment is adsorbing (A) and the other is non-adsorbing (B). Now, not only is the chain length, and ratio of adsorbing blocks important, but also the distribution and polydispersity of the different blocks within the chains. Segments which are richer in A will be closer to the surface, and shorter chains which have a higher A content may preferentially adsorb over longer chains. This is in contrast to homopolymers, where the longer chains dominate adsorption. For random copolymers the composition of the chains is more important for adsorption than the chain length. The solvent can also play a significant role, similar to block copolymers in selective solvents, where a poor solvent for A can cause multi-layer adsorption due to association of the chains, as shown in Figure 2.19.

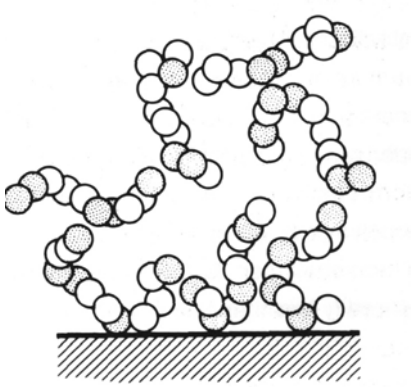

Figure 2.19: Multi-layer adsorption due to association of A groups in a poor solvent[1].

The adsorbed amount of random copolymers is usually less than that for a homopolymer of the adsorbing block, due to the non-adsorbing B segments. The bound fraction of both the total segments and A segments will decrease with increasing adsorption, because of fewer trains present. Also, as shown in Figure 2.20, the bound fraction will increase as the copolymer becomes richer in A groups, but the layer thickness will show a corresponding decrease.

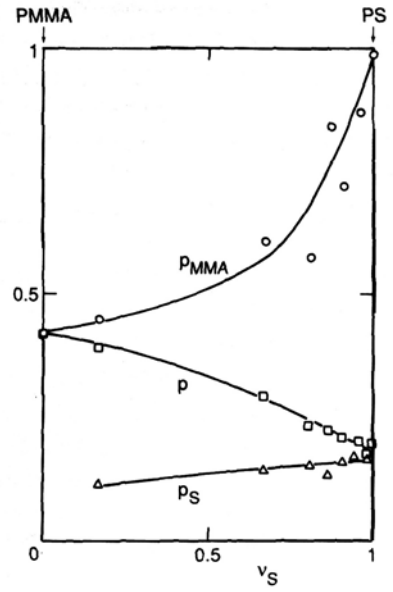

Figure 2.20: The total bound fraction p and the partial bound fraction p_{MMA} and p_S as a function of styrene content for the adsorption of random copolymers of methyl methacrylate (MMA) and styrene (S) on silica[41].

The adsorption of a random copolymer consisting of ethylene and vinyl acetate on modified silica surfaces from carbon tetrachloride has been studied[42]. The two surfaces were methylated and cyclohexylated, which are models for the methyl and methylene surfaces of a paraffin crystal. The adsorption was characterized using NMR to determine the bound fraction and the adsorption isotherm, and SANS to ascertain the segment density profile. Two model homopolymers were also studied to compare to the random

[41] Kobayashi, K.; Araki, K.; Imamura, Y.; Endo, R. *Bulletin of the Chemical Society Japan* **1990**, *63*, 511.

[42] Cosgrove, T.; Finch, N.; Vincent, B.; Webster, J. *Colloids and Surfaces* **1988**, *31*, 33.

copolymer, poly(vinyl acetate) (PVAc) and a low molecular weight paraffin, hexatriacontane, for polyethylene.

The PVAc had a low affinity type isotherm, which was attributed to the low molecular weight and the polydispersity of the sample. Both species showed a stronger affinity for the methylated surface. The random copolymer also showed a low affinity isotherm, due to polydispersity of the chain length and the composition, with higher pseudo-plateau adsorption on the methylated surface. From the SANS results, there was a rapid drop in chains with distance from the cyclohexyl surface, but more extended tails existed on the methyl surface. So, while the adsorbed layer thickness was greater for the methylated surface, the bound fraction was greater for the cyclohexylated surface.

A random copolymer with one group being charged has also been studied. A partially hydrolyzed poly(vinyl alcohol) (PVA) was studied as a copolymer containing random carboxylate groups throughout the chain[43]. For comparison, homopolymers of PVA and poly(acrylic acid) (PAA) and block copolymers of the two were also studied. The adsorption was done in an aqueous system with $BaTiO_3$, which has a positive net surface charge at the pH range studied here (8.2-8.8). Size exclusion chromatography (SEC) was used to test the samples prior to adsorption and also the supernatants after adsorption. In this manner, not only could the adsorption isotherm be determined, but also the molecular weight of the bound polymer.

The adsorption plateau for the random copolymer was about twice that of the PVA, while the block copolymer had three times the adsorbed amount than the random. It was also found that the adsorption of longer chains increased, until the plateau was reached, at which time the molecular weight of the adsorbed polymer remained constant. The only random copolymer that was able to produce a stable dispersion was that with the highest amount of carboxylate groups, which had the highest bound fraction of polymer. Thus,

[43] de Laat, A.W.M.; de Bruijn, A.W.; van der Heuvel, G.L.T. *Colloids and Surfaces A: Physiochemical and Engineering Aspects* **1994**, *82*, 99.

the surface affinity plays a stronger role in adsorption than molecular weight, but there is still preferential adsorption of longer chains.

2.1.4 Biologically Derived Polymers

The adsorption of model proteins or poly(amino acid) homopolymers has been of little interest to the biological community. Most of the research in the area of protein adsorption has been done with very complex proteins, that typically possess tertiary or quaternary structures, for the purpose of understanding the cell deposition on bioimplant materials. This section will start with a review of the relatively little work that has been done on the adsorption of poly(amino acid) homopolymers and then will review work on copolymers of poly(amino acid)s with other macromolecules, such as polyethylene oxide (PEO). The final section will give a very brief overview of the adsorption structure of more complex protein, specifically on alumina and other metal oxides, since there is a wealth of such information.

2.1.4.1 Poly(amino acid) Homopolymers

The adsorption of poly-L-(glutamic acid) (GLU) and poly-L-lysine (PLL) on hydrophilic and hydrophobic silica in water has been studied[44]. The PLL has a pK_a of 10.45, and is positively charged at pH < 9.5 and uncharged at pH > 11.5. The structure of the PLL is dominated by not only the pH dependence, but also the temperature. At low pH and T < 50°C the PLL forms an extended helix, but at T > 50°C it is in the form of a random coil. At pH > 11.5 the PLL forms a helix, but at even higher pH it is an insoluble β-sheet. The GLU is negatively charged and has a pK_a of 4-5.5. Above this pH the charge is dependent on the electrolyte concentration and the polymer forms a random coil. At low pH the GLU is in the form of an α-helix, and is insoluble below pH 3.

The adsorption of the polymers was studied using FTIR-ATR (attenuated total reflection). The PLL showed a high affinity type behavior on both substrates, with a Γ_{max}

[44] Killmann, E.; Reiner, M. *Tenside, Surfactant, and Detergent* **1996**, *33*, 220.

at pH 11. It had a higher adsorption affinity for the hydrophilic silica, as expected because of electrostatic interactions. At low ionic strength the molecular weight had little effect on the adsorbed amount, but at higher ionic strength there was a molecular weight dependence. This was due to charge screening at high salt concentrations and an increase in the number of loops and tails. The GLU did not show a high affinity type adsorption behavior, and much longer times were needed to achieve equilibrium. The maximum adsorption was at pH 3, just prior to insolubility, and no adsorption was observed at pH > 7. On the hydrophobic silica there was an increase in adsorbed amount with increasing ionic strength, similar to the PLL on the hydrophilic silica. When the polymer was highly charged it adsorbed in a very flat conformation with low adsorbed amount. As the charge was screened with increasing ionic strength, more loops and tails were formed and the adsorption increased.

Similar results for PLL adsorption on PSL were seen by another research group[45]. Specifically, as the molecular weight of the PLL was increased from a monomer to a polymer, the adsorption changed from a Langmuir type to a high-affinity type, and the pseudo-plateau adsorption value increased. The work also showed that the adsorbed amount increased more strongly with increasing ionic strength as the molecular weight was increased. Finally, the adsorbed amount increased as the pH was increased.

The adsorption and stabilization of PLL on negatively charged PSL has also been studied[46]. These researchers found no effect of molecular weight on the adsorbed amount at pH 4, and little change when the ionic strength was increased and the pH held at 4. At pH 11 the adsorbed amount was proportional to $Mw^{0.74}$, and there was less precipitation of the polymer at high salt concentration than at low ionic strength, due to better solvent quality. At high pH it was hypothesized that the helices are in an end-on formation on the surface, allowing for an increased adsorbed amount. The measured value for the

[45] Bonekamp, B.C.; van der Schee, H.A.; Lyklema, J. *Croatic Chemica Acta* **1983**, *56*, 695.

[46] Furusawa, K.; Kanesaka, M.; Yamashita, S. *Journal of Colloid and Interface Science* **1984**, *99*, 341.

layer thickness, assuming this conformation of the helix, was much less than the theoretical layer thickness calculation, perhaps due to a lower apparent surface pH than in the bulk. At pH 4 there was no steric stabilization, due to charge reversal at the surface, and a very narrow added polymer concentration range for flocculation. At pH 11 the results were very different, with a large added polymer concentration range for flocculation, and stabilization at a concentration greater than 0.7 mg/ml.

The adsorption and surface conformation of PLL on negatively charge PSL has also been studied by Bonekamp[47]. For comparison, poly-DL-lysine (PLDL) was also studied, which has no helical character. Very similar results were found for both polymers, indicating that the helical content does not effect the adsorbed amount. Using potentiometric titration, the adsorption of PLL, PLDL, GLU, and polymethacrylic acid were studied on both positively and negatively charged PSL. The polymers were studied by adsorbing at different pH and then changing the pH, to see if the adsorbed chain conformation changes with pH, or retains the same conformation as at the adsorbing pH. The results showed that only when the polymer and the surface have the same charge do conformational transitions occur, because when they have opposite charges the interactions between the two are too strong and the polymer conformation can not change.

The adsorption behavior of PLL on mica has also been studied using the Israelachvilli surface force apparatus[48]. Although there were similar surface potentials between the bare mica and the PLL covered mica, the researchers determined that the bare mica had a negative charge, while the PLL covered mica had a positive charge. So, although they have the same magnitude of force, the signs are different. This can be see from desorption experiments, where the potential for the desorbed mica samples was less than that of the uncovered or the PLL covered mica, which can only be caused by it being less positive than the PLL covered mica.

---

[47] Bonekamp, B.C. *Colloids and Surfaces* **1989**, *41*, 267.

[48] Afshar-Rad, T.; Bailey, A.I.; Luckham, P.F.; Macnaughtan, W.; Chapman, D. *Colloids and Surfaces* **1987**, *25*, 263.

The adsorption of poly(α-L-glutamic acid) (GLU) onto an inert cellulose acetate filter has also been studied by measuring the membrane characteristics[49]. The effect of the adsorption pH (4 or 8) on the hydrodynamic length, L_H, defined as the difference in the equivalent pore radius before and after adsorption, was measured. After adsorption the solution pH was varied, while monitoring the value of L_H. For adsorption at a low pH (4), the hydrodynamic length initially showed a slight increase with increasing pH, but then showed a marked decrease at pH 7. When the pH was then lowered, the value of L_H decreased even more. This irreversibility of the adsorbed layer was attributed to weak interactions between the rigid, helical structure and the surface and the lack of hydrogen bonding, which allowed desorption to occur at more alkaline conditions. When the adsorption occured at a high pH (8), the change in L_H with decreasing pH had a sigmoidal shape, with a sharp decrease from pH 7 to 5. The shape of the curve was reversible when the pH was increased, showing the strong hydrogen bonding adsorption. This result is very different from that of a typical weak polyacid, which shows the L_H leveling off above a certain pH. The difference is due to the secondary structure of the GLU polymer. At pH 8 it adsorbed in a random coil conformation, but as the pH is decreased there was a transition to a helical structure.

2.1.4.2 Poly(amino acid) Copolymers

The adsorption behavior of two copolymers containing amino acids on positively and negatively charged PSL have been studied[50]. One polymer was a tetramer of L-lysine, L-glutamyl, and L-glycine, $(LYS\text{-}GLU\text{-}GLY)_4$ and the other was a random copolymer containing 60 % D-glutamic acid and 40% D-lysine. The adsorption was measured as a function of pH and ionic strength.

---

[49] Pefferkorn, E.; Schmitt, A.; Varoqui, R. *Biopolymers* **1982**, *21*, 1451.

[50] Blaakmeer, J.; Cohen Stuart, M.A.; Fleer, G.J. *Journal of Colloid and Interface Science* **1990**, *140*, 314.

The tetramer had a fairly low affinity for the negative latex and the maximum adsorption occurred at pH 4. At higher pH the polymer becomes more negatively charged and there was repulsion with the surface. There was little effect of ionic strength on the adsorption. On the positively charged latex the tetramer had a much higher adsorbed amount, with a maximum at pH 9.5, but the results had poor reproducibility.

The random copolymer had a much higher affinity for the negative latex than the tetramer. The effect of pH was very interesting for this polymer since the pK_a for the GLU is 4 and that for the LYS is 11. The copolymer had a positive charge below pH 3, and had a small negative charge in the pH range 6-8.5. Above pH 11 the copolymer had a strong negative charge. It was expected that the adsorption at pH 4 on the negative latex should be equivalent to the adsorption at pH 9.7 on the positive latex, but the adsorption on the negative latex was twice that on the positive latex. The authors concluded that the GLU intramolecular repulsion at pH 9.7 was greater than the LYS intramolecular repulsion at pH 4, due to the longer length of the LYS side chains, i.e. the greater distance between the amine function and the backbone chain.

A comb-like copolymer containing a PLL backbone with PEG side chains has also been studied[51]. The adsorption of the copolymer on TiO_2, $Si_{0.4}Ti_{0.6}O_2$, and Nb_2O_5 was measured while varying the pH, ionic strength, and the length and number of side PEG chains. The subsequent adsorption of human serum albumin (HSA) and human fibrinogen was measured to determine if the adsorbed copolymer could inhibit adsorption. For a constant polymer architecture and molecular weight the maximum adsorbed amount increased with decreasing IEP of the metal oxide. There was also a maximum in the adsorbed amount with pH, which was different for each metal oxide. The authors were able to show a direct correlation in the adsorbed amount of both the HSA and the fibrinogen with the pre-adsorption of the graft copolymer. There was very little adsorption of the proteins when there was a large adsorbed amount of the copolymer.

[51] Kenauis, G.L.; Voros, J.; Elbert, D.L.; Huang, N.; Hofer, R.; Ruiz-Taylor, L.; Textor, M.; Hubbell, J.A.; Spencer, N.D. *Journal of Physical Chemistry B* **2000**, *104*, 3298.

2.1.4.3 Proteins

Proteins are very complex copolymers, consisting of combinations of the twenty naturally occurring primary amino acids, and their derivatives. The sequence of these amino acids is the primary structure of the protein. The peptide bonds that make up the backbone of the protein can also interact with each other through hydrogen bonding, causing the formation of helices and sheets, or secondary structures. Proteins can also have tertiary structures, resulting from interactions between side chains, such as disulfide bonds between methionine.

Due to these structural aspects, the adsorption of proteins is thus even more complicated than its synthetic synthetic polymer counterparts. Proteins are complex polyelectrolytes that generally contain, in a single chain, groups that are anionic, cationic, neutral, and hydrophobic. All of this is further complicated by the fact that some proteins will change their structure, secondary, tertiary, or quaternary during adsorption, depending on the surface and the solution conditions.

2.1.4.3.1 Adsorption Driving Forces

Two of the most important driving forces for protein adsorption are electrostatic and hydrophobic interactions. Although these types of interactions usually determine whether a protein will adsorb on a surface, there are many weaker forces which can become important. Numerous studies have been done to determine how a certain protein will adsorb on a specific surface, under particular solution conditions. It is the goal of this review to mention a few of the most important studies, in order to get a grasp of the complexity of protein adsorption.

The adsorption of two monoclonal immuno gamma globulins (IgGs) and their corresponding $F(ab')_2$ fragments onto positively and negatively charged hydrophobic

polystyrene latices and negatively charged hydrophilic latex was studied[52]. The authors used adsorption and electrophoresis measurements to distinguish between the hydrophobic effects and the electrostatic effects. On the hydrophobic surfaces there was little effect due to electrostatics. Even when the protein and surface had the same charge there was significant adsorption. The electrostatics did have an effect on the maximum adsorbed amount. This maximum occurred at a pH between the IEP of the protein and the IEP of the protein-latex complex. Calculations suggested the protein had an "end-on" orientation with respect to the surface. In contrast, the electrostatics dominated the adsorption onto the hydrophilic surface, with no adsorption occurring when the charges were the same. On the hydrophilic surface the protein was calculated to have a "side-on" orientation, i.e. the protein lay flat on the surface. This work demonstrated that the hydrophobic effects were most important, and that the protein will always adsorb on a hydrophobic surface, even if electrostatic repulsion is strong. By contrast, on the hydrophilic surface, the protein behaved like a typical polyelectrolyte, with strong adsorption in a flat conformation when the attractions were strong, and no adsorption where there was repulsion between the surface and protein.

The adsorption of four different proteins - ribonuclease, lysozyme, myoglobin, and α-lactalbumin has been studied on positive and negative polystyrene latices, and on polyoxymethylene (POM) and hematite[53]. This paper probed how the structural stability of the protein effected the adsorption. For the proteins with a high stability that did not readily denature (lysozyme and ribonuclease) hydrophobic and electrostatic effects were most important as discussed in the previous study. For the proteins with a low structural stability (myoglobin and α-lactalbumin) there was much stronger adsorption. This increase was attributed to structural rearrangements, which increase the conformational entropy of the protein. There was even evidence of adsorption on a hydrophilic surface, under electrostatic repulsion, not seen for the stable proteins. This paper stresses the

[52] Bruijs, J.; Lichtenbelt, J.W.Th.; Norde, W.; Lykelma, J. *Colloids and Surfaces B: Biointerfaces* **1995**, 5, 11.

[53] Arai, T.; Norde, W. *Colloids and Surfaces* **1990***, 51*, 1.

importance of the protein structure on adsorption. Namely, that the adsorption was greater when the protein was more flexible and had greater rotational mobility, or less α-helix and β-sheet content. From this it would seem that a flexible protein anchor block would be favorable for strong adsorption.

2.1.4.3.2 Conformational Change Due to Adsorption

It is well known that proteins can undergo conformational changes due to the adsorption on a surface. Historically, it has been difficult to probe the structure of a protein adsorbed on a surface, due to interference with the surface, and most studies have looked at the structure before adsorption and after desorption[54]. This gives only indirect information about the adsorbed conformation, because the protein may change its conformation again during desorption. More recent studies have used circular dichroism (CD) with very fine particles to determine the helix content of an adsorbed protein.

In one study the change in conformation of several proteins upon adsorption on ultra fine silica was studied[55]. The adsorbed amount and the α-helix content, via CD, were measured as function of pH. As expected, the more flexible proteins (bovine serum albumin and hemoglobin) showed the largest change in conformation, with a decrease in α-helix content upon adsorption. While the smaller, stiffer proteins (cytochrome c and ribonuclease A) showed little change in conformation with adsorption. There was also a greater change in the conformation when the protein had a higher affinity for the surface. All of the proteins showed a maximum in adsorbed amount as function of pH, with the maximum occurring near the IEP of the protein. The flexible proteins had a larger maximum value for adsorbed amount than the stiffer proteins. This maximum adsorbed amount was greater for the flexible proteins than for the stiffer proteins.

---

[54] Oscarsson, S. *Journal of Chromatography B* **1997**, *699*, 117.

[55] Kondo, A.; Oku, S.; Higashitani, K. *Journal of Colloid and Interface Science* **1991**, *143*, 214.

Another study monitored the adsorption and desorption of fibrinogen ($pK_a = 5.8$) on hydroxyapatite (HA) and on very fine TiO_2 particles[56]. CD spectroscopy was used to determine the structure of the protein before adsorption and after desorption for both surfaces, but only on the TiO_2 could the conformation of the adsorbed protein be studied. There was a marked decrease in the α-helix content from the native protein structure to the desorbed protein. With the TiO_2 experiments, it was shown that the helix content decreased slightly upon adsorption, and decreased more with successive desorption. Thus, the protein did not return to its native conformation upon desorption. When a higher ionic strength buffer was used, there was a greater change in the conformation. There was also a greater effect when the surface charge density of the TiO_2 particles became increasingly negative, by increasing pH, even though the fibrinogen had a net negative charge. The authors attribute the adsorption to local charges that are positive. Both of these results suggest that the electrostatic effects was the main interaction between the fibrinogen and TiO_2.

2.1.4.3.3 Combinatorial Library Search

The use of biological materials that strongly bind to specific substrates presents a new opportunity in material science. If a peptide sequence could be identified that has a high affinity for a surface, then that peptide could be biologically synthesized. This peptide sequence could then be used as an anchor block in block copolymers, which would have superior properties to synthetic polymers, which are incapable of such specific recognition chemistry. Additionally, every peptide chain would have the exact same sequence and number of amino acids.

A random peptide combinatorial library search is often used in biological applications to identify peptide sequences that show specific binding to an antibody, receptor or other binding protein[57]. This technique involves using a combinatorial library of different

[56] Yongli, C.; Xiufang, Z.; Yandao, G.; Nanming, Z.; Tingying, Z.; Xinqi, S. *Journal of Colloid and Interface Science* **1999**, *214*, 38.

[57] Scott, J.K.; Smith, G.P. *Science* **1990**, *249*, 386.

random peptides of a certain length, each with a different sequence. Thus, tens of millions of different peptides can be tested simultaneously. For example, the different peptide sequences are inserted into the DNA of the flagella of the *E. Coli* and are exposed to the solvent. Thus, when the cells are contacted with a surface, only those containing peptide sequences that bind to the surface will adhere, and the others will be eluted away. The bound *E. Coli* are then removed by shearing and incubated to grow new cells. This process, called panning, can be repeated several times under different conditions in order to find those peptides that show the highest affinity for the surface. The DNA sequence is then determined from those cells which showed strong binding and the amino acids in the peptides are identified.[58,59]

One group has used a similar technique to identify those peptides, containing 12 amino acids, that bound to a specific crystalline surface of several semiconductor materials[60]. A phage-display library was used instead of the direct *E. Coli* method, which adds several steps to the panning process. It was found that with successive purification, there was increased adhesion to GaAs when the number of polar groups and Lewis base groups in the peptide sequence were increased. It is believed that the Lewis base groups in the peptide may interact with the Lewis acid groups on the surface, causing specific binding. This technique was also able to show that those peptides that had a high affinity for a GaAs(100) surface, showed less binding to a GaAs(111) surface, and no binding at all to a Si(100) surface. Thus, not only were the authors able to show an affinity for different materials, but also for different crystal surfaces of the same material.

The flagella display technique[59] has several advantages over the phage display method used in the study cited above. Specifically, *E. Coli* are inexpensive and easy to grow, and there are no phages involved, which removes a step to each iteration. Secondly, the

---

[58] www.invitrogen.com

[59] Westerlund-Wikstrom, B. *International Journal of Medical Microbiology* **2000**, *290*, 223.

[60] Whaley, S.R.; English, D.S.; Hu, E.L.; Barbara, P.F.; Belcher, A.M. *Nature* **2000**, *405*, 665.

peptides are displayed in a constrained conformation in the flagella, to allow maximum interaction of the peptide sequence with the surface. Finally, the binding peptides can be directly identified, and expressed at high concentrations.

2.1.5 Surface Techniques for Analyzing Adsorbed Polymer

As shown from the above discussion many different techniques have been used to quantify and characterize the adsorption of polymers. This section will give a brief over view of some of the surface analysis methods, and the advantages and disadvantages of using each. The techniques discussed will be: FTIR-ATR, SPR, OWLS, QCM, SAR, and ellipsometry.

2.1.5.1 FTIR-ATR

Fourier transform infrared (FTIR) spectroscopy is frequently used to characterize the conformation of proteins in solution[61]. The use of attenuated total internal reflection (ATR) can be used to determine the adsorbed amount of a protein on a surface. The question remains whether FTIR-ATR can be used to observe changes in the protein secondary structure upon adsorption.

2.1.5.1.1 Basic Principles

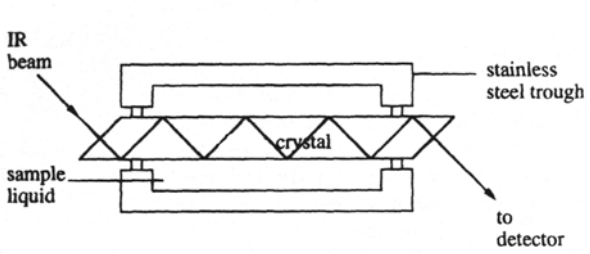

Figure 2.21: Schematic view of ATR spectroscopy sample cell[61].

[61] Ball, A.; Jones, R.A.L. *Langmuir* **1995**, *11*, 3542.

In FTIR-ATR an infrared beam is passed through an ATR crystal, as shown in Figure 2.21, typically germanium, at an angle greater than the critical angle, so that the light will be totally internally reflected in the crystal[62]. At each reflection energy is lost in the form of an evanescent wave. Proteins present in the solution will adsorb to the ATR crystal. The absorbance spectra is then obtained from the loss of this energy by the adsorbing material. The adsorbed amount can then be calculated from the following equation:

$$\Gamma = \frac{A/N - \varepsilon C_b d_e}{1000\varepsilon\left(2\,d_e/d_p\right)} \qquad \text{Equation 2.55}$$

where Γ is in units of mol/cm^2, A/N is the absorbance per reflection measured by the FTIR, and ε is the integrated molar absorptivity obtained by transmission experiments. The parameter, d_e, is the effective thickness and is defined as the thickness of adsorbed material which will give the same absorbance in transmission spectra at normal incidence as that from ATR, and is given as:

$$d_e = \frac{n_{21} E_o^2 d_p}{2\cos\theta} \qquad \text{Equation 2.56}$$

where n_{21} is the ratio of the refractive index of the solution to that of the ATR crystal, E_0 is the incident evanescent electric field, and θ is the angle that the infrared light hits the ATR crystal. The depth of penetration, d_p, is a measure of how deep the experiment probes the protein solution:

$$d_p = \frac{\lambda}{2\pi n_1 \sqrt{\left(\sin^2\theta - n_{21}^2\right)}} \qquad \text{Equation 2.57}$$

where λ is the wavelength of light, and n_1 is the refractive index of the ATR crystal.

2.1.5.1.2 Advantages and Disadvantages

One of the primary limitations for FTIR-ATR is the choice of substrate. The best material for an ATR crystal is germanium used with an incident angle of 45^o. This

[62] Chittur, K.K. *Biomaterials* **1998**, *19*, 357.

material maximizes the signal from the surface, while minimizing the signal from the bulk solution, which are both desirable. Polymers can be spin coated onto the crystal surface to measure protein-polymer interactions, but there are difficulties when trying to use metal-coated crystals[62]. One author used a silicon crystal to measure the adsorption of lysozyme[61].

Another limitation is the absorbance signal from water that overlaps the amide I band from the protein. It can be very difficult to subtract of the large water peak from the much weaker amide peak, but several techniques have been used to overcome this obstacle[62]. Another option is to use D_2O as the solvent instead of water[61]. FTIR-ATR can not differentiate between different types proteins, since the amide bonds in the backbone of the protein are the primary source of absorbance information.

One of the most significant advantages that FTIR-ATR has over other surface techniques is the possibility to observe changes in the conformation of the protein. In order to do this detailed information about the relationship between the spectra and the structure is needed. Although several authors have reported studies where the change in the secondary structure of proteins were monitored with FTIR-ATR[61,62,63], the analysis can be very ambiguous, especially for high molecular weight proteins.

2.1.5.2 SPR

Surface plasmon resonance (SPR) or surface plasmon oscillations (SPO) is another optical technique which can be used to probe adsorption on a surface. This technique has found many applications in the biotechnology field, including biosensors and immunosensors[64]. This discussion will focus on the use of SPR to determine adsorbed amounts, adsorption kinetics, and adsorbed layer thickness.

---

[63] Chittur, K.K.; Fink, D.J.; Leininger, R.I.; Hutson, T.B. *Journal of Colloid and Interface Science* **1986**, *111*, 419.

[64] Homola, J.; Yee, S.S.; Gauglitz, G. *Sensors and Actuators B* **1999**, *54*, 3.

2.1.5.2.1 Basic Principles

SPR occurs when there is a charge-density oscillation at an interface between two media, which have dielectric constants of opposite signs. The excitation of surface plasmons will not occur at all wavelengths, because the dielectric permitivity of a material is a function of the wavelength. For the infrared to visible range, metals have a negative dielectric constant, while that for a dielectric media, such as water, is positive. Metals which have been used for SPR measurements include: gold, silver, copper, and aluminum; although gold and silver are the most commonly used[65].

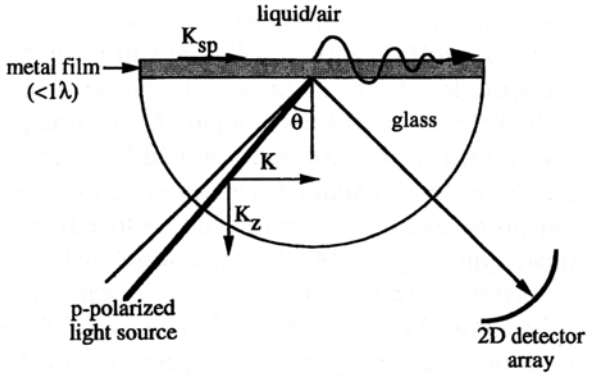

Figure 2.22: The Kretchmann configuration for SPR[65].

The Kretshmann configuration is typically used for SPR experiments. This involves using a prism with a high refractive index, as shown in Figure 2.22. A monochromatic, p-polarized light is sent through the prism, which is coated with a thin layer of metal. The surface plasmons undergo excitation when the wave vector for the evanescent field from the light source, K_x, and the wave vector for the surface plasmon, K_{sp}, are equal:

[65] Green, R.J.; Frazier, R.A.; Shakesheff, K.M.; Davies, M.C.; Roberts, C.J.; Tendler, S.J.B. *Biomaterials* **2000***, 21*, 1823.

$$K_x = \left(\frac{\omega}{c}\right) n_2 \sin\theta \qquad \text{Equation 2.58}$$

$$K_{SP} = \left(\frac{\omega}{c}\right)\left[\frac{\varepsilon_1\varepsilon_3}{(\varepsilon_1+\varepsilon_3)}\right]^{1/2} \qquad \text{Equation 2.59}$$

where, ω is the frequency of the incident light, c is the speed of light in a vacuum, n_2 is the refractive index of the prism, θ is the incident angle of light, ε_1 is the dielectric constant of the metal, and ε_3 is the dielectric constant of the dielectric media. This will occur at a specific angle of incident, where $\theta = \theta_{SPR}$[66]. The incident angle is labeled θ in Figure 2.22 when the angle is internal, and ϕ, if the angle is referenced externally, such that $\theta + \phi = 180^o$.

The measured reflectivity, R, reaches a minimum at θ_{SPR}. Close to this angle the reflectivity can be expressed as:

$$R(\theta) = 1 - \frac{4\,\mathrm{Im}(K_{SP})\,\mathrm{Im}(K^R)}{[K_x - \mathrm{Re}(K)]^2 + [\mathrm{Im}(K)]^2} \qquad \text{Equation 2.60}$$

where $K = K_{SP} + K^R + K^T$ and

$$K^R = \left(\frac{\omega}{c}\right) r_{21}\left(\frac{2}{\varepsilon_3-\varepsilon_1}\right)\left(\frac{\varepsilon_1\varepsilon_3}{\varepsilon_1+\varepsilon_3}\right)^{3/2} \exp\left(\frac{i4\pi d_1}{\lambda}\frac{\varepsilon_1}{(\varepsilon_1+\varepsilon_3)^{1/2}}\right) \qquad \text{Equation 2.61}$$

and

$$K^T = \frac{2\pi}{\lambda}\left(\frac{\omega}{c}\right)\left(\frac{\varepsilon_1\varepsilon_3}{\varepsilon_1+\varepsilon_3}\right)^2 \frac{(\varepsilon_4-\varepsilon_1)(\varepsilon_4-\varepsilon_3)}{(|\varepsilon_1|\varepsilon_3)^{1/2}(\varepsilon_3-\varepsilon_1)\varepsilon_4} d_4 \qquad \text{Equation 2.62}$$

where, r_{21} is the Fresnel coefficient between the prism and the metal, which is a function of the prism material, metal and the angle of incidence, as given in Equation 2.80, λ is the wavelength of light, d_1 is the thickness of the metal, ε_4 is the dielectric constant of the adsorbed layer and d_4 is the thickness of the adsorbed layer. It is the measurement of R(θ), as shown in Figure 2.23, and specifically, the measurement of the shift due to an adsorbed layer, the half-width of the reflectivity dip and the value of R at the minimum, which is used to characterize the adsorbed layer.

[66] Zhang, Y.; Levy, Y.; Loulergue, J.C. *Surface Science* **1987**, *184*, 214.

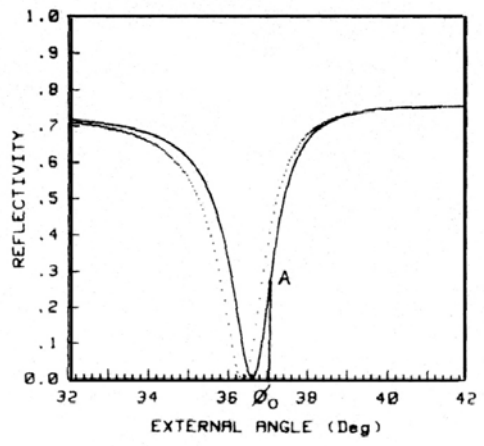

Figure 2.23: A typical angular shift of the reflectivity peak versus the external incident angle. The solid curve is the experiment data for a metal-dielectric solution. The dotted curve is the experimental data for the same system, but with an adsorbed layer of polystyrene[65].

The surface excess adsorption is given by the Lorentz-Lorenz equation:

$$\Gamma = \frac{dC}{dn} d_4 \Delta n \qquad \text{Equation 2.63}$$

where dC/dn is the inverse refractive index increment, and $\Delta n = n_4 - n_3$. When the difference between the refractive index of the adsorbed layer and that of the solution is small, $\Delta n << 1$, and the adsorbed layer thickness is small compared to the wavelength of the light source, $d_4 << l$, then the above expression for K^T can be reduced to:

$$K^T = \frac{4\pi}{\lambda} \frac{\omega}{c} \frac{|\varepsilon_1|^{3/2} \varepsilon_3}{(\varepsilon_1 + \varepsilon_3)^2} d_4 \Delta n \qquad \text{Equation 2.64}$$

This expression is then related to the angular shift, $\Delta\phi$, of the minimum in the reflectivity due to adsorption by:

$$\Delta\phi = \frac{4\pi}{\lambda} \frac{\chi}{\cos\theta} \frac{\varepsilon_3 |\varepsilon_1|^{3/2}}{(\varepsilon_1 + \varepsilon_3)^2} d_4 \Delta n \qquad \text{Equation 2.65}$$

where:

$$\chi = -\left[n_2^2 - \cos(\alpha + \phi)\right]^{1/2} \left[\sin(\alpha + \phi)\right]^{-1} \qquad \text{Equation 2.66}$$

where, α is the angle of the prism.

In order to measure the kinetics of adsorption, the reflectivity is taken at a fixed angle, ϕ_o. The angle is chosen so that it falls in the linear part of the curve of R vs. θ, as shown in Figure 2.23, and thus the following expression may be used:

$$\Delta R = m\Delta\phi \qquad \text{Equation 2.67}$$

where, m is the slope of the curve at the angle ϕ_o. This leads to the final expression for the adsorbed amount:

$$\Gamma = \frac{\cos\theta}{\chi}\frac{dC}{dn}\frac{\lambda}{4\pi}\frac{\left(\varepsilon_1+\varepsilon_3\right)^2}{\varepsilon_3\left|\varepsilon_1\right|^{3/2}}\frac{\Delta R}{m} \qquad \text{Equation 2.68}$$

In practice, the R(θ) data is first taken in air to obtain values for ε_1 and d_1 of the thin metal film. Then the same measurement is done with the solution in order to obtain a value for n_3 and to fix the incident angle, ϕ_o. The reflectivity is then collected at this fixed angle over a period of time, in order to obtain kinetic data. Either periodically or at the end of the experiment, another run of R(θ) is taken to determine $d_4\Delta n$. SPR can not independently determine either d_4 and Δn, but if one is obtained from a different technique, then the other can easily be calculated.

2.1.5.2.2 Advantages and Disadvantages

One of the main disadvantages with SPR is in the choice of substrate. Metals are most commonly used because of their reflective properties, and most authors have used gold or silver. In order to obtain excellent optical properties, the metal must be deposited in a thin film on a prism, approximately 40-50 nm thick. The thickness of the metal layer is critical for obtaining maximum efficiency of the surface plasmon waves[67]. The metal surface can also be modified by self-assembled monolayers, lipid bilayers and spin coated polymer films[65], but in reference to the current work, specific crystal faces of metal oxides would not be possible.

[67] Silin, V.; Plant, A. *Trends in Biotechnology* **1997**, *15*, 353.

One advantage that SPR has over other optical methods, such as ellipsometry, is the very low detection limit. Adsorbed amounts less than 0.5 ng/cm^2 and thickness below 0.1 nm can be detected with this technique[67]. SPR is also ideal for determining the kinetics of rapid adsorption at very short times, because of the ability to extract data at constant angles of incident. The ability to extract thickness data for the adsorbed layer is also beneficial, but it must be coupled with another technique.

SPR has been effectively used to measure the kinetics of adsorption of polystyrene[66] and a block copolymer of polystyrene and poly(vinyl-2-pyridine)[68] onto silver. For the case of the block copolymer, the authors were able to distinguish between unimer adsorption, below the cmc, and micelle adsorption, above the cmc, during the initial stages of adsorption.

2.1.5.3 OWLS

Optical waveguide lightmode spectroscopy (OWLS) is another optical technique used to characterize adsorbed species. Much of the work with OWLS has been done in the biological field, particularly with respect to: protein-membrane interactions, protein arrays, biosensors, and biocompatibility[69].

2.1.5.3.1 Basic Principles

The main principle behind OWLS is the measurement of the phase shift of guided lightmodes, caused by the adsorption of species onto a waveguide[70]. As shown in Figure 2.24, a laser beam is passed through a glass support, S, which has a refractive index, n_S, at an incident angle α. The glass support is coated with an optical waveguide film, F, which has a refractive index of n_F and thickness t_F. The waveguide film has an optical

[68] Tassin, J.F.; Siemens, R.L.; Tang, W.T.; Hadziioannou, G.; Swalen, J.D.; Smith, B.A. *Journal of Physical Chemistry* **1989**, *93*, 2106.

[69] Ramsden, J.J. *Chimia* **1999**, *53*, 67.

[70] Bernard, A.; Bosshard, H.R. *European Journal of Biochemistry* **1995***, 230*, 416.

grating imprinted along the interface between the film and the support. A bulk solution of analyte, or polymer is introduced in the flow cell, which has a bulk concentration, C, and index of refraction, n_C. The analyte will adsorb onto the film from the bulk solution, with a refractive index, n_A, and thickness, t_A.

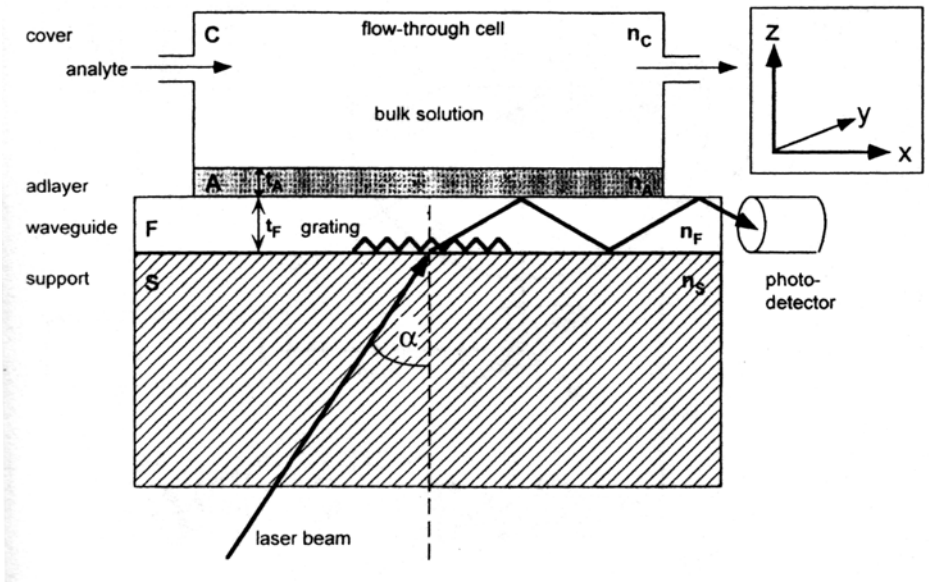

Figure 2.24: Schematic of typical OWLS instrumentation[70].

The light beam will be totally reflected between the F/S and F/A interface as long as the following is true:

$$N = n_{air} \sin\alpha + L\lambda/\Lambda \qquad \text{Equation 2.69}$$

where N is the effective refractive index of the excited guide mode for total internal reflection and is defined as the ratio of the velocity of light in a vacuum to that in the composite vaveguide structure, n_{air} is the refractive index of air, L is the order of diffraction, an integer, λ is the wavelength of light, and Λ is the line spacing of the optical grating. The parameter N is obtained by measuring the light intensity in air at various incident angles.

The adsorbed amount of analyte, Γ, can be calculated from the following equation:

$$\Gamma = \left({dn_C}/{dC} \right)^{-1} (n_A - n_C) t_A \qquad \text{Equation 2.70}$$

where dn_C/dC is the refractive index increment of the analyte solution. When analyte is adsorbed onto the waveguide film, n_A and t_A will change, and this will cause a change in the value of N. The thickness of the analyte is related to the value of N by the mode equations:

$$t_A = f[\rho = 0, n_A, N = N(TE)] \qquad \text{Equation 2.71}$$

$$t_A = f[\rho = 1, n_A, N = N(TM)] \qquad \text{Equation 2.72}$$

where f designates a function, ρ is a parameter which has a value of 0 for the transverse electric wave and a value of 1 for the transverse magnetic wave. For more information on the mode equations see reference 71. When the equation $t_A(TE) = t_A(TM)$ is solved, a value for n_A can be determined. Using this value and one of the two above mode equations, the thickness of the adsorbed layer can also be calculated. Finally, the adsorbed amount is calculated from n_A, t_A, and the above equation.

2.1.5.3.2 Advantages and Disadvantages

One of the most significant advantages to OWLS over the other optical techniques mentioned, is that it can independently determine values for the refractive index of the adsorbed layer, the thickness of the adsorbed layer, and the absolute adsorbed amount.[70] It is also beneficial because a reflective surface in not required, as with SAR[72].

The OWLS technique also has a very high detection limit,[72] with sensitivity near 0.5 ng/cm^2. It can also be used for kinetic measurements, because experiments can be carried out over very short time scales (milliseconds), or very long time scales (tens of hours).[69]

One of the limitations of OWLS is that it requires a grating coupler with lines on the order of a micron. Usually, the waveguide film is composed of $Si(Ti)O_2$, but this can be

[71] Tiefenthaler, K.; Lukosz, W. *J. Opt. Soc. Am*. **1989***, B6*, 209.

[72] Kurrat, R.; Walivaara, B.; Marti, A.; Textor, M.; Tengvall, P.; Ramsden, J.J.; Spencer, N.D. *Colloids and Surfaces B: Biointerfaces* **1998**, *11*, 187.

coated with very thin layers of other metal oxides,[51,72,73] such as TiO_2. Another draw back is that the support must be transparent and have very well-defined optical properties.[72] Most of the work to date has been done in Switzerland, where the only commercially available apparatus is produced by Artificial Sensing Instruments (ASI, Zurich, Switzerland).

2.1.5.4 QCM

Quartz crystal microbalance (QCM) is a technique that has been used to measure the deposition of thin films for over 40 years[74]. It has been used to monitor the adsorption of various species in air and liquids as well as providing electrochemical data for various applications.

2.1.5.4.1 Basic Principles

Essentially, QCM works by applying a electrical potential across a quartz crystal, which will then oscillate at a frequency proportional to the applied potential[74]. This is a piezoelectric effect. When thin films of molecules are adsorbed onto the crystal, the frequency changes according to the following equation:

$$\Delta f = -2 f_o^2 \left(\mu_q \rho_q\right)^{-½} \Delta m / A \qquad \text{Equation 2.73}$$

where Δf is the change in the frequency due to the adsorbed species, f_o is the initial frequency of the crystal before any adsorption, μ_q is the shear modulus of the crystal, ρ_q is the density of the crystal, Δm is the change in mass, and A is the piezolelectrically active area on the crystal. A number of different metals can be used for the electrode, but gold is the most common substrate.

---

[73] Kurrat, R.; Textor, M.; Ramsden, J.J.; Boni, P.; Spencer, N.D. *Rev. Sci. Instrum*. **1997**, *68*, 2172.

[74] Hepel, M. in "Interfacial Electrochemistry"; Marcel Dekker, Inc.: New York; 1999, pp. 599-630.

There are several important assumptions which go into this equation[74]. Namely, that the acoustical impedance of the quartz and the adsorbed film are the same; that the change in frequency due to adsorbed mass is independent of the radial distance from the center of the crystal; that the mass is evenly distributed over the crystal; and that the adsorbed layer acts as a rigid film. Several extensions to the initial theory have been included to account for some of these restrictions, including equations which account for viscosity effects of the dispersing media and for viscoelastic effects arising from the film[74].

2.1.5.4.2 Advantages and Disadvantages

Although QCM has very high sensitivity (~1ng/cm^2) it is not a very good technique for giving absolute adsorbed mass values. Some of the problems that arise when trying to convert changes in frequencies to changes in mass include: viscoelastic effects of the film; solvent trapping of the polymer or protein film, causing unusually high adsorbed amounts; and the possibility of the adsorbed molecule slipping on the moving electrode surface[75]. Most of the recent papers, which use the QCM technique, only report changes in frequency, and a qualitative analysis of the structure and dynamic viscoselastic properties of the adsorbed layer[75,76].

2.1.5.5 SAR

Scanning angle reflectometry (SAR) uses light reflection to characterize a surface or a thin film on a surface. SAR is very similar to ellipsometry, which will be described below. The main difference is in the polarization of the light used for the measurements, SAR only uses p-polarized light, whereas ellipsometry uses by the p- and s-polarized light. A more detailed comparison of the two techniques will follow a brief introduction to SAR.

---

[75] Hook, F.; Rodahl, M.; Brzezinski, P.; Kasemo, B. *Langmuir* **1998**, *14*, 729.

[76] Hook, F.; Rodahl, M.; Kasemo, B.; Brzezinski, P. *Proc. Natl. Acad. Sci. USA* **1998**, *95*, 12271.

2.1.5.5.1 Basic Principles

When light is passed from one media to another which has a different refractive index, some of the light is reflected and some is transmitted. Figure 2.25 shows a schematic of a light beam going through a glass-solution interface which has two layers, first a glass hydrated surface layer and then an adsorbed polymer layer.

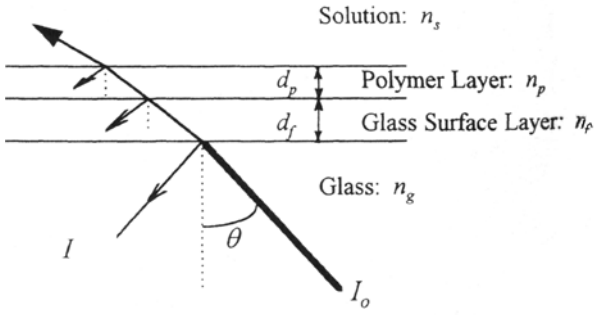

Figure 2.25: Reflectivity at a glass-solution interface containing two layers: a hydrated surface layer and an adsorbed polymer layer[77].

At each interface the light is reflected and transmitted. The angle of the transmitted light, θ_1, is related to the incident light, θ_0, by Snell's law:

$$n_0 \sin\theta_0 = n_1 \sin\theta_1 \qquad \text{Equation 2.74}$$

where n_0 is the refractive index of the first media and n_1 is that of the second. The reflectivity coefficient, r_p, of the light is given by the Fresnel equation[77]:

$$r_p = \frac{n_1 \cos\theta_0 - n_0 \cos\theta_1}{n_1 \cos\theta_0 + n_0 \cos\theta_1} \qquad \text{Equation 2.75}$$

where the reflectivity is zero at the Brewster angle, θ_B, given as:

$$\theta_B = \tan\left(n_s / n_g\right) \qquad \text{Equation 2.76}$$

for the glass-solution interface, where n_s is the refractive index of the polymer solution and n_g is for the glass. Measurements are taken near the Brewster angle, because here the reflectivity is most sensitive to changes in the adsorbed layer. The reflectivity is then defined as the ratio of the intensity of the reflected light, I, to that of the incident light, I_0:

[77] Fu, Z.; Santore, M.M. *Colloids and Surfaces A: Physiochemical and Engineering Aspects* **1998**, *135*, 63.

$$R_p = I/I_0 = |r_p|^2 \qquad \text{Equation 2.77}$$

The adsorbed amount of polymer, Γ, and the thickness of the polymer layer, d_p, are then related by the following equation[77]:

$$\Gamma = \frac{(n_p - n_s)d_p}{\left(dn_p/dc\right)} \qquad \text{Equation 2.78}$$

where n_p is the refractive index of the adsorbed polymer and dn_p/dc is the refractive index increment for the polymer in solution. This equation shows that the adsorbed amount and the layer thickness are not independent of one another. In order to calculate both parameters a model for the adsorbed layer must be introduced. The most common and simplest describes the adsorbed layer as a step function.

2.1.5.5.2 Advantages and Disadvantages

The first draw back of SAR is that it needs more calibration than ellipsometry. Not only does the residual intensity need to be calculated, but also the thickness of the oxidized layer on the glass or prism surface[78]. Another disadvantage of this method is that a highly reflective surface, such as silicon, is needed in order to get high sensitivity[79]. The silica surface can be modified to allow for more substrate options, for example spin coating of a polymer film[80], but this is not very applicable for the research described here. The choice of a model for the adsorbed layer is also critical. The calculations can become very complicated because the interfaces between the prism, the oxide layer on

[78] van Duijvenbode, R.C.; Koper, G.J.M. *Journal of Physical Chemistry B* **2000**, *104*, 9878.

[79] Gast, A.P. in Sanchez, I.C. "Physics of Polymer Surfaces and Interfaces"; Butterwork-Heinemann: Boston; 1992, ch. 11.

[80] Pagac, E.S.; Prieve, D.C.; Solomentsev, Y.; Tilton, R.D. Langmuir 1997, 13, 2993.

the surface of the prism, the adsorbed layer and the bulk solution all need to be take into account.[81]

The advantages that SAR has, are that it is an excellent method for determining adsorbed amounts and thicknesses, if the right model is used. This data can then be used to determine the conformation of the polymer chains on the surface. Also, if a well defined surface is used, SAR can be a much quicker technique than ellipsometry for obtaining the same information[78]. The SAR technique also allows for excellent kinetic data, by monitoring the reflectivity as a function of time, because of the availability of essentially instantaneous data[77,82].

2.1.5.6 Ellipsometry

Ellipsometry measures both the change in intensity and the change in polarization of a light beam, caused by the adsorption onto a surface. Thus, this technique is able to measure the layer thickness and the refractive index simultaneously.

2.1.5.6.1 Theory

When light is sent through a film-substrate system, as shown in Figure 2.26, the light is either reflected or transmitted through the interface[83]. The angles of refraction, ϕ_1 and ϕ_2, are determined by the incident angle ϕ_0, and the refractive index of the ambient, N_0, the film, N_1, and the substrate, N_2, by Snell's law:

[81] Furst, E.M.; Pagac, E.S.; Tilton, R.D. *Ind. Eng. Chem. Res*. **1996**, *35*, 1566.

[82] Pagac, E.S.; Prieve, D.C.; Tilton, R.D. *Langmuir* **1998**, *14*, 2333.

[83] Azzam, R.M.A.; Bashara, N.M. "Ellipsometry and Polarized Light"; Elsevier: Amsterdam; 1999, ch. 4.

$$N_0 \sin\phi_0 = N_1 \sin\phi_1 = N_2 \sin\phi_2 \qquad \text{Equation 2.79}$$

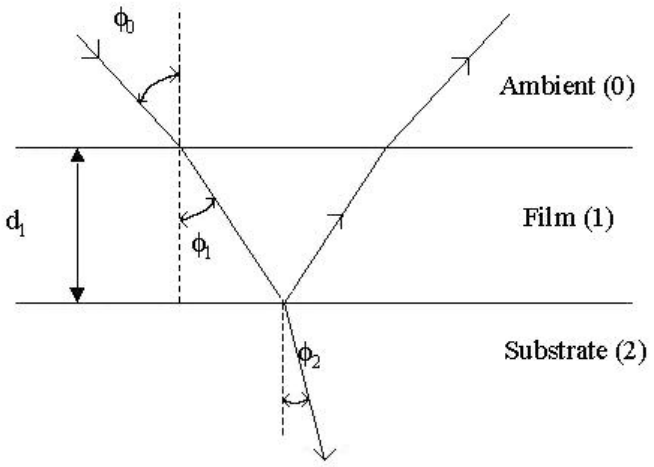

Figure 2.26: Oblique reflection and transmission of a plane wave by an ambient(0)-film(1)-substrate(2) system with parallel-plane boundaries. d_1 is the film thickness. ϕ_0 is the angle of incidence in the ambient and ϕ_1 and ϕ_2 are the angles of refraction in the film and substrate, respectively[83].

The light used in ellipsometry is linearly polarized. The electric vector that is vibrating parallel to the plane of incidence is the *p* polarization, and that vibrating perpendicular to the plane of incidence is the *s* polarization. The Fresnal reflection coefficients for these two polarization are r_p and r_s respectively, and are given in terms of two media *i* and *j* as:

$$r_{p,ij} = \frac{N_j \cos\phi_i - N_i \cos\phi_j}{N_j \cos\phi_i + N_i \cos\phi_j} \qquad \text{Equation 2.80}$$

$$r_{s,ij} = \frac{N_i \cos\phi_i - N_j \cos\phi_j}{N_i \cos\phi_i + N_j \cos\phi_j} \qquad \text{Equation 2.81}$$

where $r_{ij} = -r_{ji}$.

The phase change, β, that occurs for a wave as it is reflected multiple times through the film from one interface to the other is given by:

$$\beta = 2\pi\left(d_1/\lambda\right) N_1 \cos\phi_1 = 2\pi\left(d_1/\lambda\right)\left(N_1^2 - N_0^1 \sin^2\phi_0\right)^{1/2} \qquad \text{Equation 2.82}$$

where d_1 is the film thickness and λ is the wavelength.

In order for the light to probe the film it must pass through a series of interfaces, and thus undergoes multiple reflections, including: ambient-to-film (0-1), film-to-substrate (1-2), and again film-to-ambient (1-0). Thus, the total reflected amplitude, *R*, for each polarization is given by:

$$R_p = \frac{r_{p,01} + r_{p,12} e^{-i2\beta}}{1 + r_{p,01} r_{p,12} e^{-i2\beta}} \qquad \text{Equation 2.83}$$

$$R_s = \frac{r_{s,01} + r_{s,12} e^{-i2\beta}}{1 + r_{s,01} r_{s,12} e^{-i2\beta}} \qquad \text{Equation 2.84}$$

where $i = \sqrt{-1}$.

These reflections can be broken down into two parts, a reflection or amplitude part and a refraction or phase part, so that these effects can be studied separately:

$$R_p = \left|R_p\right| e^{i\Delta_p} \qquad \text{Equation 2.85}$$

$$R_s = \left|R_s\right| e^{i\Delta_s} \qquad \text{Equation 2.86}$$

where $|R_p|$ and $|R_s|$ denote the amplitude attenuation for the *p* and *s* polarized light and Δ_p and Δ_s are the phase shift for each polarization.

The ellipsometric ratio, ρ, is then given by:

$$\rho = \frac{R_p}{R_s} \qquad \text{Equation 2.87}$$

This can be rewritten in the form:

$$\rho = \tan\psi e^{i\Delta} \qquad \text{Equation 2.88}$$

or

$$\tan\psi = \frac{|R_p|}{|R_s|} \qquad \text{Equation 2.89}$$

$$\Delta = \Delta_p - \Delta_s \qquad \text{Equation 2.90}$$

where ψ is the differential change in the amplitude and Δ is the differential change in the phase upon reflection.

The parameters ρ, ψ, and Δ are all complicated functions of the complex refractive indices, N_0, N_1, and N_2, and of the film thickness, d_1, the wavelength of light, λ, and the angle of incidence, ϕ_0. From ellipsometry data, it is possible to calculate the refractive index of the film and the film thickness, independently, assuming a homogeneous film layer. This calculation, however, is nontrivial, due to the transcendental nature of the equation. An iterative scheme must be used, for example[84] starting with an initial guess of N_1, calculating d_1, and iterating N_1 until d_1 is a real number.

The adsorbed amount can then be calculated using:

$$\Gamma = \frac{d_1(n_1 - n_0)}{\left(dn_0 / dc\right)} \qquad \text{Equation 2.91}$$

where dn_0/dc is the refractive index increment of the polymer solution, n is the real part of the index of refraction, 0 denotes the polymer solution, and 1 the polymer layer.

The iteration procedure only yields the products $d_1 n_1$ and $d_1 n_o$, so only the adsorbed amount can be determined unambiguously, by using a dn_0/dc value of 0.186 ml/g, which is typical for many proteins[85]. Unless the refractive index of the adsorbed layer is known, the thickness can not be calculated independently. For thin, dry films, the data can be fit to a multiple parameter model, which allows for accurate calculations of the adsorbed

[84] Dorgan, J.R.; Stamm, M.; Toprakcioglu, C.; Jerome, R.; Fetters, L.J. *Macromolecules* **1993**, *26*, 5321.

[85] De Feijter, J.A.; Benjamins, J.; Veer, F.A. *Biopolymers* **1978**, *17*, 1759.

layer thickness. For solvated polymer layers these models are complicated, because the refractive index difference between the polymer film and the solution is very small[84].

2.1.5.6.2 Advantages and Disadvantages

Ellipsometry is a very powerful technique for measuring thin film thickness and the adsorption of molecules on a surface. It is capable of measuring adsorbed amounts without the destruction of the adsorbed molecule or the need for labeling[86]. Ellipsometry is also capable of measuring adsorption in situ and in real time, thereby making it possible to determine the adsorption kinetics[86].

Ellipsometry has benefits over other techniques such as SAR and SPR which require specific surfaces or surface properties[86]. Many different substrates can be used, including metals, polymer coated metals, silicon, and modified gold[86]. Ellipsometry is also very useful when the films are too thin, too numerous or too complicated, when other techniques would fail[87]. It is very sensitive to changes in surface concentration and thickness and is more reliable for fitting adsorbed layers to thickness models[78].

One of the disadvantages of ellipsometry is if the film in not homogenous, it can be difficult to resolve the refractive index and the layer thickness. However, the adsorbed amount can still be calculated as long as the product $d_1 n_1$ is known[84,86].

This section has discussed how polymers adsorb on surfaces, and specifically the conformation of the chain on the surface due to adsorption. Several surface techniques have been introduced, which allow for the measurement of the adsorbed amount, and in some case the thickness of the adsorbed polymer layer. The next section will start with an introduction into colloid stability, but the main emphasis is on how the adsorbed

---

[86] Elwing, H. *Biomaterials* **1998**, *19*, 397.

[87] McArthur, L.; Chalmers, S. *Vacuum Technology and Coating* **2000**, *Oct*., 35.

polymer will affect this stability. This will help to outline the design criteria required of the proposed polypeptide diblock to effectively stabilize alumina particles.

2.2 Colloid Stability

The stability of a colloidal dispersion must be controlled during processing. Some suspensions, such as polystyrene colloids in water, are fairly easy to stabilize, due to relatively weak van der Waals forces. Others, like alumina in water, exhibit stronger van der Waals forces and can be difficult to stabilize, especially at high solids volume fraction. It is these strong attractive forces that the brush forming polypeptide diblock will need to overcome via steric stabilization. This section will first review the relevant theories for predicting the stability of colloidal systems and then will discuss some relevant experimental work.

2.2.1 DLVO Theory

The Deryaguin-Landau-Verwey-Overbeek (DLVO) theory is the starting point for accounting for interactions between colloidal particles. This theory predicts the total pair potential interaction energy, V_T, as the sum of two terms[88]:

$$V_T = V_A + V_E \qquad \text{Equation 2.92}$$

The V_A terms accounts for the van der Waals attractive potential and V_E is the repulsive electrostatic potential.

2.2.1.1 Van der Waals Contributions

The attractive potential for two identical spheres, each with radius *a*, and separated by a center-to-center distance r is given by the following expression:

[88] Russel, W.B.; Saville, D.A.; Schowlter, W.R. "Colloidal Dispersions"; Cambridge University Press: New York, 1989.

$$V_A = -\frac{1}{6} A \left(\frac{2a^2}{r^2 - 4a} + \frac{2a^2}{r^2} + \ln\left(\frac{r^2 - 4a^2}{r^2} \right) \right) \qquad \text{Equation 2.93}$$

where A is the composite Hamaker constant, which is given by[89]:

$$A = \left(\sqrt{A_{11}} - \sqrt{A_{22}} \right)^2 \qquad \text{Equation 2.94}$$

where A_{11} is the Hamaker constant of the particles and A_{22} is that of the liquid medium. The Hamaker constant is related to the polarizability of the material by:

$$A_{jj} = \tfrac{3}{4} \pi^2 h_p v_j \alpha_j q_j^2 \qquad \text{Equation 2.95}$$

where h_p is Plank's constant, v_j is the dispersion frequency of the material, α_j is the polarizability, and q_j is the number of molecules per unit volume. The dispersion frequency assumes that all of the resonance effects occur in the ultra-violet region of the spectrum. Some typical values for Hamaker constants are given in Table 2.1. Retardation of this attraction will occur at separations greater than $c/\nu_0 2\pi$, due to a phase difference between the polarization dipole of the two surfaces[90]. Thus, the Hamaker constant is not really a constant, but becomes a function of particle separation at distances around 5-10 nm[88,89], which leads to retardation. This effect is relatively small and often ignored for simplicity.

[89] Buscal, R.; Corner, T.; Stageman, J.F. "Polymer Colloids"; Elsevier Applied Science: New York, 1985.

[90] Adamson, A.W.; Gast, A.P. "Physical Chemistry of Surfaces"; John Wiley and Sons, Inc.: New York, 1997.

Table 2.1: Hamaker constants for various materials.

Material	A_{11} (10^{-20} J)	Reference
Water	3.0 – 6.1	91
Hydrocarbons	4.6 -10	91
Poly(styrene)	5.6 – 6.4	91
Poly(methyl methacrylate)	7.11	89
Silica (SiO_2)	8.6	91
Titania (TiO_2)	11 – 31	92
Alumina (Al_2O_3)	14.8 – 15.5	92
Hematite (α-Fe_2O_3)	7.5 - 22	93

The attractive force is directly proportional to the difference in the Hamaker constants between the dispersed particles and the dispersing medium. This explains why poly(styrene) latex particles in water are easy to stabilize because both Hamaker constants fall within the same range, but alumina, which has a much higher Hamaker constant than water, is much more difficult to stabilize.

2.2.1.2 Electrostatic Contributions

The electrostatic repulsive potential for two charged spheres at constant potential is given by:

[91] Shaw, D.J. "Introduction to Colloid and Surface Chemistry"; Butterworths: Boston, 1980.

[92] Visser, J. *Advances in Colloid and Interface Science* **1972**, *3*, 331.

[93] Schudel, M.; Behrens, S.H.; Holthoff, H.; Kretzschmar, R.; Borkovec, M. *Journal of Colloid and Interface Science* **1997**, *196*, 241.

$$V_E = 2\pi\varepsilon\varepsilon_o\left(\frac{kT}{ze}\right)^2 a\Psi_s^2 \ln\left(1+e^{-\kappa h}\right) \quad \text{for } \kappa a > 10 \quad \text{Equation 2.96}$$

(thin double layer limit)

$$V_E = 4\pi\varepsilon\varepsilon_o\left(\frac{kT}{ze}\right)^2 \frac{a^2}{h+2a}\Psi_s^2 \exp(-\kappa h) \quad \text{for } \kappa a < 3 \quad \text{Equation 2.97}$$

(thick double layer limit)

where ε is the relative permittivity of the solution , ε_o is the permittivity of the vacuum, k is the Boltzmann constant, T is the temperature in Kelvin, z is the valence of the ion, e is the elementary charge, Ψ_s is the surface potential, h is the distance between the surfaces of the spheres and κ is the inverse Debye length, given by:

$$\kappa^2 = \frac{2e^2\sum\left(z^i\right)^2 n_0^i}{\varepsilon kT} \quad \text{Equation 2.98}$$

where, n_o is the number concentration of counterions in the equilibrium salt solution. κ^{-1} characterizes the length scale of the electrostatic interactions in the fluid.

2.2.2 Electrostatic Stabilization

2.2.2.1 Stability Ratio

The stability ratio, W, is often used to characterize the suspension stability, and is defined as the number of particle collisions divided by the number of particle collisions that induce coagulation, and is determined by:

$$W = 2a\int_{2a}^{\infty}\frac{\exp\left(\Phi/kT\right)}{r^2}dr \quad \text{Equation 2.99}$$

Thus, if $W \approx 1$, then the flocculation is very fast, whereas if $W > 1$, then there is slow flocculation. A suspension with a stability ratio of $W = 10^9$ can be stable for several months. When the repulsive energy barrier is large it becomes the major contribution to the stability ratio. The integral in Equation 2.99 can then be approximated as:

$$W \sim \left(-\frac{2}{\pi} \frac{d^2}{dr^2} \frac{\Phi_{max}}{kT} \right)^{-1/2} \frac{\exp\left(\frac{\Phi_{max}}{kT} \right)}{r_{mzx} - 2a} \qquad \text{Equation 2.100}$$

At very high ionic strengths, when the dispersion effects dominate, $W = W_\infty$. The stability ratio can be used to estimate the height of the potential barrier by:

$$W = W_\infty + 0.25 \left[\exp\left(\frac{\Phi_{max}}{kT} \right) - 1 \right] \qquad \text{Equation 2.101}$$

Thus, Φ_{max} = 10kT would result in a high value of W, and a stable dispersion. Figure 2.27(*a*) shows that increasing the surface charge density leads to an increase in the critical flocculation concentration, n_{crit}, which is the electrolyte concentration above which rapid coagulation occurs, and given by:

$$n_{crit} = 9.0 \left(\frac{kT}{A} \right)^{2/3} \left(\frac{ql_b}{e} \right)^{4/3} mol/l \qquad \text{Equation 2.102}$$

where l_b is the Bjernum length and is $e^2/4\pi\varepsilon\varepsilon_o kT$. This equation shows that the surface charge has a greater effect on the stability than the Hamaker constant. The effect of the Hamaker constant is shown in Figure 2.27(*b*), and shows that as A_{eff}/kT is increased, the critical flocculation concentration decreases due to increased attractive forces. Figure 2.27(*c*) shows that the particle size does not affect the critical flocculation concentration, as shown in the equation above, but a larger particle has a higher stability ratio than a smaller particle at the same ionic strength because the repulsive electrostatic interaction increases faster with size than the attractive van der Waals interactions do.

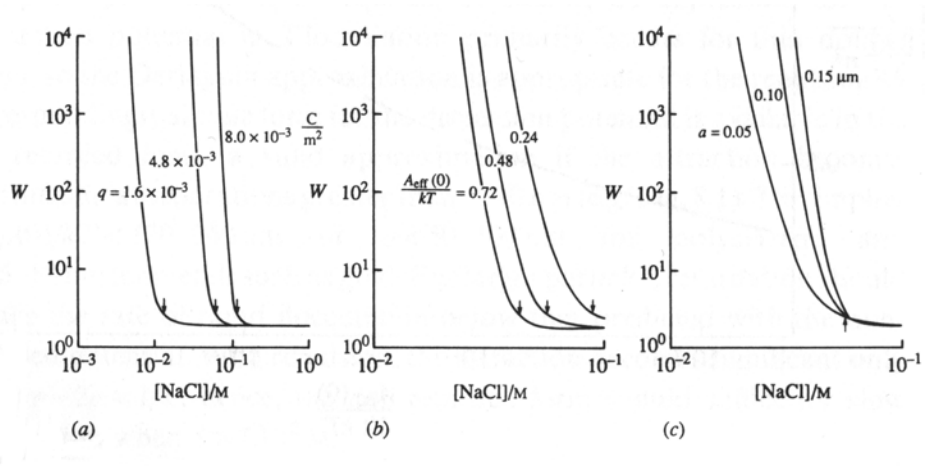

Figure 2.27: Stability ratios for flocculation of spheres in water: (*a*) Effect of surface charge density, q, for a = 0.1 μm and A/kT = 0.48. (*b*) Effect of Hamaker constant for a = 0.1 μm and q = 4.8 x 10^{-3} C/m^2. (*c*) Effect of radius for q = 4.8 x 10^{-3} C/m^2 and A/kT = 0.48. Arrors indicate the critical flocculation concentration[88].

2.2.2.2 Theory

For electrostatic stabilization of colloidal dispersions using small adsorbed molecules or ions, both the dispersion and electrostatic parts of the potential in Equation 2.92 are significant. Figure 2.28 shows a general schematic for the potentials from an attractive force and two different repulsive forces, and the resulting total potentials for each. Note the large maximum in curve V(1), this would prevent the particles from moving close enough to fall into the deep primary minimum. Curve V(2) on the other hand does not have a large enough maximum to prevent permanent flocculation, commonly referred to as coagulation.

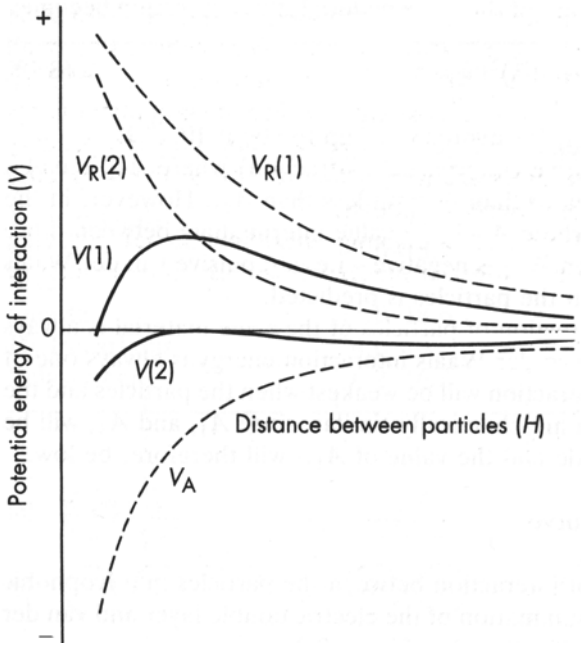

Figure 2.28: Total interaction energy curves, V(1) and V(2), obtained by the summation of an attraction curve, V_A, with different curves, $V_R(1)$ and $V_R(2)$[91].

The effect of ionic strength on the potential curves can be seen in Figure 2.29(*a*). As the salt concentration is increased, the charges become screened and the maximum in the potential decreases, until at 10^{-2} M there is no potential barrier and immediate flocculation. The effect of the Hamaker constant can been seen when Figure 2.29(*a*) and (*b*) are compared. The higher the value of the Hamaker constant, the stronger the attractive dispersion forces. This explains why the polystyrene latices are stable at 10^{-2} M, while the gold sols are not.

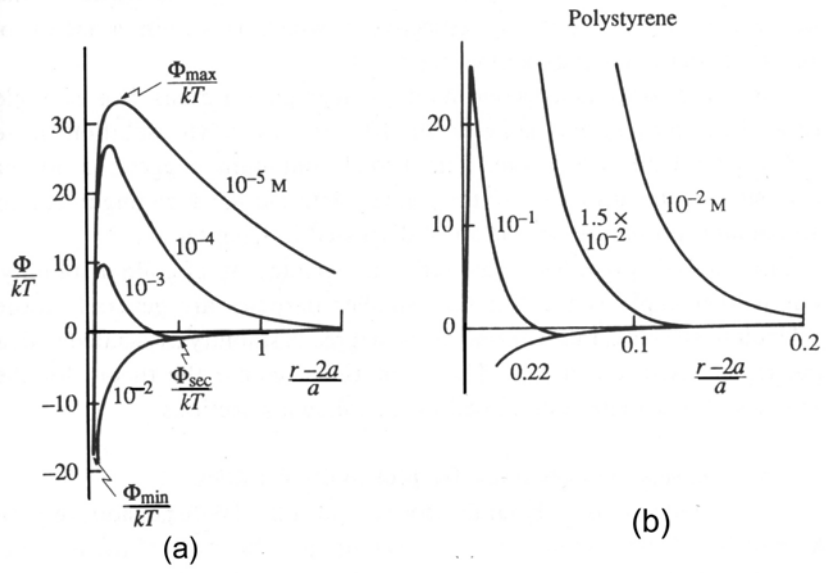

Figure 2.29: Interaction potentials for spheres with a = 0.1 μm and $e\psi_s/kT = 1.0$ in water at a range of ionic strengths: (*a*) Gold sols with A/kT = 25, (*b*) Polystyrene latices with A/kT = 2.5[88].

The particle radius also has an effect on the stability. Figure 2.30 shows the onset of a secondary minimum as the radius is increased. This is to be expected, from the van der Waals attractive potential, Equation 2.93, where the attractive energy increases with the square of the particle radius, whereas the repulsive electrostatic energy, from Equation 2.96 for $\kappa a > 10$, increases with the first power of the radius. A weak secondary minimum, which can be easily redispersed may actually be beneficial, by preventing permanent settling of the particles in tightly packed arrays over long times, which could lead to difficulties in redispersing the sediment. For example, paint companies employ this type of behavior to extend the storage life of their product. If settling does occur the paint can then be easily redispersed, prior to use.

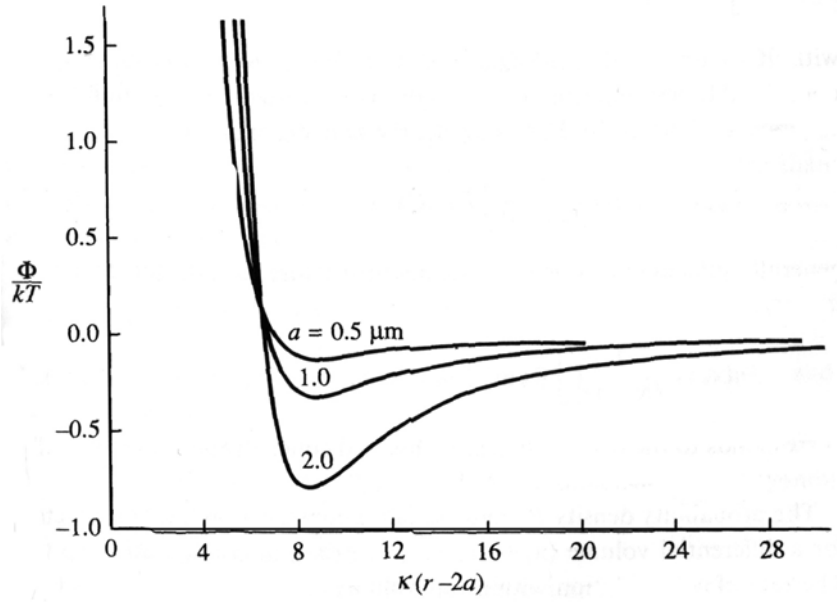

Figure 2.30: Interaction potentials between polystyrene spheres with ψ_s = 25 mV as a function of radius at I = 10^{-3} M[88].

2.2.2.3 Important Experimental Work

The effect of adsorbing different carboxylic acids on the stability of colloidal particles of α-Al_2O_3 in water has been studied[94]. The effect of this type of dispersing agent is relevant to the work discussed in this proposal, although the carboxylic acid will be used as the anchoring block in my work. The settling effects of twenty different carboxylic acids were measured at various alumina concentrations (refer to Section 2.3.3 for further details on the sedimentation experiment). It was found that those carboxylic acids containing hydroxyl groups resulted in suspensions with the best stability and the lowest viscosity. The measured adsorbed amount and the zeta potential, at various pH, of citric acid, with good dispersive properties, was compared to tricarballylic acid, a poor dispersant. Both of these molecules have three carboxylic acid groups, and the only difference in their structures is that the citric acid has an additional hydroxyl group, which the tricarballylic acid does not possess. It was found that the citric acid had a higher adsorbed amount and a more negative zeta potential at all pH values. Only at pH

[94] Tao, R.; Aksay, I.A.; Yasrebi, M.; Pellerin, N.B.; Staley, J.T. *Mat. Res. Soc. Symp. Proc*. **1994**, *330*, 113.

≥ 6 did the citric acid stabilize the alumina. The authors conclude that the main criteria for stabilization is strong adsorption of the acid. Those carboxylic acids containing hydroxyls had strong adsorption, due to hydrogen bonding, and thus were able to stabilize the particles. Under acidic conditions, pH = 4, the citric acid did not form a good dispersion, and this was attributed to insufficient charge of the adsorbed molecule, which was confirmed via zeta potential measurements.

In another study, the effects of sodium poly(methacrylic acid) (PMAA) on the stability of α-Al_2O_3 as a function of pH and polyelectrolyte concentration were measured[95]. The stability of the Al_2O_3 dispersions were characterized using adsorption, sedimentation, zeta potential, and viscosity measurements. Both the surface charge and the charge of the polyelectrolyte are functions of pH, and thus the adsorption and the resulting dispersion stability were complicated functions of pH. The pK_a for PMAA is 3.4 and its degree of ionization increases as the pH increases. The IEP for alumina is 8.7, and below this pH the surface has a net positive charge, while above pH 8.7 it has a net negative charge.

Figure 2.31 is an illustration on the adsorption and viscosity data, which yields a stability map for PMAA on colloidal α-Al_2O_3 particles, specifically AKP-30 from Sumitoma[95]. At very low pH there is no adsorption of the polyelectrolyte, due to charge neutralization and instability, but the alumina particles are stabilized electrostatically by their own positive charge. Above pH 4, a saturation limit exists which must be achieved in order for the suspension to be stable. Above this minimum in adsorbed amount the particles are stabilized via electrosteric repulsion, which is a combination of electrostatic forces from the charge on the polyelectrolyte and steric forces from the polyelectrolyte structure. At higher pH the polymer is in a very flat conformation, due to intramolecular chain repulsion, and will exhibit mainly electrostatic characteristics. At lower pH, on the other hand, the polymer is less charged, and will adsorb with loops, thus showing greater repulsive behavior. Although the alumina can be stabilized without the polyelectrolyte,

[95] Cesarano, J.; Aksay, I.A.; Bleier, A. *Journal of the American Ceramic Society* **1988**, *71*, 250.

the dispersion with PMAA showed enhanced stability over those stabilized by electrostatics alone.

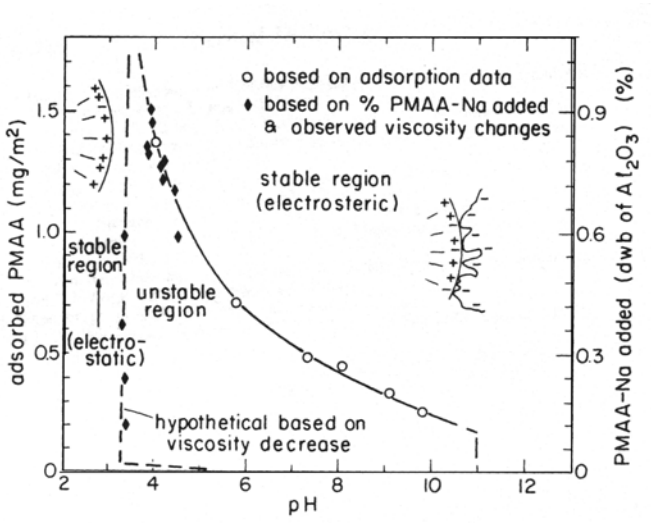

Figure 2.31: Stability map showing the amount of adsorbed PMAA required to form stable suspensions of 20 vol% AKP 30 α-Al_2O_3 as a function of pH[95].

In another system, the force as a function of distance was measured for quarternized poly(2-vinyl pyridine) (PVP) using atomic force microscopy (AFM). A colloidal silica probe was used with a flat mica surface for the measurements. Upon introduction of the PVP there was a decrease in the repulsive barrier, which was attributed to charge reversal of the surfaces. At low ionic strength the adsorbed chains had flat, train-like conformations and showed an attractive force at 8 nm. When the ionic strength was increased the polymer took on a more extended adsorbed conformation, due to screening of the electrostatic repulsion. This layer was compressible and showed no attraction at close contact. There was minimum repulsion at pH 6, which increased when the pH was either increased or decreased around 6. This minimum was attributed to the point of zero charge of the polyelectrolyte treated mica surface and the silica, where surface potentials are minimized.

2.2.3 Steric Stabilization

The potential due to polymer steric forces is a complex function of the segment distribution of the adsorbed polymer layer, which is influenced by the degree of

polymerization, the polymer-surface interactions, and the polymer-solvent interactions. Essentially, the polymer forms a layer of thickness δ around the particles, preventing close contact between particles, where the dispersion attractive forces become dominate.

As discussed in Section 2.1 a block copolymer or terminally attached polymer may extend into solution by stretching of the tail blocks, whereas a homopolymer absorbs as trains, tails, and loops. This characteristic makes block copolymers the desired choice for stabilizing colloids sterically. In order for a block copolymer to be an effective stabilizer it must have: a) strong adsorption of the anchor block; b) full coverage on the particle surface; and c) a sufficiently high tail block molecular weight.

2.2.3.1 Theory

A modified DLVO theory, which includes a steric repulsive potential, V_S, can be used to describe the interactions when there are adsorbed polymers on the surface of a colloidal particle. The total pair potential interaction energy is then the sum of three terms:

$$V_T = V_A + V_E + V_S \qquad \text{Equation 2.103}$$

When polymers are used to stabilize colloidal particles one of two situations may occur. In Figure 2.32(*a*) the potential curve for a typical nonionic polymeric stabilizer is shown. If the molecular weight is high enough, this system will be thermodynamically stable, and does not show a primary minimum. Figure 2.32(*b*) shows the potential for a polyelectrolyte, which shows both steric and electrostatic repulsion.

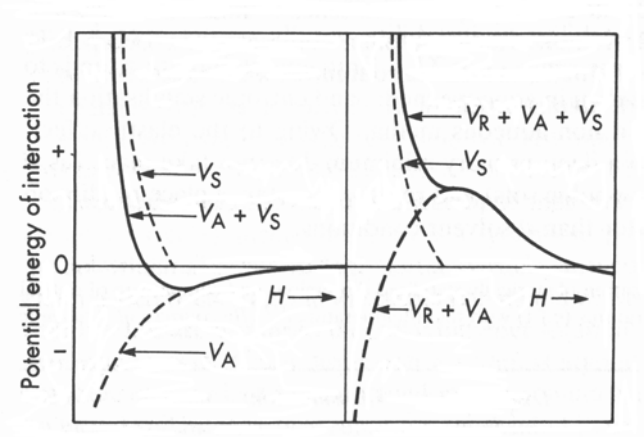

Figure 2.32: Schematic interaction energy diagrams for sterically stabilized particles: (*a*) in the absence of an electric double layer repulsion, (*b*) with electric double repulsion[91].

In the most basic model, a colloidal particle is encased in a rigid layer of adsorbed polymer, of layer thickness δ, as shown in Figure 2.33[96]. Thus, when the separation is equal to 2δ, the particles are unable to move closer together. From this most basic approximation, it is easy to see how a minimum adsorbed layer thickness is needed to overcome the van der Waals attractive forces. If, at the minimum separation, the depth of the secondary minimum is larger than several kT, then the particles will flocculate, based on the simplified interaction equation:

$$V_A = -\frac{A_{eff}\, a}{12h} \qquad \text{Equation 2.104}$$

Thus the depth of the well, or V_A, will increase with increasing particle size and decrease with increasing polymer molecular weight, which will increase *h*.

[96] Napper, D.H. "Polymeric Stabilization of Colloidal Dispersions"; Academic Press: London, 1983.

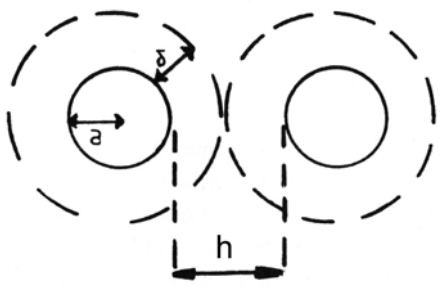

Figure 2.33: Schematic representation of the close approach of two sterically stabilized particles, with particle size *a*, steric layer thickness *d*, and minimum distance of closest approach of the particle surfaces *h*[96].

There have been many theories that have attempted to model the effect of adsorbed polymer on the pair interaction potential. Unfortunately, the steric term in the modified DLVO theory is a complicated function the particle size, polymer volume fraction, the excluded volume of the polymer, and the separation of the particles. There are two main contributions to the steric potential: entropic effects from the interaction between the polymer and the solvent, and elastic effects for compressed polymer chains. These two contributions are inherently coupled by the polymer segment density distribution in the adsorbed layer.

According to Napper, two main schools of thought have existed for the theories of polymeric stabilization: pragmatic theories, which assume a segment density distribution; and *ab initio* theories, such as the self-consistent mean field theory, which do not separate the entropic and elastic effects. A detailed description of these theories will not be given here, but rather a summary of the important findings.

In the pragmatic theory, the steric potential for free interpenetration of the chains is given simply as the contribution to the free energy of mixing at large separations, and the sum of the contributions from mixing and the elastic effects at small separations:

$$V_S = \Delta G_M \qquad \text{for } \delta < h < 2\delta \qquad \text{Equation 2.105}$$

$$V_S = \Delta G_M + \Delta G_{EL} \qquad \text{for } h < \delta \qquad \text{Equation 2.106}$$

For spherical particles these equations become:

$$V_S = \frac{2\pi akT}{V_1}\phi_2\left(\frac{1}{2} - \chi\right)S_M \qquad \text{for } \delta < h < 2\delta \qquad \text{Equation 2.107}$$

$$V_S = \frac{2\pi akT}{V_1}\phi_2\left(\frac{1}{2} - \chi\right)S_M^* + \frac{2\pi akT}{V_1}\phi_2 S_{EL} \qquad \text{for } h < \delta \qquad \text{Equation 2.108}$$

where S_M, S_M^*, and S_{EL} are geometric functions which are dependent on the segment density distribution function chosen. For example, a uniform segment density distribution function can be chosen, which is a constant between separations 0 and L and is zero at larger separations. For this model, $V_S/kT \sim aN/V^{1/3}$, where a is typically of the order $10^3 V^{1/3}$. Thus it is easy to see that the steric repulsion can be very large, especially for high molecular weight polymers.

The stability of colloidal particles with adsorbed polymer is dependent on several dimensionless parameters, which are shown in Table 2.2. N is the number of segments per chain, proportional to the molecular weight; l is the Kuhn segment length; v is the segment-segment excluded volume; ϕ_p is the dimensionless surface coverage of the polymer; w is the physical volume of the segment, and n_p is the number of attached chains per unit area. The excluded volume is related to the Flory parameter, χ, which is a measure of the solvent quality by:

$$\upsilon = \frac{C_\infty \upsilon_o m_o (1 - 2\chi)}{N_A} \qquad \text{Equation 2.109}$$

where, C_∞ is the characteristic ratio of the polymer chain, ν_o is the specific volume, m_o is the repeat unit molecular weight, and N_A is Avogadro's number.

At large separations, or for an isolated polymer layer, the dimensionless layer thickness $\alpha \rightarrow \alpha_o$. In good solvents, $\alpha_o > 1$, while in poor solvents $\alpha_o < 1$. In a theta solvent, $v = 0$

and thus the excluded volume is also equal to zero, and is positive in a good solvent and negative in a poor solvent. At high surface coverage, $\phi_p > 1$, while at low coverage $\phi_p < 1$.

Table 2.2: Important parameters and their dimensionless forms.

Parameter	Dimensionless Form
Separation	$H = \frac{r - 2a}{N^{1/2} l} = \frac{h}{N^{1/2} l}$
Excluded volume	$\upsilon = \frac{N^{1/2} v}{l^3}$
Ratio of particle to segment size	a/l
Surface coverage	$\phi_p = \frac{N n_p w^{1/2}}{l}$
Hamaker constant	A/kT
Frequency characterizing retardation	Ω
Layer thickness	$\alpha = \frac{L}{N^{1/2} l}$

The solvent quality with respect to the tail blocks is also an important factor which will affect how well the particle is stabilized. If the tail block is in a good solvent and the surface is fully covered, osmotic effects will prevent interpenetration of the chains, which will cause a repulsive force for surface separations between $\delta \leq h \leq 2\delta$, as shown in Figure 2.34. For poor solvents at low coverage, on the other hand, there is an extension of chains and thus an attractive force, at the same separations. For all cases, at $h \leq \delta$, there is elastic compression of the chains, which is truly repulsive, and if the layer thickness is sufficient, will thermodynamically stabilize the particles.

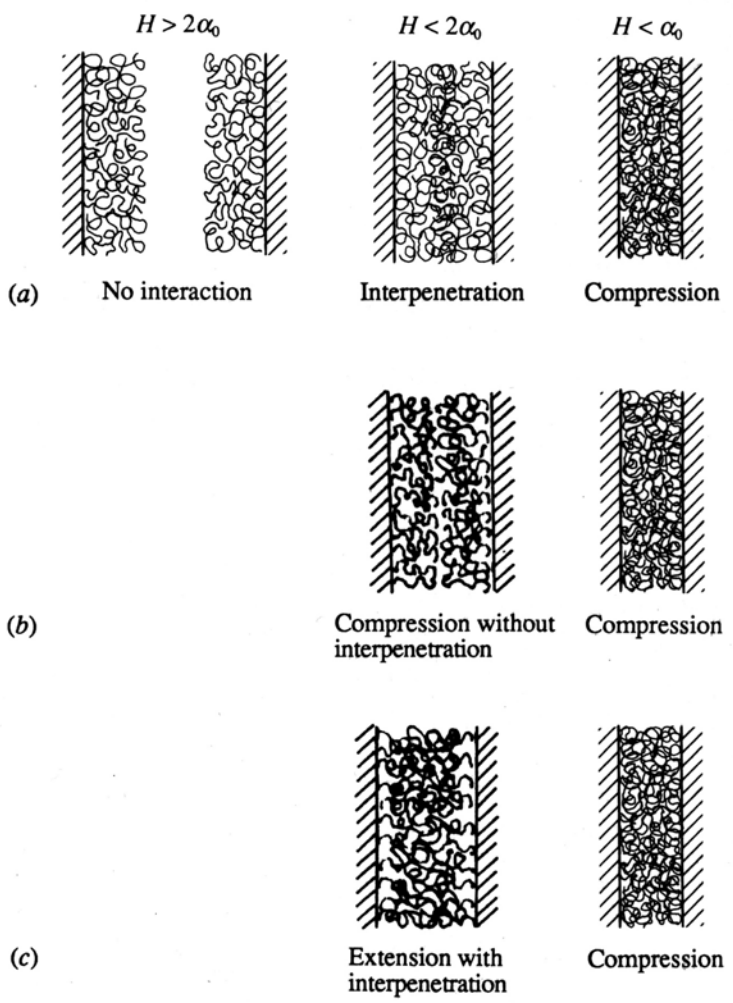

Figure 2.34: Modes of interaction between polymer layers according to the mean-field theory for (*a*) low coverage at theta conditions, (*b*) moderate coverage in a good solvent, and (*c*) low coverage in a poor solvent[88].

The interaction potential between two spheres with end-attached polymer chains was approximated by Russel[88] as:

$$\Phi = \pi a \int_{r-2a}^{\infty} \Phi_{fp}\, dh - \frac{1}{6} A_{eff}(r-2a)\left(\frac{2a^2}{r^2-4a^2} + \frac{2a^2}{r^2} + \ln\frac{r^2-4a^2}{r^2}\right) \quad \text{Equation 2.110}$$

where Φ_{fp} is the interaction potential due to adsorbed polymer on two flat plates:

$$\Phi_{fp} = 2n_p\left[A(H,z,\phi_p) - A_0(z,\phi_p)\right] \quad \text{Equation 2.111}$$

A is the free energy per chain of the adsorbed polymer layer as a function of the separation, which is given by:

$$\frac{A}{kT} = \frac{3}{2}\left(\alpha^2 + \alpha^{-2} - 2\right) + \frac{3}{2}\frac{z}{\alpha}\left(1 - \frac{H}{3\alpha}\right) + \frac{7}{6}\frac{\phi_p^2}{\alpha^2}\left(1 - \frac{3}{7}\frac{H}{\alpha}\right) \qquad \text{Equation 2.112}$$

and A_0 is the free energy per chain of an isolated adsorbed layer, at large separation:

$$\frac{A_0}{kT} = \frac{3}{2}\left(\alpha_0^2 + \alpha_0^{-2} - 2\right) + \frac{N\upsilon n}{2} + \frac{Nwn^2}{6} \qquad \text{Equation 2.113}$$

recalling that α_0 is the dimensionless layer thickness for isolated chains.

The effect of the molecular weight of an end grafted polymer on the interparticle potential as a function of separation is shown in Figure 2.35. As the molecular weight of the polymer is increased, the secondary minimum in the potential curve becomes less negative. As a general rule of thumb, flocculation occurs if the potential minimum, $-\Phi_{sec}/kT$, is between 2 and 10. Thus, curve (*a*) will show immediate phase separation. For the other extreme, dispersion forces become insignificant, $-\Phi_{min}/kT << 0.1$, only for curve (*d*), at the highest molecular weight. Curves (*b*) and (*c*) will both eventually show flocculation, but will be easy to redisperse.

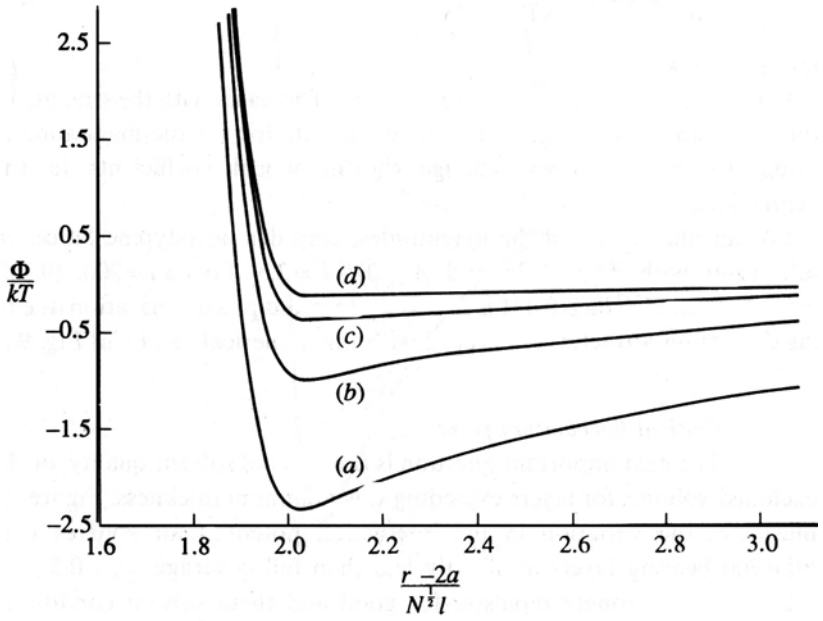

Figure 2.35: The total interparticle potential for polystyrene latices, with A/kT = 2.5 and lΩ/a = 0.25, with polymer layers of ϕ_p = 1.0 and a/l = 200, at theta conditions: (*a*) N = 16, (*b*) N = 40, (*c*) N = 100, (*d*) N = 250[88].

The separation at the minimum in the potential curve is independent of the molecular weight and occurs at $r - 2a \approx 2N^{1/2}l$. This can then be used to determine the minimum molecular weight, and thus layer thickness, needed for stabilization:

$$\frac{Nl}{a} \geq 0.019 \frac{a}{l\Omega} \frac{A}{kT} \; for \; \frac{\Omega A}{kT} >> 1 \qquad \text{Equation 2.114}$$

$$\frac{N^{1/2}l}{a} \geq 0.021 \frac{A}{kT} \; for \; \frac{\Omega A}{kT} << 1 \qquad \text{Equation 2.115}$$

These two equations show that as the Hamaker constant is increased, or the attractive dispersion forces are increased, a higher molecular weight polymer is needed to maintain stability.

In Figure 2.36 the effect of solvent quality, or the dimensionless excluded volume, on the interaction potential is shown. As the solvent quality is decreased, going from curve (*a*) to curve (*d*), there is an abrupt transition where flocculation occurs. This transition occurs at conditions slightly below the theta condition. This graph shows that even under poor solvent conditions, a colloidal dispersion can be stable, if the brush is dense enough.

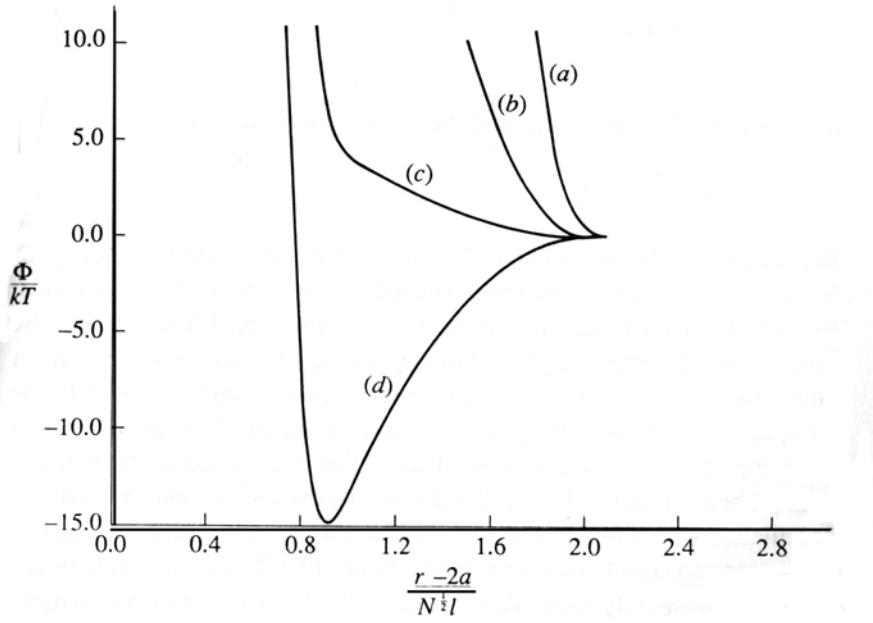

Figure 2.36: The total interparticle potential for spheres with $a/l = 200$ with polymer layers of $\phi_p = 0.5$ at $N^{1/2}v/w^{1/2}$ = (*a*) 2.24, (*b*) 0.0, (*c*) –0.45, (*d*) –0.67[88].

The transition from a stable to a flocculated system can be measured experimentally several different ways. The solvent can be changed, as shown above, which changes the segment to segment excluded volume. Also, the temperature can be varied, if temperatures near the theta temperature are accessible. Another alternative is to add a non-solvent to the system, and monitor the changes in the colloidal stability as a function of added non-solvent concentration.

The effects of the solvent quality, excluded volume, and the surface coverage of polymer on the critical flocculation point and on phase behavior of the polymer are shown in Figure 2.37. Several different regions are of interest. When the excluded volume is only slightly negative, greater than -2, all but the most sparsely covered particles are stable. For highly negative values of excluded volume and low surface coverage, the system is flocculated, due to the dominance of the dispersion forces. There is a window that occurs at moderately negative values of excluded volume and high surface coverage, where even though the polymer solution is in a two phase region, the colloidal dispersion is stable. The occurs because the surface coverage of the polymer is high enough to overcome dispersion forces and the poor solvent quality.

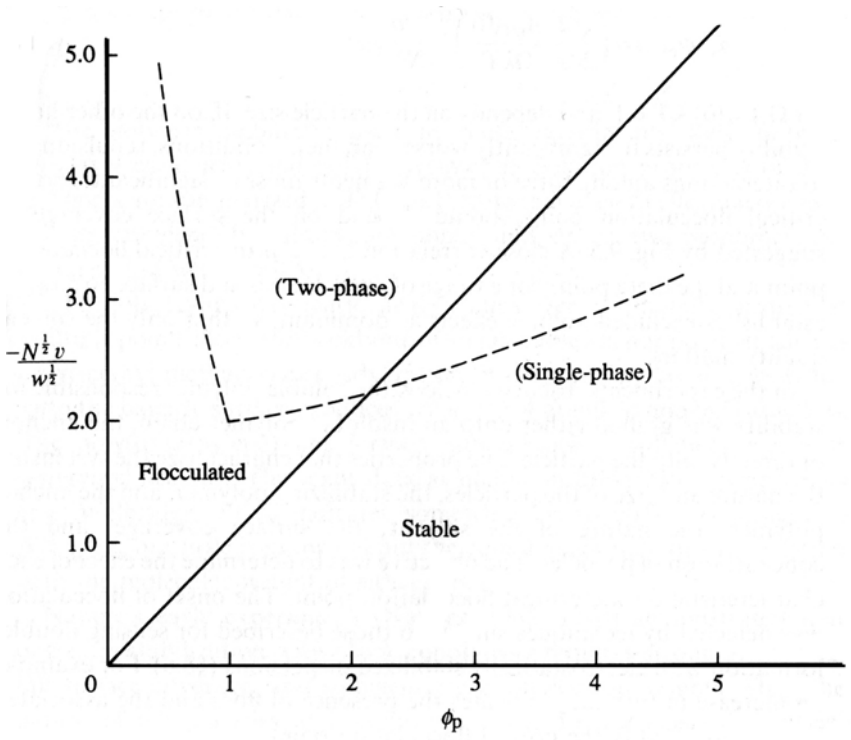

Figure 2.37: Values of the dimensionless excluded volume, $-N^{1/2}v/w^{1/2}$, corresponding to the critical flocculation point (—) for colloidal particles with surface coverage $\phi_p = Nw^{1/2}n_p/l$ and the phase boundary (---) for polymer solutions at concentration $\phi_p/N^{1/2} = N^{1/2}w^{1/2}n_p l$[88].

2.2.3.2 Important Experimental Work

2.2.3.2.1 Terminally Attached Polymers

In one study, the stability of dispersed latices with end grafted poly(oxyethylene) in a melt containing the same polymer was studied[97]. By doing this, the stability was determined only by the elastic compression of the chains and the dispersion forces. Figure 2.38 shows the particle size range that can be effectively stabilized by a particular molecular weight polymer. The slope of the line was fit to Equation 2.114 for the molecular weight dependence and predicted $aA/\Omega lkT = 4$, which is a reasonable value for the minimum layer thickness needed to stabilize polymeric particles in an organic solvent.

[97] Smitham, J.B.; Napper, D.H. *Journal of Colloid and Interface Science* **1976**, *54*, 467.

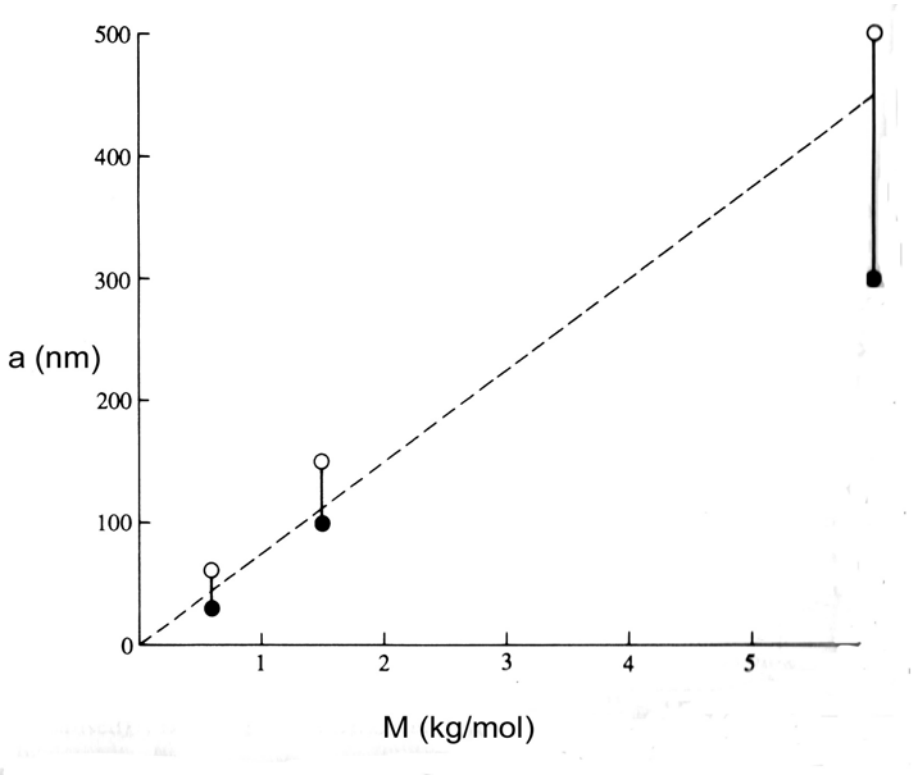

Figure 2.38: The maximum stable (●) and minimum unstable (○) particle radii a for latex spheres with poly(oxyethylene) chains of molecular weight M dispersed in a melt of the same composition. The broken line represents the prediction of (9.2.5)[88].

2.2.3.2.2 Physisorbed Polymers

2.2.3.2.2.1 Homopolymers

The forces between mica surfaces coated with polystyrene (PS) in cyclohexane have been studied using the Israelachvili surface forces apparatus, described in the previous section[98]. Measurements were done at partial and full surface coverage and at temperatures above and below the theta temperature for PS in cyclohexane. Figure 2.39 shows a schematic summary of the data obtained in this work. By comparing curve *i* to curve *iii*, it is shown that when the surface was not completely covered the attractive forces between the surfaces were much greater than at full coverage. This was probably due to bridging of the polymer between the surface at partial saturation conditions. Also, the separation distance at which the forces became repulsive for the partial coverage case

[98] Israelachvili, J.N.; Tirrell, M.; Klein, J.; Almog, Y. *Macromolecules* **1984**, *17*, 204.

was much closer because the thickness of the polymer layer was less. For temperatures above the theta temperature the forces were still attractive, as shown in curve *ii*, but the magnitude of this attraction was less than at conditions below theta. Even though the polymer was in a slightly better than theta solvent, there were still attractive forces between the surfaces.

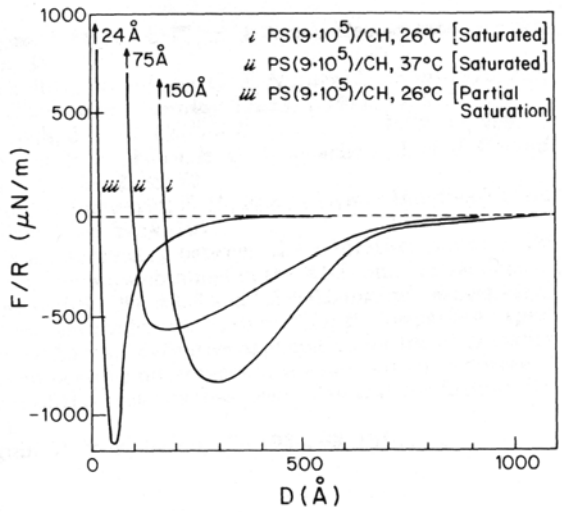

Figure 2.39: Schematic comparison of data for PS (9 X 10^5 molecular weight)[98].

2.2.3.2.2.2 Brush Formers

A block copolymer was studied for its stabilizing ability on colloidal particles of α-Fe_2O_3[99]. The anchor block of the copolymer was a charged poly(vinyloxy-4-butyric acid) (PVOBA), while the tail block was the uncharged poly(vinylmethylether) (PVME). Various polymers of different tail block molecular weights were tested, along with the homopolymers of each block. The effect of the ionic strength of the aqueous dispersion on the stability for each copolymer was also studied.

All of the adsorbing polymers were shown to stabilize the particles, by using optical microscopy. Rheological measurements were used to determine the stability based on which systems showed non-Newtonian behavior, or specifically a Bingham yield stress. The copolymers with low molecular weight tails (< 200 DP) showed a yield stress at low

[99] de Laat, A.W.M.; Schoo, H.F.M. *Colloid and Polymer Science* **1998**, *276*, 176.

ionic strengths, which increased in value when the salt concentration was increased. Those copolymers with high molecular weight tail blocks (> 400 DP) displayed no yield stress, regardless of ionic strength. Thus, when the tail length was low the electrostatic effects from the anchor block dominate the stability of the α-Fe_2O_3 particles, as seen by the stability differences with ionic strength. For longer tail blocks though, the steric effects dominated, and the electrostatics do not affect the stability.

In another study a block copolymer was used to stabilize SiO_2 particles[100]. The tail block was the uncharged poly(dihydroxypropyl methacrylate) (HMA), and the anchor block had a positive charge, poly(dimethylaminoethyl methacrylate) (AMA). The adsorbed amount and the stabilization effect of the block copolymer were measured at various block length ratios and at different ionic strengths and pH. The total molecular weight of the copolymer was kept constant at about 20 kg/mol.

The adsorbed amount showed a maximum at an AMA fraction of 0.1, which is close to the value of 0.05 predicted by the MJ theory discussed in the previous section. As shown in Figure 2.40 there was a minimum in the stability near this same molecular composition, which was independent of the ionic strength. At pH 4.5 there was a decrease in stability with increasing ionic strength for $\nu_{AMA} > (\nu_{AMA})_{min}$. This shows that as the anchor block molecular weight is increased the electrostatic effects begin to dominate, and the stability decreased at high ionic strengths. These results show that even at high adsorbed amounts the electrostatic effects dominate the stability by charge neutralization. As shown in Figure 2.40(b) for pH 7, there was little affect of ionic strength on the stability above I = 0.1 M. The results at high anchor block content were expected to be similar to those at pH 4.5 because of the electrostatics, and it is unclear why the system remained stable at high ionic strength.

[100] Hoogeveen, N.G.; Cohen Stuart, M.A.; Fleer, G.J. *Colloids and Surfaces A* **1996**, *117*, 77.

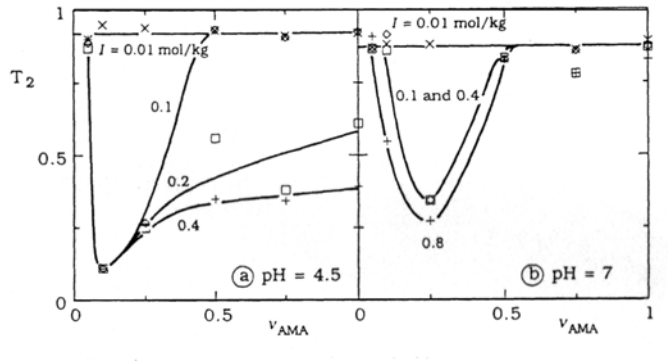

Figure 2.40: The transmission in a spectrophotometer, used to measure the stability of SiO_2 dispersions covered with HMA-AMA block copolymers as a function of the composition at various ionic strengths at: (*a*) pH 4.5, (*b*) pH 7. The polymer concentration was 1000 mg/kg[100].

The stabilization effects from a graft copolymer on polystyrene latex (PSL) in water was studied by several different methods[101]. The copolymer used had a poly(methyl methacrylate) (PMMA) backbone with methoxy capped poly(ethylene oxide) (PEO) side chains. The side chains were approximately 17 repeat units long and were spaced one every 15 backbone units. The stability was measured with direct force measurement of mica crossed cylinders and by osmotic pressure, π, and rheology of PSL dispersions.

The force measurement curves were typical for a terminally attached polymer, which the graft copolymer resembles. The curves showed an exponential decrease in the interaction energy with increasing separation. The osmotic pressure data were converted to interaction energy and showed good qualitative agreement with the direct measurements. The rheological data showed that, at low particle volume fractions, the dispersions were more "liquid-like", but at higher volume fractions they were more "solid-like". The SFA data was converted into a high frequency storage modulus, and the results were compared to the rheological data. Again, the trends were qualitatively similar, although the rheological results seemed to be more sensitive at large separations.

[101] Costello, B.A..; Luckham, P.F.; Tadros, TH.F. *Journal of Colloids and Interface Science* **1992**, *152*, 237.

From the theory and experiments presented in this section it is clear that the interaction potential between two particles can be modified by the adsorption of a brush forming block copolymer. These interaction forces can be measured using the AFM technique in Professor Ducker's group. Specifically, by increasing the molecular weight of the tail block in the polypeptide diblock, the Al_2O_3 particles can be sterically stabilized. The stabilization can be monitored using rheology and sedimentation experiments, discussed in Section 2.3.

2.2.4 Depletion Flocculation

Nonadsorbing polymers can also affect the stability of colloidal dispersions. If the polymer concentration is high enough, the polymer coils can cause the particles to aggregate, a situation called depletion flocculation. This flocculation is reversible, because the polymer is not adsorbed on the surface, and the suspension can be restabilized upon dilution. A discussion on one of the theories currently being used to model this phenomena will be followed up by a brief summary of some of the important experimental work in this field.

2.2.4.1 Theory

When a nonadsorbing polymer, or hard sphere, is introduced into a stable colloidal suspension the polymer coil will be displaced from the particles due to restrictions on the conformational entropy. This depletion zone, as shown in Figure 2.41, will have a size on the order of the radius of gyration of the polymer coil[102]. As two particles come into close contact, these depletion zones will overlap, causing expulsion of the polymer coil. Now there is a difference in the chemical potential between the bulk solution and that in the overlapping depletion zone. This in turn, will drive the solvent molecules out of the gap, lowering the free energy. The particles are essentially forced together by the osmotic pressure difference due to the free polymer.

[102] Jenkins, P.; Snowden, M. *Advances in Colloid and Interface Science* **1996**, *68*, 57.

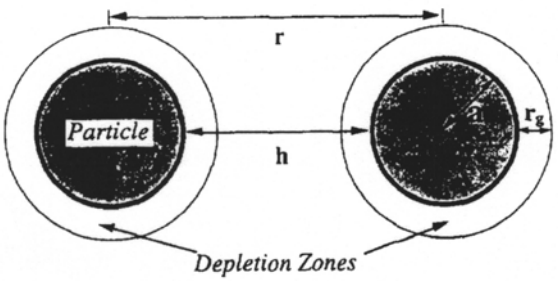

Figure 2.41: Depletion Zone caused by nonadsorbing polymer, r is the center-to-center separation of the particles, h is the surface-to-surface separation, and r_g is the radius of gyration of the polymer coil, which determines the depletion layer thickness[102].

In order for depletion flocculation to occur, a minimum polymer concentration must be achieved in the bulk, or a critical volume fraction for flocculation, ϕ^*. Below this concentration the particles will remain stable. At very high polymer concentrations the system may actually regain stability. However, the reasons behind this restabilization, and whether it is of thermodynamic or kinetic origins, is still unknown.

One of the first theories on depletion flocculation was introduced by Asakura and Oosawa[103], and is categorized as a volume exclusion theory[102]. The interaction between two spherical particles was given as the free energy required to bring two particles together from an infinite separation to a separation h, where $h < 2r_g$:

$$\Delta G^{dep} = \Delta\Pi\Delta V \qquad \text{Equation 2.116}$$

where ΔV is the extra volume available due to the overlapping of the depletion zones, and is given by:

$$\Delta V = \frac{4}{3}\pi\left(a + r_g\right)^3\left(1 - \frac{3r}{4\left(a + r_g\right)} + \frac{r^3}{16\left(a + r_g\right)^3}\right) \quad \text{for } 2a < h < 2(a + r_g) \qquad \text{Equation 2.117}$$

$$\Delta V = 0 \qquad \text{for } h > 2(a + r_g) \qquad \text{Equation 2.118}$$

where ρ is the center-to-center distance between the particles, and a is the radius of the particles. Thus, as the particles move apart, the extra volume decreases, until the depletion zones no longer overlap, at $h = 2(a + r_g)$.

[103] Asakura, S.; Oosawa, F. *Journal of Polymer Science* **1958**, *33*, 183.

The other factor in the free energy is ΔΠ, which is the difference in the osmotic pressure between the bulk solution and that in the depletion zone, and is given by:

$$\Delta\Pi = -\rho kT \qquad \text{Equation 2.119}$$

where ρ is the number density of polymer molecules in the bulk solution. Combining these expressions yields the depletion free energy:

$$\Delta G^{dep} = 0 \qquad \text{for } r < 2a \qquad \text{Equation 2.120}$$

$$\Delta G^{dep} = -\frac{4\pi}{3}\left(a + r_g\right)^3\left(1 - \frac{3r}{4\left(a + r_g\right)} + \frac{r^3}{16\left(a + r_g\right)^3}\right)\rho kT \qquad \text{Equation 2.121}$$

$$\text{for } 2a < r < 2(a + r_g)$$

$$\Delta G^{dep} = 0 \qquad \text{for } 2(a + r_g) < r \qquad \text{Equation 2.122}$$

Thus, at the two extremes (the particles are in contact or their depletion zones do not overlap) the attractive energy is zero, but within this region there is an attractive energy well, forcing flocculation.

One of the major drawbacks of this theory is that it predicts that the attractive energy will increase continuously with increasing polymer concentration, via ρ. As previously discussed, there is expected to be a decrease in the attraction at high polymer concentrations. Several extensions to this model have been introduced to try to overcome this deficiency[102], but they will not be discussed here.

2.2.4.2 Important Experimental Work

There are two very different approaches, experimentally, to studying depletion flocculation. The first is by directly measuring the interactions via atomic force microscopy (AFM) or total internal reflectance microscopy (TIRM). This would obviously be the most beneficial way to measure depletion flocculation, because a direct comparison with theoretical calculations could then be made.

The other approach is to monitor the flocculation indirectly, using rheological techniques, settling experiments, and phase separation, which monitor the colloidal stability. Most of

the earlier work in this field used these more qualitative methods to investigate depletion flocculation[104,105]. The details of rheological and sedimentation experiments can be found in Section 2.3, and only the direct techniques will be discussed here.

Most of the more recent work in depletion flocculation has used AFM to directly measure the depletion interactions. Even with a very sensitive instrument, such as AFM, it is often difficult to separate the weak depletion interactions from the van der Waals and electrostatic interactions. One group of researchers has found a way to overcome this difficulty by minimizing the other interactions[106]. They chose a low-polarity solvent to minimize the electrical double-layer interactions, which also had a refractive index close to the particles studied to minimize the effective Hamaker constant and thus the van der Waals interactions. In this study the interactions between a silica sphere and a silica surface, both covered with terminally attached n-octadecyl alcohol chains, in a cyclohexane solution containing the nonadsorbing free polymer, poly(dimethyl siloxane) (PDMS).

The authors found no attractive minimum when pure cyclohexane was used in the AFM, and only the repulsive force due to compression of the terminally attached chains was observed at very close contact. However, when the PDMS was added a significant attractive minimum was observed, as shown in Figure 2.42, before the octadecyl chains became compressed and exerted a repulsive force. The length of the depletion zone from the curves was calculated to be around 10 nm, which is comparable to the radius of gyration of the PDMS. Another observation was that the repulsive barrier occurred at around 3-4 nm, which would indicate that there was no free polymer in the gap, on the octadecyl chains. The magnitude of the depletion forces measured with AFM were on the order of those determined from theoretical calculations.

---

[104] Sperry, P.R.; Hopfenberg, H.B.; Thomas, N.L. *Journal of Colloid and Interface Science* **1981**, *82*, 62.

[105] De Hek, H.; Vrij, A. *Journal of Colloid and Interface Science* **1981**, *84*, 409.

[106] Milling, A.J.; Biggs, S. *Journal of Colloid and Interface Science* **1995**, *170*, 604.

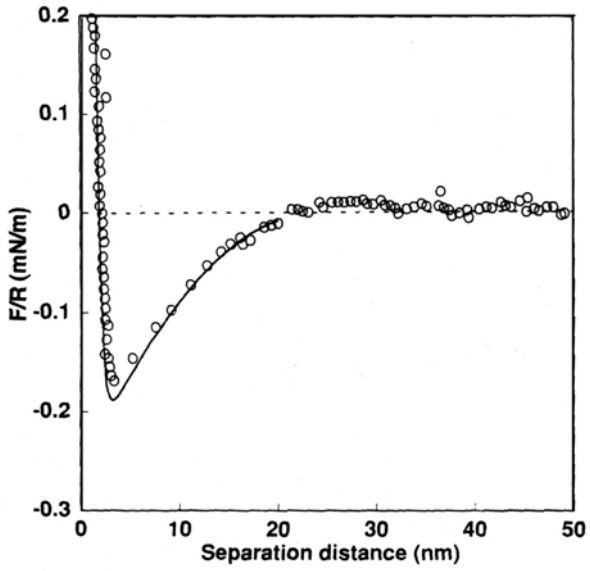

Figure 2.42: The force as a function of surface separation for a stearylated silica probe interacting with a flat sterarylated silica surface mediated by a cyclohexane solution of PDMS. The solid line represents a fitted steric plus depletion interaction forces. Modified from reference 106.

In another study, the depletion forces were measured for a nonadsorbing polyelectrolyte using AFM[107]. It is expected that the depletion interactions will be significantly larger for a charged polymer than for the neutral polymer, due to electrostatic interaction between the polymer and the solvent. The interaction force between a silica particle and a silica surface was measured with added poly(acrylic acid) at different ionic strengths and polymer concentrations. A schematic of a typical force versus separation curve is shown in Figure 2.43. Note the depletion minimum, and that the depletion zone thickness, Δ, is equal to one half times the separation at the onset of the flocculation minimum. In a few experiments an oscillatory curve was found, which is attributed to a structural force. When no salt was added there was an observed depletion force, which increased in magnitude with increasing polymer concentration. Long-range structural forces were also observed, due to the strong electrostatic interactions between the polymer and the solvent. At higher ionic strengths adsorption of the polymer was observed, which lead to a repulsive interaction at very high polymer concentration.

[107] Milling, A.J.; Kendall, K. *Langmuir* **2000**, *16*, 5106.

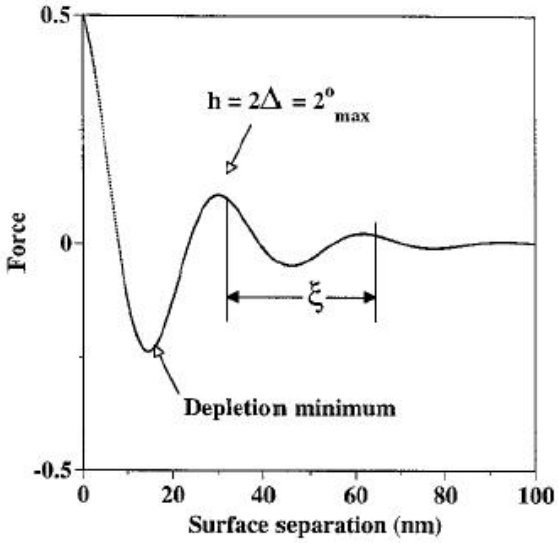

Figure 2.43: Typical force versus surface separation curve for depletion flocculation measured with AFM for a non-adsorbed polyelectrolyte[107].

The depletion flocculation due to a polyelectrolyte has also been studied using TIRM. In one experiment the effect of sodium polystyrene sulfonate (SPSS) on the interaction between a polystyrene particle and a glass slide was measured in water at different ionic strengths and polymer concentration[108]. TIRM is used to monitor the separation distance over a long time period. The probability, *p(h)* of finding the particle at a specific separation is then related to the total potential energy, E_{tot}, by the probability function:

$$p(h) = A\exp\left(\frac{-E_{tot}(h)}{kT}\right) \qquad \text{Equation 2.123}$$

where A is a normalization coefficient. For this work, 50,000 measurements were taken for each experiment. Again, the addition of the polyelectrolyte caused significant changes in the interaction and flocculation. At high polymer concentrations long-range structural forces were also observed. The authors compared these results with previous ones from an experiment were charged spheres were used instead of the polyelectrolyte. There was a much greater effect of ionic strength seen for the polymeric system, which

[108] Sharma, A.; Tan, S.N.; Walz, J.Y. *Journal of Colloid and Interface Science* **1997**, *191*, 236.

was attributed to geometric factors. Specifically, at low ionic strengths the polymer is extended like a rigid rod and at high ionic strength it is a random coil. The hard spheres on the other hand, do not change shape, and little effect of ionic strength is observed.

2.3 Rheology of Colloidal Dispersions

The rheology of colloidal dispersions is complicated by the particle-particle and particle-fluid interactions that affect colloidal stability. There are many factors which can effect the rheology, including the dispersant viscosity, the particle size, the particle volume fraction, and any additional polymers or surfactants. In order for a colloidal dispersion to be processable, the rheology must be controlled, so that the flow behavior can be predicted in a given flow geometry. The stability of the colloidal dispersion is crucial and can change the rheology dramatically, greatly affecting the processability. For example, when a suspension becomes colloidally unstable the viscosity can increase by several orders of magnitude and a yield stress can develop. Table 2.3 shows the typical range of shear rates for several different processing applications. This table demonstrates that the viscosity must be controlled over a range of shear rates, dependent on the application.

Table 2.3: Typical range of shear rates for various processing situations and the corresponding relevant applications. Excerpt from reference 109.

Situation	Typical range of shear rates (s^{-1})	Application
Sedimentation of fine powders	10^{-6} - 10^{-4}	Medicines, paints
Extruders	10^{0} - 10^{2}	Polymers
Chewing and swallowing	10^{1} - 10^{2}	Foods
Pipe flow	10^{0} - 10^{3}	Pumping, blood flow
Spraying and brushing	10^{3} - 10^{4}	Spray-drying, paints
High speed coating	10^{5} - 10^{6}	Paper
Lubrication	10^{3} - 10^{7}	Gasoline Engines

[109] Barnes, H.A.; Hutton, J.F.; Walters, K. "An Introduction to Rheology"; Elsevier: Amsterdam, 1989.

This section will focus on model colloidal systems to show the effects that different factors have on the suspension rheology. In particular, the parameters discussed will be the shear rate dependent viscosity, $\eta(\dot{\gamma})$; the storage and loss moduli, G' and G"; and the apparent yield stress, τ_o. The dependence of the parameters on: the particle volume fraction, ϕ; the viscosity of the medium, η_s; and the specific interactions between particles, including: hard sphere interactions, electrostatic interactions, the interactions between sterically stabilized spheres, and the interactions in weakly flocculated systems will also be discussed.

2.3.1 Theory – Viscosity Models

There are a number of rheological experiments that can be done to measure the properties of colloidal dispersions. The most common rheological tests are: simple shear, sinusoidal oscillation, and a transient test of either creep or stress relaxation. Details of these experiments and the governing equations can be found in Bird, Armstrong, and Hassager[110].

The viscosity of very dilute hard spheres in a Newtonian medium was first modeled by Einstein. When intrinsic viscosity, $[\eta]$, is expressed as a virial expansion in ϕ, Einstein showed that the first order term had a value of 2.5, reflecting single particle effects, which was independent of the particle size or the viscosity of the dispersing medium. This was then related to the viscosity of the suspension, η, and the viscosity of the medium, η_s, or the reduced viscosity, by:

$$\eta / \eta_s = 1 + 2.5\phi \qquad \text{Equation 2.124}$$

For $\phi > 0.02$, additional terms are needed to account for multiparticle interactions.

[110] Bird, R.B.; Armstrong, R.C.; Hassager, O. "Dynamics of Polymeric Liquids"; John Wiley and Sons: New York, 1987.

A typical viscosity versus shear stress curve shown in Figure 2.44 indicates the four flow regimes that a concentrated colloidal dispersion may exhibit. In regime I there is a zero shear Newtonian viscosity, η_o, of the randomly packed dispersion. Regime II shows the shear thinning that occurs as the three-dimensional dispersion breaks down into two-dimensional layers. In regime III the fluid exhibits an infinite shear viscosity, η_∞, which consists of thick two-dimensional ordered layers with a thickness approximately equal to a particle diameter. Finally, in regime IV the viscosity increases, and becomes dilatant, as the dispersion becomes unstable due to the hindered rotations and the mutual interference of the particle motion.

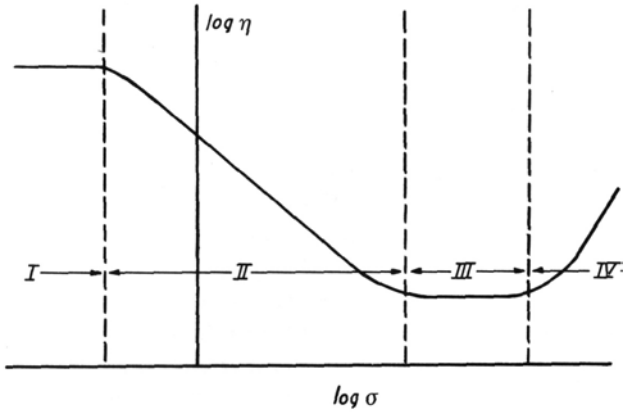

Figure 2.44: Possible flow regimes for colloidal dispersion, see text for description[111].

For steady simple shear flow the velocity in the direction of shear, as shown in Figure 2.45, is given by:

$$v_x = \dot{\gamma}_{yx} y$$

where $\dot{\gamma}_{yx}$ is the velocity gradient, whose absolute value is called the shear-rate $\dot{\gamma}$. The shear-rate dependent viscosity is defined in terms of the shear stress and the shear rate by:

$$\sigma_{yx} = \eta(\dot{\gamma}_{yx})\dot{\gamma}_{yx}$$

[111] Buscal, R.; Corner, T.; Stageman, J.F. "Polymer Colloids"; Elsevier Applied Science: New York, 1985.

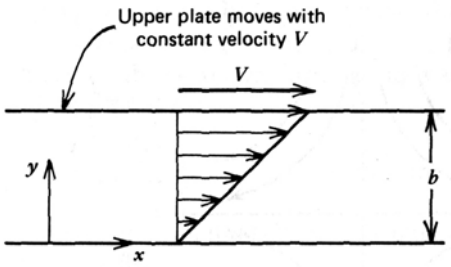

Figure 2.45: Steady simple shear flow with a shear rate $\gamma = V/b$[110].

For small amplitude oscillatory shear the plate in Figure 2.45 is now oscillated with a frequency ω, and:

$$v_x = \dot{\gamma} y \sin \omega t$$

The shear stress can now be written in terms of its in-phase and out of phase components by defining the storage modulus, G', and the loss modulus, G":

$$\sigma_{yx} = -G'(\omega)\gamma^o \sin \omega t - G''\gamma^o \cos \omega t \qquad \text{Equation 2.125}$$

where γ^o is the amplitude of the shear strain.

Another common rheological parameter encountered in colloidal dispersions is a yield stress, τ_y, which is the stress that must be applied in order for flow to occur, as shown in Figure 2.46. This occurs for suspensions exhibiting weak attraction forces, which causes the formation of a network. Below the yield stress the three-dimensional structure of the colloidal dispersion prevents fluid flow.

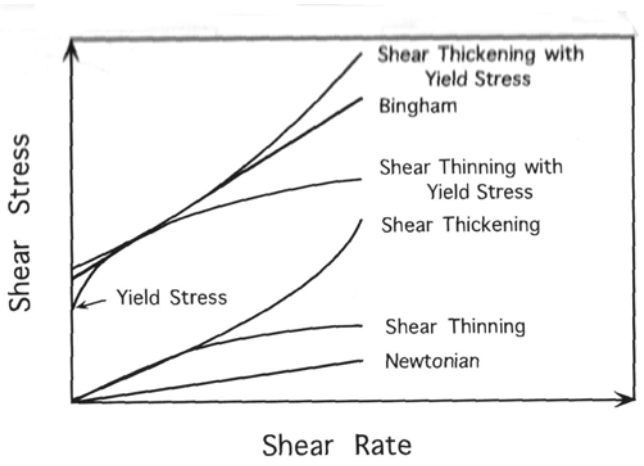

Figure 2.46: Effect of shear rate on the shear stress for different flow behavior models[112].

In order to describe the stress-strain behavior of more complex fluids, many constitutive equations have been developed. Particularly for colloidal dispersions, the Bingham, Casson, and Cross equations are very useful for fitting data into a predictive model. Experimentally there are two different methods which can be used to measure the yield stress. Typically, the value of the yield stress, τ_B is extrapolated using a constant rate rheometer and one of the previously mentioned constitutive equations. The problem with this method is that it only approximates the value of the yield stress and does not give a true yield stress. In order to obtain a true yield stress, a constant stress rheometer must be used, which directly measures τ_y.

2.3.2 Particle Interactions – Effect on Rheology

Now that an overview of the rheology of colloidal dispersions has been provided, some experimental results will be discussed that illustrate the role of particle interactions. Four principle interactions will be discussed including those between: hard spheres, charged spheres, polymerically stabilized particles, and weakly flocculated particles.

[112] Reed, J.S. "Principles of Ceramic Processing"; John Wiley and Sons: New York, 1995, p. 281.

2.3.2.1 Hard Sphere Interactions

The viscoelastic response of hard sphere dispersions is governed by viscous forces, Brownian motion, and the excluded volume of the particles. When the reduced viscosity is plotted against a reduced shear-rate, or the Peclet number, which is the ratio of the convection forces to the diffusion forces, the curves for different particle sizes and different medium viscosity at a constant volume fraction superimpose, as shown in Figure 2.47. At low Peclet values, Pe < 1, the microstructure is in equilibrium and dominated by Brownian motion, whereas at Pe >> 1, the convection forces dominate and it is difficult to reach equilibrium. Only the particle volume fraction affects the reduced viscosity. These data can then be fitted to one of the constitutive equations mentioned above for each value of ϕ.

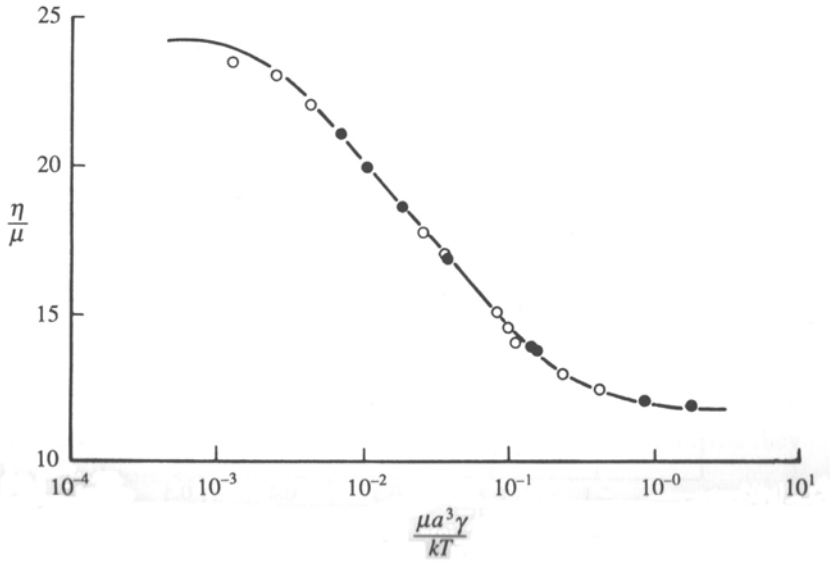

Figure 2.47: Relative steady shear viscosity as a function of the reduced shear rate for polystyrene latices[113].

An empirical equation was developed by Dougherty and Krieger to predict the effect of ϕ on the reduced viscosity. Their approach defines the final suspension as the sum of two consecutive additions of particles. A co-volume factor, *k*, is included because not all of

the particles in the suspension after the first addition are accessible to the particles in the second addition, which gives the functional equation[113]:

$$\eta_r(\phi_1+\phi_2)=\eta_r(\phi_1)\eta_r\left(\frac{\phi_2}{1-k\phi_1}\right)=\eta_r(\phi_2)\eta_r\left(\frac{\phi_2}{1-k\phi_1}\right) \quad \text{Equation 2.126}$$

The solution to this is:

$$\frac{\eta}{\eta_s}=\left[1+\frac{\varphi}{\varphi_m}\right]^{-[\eta]\varphi_m} \quad \text{Equation 2.127}$$

where [η] is the intrinsic viscosity, given above for hard spheres as 2.5, and ϕ_m is the maximum packing fraction at which flow can occur and is equal to 1/*k*.

The effect of the particle volume fraction on the reduced zero-shear and high-shear limiting viscosity is shown in Figure 2.48, as taken from Russel, et. al.[113]. The zero-shear viscosity increases more rapidly to an asymptote than the infinite-shear viscosity. This is due to the more ordered structure that the dispersion takes on at high shear rates, which allows for a higher fraction of particles to be incorporated into the suspension.

[113] Russel, W.B.; Saville, D.A.; Schowalter, W.R. "Colloidal Dispersions"; Cambridge University Press: New York, 1989.

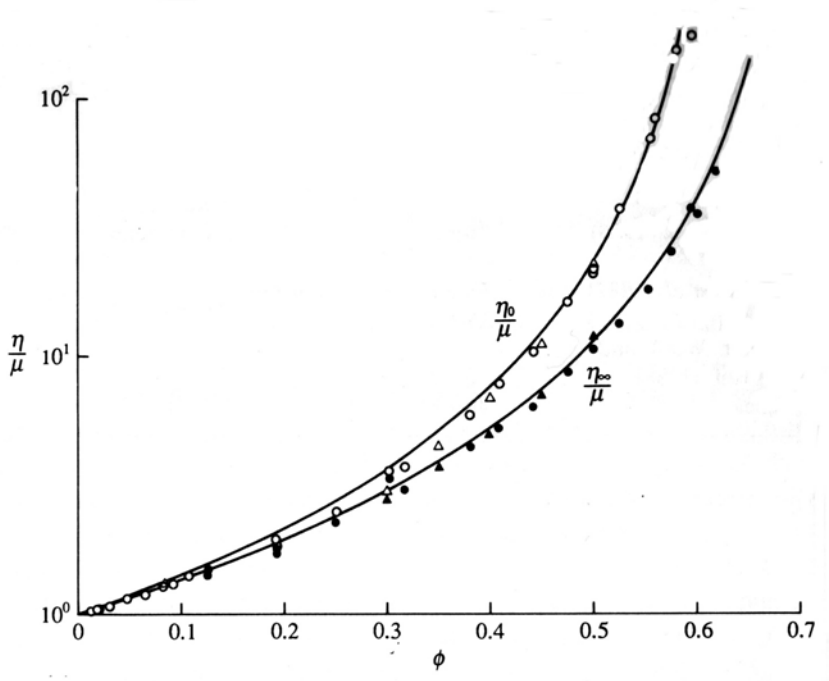

Figure 2.48: Zero (open symbols) and high (filled symbols) shear limiting viscosity for dispersions of hard spheres[113].

The data in the curves in Figure 2.48 have been correlated over the range of volume fractions using a Krieger type equation[113]:

$$\frac{\eta_o}{\eta_s} = \left(1 - \frac{\phi}{0.63}\right)^{-2} \qquad \text{Equation 2.128}$$

$$\frac{\eta_\infty}{\eta_s} = \left(1 - \frac{\phi}{0.71}\right)^{-2} \qquad \text{Equation 2.129}$$

where the factor 0.63 is the maximum packing fraction for randomly close packed spheres and 0.71 is that for face-centered cubic or hexagonal close packed spheres. For dilute suspensions these equations can be written as virial expansions[114]:

[114] De Kruif, C.G.; van Iersel, E.M.F.; Vrij, A.; Russel, W.B. *Journal of Chemical Physics* **1986**, *83*, 4717.

$$\eta_o/\mu = 1 + 2.5\phi + (4 \pm 2)\phi^2 + (42 \pm 10)\phi^3 + \ldots \qquad \text{Equation 2.130}$$

$$\eta_\infty/\mu = 1 + 2.5\phi + (4 \pm 2)\phi^2 + (25 \pm 7)\phi^3 + \ldots \qquad \text{Equation 2.131}$$

The variation between the two is not evident until the higher order interactions, the ϕ^3 term. This illustrates the lack of the long-range structure in these systems, which require three-body interactions.

The effect of the particle volume fraction on the reduced viscous stress, σ_c, which is the stress at $\eta = (\eta_o - \eta_\infty)/2$ that characterizes the shear thinning, is shown in Figure 2.49. The hard sphere points describe nondeformable, hard particles, whereas the soft sphere points describe deformable particles, such as when a polymer brush layer is adsorbed on the surface. The plot shows a maximum at $\phi \approx 0.5$, where a disorder-order transition occurs for the hard sphere case. Above $\phi = 0.63$, the characteristic shear thinning stress is zero, due to a lack of flow.

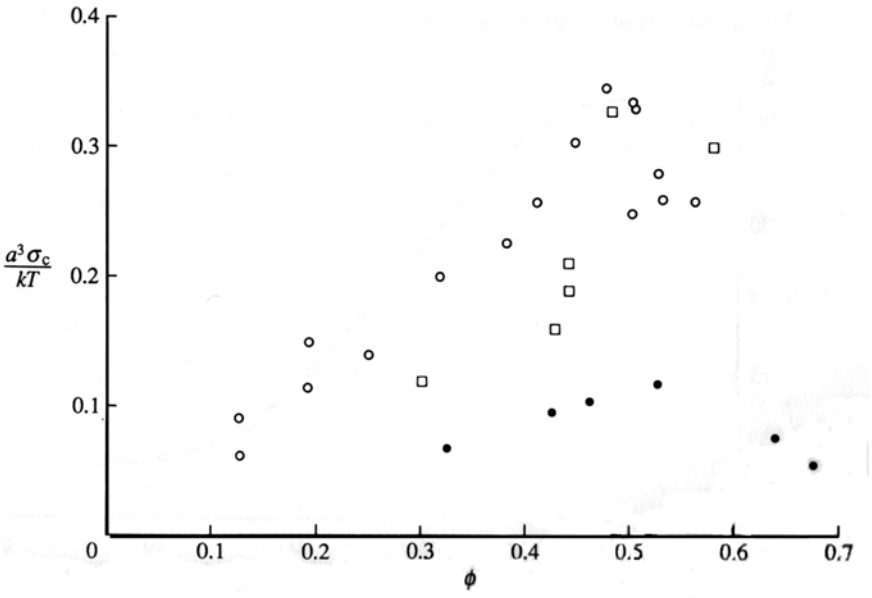

Figure 2.49: Dimensionless characteristic stresses for dispersions of hard spheres (open symbols) and soft spheres (filled symbols)[113].

Figure 2.50 shows the frequency dependence of the dynamic viscosity and the dynamic shear modulus. The important features of this graph are: (1) the data for two different sized silica particles superimpose as expected for hard spheres. (2) the high frequency dynamic viscosity does not equal the high shear viscosity. This demonstrates that for the steady shear experiments there is a hydrodynamically dominated structure at high shear rates, but at high frequencies there is only a perturbation in the equilibrium microstructure.

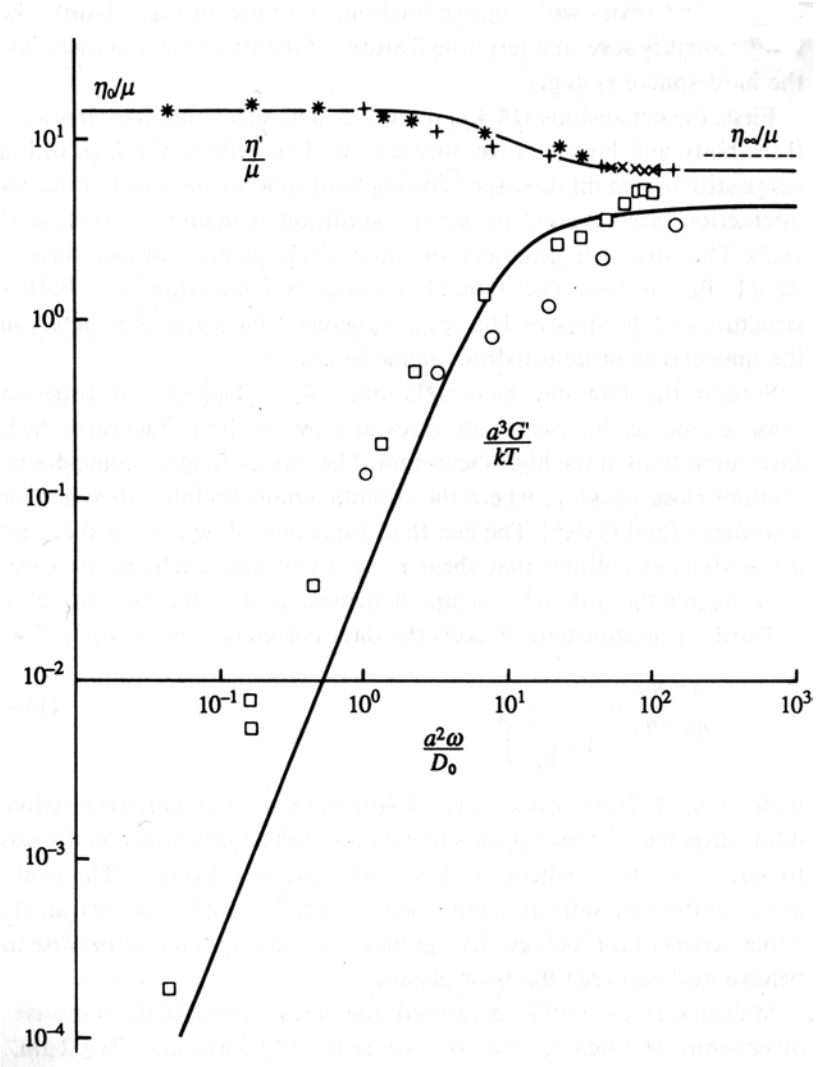

Figure 2.50: Shear moduli and dynamic viscosity for hard sphere silica particles[113].

2.3.2.2 Electrostatic Interactions

If the colloidal particles are charged, additional complexities become important, such as ionic strength and pH. At moderate salt concentrations, $a\kappa >> 1$, the thin double layer limit, the charges are screened and the rheology resembles that for hard spheres. At low values of ionic strength, there are long-range interparticle repulsion, which will dramatically effect the rheology, increasing the viscosity and possibly causing the onset of a yield stress.

The primary electroviscous effect is a relatively weak rheological factor that is caused by the deformation of the electrical double layer due to shear flow. The effect of this phenomena on the rheology is so small, and many instruments are not sensitive enough to measure it since it typically requires very high shear rates.

A much stronger contribution is from the secondary electroviscous effect. This is caused by the increase in the effective diameter, and thus the excluded volume, of charged particles due to the electrostatic repulsive forces. This is what causes the dramatic effects discussed above at low ionic strength. The Debye length, κ^{-1}, which defines the decay length for electrostatic interactions in solution, is calculated from:

$$\kappa^2 = \frac{2e^2 \sum n_0^i \left(z^i\right)^2}{\varepsilon kT}$$

where, n_o is the number concentration of counterions in the equilibrium salt solution, z is their valency, e is the elementary charge, ε is the dielectric permittivity of the solvent medium, and kT is the thermal energy. This is related to the effective particle volume fraction, ϕ_{eff}, due to the charge by[115]:

$$\phi_{eff} = \phi\left[1 + \frac{\kappa^{-1}}{a}\right]^3 \qquad \text{Equation 2.132}$$

This approximates the exponential decay of the electrostatic interactions with a step function, and is rather like a hard-sphere potential, which presumably should be

[115] Tadros, Th.F. *Advances in Colloid and Interface Science* **1996**, *68*, 97.

approached as $a\kappa >> 1$. Another approximation of this decay is given by Russel[113], where the decay length of the electrostatic repulsion is given by:

$$d \sim \frac{1}{\kappa} \ln\{\alpha / \ln[\alpha / \ln(\alpha / ...)]\} \qquad \text{Equation 2.133}$$

$$\alpha = \frac{4\pi\varepsilon\varepsilon_0 \psi_s^2 a^2 \kappa \exp(2a\kappa)}{kT} \qquad \text{Equation 2.134}$$

the effective hard-sphere particle volume fraction is then given as:

$$\phi_{eff} = \phi\left(\frac{d}{2a}\right)^3 \qquad \text{Equation 2.135}$$

The effective excluded volume of the spheres plays an important role in determining the maximum packing of the particles and thus on the rheology. An expression has been developed based on geometric arguments that gives the average surface-to-surface separation between neighbors, *h*, in terms of the particle diameter, *a*, as a function of the particle volume fraction[109]:

$$\frac{h}{2a} = \left[\left(\frac{1}{3\pi\phi} + \frac{5}{6}\right)^{1/2} - 1\right] \qquad \text{Equation 2.136}$$

In Figure 2.51 this equation is plotted as the average separation distance between particles versus the particle volume fraction. The top horizontal line gives the effective length scale for electrostatic interactions at I = 5 x 10^{-4} M or κ^{-1} = 14 nm. The bottom horizontal line give the layer thickness, δ, due to steric forces from an adsorbed polymer where, for example, δ is chosen to be 4 nm. The graph shows that for the electrostatically stabilized spheres the interparticle forces become important at $\phi < 0.25$, for a particle with a radius of 110 nm, at which point the viscosity would begin to increase sharply. For the polymerically stabilized system, the range of interactions is less, and thus for similarly sized particles, the interparticle forces do not become important until $\phi \geq 0.45$. Figure 2.51 also shows that if the size of the particles is increased, the maximum volume fraction before the onset of strong interactions between the particles increases.

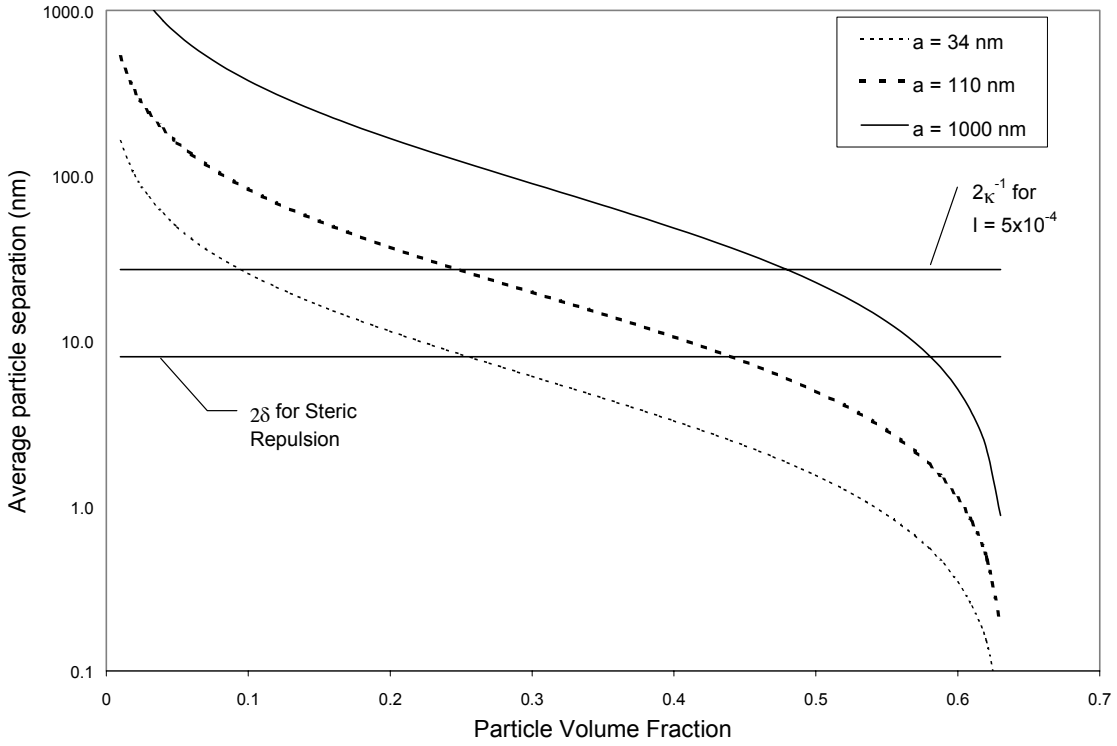

Figure 2.51: Average particle separation as a function of the particle volume fraction, for three different sized spheres. The top horizontal line shows the minimum separation allowable for a charged sphere at $I = 5 \times 10^{-4}$ M or $\kappa^{-1} = 14$ nm, and the lower line gives this value for a sterically stabilized suspension with layer thickness, $\delta = 4$ nm. Modified from reference 109.

The effect of electrostatic interactions is illustrated in Figure 2.52, which shows that the zero shear viscosity diverges at relatively low particle volume fractions, $\phi = 0.15$ at low ionic strength, compared to the hard sphere data in Figure 2.48. At this same value of ϕ there is the sudden appearance of a shear modulus, which is indicative of a disorder-order transition, and a yield stress.

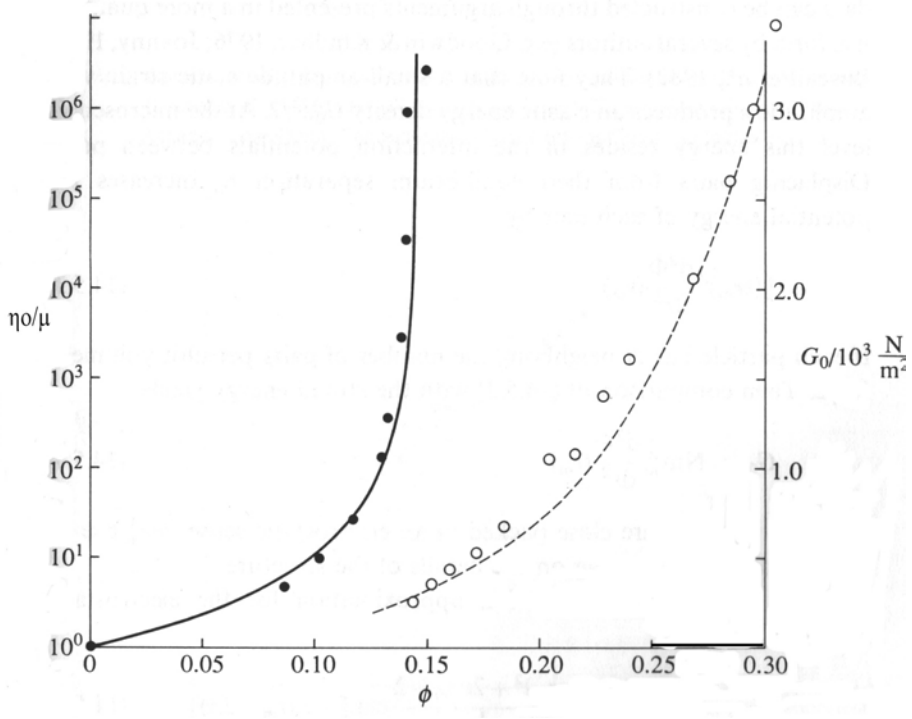

Figure 2.52: Zero-shear limiting viscosities and static shear moduli for polystyrene latices (a = 34 nm) in 5 x 10^{-4} M NaCl: ●, η_o; ○, G_o[113].

Experimental results have shown that the high shear viscosity limit, is not affected by varying the ionic strength, as shown in Figure 2.53. At high shear rates the hydrodynamic forces are stronger than the electrostatic forces, giving rise to a single value of η_∞ for a specific colloidal dispersion, independent of the salt concentration. The low shear viscosity limit, however, shows a significant effect due to ionic strength. As the ionic strength decreases, the interparticle electrostatic repulsion becomes stronger and thus η_o increases, as shown in Figure 2.53. Below a certain ionic strength there is a disorder-order transition, and the onset of a yield stress, evident at 1.9 X 10^{-3} M HCl.

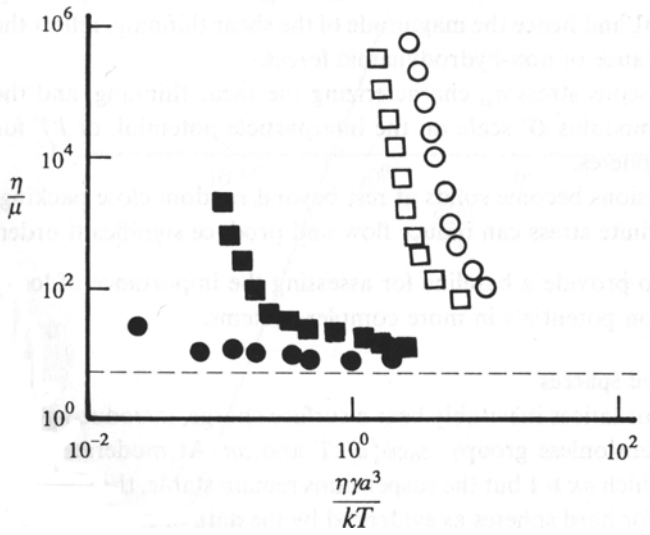

Figure 2.53: Steady shear viscosities for polystyrene latices (a = 110 nm) at $\phi = 0.40$ in water: ○, deionized; □, 1.9 x 10^{-4} M HCl; ■, 1.9 x 10^{-3} M HCl; ●, 1.9 x 10^{-2} M HCl; ---, hard spheres[113].

The effect of the ionic strength is even more evident in Figure 2.54. The onset of the yield stress, and the divergence from Newtonian behavior at 4 x 10^{-5} M HCl is quite obvious. Also, the jump in the shear stress seen in the 4 x 10^{-5} M HCl curve shows exactly where the system becomes disordered, and causes the viscosity to increases very quickly. There was also a visible transition in this system, the dispersions with yield stresses were iridescent while the disordered ones were not.

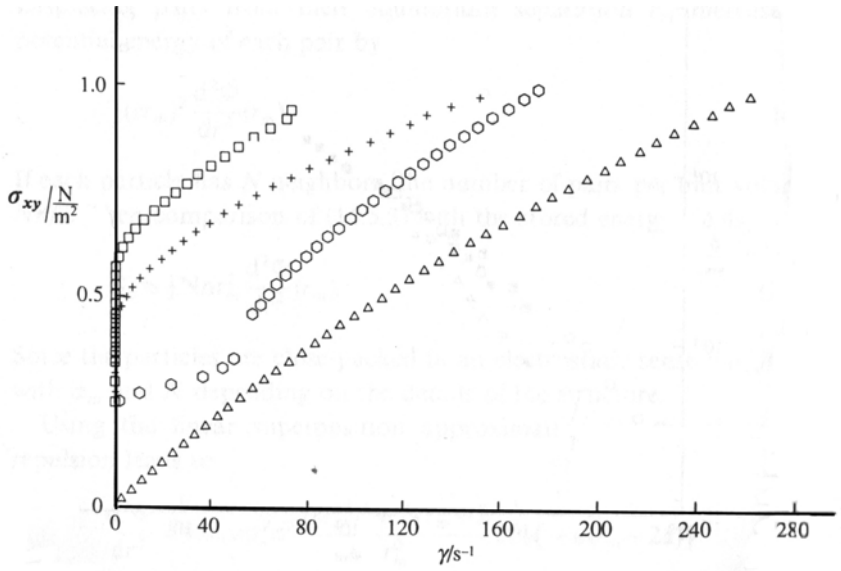

Figure 2.54: Shear stress as a function of shear rate for polystyrene latices (a = 45 nm) at $\phi = 0.04$ in □, deionized water; +, 1 x 10^{-5} M HCl; hexagons, 4 x 10^{-5} M HCl; △, 5 x 10^{-5} M HCl[113].

The adsorption of polyelectrolytes on colloidal particles will greatly affect the rheology. The effect of the addition of poly(methacrylic acid) (PMAA) and poly(acrylic acid) (PAA) on the stability and rheology of α-Al_2O_3 aqueous suspensions has been studied[116]. As shown in Figure 2.55, as the amount of solids was increased there was a more pronounced affect of pH on the viscosity. Not only did the viscosity increase with increasing Al_2O_3 volume fraction but the stable pH range decreased, with a minimum at pH 8.8, which is the pzc (point of zero charge) for the alumina. Below pH 8, the PMAA has a more neutral charge and more polymer is needed to stabilize the alumina. This was also due to an increase in the ionic strength, and thus screening of electrostatic repulsion, due to an increased concentration of ions associated with the polymer during pH adjustment. These two factors results in less electrosteric repulsion and an increase in viscosity. At high pH, above 9, the adsorption is not of the 'high affinity' type and there is excess polymer in the solution, which causes depletion flocculation and an increase in viscosity.

[116] Cesarano, J.; Aksay, I.A. *Journal of the American Ceramic Society* **1988**, *71*, 1062.

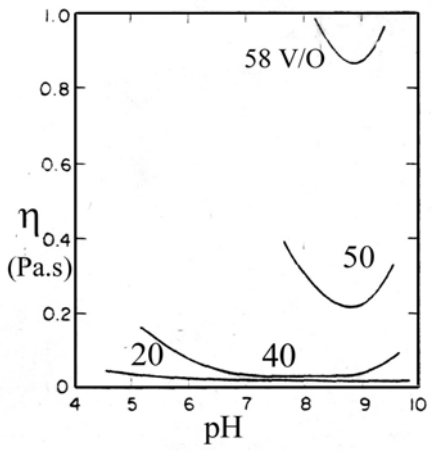

Figure 2.55: Viscosity versus pH for PMAA-stabilized alumina, at 9.3 s^{-1} at various particle volume percentages[116].

In Figure 2.56 the effect of varying the molecular weight of the PAA on the viscosity is shown. As the molecular weight is increased the effective operating window of polymer concentration is decreased. As polymer is added the particles become stabilized, and the viscosity reaches a minimum. At high polymer concentrations there is excess polymer in solution and depletion flocculation, which causes the viscosity to increase.

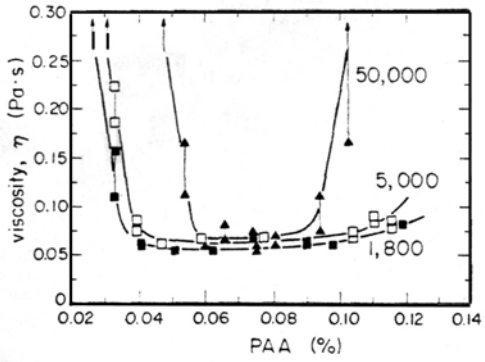

Figure 2.56: Viscosity versus PAA concentration for various molecular weights for 50% α-Al_2O_3 suspensions at pH 9. Open symbols are at 0 min and filled symbols are 10 min at a shear rate of 9.3 s^{-1}.[116]

2.3.2.3 Steric Stabilization

The adsorption of polymers and surfactants on dispersed particles can also greatly effect the rheology of colloidal dispersions. An adsorbed polymer layer with thickness δ has two primary effects, first to increase the effective particle volume fraction, ϕ_{eff}, by the following equation:

$$\varphi_{eff} = \varphi\left(1 + \delta/a\right)^3 \qquad \text{Equation 2.137}$$

This additional excluded volume causes the viscosity to be higher than the hard sphere case. Secondly, the adsorbed layer fixes the range of interactions between particles, thus eliminating the problems caused by the long-range electrostatic repulsion of charged particles. The charge on the particle and thus the effective volume fraction of the system will fluctuate when the ionic strength changes, as shown in Equation 2.132.

Sterically stabilized colloidal dispersions show scaling of the reduced viscosity with reduced shear-rate similar to hard sphere dispersions. The data can also be fitted to the Krieger equation, by replacing the particle volume fraction, ϕ, with the effective particle volume fraction, ϕ_{eff}.

Steric stabilization can be illustrated with the example of the effect of an ionic surfactant, poly(12-hydroxystearic acid), on the rheology of poly(methyl methacrylate) (PMMA) spheres in decalin[117]. For this system the ratio of the radius of the spheres to the layer thickness (a/δ) was varied from 5 to 61. For large particles or thin layers, the rheological behavior resembles that of hard spheres. When the adsorbed layer is thick with respect to the radius of the spheres, there is significant deviation from hard sphere behavior, and the particles are "soft". Figure 2.57 shows that similar to the hard sphere case, the viscosity increases with increasing effective particle volume fraction, and above $\phi_{eff} \approx 0.5$ there is the onset of a yield stress.

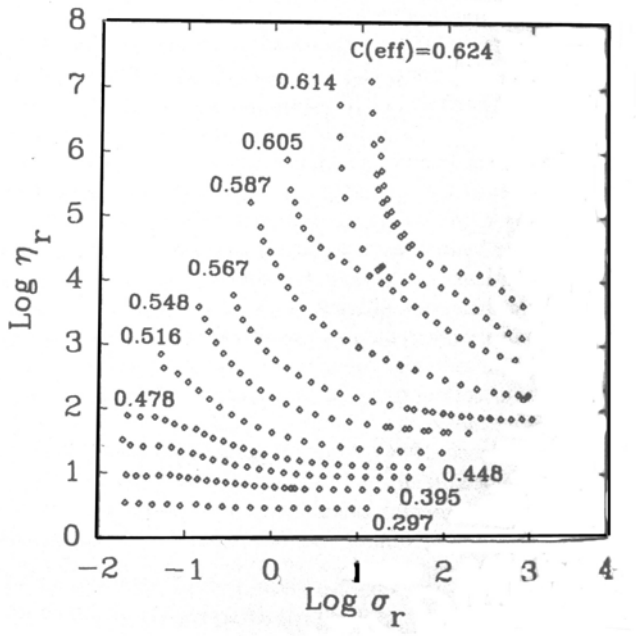

Figure 2.57: Change in the reduced viscosity versus reduced shear stress curves for different values of ϕ_{eff} = c(eff)[117].

The softness of the stabilized particles can be measured using the values for the zero and high shear viscosity at the maximum packing volume fraction. In Figure 2.58 the ratio of the equivalent hard sphere volume fraction to the effective volume fraction that produce the same viscosity at a particular shear rate is plotted against the effective volume fraction. The deviation from unity gives the degree of softness. The results show that the high shear viscosity shows more compressibility and softness than the zero shear viscosity. This is due to the ordering of the particles that takes place at high shear, as discussed above.

[117] Mewis, J.; Frith, W.J.; Strivens, T.A.; Russel, W.B. *AIChE Journal* **1989**, *35*, 415.

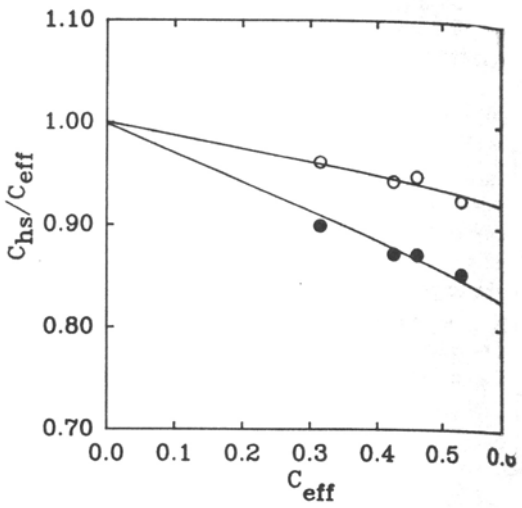

Figure 2.58: Ratio of the equivalent hard sphere volume to the effective volume fraction versus the effective volume fraction: ○, zero-shear viscosity; ●, high-shear viscosity. A measure of the softness of the stabilizing layer[117].

In Figure 2.59 the data for the viscosity are scaled with respect to the zero and high shear viscosity limits, giving a degree of shear thinning of the colloidal dispersion. This is plotted against the log of a reduced shear rate. This proves to be a viable technique to scale data for sterically stabilized systems, because all of the curves superimpose for different effective particle volume fractions.

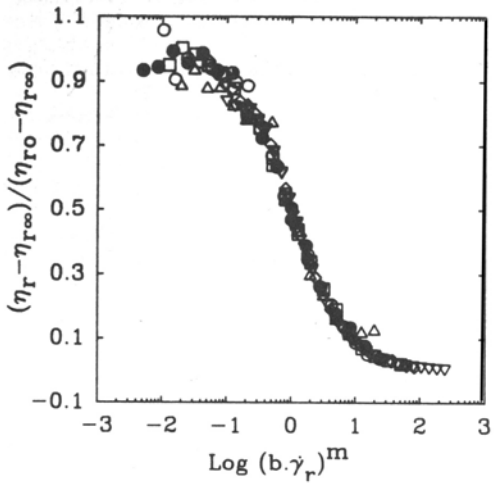

Figure 2.59: Intrinsic shape of the viscosity curve for soft spheres versus the relative shear rate for different effective volume fractions[117].

These model system studies were valuable because they demonstrate the general trends seen for sterically stabilized colloidal dispersions. These trends can also seen in more complex particle systems where size and shape are not well controlled. For example the effects of various surfactants and polymers on the rheology of coal/water dispersions was studied[118]. An ionic surfactant, Ufoxane 3A, which is a sodium lignosulfonate polyelectrolyte, was studied. This type of molecule is interesting in that it can stabilize via electrostatic and steric repulsion mechanisms. As shown in Figure 2.60, as the concentration of surfactant was increased, the adsorbed amount showed the typical shape for polymers. The complex modulus decreased dramatically at almost the same polymer dosage that the adsorption isotherm showed a sharp increase. At low Ufoxane concentrations, there was a flocculated structure, but as the amount of surfactant was increased, stabilization occurred. When the system was flocculated there was a very soft, thick, and easily redispersed sediment, but the stable dispersion settled into a very hard and dilatant sediment. These are typical results for sedimentation experiments, as will be discussed in Section 2.3.3.

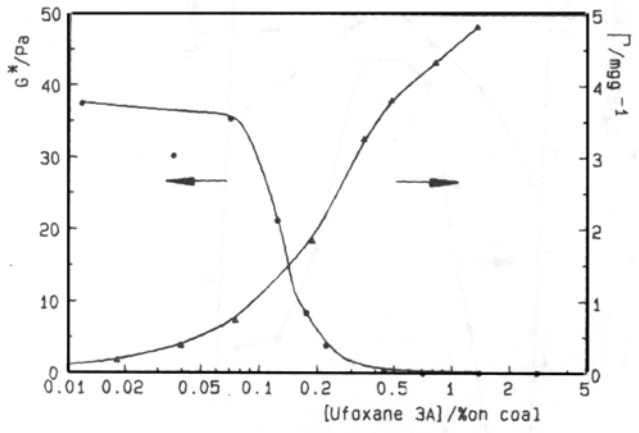

Figure 2.60: Effect of the ionic surfactant, Ufoxane 3A, concentration on the complex modulus and the adsorbed amount[118].

A nonionic surfactant, a hexamethylenediamine derivative with 4 tails of 10 propylene oxide and 55 ethylene oxide units extending out from the methylene center, called EL1602P, was also tested as a possible stabilizer for the coal. As shown in Figure 2.61,

[118] Tadros, Th.F.; Taylor, P.; Bognolo, G. *Langmuir* **1995**, *11*, 4678.

the viscosity, yield stress, and complex modulus all show a maximum around 0.1% EL1602P. This was attributed to a reorientation of the surfactant molecules on the surface as the adsorbed amount began to increase. At low polymer concentrations the PEO chains would adsorb on the surface via hydrogen bonding, and interactions between the center methylene groups that would face outward caused flocculation. Above a saturation concentration, further adsorption was due to the hydrophobic segments of the surfactant on the surface, and the PEO chains acted to sterically stabilize the particles.

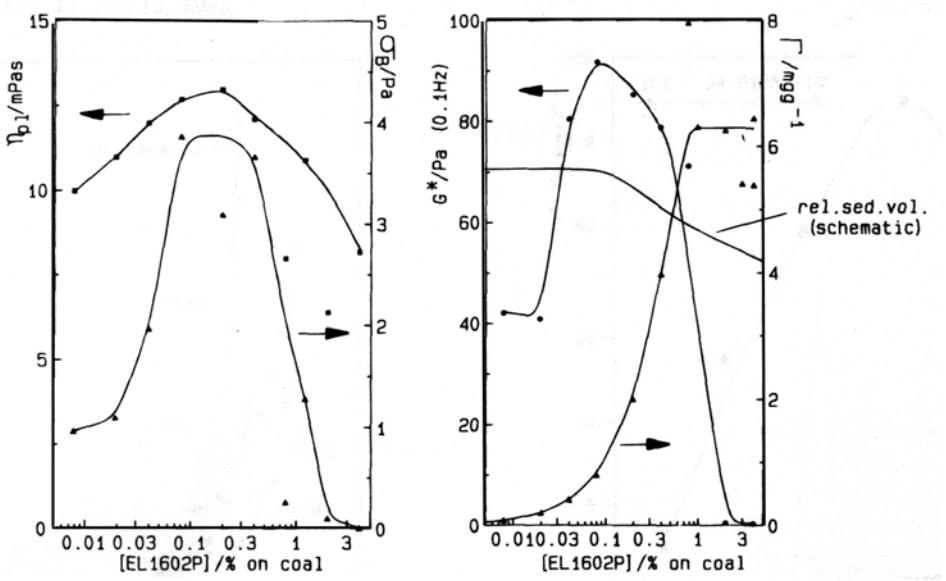

Figure 2.61: Effect of the nonionic surfactant, EL1602P, concentration on the viscosity, yield stress, complex modulus, relative sediment volume and the adsorbed amount[118].

A nonionic block copolymer was also studied for its effect on the rheology of coal/water dispersions. Several PEO-PPO-PEO, Pluronic™, block copolymers were studied with varying PEO block lengths, but with a constant PPO block length. For Pluronics, the PEO chain length increases with the ID number. It was expected that the PPO would adsorb onto the surface, while the two PEO chains would act as tail blocks for the stabilization of the coal particles. In Figure 2.62(a), the effect of tail length on the complex modulus, G*, is clearly visible. As the length of the tail is increased the complex modulus decreases, and the maximum volume fraction of particles increases. This shows an increased stability at longer PEO tails, as expected. The viscosity data for the same dispersions are shown in Figure 2.62(b). In this graph the differences between

the various stabilizers are not as visible, and all of the curves roughly superimpose. This shows that rheological measurements of flocculated structures are most accurate using a technique that causes minimal disruption to the microstructure. At high shear rates all of the dispersions resemble each other, and thus no differences are noticed in the viscosity data.

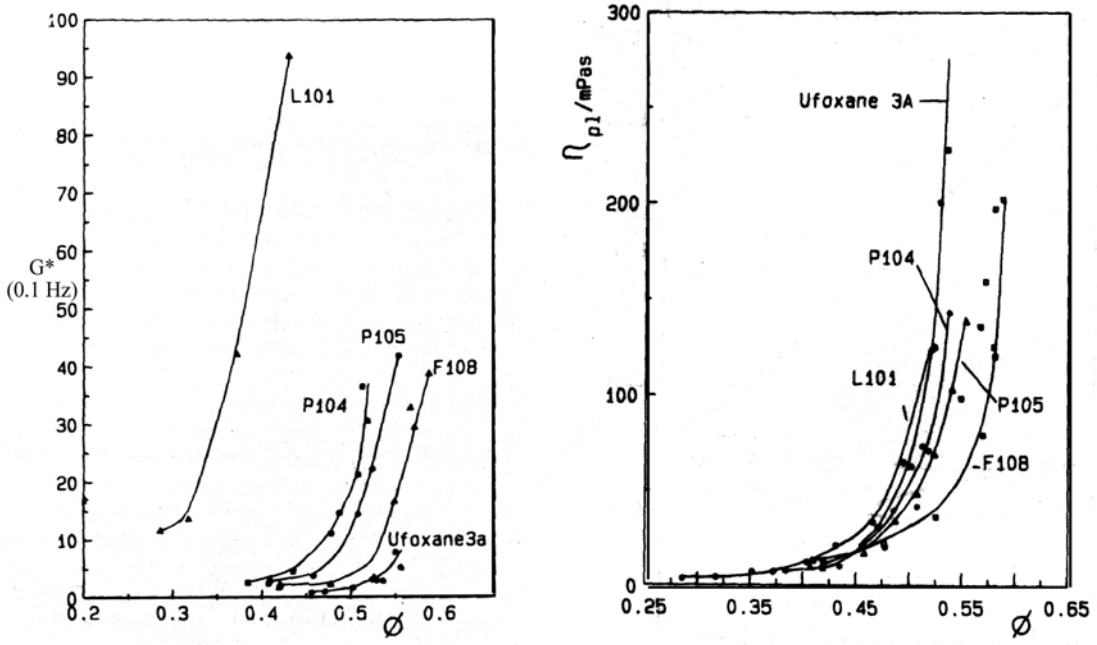

Figure 2.62: Effect of the volume fraction of coal for various PEO-PPO-PEO block copolymers and Ufoxane 3A (1% based on the weight of the coal) on (a) the complex modulus and (b) the viscosity[118].

The rheology of hydrophobically modified silica particles in water, stabilized with an ionic graft copolymer, has also been studied[119]. The copolymers used were designated as PAA N-XCn, where each has a backbone of poly(sodium acrylate) with N molecular weight, X – molar percentage of hydrophobic moieties in the copolymer and n carbon atoms on the side chains. The alkyl grafts would adsorb onto the silica surface, while the PAA backbone did not adsorb. In Figure 2.63(a) and (b) the effect of the added polymer concentration on the viscosity versus shear rate data is measured at two different particle

[119] Poncet-Legrand, C.; Lafuma, F.; Audebert, R. *Colloids and Surfaces A: Physiochemical and Engineering Aspects* **1999**, *152*, 251.

volume fractions. In both graphs, the viscosity varies with the polymer concentration with a minimum occurring around Cp = 0.2. This is conceptually shown in Figure 2.64. At very low polymer concentration, the particles are aggregated due to bridging flocculation and the viscosity is high. The viscosity continues to drop as more polymer is introduced into the system, until each particle is coated. Any additional polymer causes depletion flocculation between the particles, which results in an increase in the viscosity.

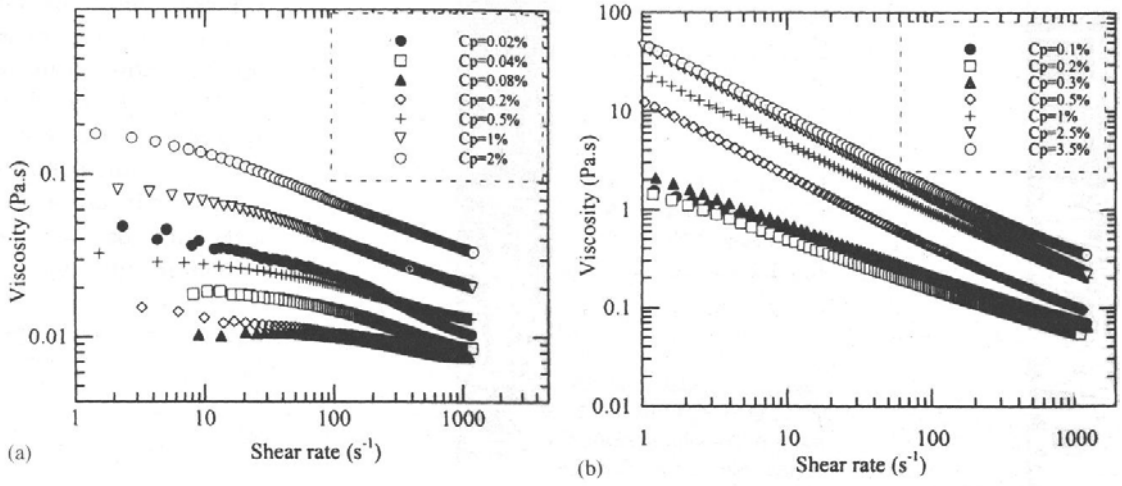

Figure 2.63: Effect of polymer concentration, PAA 20-5C12, on the rheology of the hydrophobic silica suspensions stabilized in water for two different particle volume fractions: (a) $\phi = 0.30$, (b) $\phi = 0.40$[119].

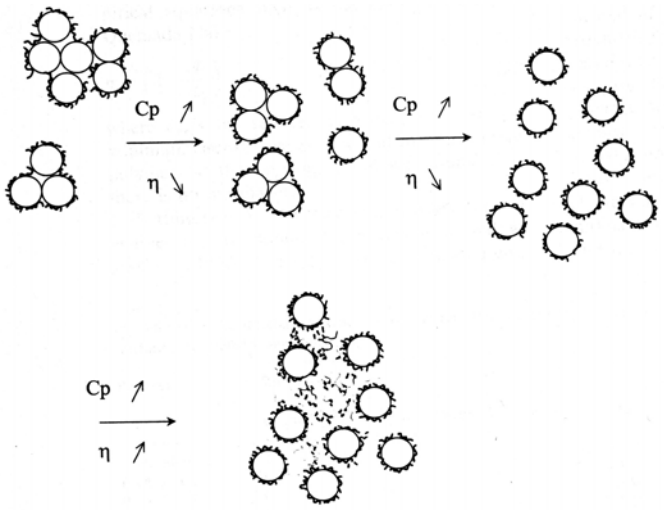

Figure 2.64: Schematic showing the evolution of the size of the aggregates and the change in the viscosity when the polymer concentration increases[119].

The addition of salt to this system can also affect the rheology of these polyelectrolyte stabilized dispersions, as shown in Figure 2.65. At low polymer concentrations, the addition of salt increases the viscosity by two orders of magnitude, compared to the suspension with no salt. This is due to screening of the electrostatic repulsion, which stabilize the silica particles. At polymer concentrations above 0.2% the two curves collapse at a low viscosity. When the amount of polymer is sufficiently high, the surface of the silica particles becomes saturated, and thus both steric and electrostatic repulsion are used to stabilize the system, and the effect of ionic strength becomes negligible.

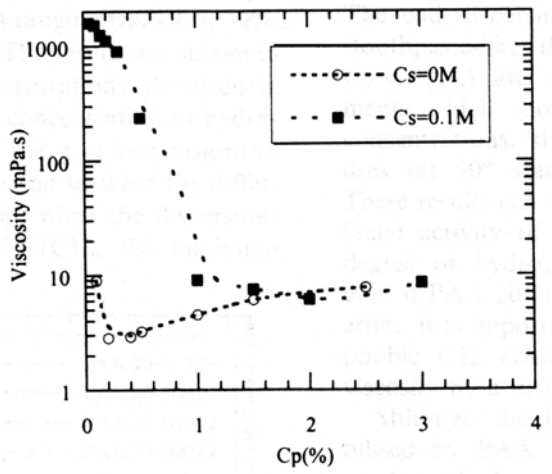

Figure 2.65: Effect of salt and polymer concentration on the viscosity of the hydrophobic silica suspensions stabilized by PAA 5-3C12, $\phi = 0.25$, viscosity measured at $100s^{-1}$.[119]

The amount and length of the alkyl chain will also effect the rheology. As shown in Figure 2.66, as the percentage of the hydrophobic component is increased, there is a reduction in the viscosity by an order of magnitude. Similar results were seen when the length of the alkyl chain was systematically increased. A minimum alkyl content, of a certain length, is required to stabilize the particles. Once this minimum is reached the viscosity changes very little with the addition of more hydrophobic character, because the polymer is already well anchored to the surface.

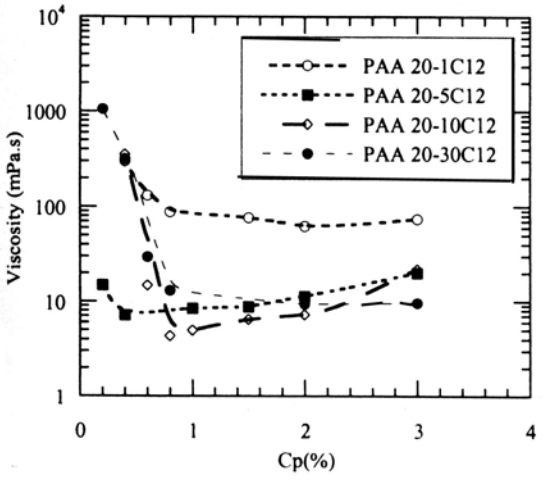

Figure 2.66: Effect of hydrophobicity of the polymer, due to a higher percentage of alkyl moieties in the copolymer, on the viscosity of the dispersions; $\phi = 0.25$, Cs = 0.1 mol/l, viscosity measured at 100 s^{-1}.[119]

The rheology of a system mentioned in Sections 2.1.1.2, a block copolymer containing poly(vinylmethylether) (PVME) and poly(vinyloxy-4-butyric acid) (PVBA) for the stabilization of α-Fe_2O_3, has also been studied[120]. The PVBA strongly adsorbs on the surface of the particles, while the PVME acts a tail block for stabilization. In this study, the molecular weight of the PVME was systematically varied, to determine its effect on the stability of the system. As the sample designation was varied from F1 to F6 the number of repeat units of PVME was varied from 0 to 612, while the PVBA degree of polymerization remained fairly constant at about 40-50 repeat units.

As shown in Figure 2.67, there was flocculation upon heating for most of the polymers containing PVME. As the length of the PVME chain was increased, the temperature at which flocculation occurred decreased. When there was no PVME there was no flocculation, and for the shortest PVME-containing copolymer, electrostatic interactions dominated and prevented flocculation. The temperature of flocculation was forced to lie between the θ temperature for the PVME and the LCST of the block copolymer. The length of the PVME chain determined where the flocculation will occur, relative to these two extremes.

[120] de Laat, A.W.M.; Schoo, H.F.M. *Journal of Colloid and Interface Science* **1998**, *200*, 228.

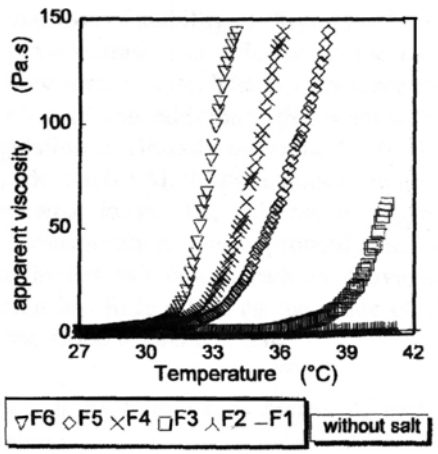

Figure 2.67: Effect of the tail block molecular weight on the viscosity as a function of temperature[120]. F1 has no PVME and F6 has the longest PVME blocks.

The ionic strength also had an effect on the rheology of these systems due to the electrostatic nature of the PVBA anchor block. As shown in Figure 2.68, as the salt concentration was increased, the viscosity increased and the temperature of flocculation decreased. This was due to screening of repulsive electrostatic interactions, which contribute to the stabilization of the particles. This result was not seen at higher PVME chain lengths, where the viscosity was independent of ionic strength because the steric forces dominated.

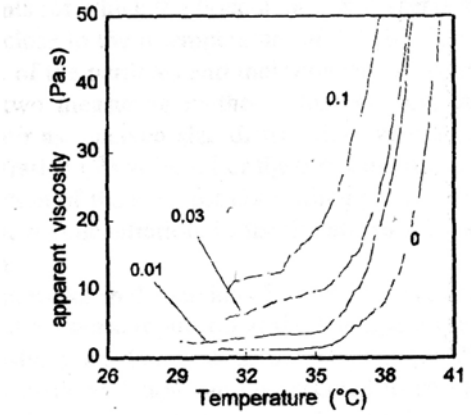

Figure 2.68: Effect of ionic strength on the viscosity as a function of temperature for polymer F3 dispersions at 0, 0.01, 0.03, and 0.1 M KNO_3[120].

2.3.2.4 Weakly Flocculated Particle Systems

Weakly flocculated colloidal dispersions respond elastically to deformation because of the non-hydrodynamic interactions between the particles. Although these systems are not thermodynamically stable, and will show macroscopic phase separation over time, they do form a metastable phase that can change little over the course of typical experimental measurements (minutes to hours). Thus, these systems do recover reproducibly after deformation. The complex rheological behavior of weakly flocculated particles is due to the non-equilibrium nature of these systems, and their history-dependent, or thixotropic, behavior.

A model system consisting of polystyrene latices stabilized with Triton X-405, and then flocculated via depletion flocculation with dextran has been studied[113]. The effect of the particle size, particle volume fraction, and polymer concentration or the depth of the attractive minimum, on the shear stress and dynamic modulus are shown for viscosity and storage modulus in Figure 2.69(a) and (b), respectively. The plots are complementary to each other. First, when the depth of the pair interaction secondary potential minimum is increased there is an onset of a yield stress, as shown by a minimum stress of 10^{-1} N/m2 needed for flow in (a) and the existence of a dynamic modulus at very low frequencies in (b). When the particle volume fraction was increased from 0.20 to 0.30, with the secondary potential minimum was kept constant, the shear stress needed for flow increased and the dynamic modulus at low frequencies increased.

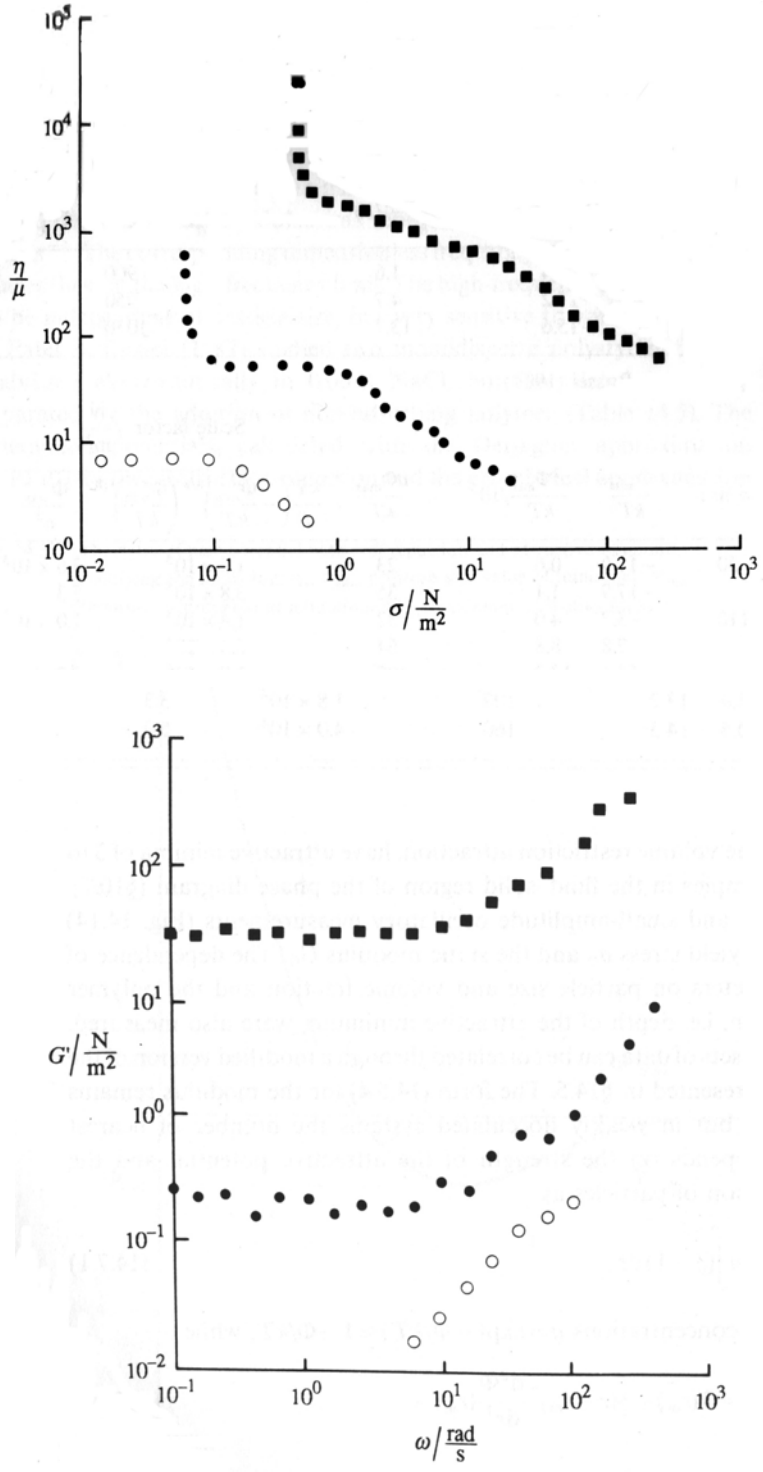

Figure 2.69: (a) Reduced shear viscosity plotted against the shear stress and (b) Shear modulus plotted against frequency: for polystyrene latices (a = 220 nm) in water at 0.06 M NaCl and 1.5 percent Triton X-405 with soluble dextran (Mw = 600 kg/mol, r_g = 33 nm added: ○, $\phi = 0.20$, $\Phi = -1.5kT$; ●, $\phi = 0.20$, $\Phi = -20kT$; ■, $\phi = 0.30$, $\Phi = -20\ kT$[113].

In a similar study, monodisperse polystyrene latex was first stabilized using a graft copolymer consisting of a poly(methyl methacrylate) backbone with PEO side chains. The addition of different molecular weights of hydroxyethyl cellulose (HEC) on the rheology, and particularly on the extrapolated yield stress value, τ_B, was measured[121]. As shown in Figure 2.70, the yield stress value increased with increasing HEC polymer volume fraction, ϕ_p, similar to the behavior shown above for the dextran study. Also, the yield stress increased very dramatically when the HEC molecular weight was increased, and showed an even greater effect when a hydrophobically modified HEC polymer, containing long chain alkyl groups, was used.

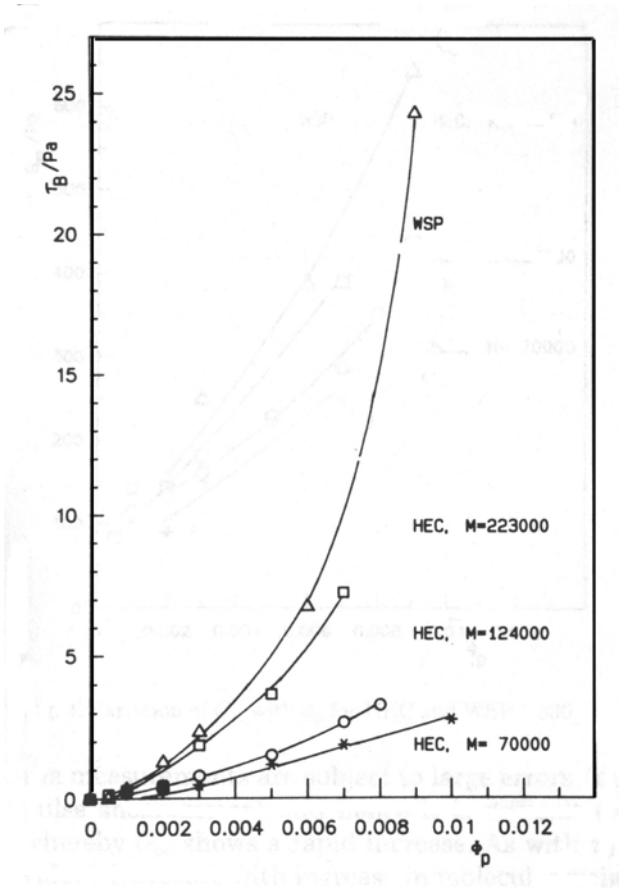

Figure 2.70: Effect of HEC concentration, ϕ_p, and HEC molecular weight on the extrapolated yield stress, τ_B[121].

[121] Tadros, Th.F.; Zsednai, A. *Colloids and Surfaces* **1990**, *49*, 103.

2.3.3 Sedimentation

Sedimentation is another experiment that can be done to qualitatively assess the stability of colloidal suspensions. Due to the difference in density between the particles and the surrounding medium, most colloidal systems will settle with time. For those cases where the particle density is greater than the fluid density, the particles will tend to settle due to gravitational forces. If the particles are submicron in size (as they are for this proposed work) these forces will be opposed by Brownian motion due to the translational kinetic energy. If the gravitational potential energy is much greater than the kinetic energy then the suspension will undergo complete settling,[122] i.e. when:

$$\tfrac{4}{3}\pi a^3 \Delta\rho g L >> kT \qquad \text{Equation 2.138}$$

where a is the radius of the particle, $\Delta\rho$ is the density difference between the particles and the medium, g is the acceleration due to gravity, and L is the height of the container. If the kinetic energy is greater than the gravitational force than there will be very little sedimentation. This latter case will occur for either very small particles or if the particles are in a medium of similar density.

The type of sediment formed will depend on the state of aggregation of the suspension and on the interparticle forces, discussed in Section 2.2. Figure 2.71 shows the typical settling behavior of different types of systems[123]. If the particles are stabilized, but yet have a large density difference (such as inorganic powder in water) then the sediment will resemble that shown in Figure 2.71(a). For this case, the repulsive interactions that keep the system stabilized will allow the particles to move to a position of lowest free energy, which is a dense sediment. This type of sedimentation is often called "claying" and is characterized by a very low sediment volume with a high settling density, which is dilatant and difficult to redisperse.

---

[122] Tadros, Th.F.; "Solid/Liquid Dispersion"; Academic Press: London, 1987.

[123] Armstrong, G.H.; Johnson, L.; Parker, A.A. *Journal of Applied Polymer Science* **1994**, *52*, 997.

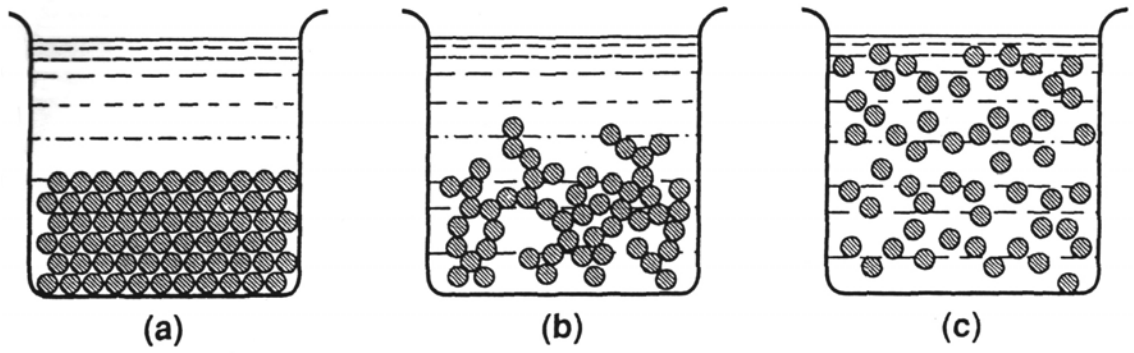

Figure 2.71: Schematic diagram of typical settling behavior for (a) stabilized inorganic powder, (b) a flocculated inorganic powder, (c) a stabilized polymer dispersion[123].

For systems which have an attractive interaction and are flocculated suspensions, the aggregates will adhere to each other upon settling, and will resemble the sediment in Figure 2.71(b). This type of sediment is characterized by high sediment volumes, which have a low settling density and a very fluffy. If the attractions are not too strong, then the system can be easily redispersed with applied shear. Often times this type of behavior is desirable for industrial applications, in order to avoid the formation of clays that occurs in stabilized systems. Frequently, this weak flocculation is intentionally incorporated into the system by the addition of very small colloidal particles, which cause hetercoagulation, or by adding polymers to the suspension, which will cause either bridging flocculation or depletion flocculation (discussed in Section 2.2.4) depending on if the polymer adsorbs on the particles or not.

Figure 2.71(c) shows a schematic for a system which is not only stable, but the particles also have a low density (i.e. a polymer latex in an organic solvent) and do not settle over time. Obviously, this type of behavior would be the most desirable, but is inaccessible for many industrial applications.

In a paper, previously discussed with respect to polyelectrolyte adsorption, the effect of poly(methacrylic aicd) (PMMA) on α-Al_2O_3 in water was studied[18]. At low polyelectrolyte levels there was a positive zeta potential and a large sediment height, representative of an unstable suspension, as shown in Figure 2.72. As the polymer

concentration was increased the zeta potential decreased to negative values before leveling off, at which point there was a small sediment height, indicative of a stable system. The two sets of data thus compliment each other, and show the polymer concentration where the suspension becomes stable due to electrosteric repulsion.

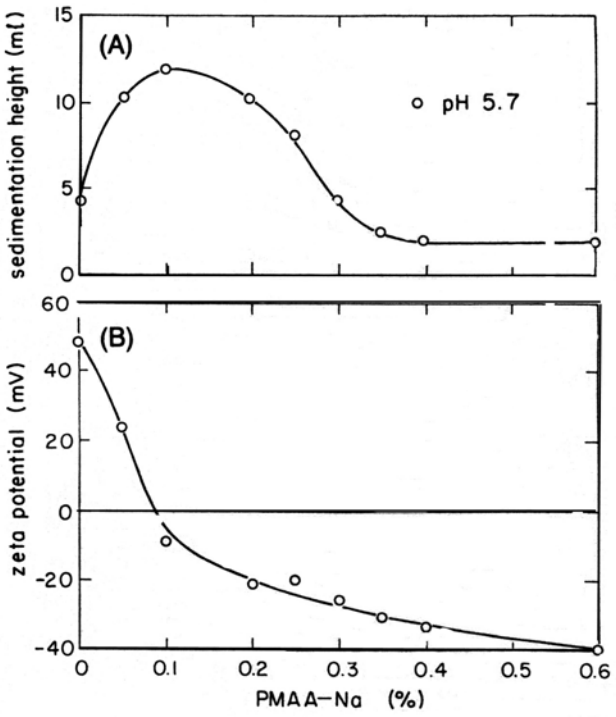

Figure 2.72: (A) Sedimentation height and (B) zeta potential versus percent PMMA-Na for 2 vol% suspensions of α-Al_2O_3[18].

In another study the effect of several different polymers on the sedimentation of α-Al_2O_3 in 90:10 wt% toluene-ethanol mixtures was studied[123]. In this work the results were reported in terms of theoretical sediment density, which was defined as the ratio between the measured cake density divided by the density of the alumina particles. Thus, a stable system would have a large sediment density, or a small sediment height, and the authors chose a value of 45-50% as the theoretical sediment density for a stable suspension. An unstable system would have a low sediment density, or a large sediment height. It was determined that sulfonated derivatives of polystyrene (60k) and Kraton (a styrene/ ethylene-butylene block copolymer, 40k) were effective in stabilizing the alumina. The low molecular weight (10k) sulfonated polystyrene, the homopolymer polystyrene and, the unfunctionalized Kraton did not stabilize the particles. The authors conclude that in

order to stabilize the suspension, effective anchoring of the polymer needed to take place, which occurred only for the sulfonated polymers.

3 Characterization and Adsorption of Homopolymer Polypeptides on Colloidal α-Al_2O_3 Surfaces

Abstract

The adsorption of several homopolymer polypeptides on α-Al_2O_3 was investigated to identify possible anchor and tail blocks for brush-forming block copolymers. Poly-L-(glutamic acid) (GLU) and poly-L-(aspartic acid) (ASP) were found to adsorb on α-Al_2O_3 particles at pH 7 and 9, below and at the isoelectric point of the alumina, respectively. Poly-L-proline (PRO) adsorbed only slightly on the α-Al_2O_3 at both pH values. Similar results were found for competitive adsorption experiments using a mixture of GLU and PRO. These findings are useful in designing a block copolymer consisting of PRO and GLU that would form brush-like layers with the GLU acting as the anchor block and the PRO as the tail block.

Keywords: Protein Adsorption, Steric Stabilization, Alumina

3.1 Introduction

Suspensions of metal oxide particles in water have numerous applications, from ceramic processing, adhesives, and coatings, to biomedical uses such as drug delivery vehicles. Controlling the state of aggregation of these suspensions is critical for controlling rheology and processing,[1,2,3,4,5,6] particularly in aqueous systems, where aggregation is

[1] Ring, T.A., 'Processing of Fine Ceramic Powders', *MRS Bulletin* **1990**, *15*, 34-40.

[2] Sheppard, L.M., 'Fabrication of Ceramics: The Challenges Continues', *Ceramic Bulletin* **1989**, *68*, 1817-1820.

typically more pronounced than in organic solvents. Polyelectrolytes are commonly used to stabilize metal oxide particles in water, but the stabilization imparted by this method is often sensitive to changes in pH and ionic strength.[7,8] Sterically stabilized systems provide a more robust system for stabilization, because they are not as sensitive to these types of fluctuations. The most promising steric stabilizers are block copolymers[9,10,11] that consist of a strongly adsorbing anchor block and a weakly or non-adsorbing, soluble, nonionic tail block. When designed properly, these copolymers form self-assembled

---

[3] Cesareno, J.; Aksay, I.A.; Bleier, A., 'Stability of Aqueous α-Al_2O_3 Suspensions with Poly(methacrylic acid) Polyelectrolyte', *Journal of the American Ceramic Society* **1988**, *71*, 250-255.

[4] Cesareno, J.; Aksay, I.A., 'Processing of Highly Concentrated Aqueous α-Al_2O_3 Suspensions Stabilized with Polyelectrolytes', *Journal of the American Ceramic Society* **1988**, *71*, 1062-1067.

[5] Goodwin, J.W., 'Rheology of Ceramic Processing', *Ceramic Bulletin* **1990**, *69*, 694-698.

[6] Horn, R.G., 'Surface Forces and Their Action in Ceramic Materials', *Journal of the American Ceramic Society* **1990**, *73*, 1117-1135.

[7] Reed, J.S. *Principles of Ceramic Processing*, Wiley-Interscience: New York, 1995.

[8] Gilde, G.; Gazza, G. in Silicon Nitride Ceramics, Mat. Res. Soc. Symp. Proc., Vol 287, 257, 1993.

[9] DeLaat, A.W.M.; Schoo, H.F.M., 'Novel Poly(vinyl ether) Block Copolymers: Synthesis and Colloidal Stabilization of α-Fe_2O_3 in Water and Organic Solvents', *Colloid and Polymer Science* **1998**, *176*, 176-185.

[10] DeLaat, A.W.M.; Schoo, H.F.M., 'Novel Poly(vinyl ether) Block Copolymers: Adsorption from Aqueous Solutions on α-Fe_2O_3 (Hematite) and the Mechanism of Colloidal Stabilization', *Colloid and Interface Science* **1997**, *191*, 416-423.

[11] DeLaat, A.W.M.; Schoo, H.F.M., 'Reversible Thermal Flocculation of Aqueous α-Fe_2O_3 Disperions Stabilized with Novel Poly(vinylo ether) Block Copolymers', *Colloid and Interface Science* **1998**, *200*, 228-234.

layers on a surface, with brush-like tails extending from the surface into solution that generate repulsive steric forces.[12,13,14,15]

While numerous block copolymers have been developed that form brushes on polar and hydrophobic surfaces in organic solvents,[12,13,14] relatively few copolymers form brushes on surfaces in contact with water. The Pluronics triblock copolymers, consisting of polyethylene oxide (PEO) tail blocks and a polypropylene oxide (PPO) anchor block form brushes on hydrophobic polymer latexes,[16,17] but do not do so on silica in contact with water.[18,19] There are relatively few examples of water-soluble copolymers that form brushes on metal oxides-most rely on electrostatic interactions to anchor the brush to an oxide surface. Poly(vinylmethylether)-b-poly(vinyloxy-4-butyric acid) forms brush layers on α-Fe_2O_3,[9,10,11] while poly(methacrylic acid)-b-PEO was shown to sterically

---

[12] Fleer, G.J; Cohen Stuart, M.A.; Scheutjens, J.M.H.M.; Cosgrove, T.; Vincent, B. *Polymers at Interfaces*, Chapman and Hall: London, 1993.

[13] Guzonas, D.; Hair, M.L. Cosgrove, T., 'Adsorption of Block Copolymers from Nonselective Solvents', *Macromoecules* **1992**, *25*, 2777-2779.

[14] Halperin A.; Tirrell M.; Lodge T.P., 'Macromolecules: Synthesis, Order and Advanced Properties', *Advances in Polymer Science* **1992**, *100*, 31-71.

[15] Gast, A., 'Structure, Interactions and Dynamics in Tethered Chain Systems', *Langmuir* **1996**, *12*, 4060-4067.

[16] Baker, J.A.; Berg, J.C., 'Investigation of the Adsorption Configuration of Poly(ethylene oxide) and its Copolymers with Poly(propylene oxide) on Model Polystyrene Latex Dispersions', *Langmuir* **1988**, *4*, 1055-1061.

[17] Baker, J.A,; Pearson, R.A.; Berg, J.C., 'Influence of Particle Curvature on Polymer Adsorption Layer Thickness', *Langmuir* **1989**, *5*, 339-342.

[18] Malmsten, M.; Linse, P.; Cosgrove, T., 'Adsorption of PEO-PPO-PEO Block Copolymers at Silica', *Macromolicules* **1992**, *25*, 2474-2481.

[19] Killman, E.; Maier, H.; Baker, J.A., 'Hydrodynamic Layer Thickness of Various Adsorbed Polymers on Precipitated Silica and Polystyrene Latex', *Colloids and Surfaces* **1988**, *31*, 51-71.

stabilize α-Al_2O_3 particles in water.[20] The diblock poly(diethylaminoethyl methacrylate)-b-poly(dihydroxypropyl methacrylate) or DMAEM-b-HMA was found to sterically stabilize TiO_2 and SiO_2 for very low DMAEM compositions, where adsorption was the greatest and a mixed layer conformation existed.[21,22] Diblocks of DMAEM-b-BMA were shown to form brush layers on SiO_2 in contact with isopropanol due to adsorption of the protonated DMAEM block.[23] A comb copolymer consisting of a poly-L-lysine (PLL) backbone with grafted PEO side chains was found to strongly adsorb onto TiO_2, SiO_2, and Nb_2O_5 from water due to anchoring of the positively charged PLL block. The PEO sidechains formed extended brush layers and prevented.[24]

Block copolymers of polypeptides that form brush layers have several potential advantages over block copolymers made by classical synthetic methods. The most important of these is that by using recombinant DNA technology, monodisperse polymers

---

[20] Orth, J.; Meyer, W.H.; Bellmann, C.; Wegner, G., 'Stabilization of Aqueous α-Al_2O_3 Suspensions with Block Copolymers', *Acta Polymer* **1997**, *48*, 490-501.

[21] Hoogeveen, N.G.; Cohen Stuart, M.A.; Fleer, G.J., 'Adsorption of Charged Block Copolymers with Two Adsorbing Blocks', *Faraday Discussions* **1994**, *98*, 161-172.

[22] Hoogeveen, N.G.; Cohen Stuart, M.A.; Fleer, G.J., 'Can Charged (Block Co)Polymers Act as Stabilisers and Flocculants of Oxides', *Colloids and Surfaces A: Physicochemical and Engineering Aspects* **1996**, *117*, 77-88.

[23] Wu, D.T.; Yokoyama, A.; Setterquist, R.L., 'An Experimental Study on the Effect of Adsorbing and Non-Adsorbing Block Sizes on Diblock Copolymer Adsorption', *Polymer Journal* **1991**, *23*, 709-714.

[24] Kenausis, G.L.; Voros, J.; Elbert, D.L.; Huang, N.; Hofer, R.; Ruiz-Taylor, L.; Textor, M.; Hubbell, J.A.; Spencer, N.D., 'Poly(L-lysine)-g-Poly(ethylene glycol) Layers on Metal Oxide Surfaces: Attachment Mechanism and Effects of Polymer Architecture on Resistance to Protein Adsorption', *Journal of Physical Chemistry B* **2000**, *104*, 3298-3309.

with an exact sequence can be synthesized with no polydispersity.[25,26] This permits model block copolymer systems to be made with precisely tailored compositions, including end groups. Monodisperse stabilizers are important for forming uniform brush layer on the surface.[12,27,28,29]

The objective of this work was to find a combination of polypeptides that would serve as anchor and tail blocks for diblock and triblock copolymers designed to form brushes at the interface between Al_2O_3 and water. This is done by measuring the adsorption of selected homopolymers of amino acids from both pure solutions and from mixtures. Relatively little work has been reported on the adsorption of synthetic, unstructured polypeptides,[30,31] and none has been reported with aim to define candidate anchor and tail blocks for a designed copolymer. Our focus was on pH 7, which is below the IEP of Al_2O_3 and therefore the Al_2O_3 is positively charged, and pH 9 which is near the IEP. Three poly(amino acids) were studied, poly-L-proline (PRO), poly-L-(glutamic acid) (GLU), and poly-L-(aspartic acid) (ASP). Both GLU and ASP have carboxylate side

---

[25] van Hest J.C.M.; Tirrell D.A., 'Protein-Based Materials, Toward a New Level of Structural Control', *Chem Commun* **2001**, *19*, 1897-1904.

[26] Yu S.J.M.; Tirrell D.A., 'Thermal and Structural Properties of Biologically Derived Monodisperse Hairy-Rod Polymers', *Biomolecules* **2000**, *3*, 310-312

[27] Tirrell, M.; Levicky, R., 'End Tethered Chain Molecules at Liquid Interfaces', *Current Opinion in Solid State and Materials Science* **1997**, *2*, 668-672.

[28] Currie, E.P.K.; Wagemaker, M.; Cohen Stuart, M.A.; van Well, A.A., 'Structure of Monodisperse and Bimodal Brushes', *Macromolecules* **1999**, *32*, 9041-9050.

[29] Levicky, R.; Koneripalli, N.; Tirrell, M., 'Stratification in Bidisperse Polymer Brushes from Neutron Reflectivity', *Macromolecules* **1998**, *31*, 2616-2621.

[30] Blaakmeer, J.; Cohen Stuart, M.A.; Fleer, G.J., 'The Adsorption of Polyampholytes on Negatively and Positively Charged Polystyrene Latex', *Journal of Colloid and Interface Science*, **1990**, *140*, 314-325.

[31] Killmann, E.; Reiner, M., 'Adsorption of Poly-L-Lysine and Poly-L-(glutamic acid) on Silica Surfaces', *Tenside, Surface, Detergent* **1996**, *33*, 220-227.

groups with a pKa of 4.07 for GLU and 3.90 for ASP[32] and therefore are negatively charged at pH 7 and 9.

3.2 Experimental

3.2.1 Materials

The polypeptides used were all purchased from Sigma and used as received. The structures of the polymers are shown in Figure 3.1. Two samples of poly-L-proline, two poly-L-(glutamic acid) samples, and poly-L-(aspartic acid) were used. A correction for the water content in the polymers was made using analytical data from the supplier. All adsorption experiments were performed with alumina (Sumitomo Chemical Company, Ltd., α-Al_2O_3, AKP-30, > 99.99% Purity, Specific Surface Area: 7.1 m^2/g, Mean Particle Size: 0.40 μm), the IEP was measured to be 8.6, in agreement with reported literature values.[3] Deionized (DI) water, purified using a NANOpure II ion exchanger from Barnstead with a specific resistance above 17 MΩ·cm, was used for all experiments. ACS Reagent grade sodium chloride, potassium nitrate, sodium hydroxide, potassium hydroxide, nitric acid and hydrochloric acid from Fisher were used for ionic strength and pH adjustment.

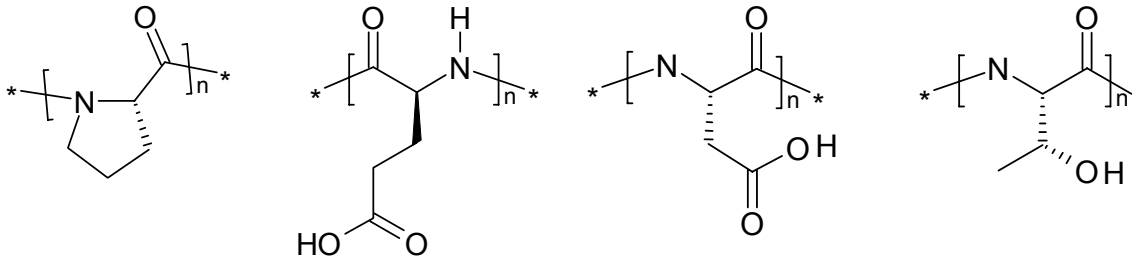

Figure 3.1: Structures of polymers used in adsorption experiments: a) poly-L-proline (PRO), b) poly-L-(glutamic acid) (GLU) pKa = 4.07,[32] c) poly-L-(aspartic acid) (ASP) pKa = 3.90.[32]

[32] Tropp, B.E. *Biochemistry*, Brooks/Cole Publishing Company: Pacific Grove, CA, 1997, pg. 111.

3.2.2 Electrophoretic Light Scattering

The zeta potential of the α-Al_2O3 particles was measured with the ZetaSizer 3000 from Malvern Instruments, Ltd. In the limit of a thin double layer, $a/\kappa^{-1} >> 1$, the zeta potential, ζ, is related to the electrophoretic mobility, u, by the following equation:

$$u = \frac{\zeta \varepsilon}{\eta} \qquad \text{Equation 3.1}$$

where ε is the electric permitivity of the liquid, η is the viscosity, a is the radius of the particle, and k^{-1} is the Debye length.[33] By measuring the zeta potential over a range of pH the IEP can be determined. A stock solution of alumina particles at 0.15 g/L was first made and the ionic strength of the solution was adjusted to 0.1M by the addition of sodium chloride, potassium nitrate. The stock solution was then divided, and the pH of each aliquot was adjusted using either potassium hydroxide of nitric acid, to encompass a range over the expected IEP.

3.2.3 Dynamic Light Scattering

Dynamic light scattering (DLS) measurements were performed at 836 nm with a DynaPro-801 TC from Protein Solutions Inc. All experiments were done at 25°C and controlled to ± 0.2°C and all samples were filtered with a 0.02 μm Whatman Anotop syringe filter. At the start of each experiment, the sample chamber was flushed with 1-2 ml of DI water. Bovine serum albumin (BSA) standard (from Pierce at 2mg/ml) was used periodically to check the optical alignment. Approximately 0.5 ml of the sample was injected into the sample chamber, making sure there were no air bubbles in the syringe prior to injection. Initially, a stable intensity count rate was established before measurements were taken. Typically 15 measurements were taken to get an accurate average. Size distribution analyses were conducted using two algorithms in the

[33] Hunter, R.J. *Zeta Potential in Colloid Science: Principles and Applications*, Academic Press: London, 1981.

Dynamics software.[34] The first is the Regularization algorithm, which calculates up to three peaks and gives the relative scattering percentages for each. The second algorithm, Dynals, can report more than three peaks and gives relative scattering percentages for each. The hydrodynamic radius was determined using the Stokes-Einstein equation:

$$R_H = \frac{k_b T}{6\pi\eta D_T} \qquad \text{Equation 3.2}$$

where: k_b is Boltzmann's constant, T is temperature, η the solvent viscosity and D_T is the translational diffusion coefficient which is calculated from the autocorrelation function. Measurements were taken at polymer concentrations ranging from 1-4 mg/ml. The values of R_H did not vary with concentration in all cases studied, confirming that this is in the dilute range.

3.2.4 Static Light Scattering

The weight average molecular weight and the second viral coefficient, A_2, were measured using the DynaPro 801 in the static scattering mode. From scattering theory, the Rayleigh ratio, R_θ or the reduced relative scattering intensity is related to the concentration, c, by:

$$\frac{Kc}{R_\theta} = \frac{1}{M_w} + 2A_2 c \qquad \text{Equation 3.3}$$

where K is an optical constant defined as:

$$K = \frac{2\pi^2 n_o^2 \left(dn/dc\right)^2}{N_A \lambda^4} \qquad \text{Equation 3.4}$$

[34] Ivanova, M.A.; Arutyunyan, A.V.; Lomakin, A.V.; Noskin, V.A., 'Study of DNA Internal Dynamics by Quasi-Elastic Light Scattering' *Applied Optics* **1997**, *36*, 7657-7663.

where n_o is the refractive index of the solvent, (dn/dc) is the refractive index increment, and and λ is the wavelength of light used in the experiment.[35] The dn/dc value used for the solutions was 0.186 ml/g, a typical value for proteins at wavelengths greater than approximately 730 nm.[36] The other instrumental parameter required was the scattering intensity of toluene, I(toluene), which was calculated using a standard. This calibration procedure was recommended by Protein Solutions as a convenient way to avoid contaminating the cell with toluene. Lysozme, from Sigma which has a known molecular weight of 14,400 g/mol, was run before every series of static measurements under the same conditions as the polymers (pH 7, with 0.1 M NaCl), and the I(toluene) parameter was adjusted to obtain the known molecular weight. This value was then used to calculate the molecular weight and the second virial coefficient for the polymer solutions. A typical experiment consisted of measurements taken at seven different polymer concentrations, ranging from 1 to 4 mg/ml.

3.2.5 Homopolymer Adsorption Isotherms

Adsorption isotherms of the poly(amino acids) were measured using the depletion method. A stock solution of polymer in water, at 4 mg/ml, was stirred overnight, and then filtered with a 0.45 μm Nalgene Surfactant-Free Cellulose Acetate (SFCA) filter. The stock solution was diluted to the initial concentration with 0.1 M NaCl and at the appropriate pH (7 or 9), which was obtained using either 0.1 M NaOH or 0.1 M HCl. Depletion experiments require measurements of the initial polymer concentration, C_A, and the concentration in equilibrium with the Al_2O_3, C_S of the polymer. First, C_A was determined by measuring the absorbance at 220 nm using the spectrophotometer. Next, 1 g of Al_2O_3 was added to the solution and agitated overnight (longer than 16 hours). The sample was then centrifuged for 15 min. at approximately 15,000 g's in a Marathon 21K Centrifuge. The supernatant was carefully pipetted and filtered with a 0.2 μm Whatman

[35] Burchard, W., 'Polymer Characterization – Quasi-Elastic and Elastic Light-Scattering', *Makromol. Chem., Macromol. Symp*. **1988**, *18*, 1-35.

[36] Huglin, M.B. *Light Scattering from Polymer Solutions*, Academic Press: London, 1972.

Anotop 25 mm syringe filter. The equilibrium supernatant concentration, C_S, was then measured and the adsorbed amount, Γ, was calculated from:

$$\Gamma = \frac{(C_A - C_S)V_T}{M_P A_S} \qquad \text{Equation 3.5}$$

where: V_T is the volume of solvent used, M_P is the mass of solid, and A_S is the specific surface area of the solid particles. Duplicate measurements of the initial and final concentrations were taken for each sample.

3.2.6 Competitive Adsorption

The competitive adsorption of PRO and GLU on Al_2O_3 was also characterized using the depletion method. Separate solutions of GLU and PRO were made in water at 1 mg/ml and stirred overnight. Each solution was then filtered using a 0.45 μm Nalgene SFCA filter. The GLU and PRO solutions were then mixed in the appropriate amounts to make a 0.75 mg/ml Pro, 0.25 mg/ml GLU, 0.1 M NaCl stock solution, and the pH was adjusted using either 0.1 M NaOH or 0.1 M HCl to the desired pH (7 or 9). This solution gives approximately a 1:1 chain ratio based on the molecular weight values calculated from the SLS measurements. This 1:1 chain ratio in the mixture roughly replicated a diblock composition. Next, 12 ml of the stock solution was placed into a centrifuge tube and 2 ml were removed from each sample for determining the initial concentration using capillary zone electrophoresis (CZE). A series dilution of standards were made using the stock as the maximum concentration and diluting in half three consecutive times. These standards were run on CZE to create a calibration curve for each polymer. Then, 1 g of alumina was added to each sample, leaving a control containing polymer with no alumina, and then all samples were shaken overnight. The tubes were centrifuged at 10,000 rpm for 15 min., to separate the alumina, and the supernatant was carefully removed and filtered with a 0.2 μm Whatman Anotop filter. The final concentration was calculated using the CZE technique and the calibration curve and the adsorbed amount for each species was calculated using Equation 4. Four replicates were made at each pH.

3.2.7 Capillary Zone Elelctrophoresis

The CZE measurements were done using a Beckman P/ACE 5000 instrument with 200 or 214 nm UV detection and the capillary outlet at the cathode. The electrolyte buffer was 100 mM sodium tetraborate, pH = 8.3. A 75 μm I.D. fused silica capillary (Beckman) with 37 cm total length (30 cm to detection window) was used for all analyses. Samples were injected by pressure (0.5 psi) and separations were run at 18 kV. Calibration curves were created by integrating the areas for standard solutions of pure polymer.

3.3 Results and Discussion

3.3.1 Characterization of α-Al_2O_3 Particles

Figure 3.2 and Figure 3.3 show the results for the zeta potential measurements as a function of pH with KNO_3 and NaCl as the background ionic strength, respectively. At pH 8.6 in Figure 3.2 and at pH 8.7 in Figure 3.3 the zeta potential is approximately zero, indicating this is the IEP for the particles. These results are in good agreement with those found by Wiese and Healy of 8.8.[37] The particles have a net positive charge for pH < 8.6 and a net negative charge for pH > 8.6.

[37] Wiese, G.R.; Healy, T.W. *Journal of Colloid and Interface Science* **1975**, *51*, 427.

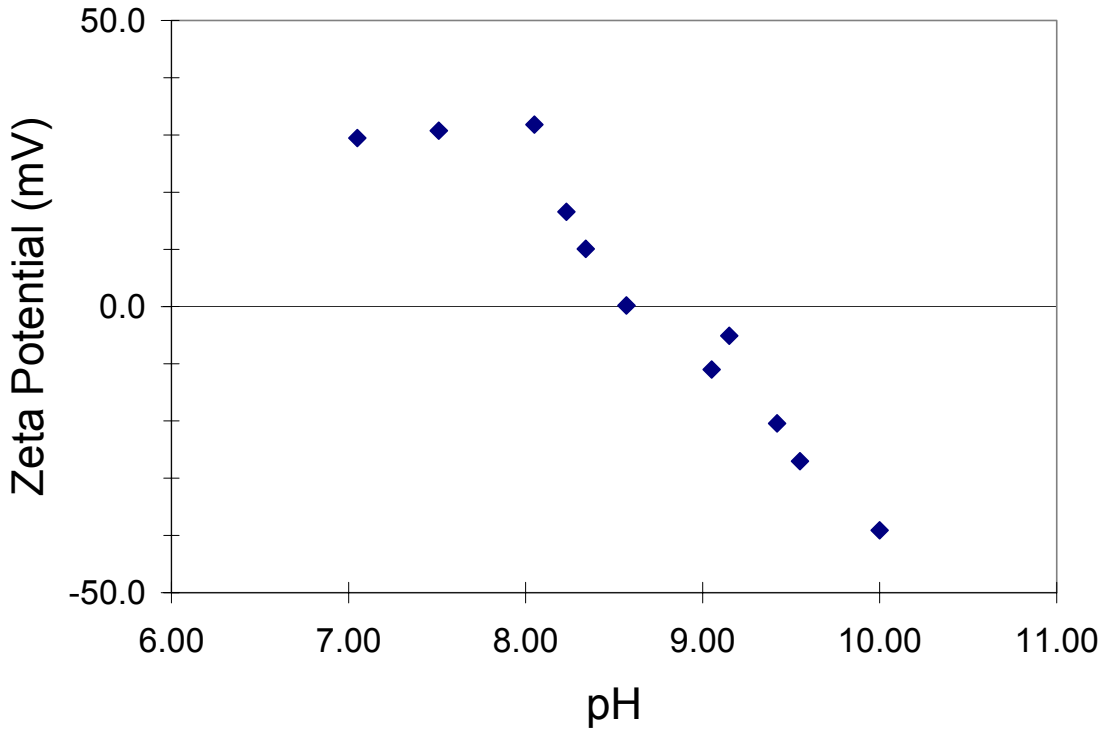

Figure 3.2: Zeta potential measurements for α-Al_2O_3 particles as a function of pH, at 0.15 g/L particles and 0.1 M KNO_3.

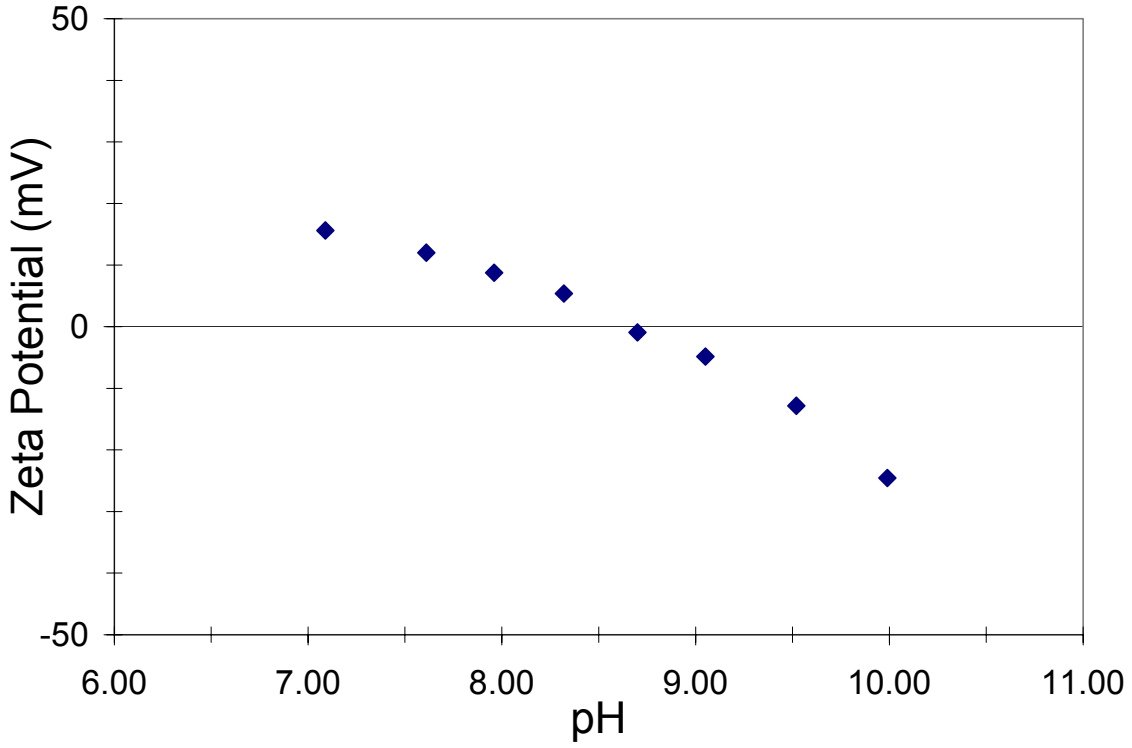

Figure 3.3: Zeta potential measurements for α-Al_2O_3 particles as a function of pH, at 0.15 g/L particles and 0.1 M NaCl.

3.3.2 Solution Properties of Pure Poly(Amino Acids)

The weight-average molecular weight, M_w, and the second virial coefficient, A_2, were calculated using equations (2) and (3). These results are shown in Table 3.1.

Table 3.1: Weight-average molecular weights and second virial coefficients from light scattering measurements, (± standard deviation), made at pH 7 and 9, in 0.1 M NaCl, at 25°C. M_w values are averages of values obtained at pH = 7 and 9.

Polymer	Mw[a]	A_2[a] pH 9	A_2[a] pH 7
	g/mole	$m^3kg^{-2}mol$	$m^3kg^{-2}mol$
PRO (18.0k)	18000 ± 800	0.005 ± 0.001	0.004 ± 0.001
PRO (22.2k)	22200 ± 600	0.004 ± 0.001	0.003 ± 0.001
GLU (8.1k)	8100 ± 800	0.023 ± 0.003	0.028 ± 0.001
GLU (12.0k)	12000 ± 1000	0.010 ± 0.002	0.004 ± 0.001
ASP (12.4k)	12400 ± 2200	0.029 ± 0.001	0.025 ± 0.003

a) Calculated using Equation 2.

The second virial coefficient A_2 is a measure of the intermolecular forces between the polymer and the solvent and reflects the solubility of the polymer in solution: A_2 increases as the polymer becomes more soluble. This is not a measure of the maximum solubility of the polymer in water, but rather a relative comparison of the polymer-solvent interactions in dilute solution. Shorter chains are more soluble and thus have a larger A_2. Comparing the two molecular weight samples of PRO and of GLU shows this. For both cases, the lower molecular weight samples have a higher A_2. From the structures in Figure 3.1, ASP has one less methylene unit in its side group, and thus should be more soluble in water than GLU. This is indeed seen by comparing the A_2 value of ASP (12.4k) with that of the GLU (12.0k) which have similar weight average molecular weights. The polydispersity of the polymers is expected to be near two, given the fact that they were synthesized by condensation polymerization.

Before the adsorption experiments were made, the aggregation behavior of the polymers in solution was characterized by DLS in 0.1 M NaCl at pH 7 and 9. The results from the Dynals algorithm and the regularization algorithm were comparable, with both showing only one peak. The measured R_H values from these two algorithms typically agreed to within 2 nm and thus the Regularization results are presented here. The results for the hydrodynamic radii were compared with freely jointed chain statistic calculations for

chain dimensions, using the following equations for the end-to-end distance, R, and radius of gyration, R_g, respectively:

$$\left\langle R^2 \right\rangle = nl^2 C_\infty \qquad \text{Equation 3.6}$$

$$\left\langle R_g^2 \right\rangle = \frac{\left\langle R^2 \right\rangle}{6} \qquad \text{Equation 3.7}$$

where, n is the number of backbone bonds (three times the degree of polymerization for the poly(amino acids)), l is the average length of these bonds, and C_∞ is the characteristic ratio (C_∞ = 13.7 for PRO in water[38]; C_∞ = 8.8 for GLU in 0.3M sodium phosphate buffer at pH 7.85;[39] this latter value represents a lower bound for our experiments). The hydrodynamic radius can then be calculated from the radius of gyration, assuming a non-draining sphere,[40] by:

$$R_H = 0.875 R_g \qquad \text{Equation 3.8}$$

Table 3.2 shows the calculated R_H values for various degrees of polymerization for PRO and GLU. DLS results using the Regularization algorithm, were compared to the calculated values and were found to agree within 1-2 nm.

[38] Mattice, W.L.; Mandelkern, L., 'Conformational Properties of Poly-L-Proline Form II in Dilute Solution', *Journal of the American Chemical Society* **1971**, *93*, 1769-1777.

[39] Brandup, J.; Immergut, E.H. *Polymer Handbook, 3rd ed.*, John Wiley and Sons: New York, 1989, pg.

[40] Tanford, C. *Physical Chemistry of Macromolecules*, John Wiley and Sons: New York, 1962, pg. 20.

Table 3.2: Comparison of calculated and measured hydrodynamic radii at pH 9, 0.1 M NaCl, and 25°C. C_∞ for PRO is 13.7,[38] and C_∞ for GLU is 8.8.[39]

	DP	R [a]	Rg [b]	R_H [c]	R_H (DLS)
		nm	nm	nm	nm
PRO (18.0k)	175	12.1	5.0	4.3	4.4
PRO (22.2k)	200	13.0	5.3	4.6	7.8
GLU (8.1k)	50	5.2	2.1	1.9	2.3
GLU (12.0k)	75	6.4	2.6	2.3	4.7
ASP (12.4k)	100	7.3[d]	3.0[d]	2.6[d]	1.9

a) End-to-end distance calculated using Equation 3.6.

b) Radius of gyration calculated using Equation 3.7.

c) Hydrodynamic radius calculated using Equation 3.8.

d) Using C_∞ for GLU[39].

These results for GLU and PRO are consistent with published reports. At pH < 4, GLU forms an α-helix which self-aggregates, and is not soluble in water.[41,42] At pH > 6, the conformation of GLU changes to a charged random coil, which is soluble in water.[43] At intermediate pH values, a combination of helical and random coil conformations exist. The PRO chain exists in its form II state in aqueous solution, that is the left-handed helical form with the peptide bonds in the trans configuration.[44,45]

[41] Blout, E.R.; Idelson, M., 'Polypeptides. VI. Poly-a-L-Glutamic Acid: Preperation and Helix-Coil Transition', *Journal of the American Chemical Society* **1956**, *78*, 497.

[42] Fasman, G.D.; Lindblow, C.; Bodenheimer, E. *Biochemistry* **1964**, *3*, 155.

[43] Nakajima, A.; Shinoda, K.; Hayashi, T.; Sata, H., 'Interactions Between Oppositely Charged Polypeptides', *Polymer Journal* **1975**, *7*, 550-557.

[44] Steinberg, I.Z.; Harrington, W.F.; Berger, A.; Sera, M.; Katchalski, E., 'The Configurational Changes of Poly-L-proline in Solution', *Journal of the American Chemical Society* **1960**, *82*, 5263.

[45] Smith, M.; Walton, A.G.; Koenig, J.L., 'Raman Spectroscopy of Poly-L-Proline in Aqueous Solution', *Biopolymers* **1969**, *8*, 173.

3.3.3 Phase Separation

Since the competitive adsorption experiments involve mixtures of PRO and GLU, the solution properties of the mixtures were also studied. Mixtures of PRO 22.2k and GLU 8.1k were studied by DLS and it was found that there was phase separation of these polymers at concentrations greater than 1 mg/ml. The initial experiment involved using a roughly 1:1 molar chain ratio of the polymers, with a $(C_A)_{GLU}$ at 1 mg/ml which resulted in a $(C_A)_{PRO}$ of 9.45 mg/ml. This was a very turbid mixture, with obvious phase separation. Further experiments were done to determine the maximum total polymer concentration where there was no aggregation. Table 3.3 shows the DLS results using the Regularization algorithm for the three total polymer concentrations studied. In the R_H column the number in parenthesis is the percentage of the total peak area attributed to that peak.

Table 3.3: Dynamic light scattering results on phase separation of PRO 22.2k and GLU 8.1k mixtures at different total polymer concentrations, and at pH 9, 25°C, and 0.1 M NaCl. R_H values were calculated using the Regularization algorithm.

$(C_p)_{Total}$	$(C_p)_{GLU}$	$(C_p)_{PRO}$	R_H (Percentage)
mg/ml	mg/ml	mg/ml	nm
1	0.13	0.87	0.55 (8), 4.5 (92)
2	0.27	1.73	0.37 (3), 6.1 (81), 87.0 (16)
3	0.4	2.6	19.0 (broad)

It is well known that solutions of polymer mixtures containing two or more polymers can exhibit phase separation.[46] If the polymer-polymer interaction is repulsive, then excluded volume interactions between the two polymers will dominate the entropy of mixing and two separate phases will form, each rich in one of the polymers. This type of behavior has been observed with mixtures of sodium dextran sulfate and poly(ethylene glycol) (PEG) in salt solutions. Above a certain added PEG concentration, there is phase separation and, at higher ionic strengths, phase separation occurs at lower PEG

[46] Albertsson, P. *Partition of Cell Particles and Macromolecules*, John Wiley and Sons: New York, 1986.

concentrations due to a reduced excluded volume. This system is similar to the PRO-GLU combination in that both have an anionic polymer and neutral polymer with hydrogen bonding sites. If the polymer-polymer interaction is attractive, two phases will still form, with one phase being rich in both polymers and the other depleted in both. This latter case readily occurs with binary mixtures of opposite charged polyelectrolytes. The structure of the two polymers must be very similar in order for a binary polymer solution to form one homogenous phase over a wide range of concentrations, thus, most systems will form two phases.

The results in Table 3.3 show, that at 1 mg/ml total polymer concentration, there was no polymer aggregation. The DLS data show two peaks, which are in the expected range for the two polymers in solution, as shown in Table 3.2. The lower detection limit for the DynaPro instrument is $R_H < 1$ nm, thus the peak at 0.55 nm was ignored. At 2 mg/ml a larger peak appeared which can be attributed to phase separation. At the highest polymer concentration, 3 mg/ml, there was only one broad peak, with a mean of 19 nm. This is also indicative of phase separation. For this polymer mixture, only at low polymer concentrations can one homogenous phase be formed and no aggregation appears, indicating the interactions between GLU and PRO are repulsive. Based on these results, a total polymer concentration of 1 mg/ml was used for the competitive adsorption experiments.

3.3.4 Homopolymer Adsorption

Figure 3.4 and Figure 3.5 show the homopolymer adsorption isotherms in 0.1 M NaCl at pH 9 and pH 7 on alumina. The adsorption of GLU and ASP was much greater than the adsorption of PRO, exceeding 0.5 mg/m^2. The adsorbed amounts for the PRO were very low and within the noise level of the experiment. This difference is expected because GLU and ASP adsorption is driven by electrostatic attraction whereas the adsorption of PRO is not. The PRO results were comparable to previous results for the adsorption of

PEO on alumina. Prior work done in our laboratory[47] and others[48] has shown that PEO and nonionic poly(ethyl oxazoline) (PEOX) do not adsorb on Al_2O_3, presumably because the polymer-water and water-oxide interactions are larger in magnitude than the polymer-oxide interactions. It was hypothesized that PRO might prove to be similar to PEOX in its adsorption characteristics and adsorb weakly or not at all on Al_2O_3 and thus be a good tail block. It was expected that the GLU and ASP should adsorb strongly on the Al_2O_3 surface and be good anchor blocks.

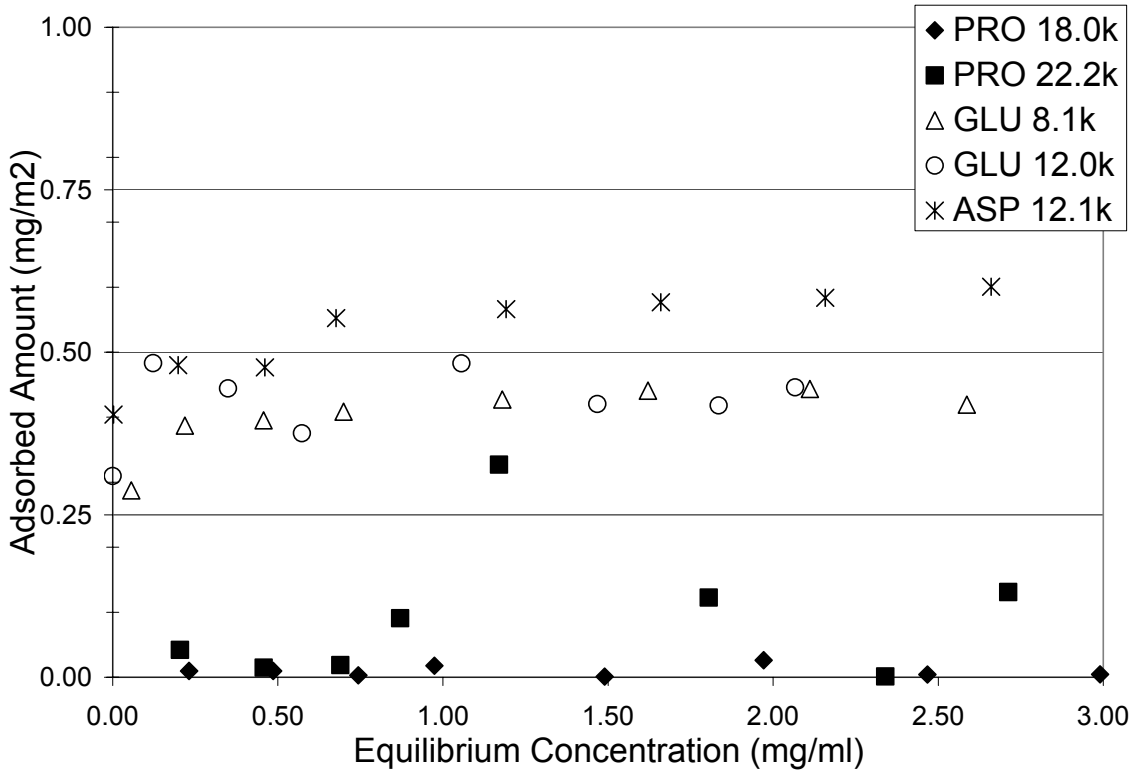

Figure 3.4: Adsorption isotherms of poly(amino acids) on α-Al_2O_3 at 0.1 M NaCl and pH 9. Calculated from Equation 3.5.

[47] Gibson, F.W. *Stabilization of Submicron Metal Oxide Particles in Aqueous Media*, Ph.D. Dissertation, Virginia Tech, 1998.

[48] Mathur, S.; Moudgil, B.M., 'Adsorption Mechanism(s) of Poly(ethylene oxide) on Oxide Surfaces', *Journal of Colloid and Interface Science*, **1997**, *196*, 92-98.

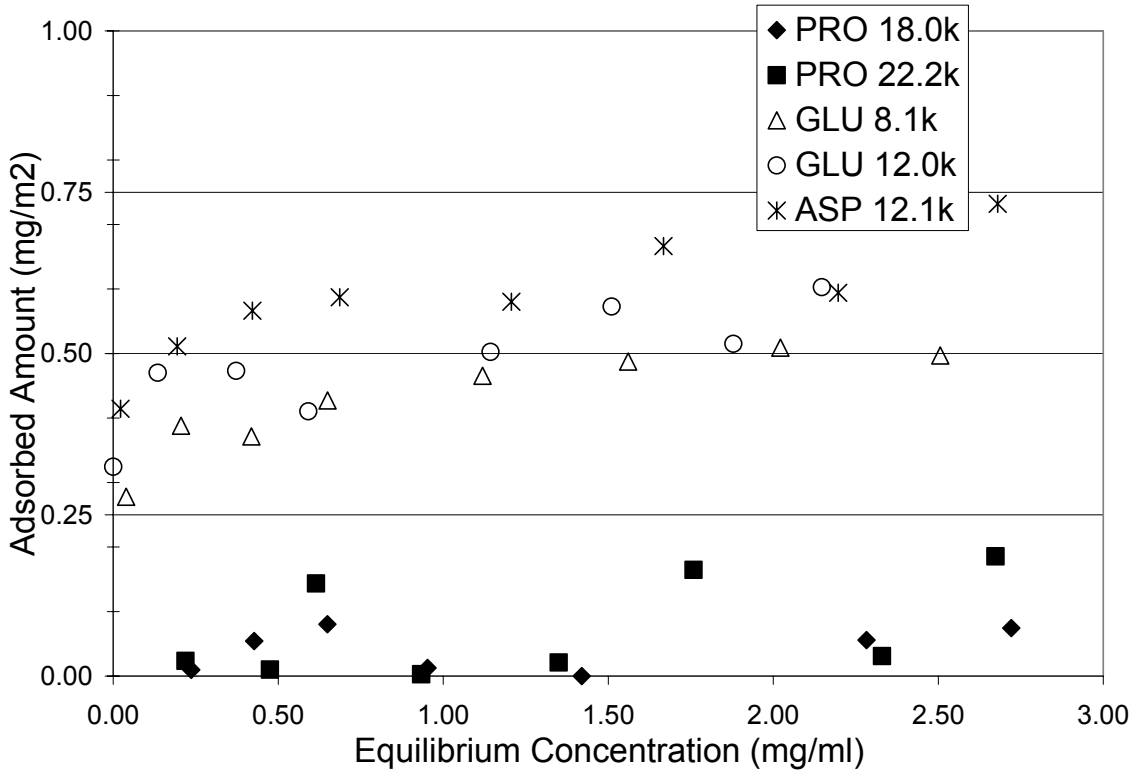

Figure 3.5: Adsorption isotherms of poly(amino acids) on α-Al_2O_3 at 0.1 M NaCl and pH 7. Calculated from Equation 3.5.

Typically, for adsorbing polymers, the adsorbed amount increases with increasing equilibrium concentration, until a plateau is reached.[12] The adsorbed amount of the charged polymers, GLU and ASP, was higher at pH 7 than at pH 9. This is expected because, at pH 7, the surface has a net positive charge that would attract the negatively charged polymer groups. At pH 9, the net charge on the surface was slightly negative and the electrostatic interactions between the surface and polymer were minimized. Previous work done by Cesareno et al.[3] showed that the sodium salt of poly(methacrylic acid), with a molecular weight of 15,000 in 0.1 M NaCl, exhibited stronger adsorption on α-Al_2O_3 at pH < IEP (at pH 7.5, $\Gamma \approx 0.5$ mg/m^2), but still adsorbed at pH > IEP (at pH 9.2, $\Gamma \approx 0.3$ mg/m^2).

An adsorption study on positively and negatively charged polystyrene latex was done using a random copolymer consisting of 60 %mole GLU and 40 %mole lysine (LYS) and

a tetramer of (LYS-GLU-GLY)4.[32] Both polymers exhibited greater adsorption on the negatively charged latex than on the positively charged latex. At high pH, intramolecular electrostatic repulsion prevented high adsorption levels even with an oppositely charged surface. It was also determined that strong nonelectrostatic attractions were present, due to the fact that adsorption occurred even when the polymer and the surface had the same charge. In another study the adsorption of poly-L-(glutamic acid) on hydrophobic silica was found to be greater than on hydrophilic silica, but there was very little adsorption on either surface above pH 8.[32] The trends showed, that as the degree of ionization increased, the adsorption decreased due to increasing electrostatic repulsion between the negatively charged silica and the GLU.

It is also expected that the plateau adsorbed amount will increase with increasing polymer molecular weight for nonionic polymers.[12] We were not able to delineate the effect of molecular weight on the adsorption of PRO due to polydispersity effects and due to the low adsorbed amounts. Polydispersity effects also obscured the effects of molecular weight on the adsorption of GLU. In addition, the GLU adsorption showed no effect of molecular weight due to its adsorption in mostly flat, train-like conformation and due to intramolecular electrostatic repulsions between adsorbed chains, which limits coverage.[30] An adsorbed amount of 0.5 mg/m^2 is equivalent to 0.43 nm^2 of surface per GLU residue, which is consistent with the work by Blaakmeer et al.,[30] who estimated that one amino acid residue occupied approximately 0.43 nm^2 on the surface. This is consistent with the GLU adsorbing mainly in a train-like conformation.

3.3.5 Competitive Adsorption

Analysis of competitive adsorption experiments requires separation and quantification of the two polymer components. CZE separates species based on a charge-to-mass ratio differences. Species containing no charge (e.g., PRO) will migrate with the electro-osmotic flow (towards the cathode); the migration rate of negatively charged species (e.g., GLU) will be a balance between electrophoretic and electroosmotic velocities. The polydispersity of the polymers contributes to the broad peaks observed, but baseline

resolution is still obtained and the concentrations of the two polymers can be determined. Table 3.4 summarizes the competitive adsorption experiments run at 0.1 M NaCl and pH 7 and 9. To avoid phase separation, the total polymer concentration was kept at 1 mg/ml with roughly a 1:1 molar chain ratio of the PRO 22.2k and GLU 8.1k. Baseline resolution between PRO and GLU peaks enabled integration of peak areas, as shown in Figure 3.6.

Table 3.4: Competitive adsorption on Al_2O_3 particles of PRO 22.2k and GLU 8.1k mixtures at 1:1 molar chain ratio, with 0.1 M NaCl. Values of Γ were calculated using Equation 3.5.

pH 7				pH 9			
PRO		GLU		PRO		GLU	
C_s	Γ	C_s	Γ	C_s	Γ	C_s	Γ
mg/ml	mg/m^2	mg/ml	mg/m^2	mg/ml	mg/m^2	mg/ml	mg/m^2
0.70	0.07 ± 0.02	0.03	0.30 ± 0.02	0.73	0.03 ± 0.04	0.05	0.28 ± 0.01
0.70	0.02 ± 0.02	< 0.01	0.32 ± 0.02	0.74	< 0.01 ± 0.04	0.04	0.30 ± 0.01
0.69	0.08 ± 0.01	< 0.01	0.42 ± 0.02	0.98	< 0.01 ± 0.04	0.01	0.34 ± 0.01
0.70	0.08 ± 0.01	< 0.01	0.37 ± 0.02	0.99	< 0.01 ± 0.04	0.02	0.36 ± 0.01

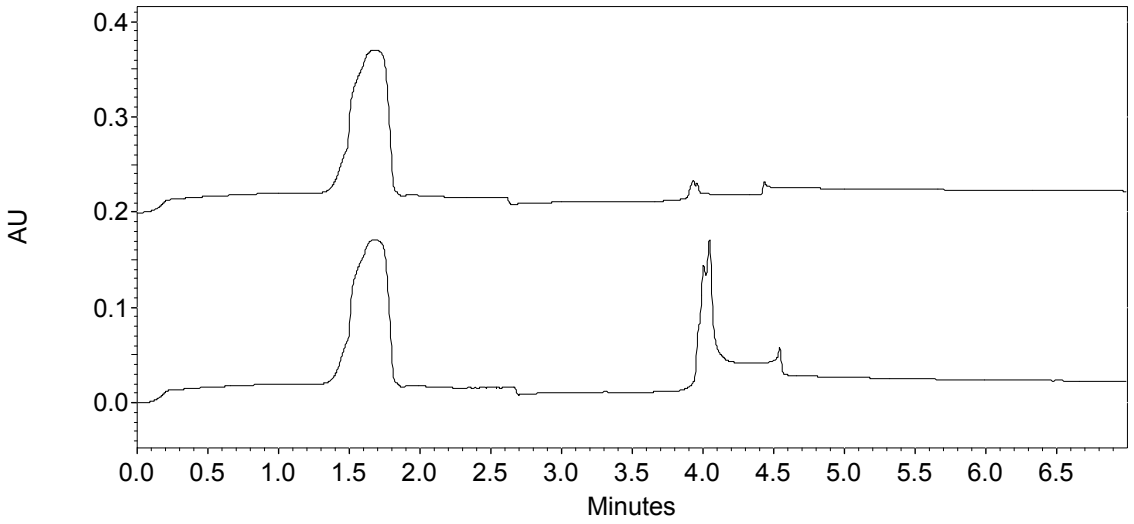

Figure 3.6: CZE electropherogram for the competitive adsorption with PRO (22.2 kg/mole) at 0.75 mg/ml and GLU (8.1 kg/mole) at 0.25 mg/ml initial polymer concentrations at pH 7 with 0.1 M NaCl. The bottom curve shows the polymer concentrations before contact with the alumina, and the top curve shows the supernatant concentrations. Run conditions for CZE: fused silica capillary with 75 μm I.D. and 37 cm total length (30 cm to detection window), electrolyte buffer of 100 mM sodium tetraborate at pH = 8.3, injection pressure of 0.5 psi, and voltage of 18 kV.

Almost all of the GLU adsorbed, as is evident from the measured supernatant concentrations, which show a minimum of 80% of the GLU adsorbed, even at pH 9. Conversely, very little PRO adsorbed, and the supernatant concentrations only drop a maximum 8% from the initial polymer concentration. For both pH 7 and 9, the GLU adsorbed amounts were relatively high, approximately 0.3-0.4 mg/m^2, which is similar to the values obtained from pure GLU adsorption, while the PRO adsorption was much lower, even though the initial concentration was relatively higher. For pH 9 the adsorbed PRO amount lay in the noise level of experiment. The adsorption of PRO increased slightly when the pH was lowered to 7. In fact the equilibrium PRO adsorption, at pH 7, was about the same as in the absence of GLU. Thus, GLU does not appear to promote the co-adsorption of PRO. This is consistent with the light scattering results for the PRO-GLU mixture, which showed the interactions between PRO and GLU are repulsive. The

strong adsorption of GLU in the presence of PRO and the weak adsorption of PRO in the presence of GLU suggest that a PRO-GLU diblock would make a good brush for stabilizing alumina.

3.4 Conclusions

Homopolymer adsorption isotherms showed that both poly-L-(glutamic acid) and poly-L-(aspartic acid) adsorb onto alumina at reasonably high levels, $\Gamma \approx 0.5$ mg/m^2 for $C_S = 2.5$ mg/ml. It was found that these polypeptides show adsorption behavior similar to synthetic polyelectrolytes. Poly-L-proline, on the other hand, showed relatively little adsorption, even at high polymer concentrations. Competitive adsorption experiments were done to determine which polymer, PRO or GLU, would selectively adsorb when both were present. The results showed that the PRO adsorption was very small, compared to that for the GLU, even though the initial concentration of PRO was three times that of GLU. These results show that either GLU or ASP would make a good adsorbing anchor block, while PRO would make a good non-adsorbing tail block for a brush forming copolymer on alumina that would sterically stabilize Al_2O_3 particles in aqueous solutions.

3.5 Acknowledgements

The authors gratefully acknowledge the Center for Adhesive and Sealant Science at Virginia Tech and the Adhesive and Sealant Council Education Foundation for fellowship support for Jody Krsmanovic. This work was funded by the National Science Foundation Grant # BES-0086875.

4 Polypeptide Adsorption on Al_2O_3 and SiO_2 Colloidal Particles

Abstract

The adsorption of several poly(amino acid)s were studied on colloidal particles of α-Al_2O_3 and SiO_2. On alumina, poly-L-(glutamic acid) (GLU) adsorbed strongly, while the poly-L-proline (PRO) showed very little adsorption. Conversely, on silica the PRO showed high affinity adsorption, while the GLU did not adsorb. A hydroxylated version of PRO, poly-L-(hydroxyproline) (HPRO), did not adsorb strongly on either surface. Greater adsorbed amounts for GLU on Al_2O_3 were obtained at higher ionic strengths, indicating that unstructured proteins behave like classical synthetic polymers.

Keywords: Protein Adsorption, Steric Stabilization, Alumina, Silica

4.1 Introduction

Brush-forming block copolymers are very effective for modifying the properties of surfaces. The most promising steric stabilizers are block copolymers[1,2,3] that consist of a strongly adsorbing anchor block and a weakly or non-adsorbing, soluble, nonionic tail block. When designed properly, these copolymers form self-assembled layers on a

[1] DeLaat, A.W.M.; Schoo, H.F.M. 'Novel Poly(vinyl ether) Block Copolymers: Synthesis and Colloidal Stabilization of α-Fe_2O_3 in Water and Organic Solvents', *Colloid and Polymer Science* **1998**, *176*, 176-185.

[2] DeLaat, A.W.M.; Schoo, H.F.M. 'Novel Poly(vinyl ether) Block Copolymers: Adsorption from Aqueous Solutions on α-Fe_2O_3 (Hematite) and the Mechanism of Colloidal Stabilization', *Colloid and Interface Science* **1997**, *191*, 416-423.

[3] DeLaat, A.W.M.; Schoo, H.F.M. 'Reversible Thermal Flocculation of Aqueous α-Fe_2O_3 Dispersions Stabilized with Novel Poly(vinyl ether) Block Copolymers', *Colloid and Interface Science* **1998**, *200*, 228-234.

surface, with brush-like tails extending from the surface into solution that generate repulsive steric forces.[4,5,6,7]

While numerous block copolymers have been developed that form brushes on polar and hydrophobic surfaces in organic solvents,[4,13,14] relatively few copolymers form brushes on surfaces in contact with water. The Pluronics triblock copolymers, consisting of polyethylene oxide (PEO) tail blocks and a polypropylene oxide (PPO) anchor block form brushes on hydrophobic polymer latexes,[8,9] but do not do so on silica in contact with water.[10,11] There are relatively few examples of water-soluble copolymers that form brushes on metal oxides-most rely on electrostatic interactions to anchor the brush to an oxide surface and most employ uncharged, soluble chains as tail blocks. Poly(vinylmethylether)-b-poly(vinyloxy-4-butyric acid) forms brush layers on α-

---

[4] Fleer, G.J; Cohen Stuart, M.A.; Scheutjens, J.M.H.M.; Cosgrove, T.; Vincent, B. *Polymers at Interfaces*, Chapman and Hall: London, 1993.

[5] Guzonas, D.; Hair, M.L. Cosgrove, T. 'Adsorption of Block Copolymers from Nonselective Solvents', *Macromoecules* **1992**, *25*, 2777-2779.

[6] Halperin A.; Tirrell M.; Lodge T.P. 'Macromolecules: Synthesis, Order and Advanced Properties', *Advances in Polymer Science* **1992**, *100*, 31-71.

[7] Gast, A. 'Structure, Interactions, and Dynamics in Tethered chain Systems', *Langmuir* **1996**, *12*, 4060-4067.

[8] Baker, J.A.; Berg, J.C. 'Investigation of the Adsorption Configuration of Poly(ethylene oxide) and its Copolymers with Poly(propylene oxide) on Model Polystyrene Latex Dispersions', *Langmuir* **1988**, *4*, 1055-1061.

[9] Baker, J.A,; Pearson, R.A.; Berg, J.C. 'Influence of Particle Curvature on Polymer Adsorption Layer Thickness', *Langmuir* **1989**, *5*, 339-342.

[10] Malmsten, M.; Linse, P.; Cosgrove, T. 'Adsorption of PEO-PPO-PEO Block Copolymers at Silica', *Macromolicules* **1992**, *25*, 2474-2481.

[11] Killman, E.; Maier, H.; Baker, J.A. 'Hydrodynamic Layer Thickness of Various Adsorbed Polymers on Precipitated Silica and Polystyrene Latex', *Colloids and Surfaces* **1988**, *31*, 51-71.

Fe_2O_3,[1,2,3] while poly(methacrylic acid)-b-PEO was shown to sterically stabilize α-Al_2O_3 particles in water.[12] The diblock poly(diethylaminoethyl methacrylate)-b-poly(dihydroxypropyl methacrylate) or DMAEM-b-HMA was found to sterically stabilize TiO_2 and SiO_2 for very low DMAEM compositions, where adsorption was the greatest and a mixed layer conformation existed.[13,14] Diblocks of DMAEM-b-BMA were shown to form brush layers on SiO_2 in contact with isopropanol due to adsorption of the protonated DMAEM block.[15] A comb copolymer consisting of a poly-L-lysine (PLL) backbone with grafted PEO side chains was found to strongly adsorb onto TiO_2, SiO_2, and Nb_2O_5 from water due to anchoring of the positively charged PLL block. The PEO sidechains formed extended brush layers and prevented protein adsorption.[16]

Block copolymers of polypeptides that form brush layers have several potential advantages over block copolymers made by classical synthetic methods. The most important of these is that by using recombinant DNA technology, monodisperse polymers

---

[12] Orth, J.; Meyer, W.H.; Bellmann, C.; Wegner, G. 'Stabilization of Aqueous a-Al2O3 Suspensions with Block Copolymers', *Acta Polymer* **1997**, *48*, 490-501.

[13] Hoogeveen, N.G.; Cohen Stuart, M.A.; Fleer, G.J. 'Adsorption of Charged Block Copolymers with Two Adsorbing Blocks', *Faraday Discussions* **1994**, *98*, 161-172.

[14] Hoogeveen, N.G.; Cohen Stuart, M.A.; Fleer, G.J. 'Can Charged (block co) Polymers Act as Stabilizers and Flocculants of Oxides*Colloids and Surfaces A: Physicochemical and Engineering Aspects* **1996**, *117*, 77-88.

[15] Wu, D.T.; Yokoyama, A.; Setterquist, R.L. 'An Experimental Study on the Effect of Adsorbing and Non-Adsorbing Block Sizes on Diblock Copolymer Adsorption', *Polymer Journal* **1991**, *23*, 709-714.

[16] Kenausis, G.L.; Voros, J.; Elbert, D.L.; Huang, N.; Hofer, R.; Ruiz-Taylor, L.; Textor, M.; Hubbell, J.A.; Spencer, N.D. 'Poly(L-lysine)-g-Poly(ethylene glycol) Layers on Metal Oxide Surfaces: Attachment Mechanism and Effects of Polymer Architecture on Resistance to Protein Adsorption', *Journal of Physical Chemistry B* **2000**, *104*, 3298-3309.

with an exact sequence can be synthesized with no polydispersity.[17,18] This permits model block copolymer systems to be made with precisely tailored compositions, including end groups. Monodisperse stabilizers are important for forming uniform brush layers on the surface.[19,20,21]

In Chapter 3 the potential use of polypeptides for brush forming steric stabilizers was introduced. Specifically, poly-L-(glutamic acid) (GLU) was identified as a potential anchor block for α-Al_2O_3 particles in water and poly-L-proline (PRO) was found to be a candidate tail block. Although this study began to address polypeptide adsorption, there are other important issues that the prior chapter and prior published literature have not fully addressed.

One issue is the effect of varying the substrate surface chemistry from a Lewis base (e.g. Al_2O_3) to a Lewis acid (e.g. SiO_2) on the adsorption of polypeptides. This type of study is important because a wide range of surface chemistries are encountered in colloid applications. The adsorption of GLU on hydrophilic and hydrophobic silica has been studied.[22] There was greater adsorption on the hydrophobic surface than on the hydrophilic surface, and there was very little adsorption on either surface above pH 8. An adsorption study on positively and negatively charged polystyrene latex has also been

---

[17] van Hest J.C.M.; Tirrell D.A. 'Protein-Based Materials, Toward a New Level of Structural Control', *Chem Commun* **2001**, *19*, 1897-1904.

[18] Yu S.J.M.; Tirrell D.A. 'Thermal and Structural Properties of Biologically Derived Monodisperse Hairy-Rod Polymers', *Biomolecules* **2000**, *3*, 310-312

[19] Tirrell, M.; Levicky, R. 'End Tethered Chain Molecules at Liquid Interfaces', *Current Opinion in Solid State and Materials Science* **1997**, *2*, 668-672.

[20] Currie, E.P.K.; Wagemaker, M.; Cohen Stuart, M.A.; van Well, A.A. 'Structure of Monodisperse and Bimodal Brushes', *Macromolecules* **1999**, *32*, 9041-9050.

[21] Levicky, R.; Koneripalli, N.; Tirrell, M. 'Stratification in Bidisperse Polymer Brushes from Neutron Reflectivity', *Macromolecules* **1998**, *31*, 2616-2621.

[22] Killmann, E.; Reiner, M. 'Adsorption of Poly-L-Lysine and Poly-L-(glutamic acid) on Silica Surfaces', *Tenside, Surface, Detergent* **1996**, *33*, 220-227.

done using a random copolymer consisting of 60 mole% GLU and 40 mole% PLL and a tetramer of lysine-glutamic acid-lysine (LYS-GLU-GLY)4.[23] The results for both polymers showed that adsorption was greater on the negatively charged surface at all pHs than on the positive latex. This effect has also been studied on synthetic polymer, in particular (PEO). PEO, which is a Lewis base, was found to adsorb on SiO_2 (a Lewis acid), but not on Al_2O_3 (a Lewis base).

Another issue that has not been addressed to date is the effect of hydroxylation of a nonionic, soluble polypepetide on the solution properties and adsorption behavior. For synthetic polymers it is has been found that hydroxylated polymers adsorb on Al_2O_3, such as poly(vinyl alcohol).[24] This important for understanding polypeptide adsorption because there are several hydroxylated nonionic amino acids (e.g. threonine and serine) that might be included in future copolymers, made by biosynthesis.

It is also desirable to study the effect of salt concentration and different salt types on adsorption. This has both scientific and practical benefits, in that it is often difficult to control the background electrolyte in a processing situation. In this chapter the adsorption from a NaCl solution will be compared to that from a $NaCl/CaCl_2$ solution. Of particular interest is the possible association between the charged GLU and the divalent Ca^{2+} ions. Prior work has shown that multivalent ions can reduce the intermolecular repulsions between polyelectrolyte chains to an extent that can not be explained by the Debye-Huckel model alone.[25,26] It has also been shown that the Ca^{2+}

---

[23] Blaakmeer, J.; Cohen Stuart, M.A.; Fleer, G.J. 'The Adsorption of Polyampholytes on Negatively and Positively Charged Polystyrene Latex', *Journal of Colloid and Interface Science* **1990**, *140*, 314-325.

[24] Santhiya, D.; Subramanian, S.; Natarajan, K.A.; Malghan, S.G., 'Surface Chemical Studies On The Competitive Adsorption Of Poly(Acrylic Acid) And Poly(Vinyl Alcohol) Onto Alumina', *Journal of Colloid Interface Science* **1999**, *216*, 143-153.

[25] Mahltig, B.; Walter, H.; Harrats, C.; Muller-Buschbaum, P.; Jerome, R.; Stamm, M. 'Adsorption of Polyampholyte Copolymers at the Solid/Liquid Interface: The Influence

ions will specifically adsorb on the silica surface.[27] Thus the Ca^{2+} ions may act as a bridging unit between the GLU and the SiO_2 surface that facilitates adsorption.

The objective of this work was to investigate the adsorption of poly(amino acids) from aqueous solutions on Al_2O_3 and SiO_2. All adsorption experiments were done at pH 7, which is below the IEP of Al_2O_3[28] and therefore the Al_2O_3 was positively charged. The IEP of SiO_2 is 2-3 and so the silica was negatively charged. The focus of this work is on homopolymers and copolymers that do not exhibit any tertiary or quaternary structure. Four poly(amino acids) were studied, poly-L-proline (PRO), poly-L-hydroxyproline (HPRO), poly-L-(glutamic acid) (GLU), and a copolymer consisting of the trimer proline-glycine-proline (PGP). The GLU has carboxylate side groups with a pKa of 4.07[29] and therefore is negatively charged at pH 7. In the previous chapter, it was shown that this is an interesting candidate for an anchor block that adsorbs onto positively charged surfaces. PRO is the only naturally occurring, nonionic, water-soluble polypeptide and, in Chapter 3, it was shown that this could make an effective steric tail block for alumina surfaces when copolymerized with GLU.

---

of pH and Salt on the Adsorption Behaviour', *Physical Chemistry Chemical Physics* **1999**, *1*, 3853-3856.

[26] Zhang, Y.; Tirrell, M.; Mays, J.W. 'Effects of Ionic Strength and Counterion Valency on Adsorption of Hydrophobically Modified Polyelectrolytes', *Macromolecules* **1996**, *29*, 7299-7301.

[27] Meagher, L. 'Direct Measurement of Forces Between Silica Surfaces in Aqueous $CaCl_2$ Solutions Using an Atomic Force Microscope', *Journal of Colloid and Interface Science* **1992**, *152*, 293-295.

[28] Cesareno, J.; Aksay, I.A.; ' Processing of Highly Concentrated Aqueous α-Alumina Suspensions Stabilized with Polyelectrolytes', *Journal of the American Ceramic Society* **1988**, *71*, 1062-1067.

[29] Tropp, B.E. *Biochemistry: Concepts and Applications*, Brooks/Cole Publishing Company: Pacific Grove, CA, 1997, p. 111.

HPRO was studied to determine what effect, if any, the pendent hydroxyl group had on adsorption. A copolymer consisting of the trimer PRO-GLY-PRO was also studied to determine the effect on adsorption of adding other monomers into the PRO chain. Organisms typically do not form long chains of only one amino acid, and thus other amino acids are needed to create the long chain needed for the buoy block.

4.2 Experimental

4.2.1 Materials

The polypeptides used were all purchased from Sigma, with the following lot numbers: poly-L-proline - 029H5914, 020K5901, 089H5912; poly-L-hydroxyproline – 096H5511; poly-L-(glutamic acid) – 127H5908; poly-(PRO-GLY-PRO) – 035H5520. The structures of the polymers are shown in Figure 4.1. The alumina particles used for the adsorption experiments consisted of α-Al_2O_3 (Sumitomo Chemical Company, Ltd, AKP-30, Lot #: HB-9801, > 99.99% Purity, Specific Surface Area: 7.1 m^2/g, Mean Particle Size: 0.40 μm). In Chapter 3 the IEP of the alumina particles was measured to be 8.6 in KNO_3 and 8.7 in NaCl, which is in good agreement with that found in the literature of 8.8.[28] The silica was (Cabot Corporation), Cab-O-Sil LM-130, BET surface area: 130 m^2/g, average particle aggregate: 0.2 – 0.3 μm) which has an IEP ~ 3. The silica was dried in a convection oven at 110-115^oC for at least four hours just prior to use. Deionized water, purified using a NANOpure II ion exchanger from Barnstead with a specific resistance above 17 MΩ·cm, was used for all experiments. ACS Reagent grade sodium chloride, sodium hydroxide and hydrochloric acid from Fisher were used for ionic strength and pH adjustment.

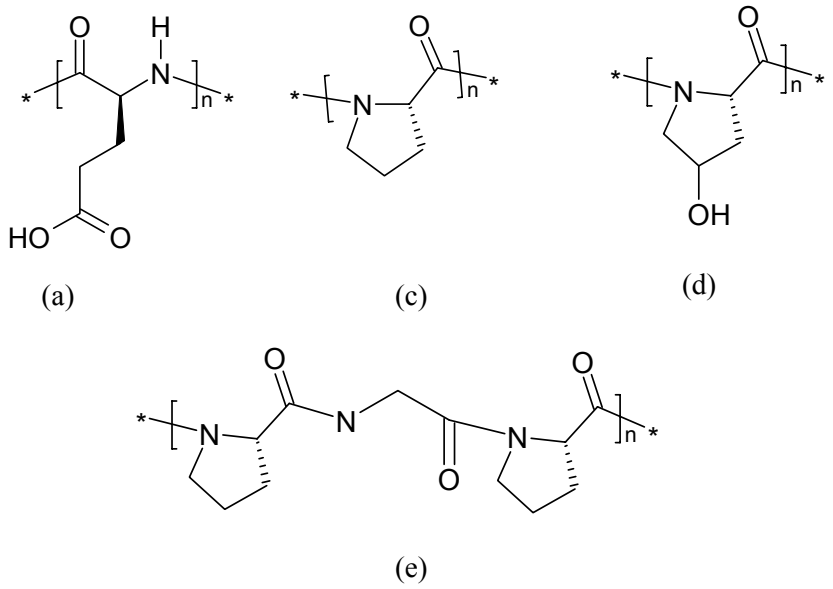

Figure 4.1: Polymer Stuctures: a) poly-l-(glutamic acid), b) poly-l-proline (PRO), c) poly-l-hydroxyproline (HPRO), d) poly(PRO-GLY-PRO) (PGP).

4.2.2 Dynamic Light Scattering

Dynamic light scattering (DLS) measurements were performed with a DynaPro-801 TC from Protein Solutions Inc operating at a wavelength of 836.4 nm. All experiments were done at 25^{o}C and controlled to ± 0.2^{o}C. At the start of each experiment, the sample chamber was flushed with 1-2 ml of DI water, filtered with a 0.02 μm Whatman Anotop syringe filter. Bovine serum albumin (BSA) standard (from Pierce at 2mg/ml) was used periodically to check the optical alignment. Approximately 0.5 ml of the sample was injected, after filtering with a 0.02 μm Whatman Anotop syringe filter, into the sample chamber, making sure there were no air bubbles in the syringe prior to injection. Initially, a stable count rate needed to be established before measurements could be taken. Enough measurements were taken so that a good average could be calculated (at least 15). Size distribution analyses were conducted using two algorithms in the

Dynamics software[30]. The first is the Regularization, which calculates up to three peaks and gives the relative scattering percentages for each. The second, Dynals, can report more than three peaks, subpeaks, and gives relative scattering percentages for each. Both of these methods will only give a value for the hydrodynamic radius, unless it is known how the molecular weight varies with radius, as is the case for globular proteins like BSA. The hydrodynamic radius is determined using the Stokes-Einstein equation:

$$R_H = \frac{k_b T}{6\pi\eta D_T} \qquad \text{Equation 4.1}$$

where k_b is Boltzman's constant, T is temperature, η is the solvent viscosity and D_T is the diffusion coefficient which is comes from the autocorrelation function.

4.2.3 Static Light Scattering

Static light scattering experiments were also performed with the DynaPro to measure the weight average molecular weight and the second viral coefficient, A_2. In order to calculate these values, scattering intensities were measured at different polymer concentrations. From scattering theory for dilute solutions:

$$\frac{Kc}{R_\theta} = \frac{1}{M_w} + 2A_2 c \qquad \text{Equation 4.2}$$

where R_θ is the Rayleigh ratio or the reduced relative scattering intensity, c is the concentration of polymer, and K is an optical constant defined as:

$$K = \frac{2\pi^2 n_o^2 \left(dn/dc\right)^2}{N_A \lambda^4} \qquad \text{Equation 4.3}$$

[30] Ivanova, M.A.; Arutyunyan, A.V.; Lomakin, A.V.; Noskin, V.A., 'Study of DNA Internal Dynamics by Quasi-Elastic Light Scattering' *Applied Optics* **1997**, *36*, 7657-7663.

where n_o is the refractive index of the solvent, (dn/dc) is the refractive index increment, and and λ is the wavelength of light used in the experiment[31]. The dn/dc value used for the solutions was 0.186 ml/g, a typical value for proteins at wavelengths greater than approximately 730nm[32]. The other instrumental parameter required was the intensity of toluene, I(toluene), which was calculated using a standard. Lysozme, from Sigma (product number L7651, Lot number 57H7045) which has a known molecular weight of 14,400 g/mol, was first run before every series of static measurements under the same conditions as the polymers (pH 7, with 0.1 M NaCl), and the I(toluene) parameter was adjusted to obtain the known molecular weight. This value was then used for the polymer solution analysis to calculate the molecular weight and the second virial coefficient. A typical experiment consisted of measurements taken at seven different polymer concentrations, ranging from 1 to 3 mg/ml. Within this range there was no dependence on the hydrodynamic radius with polymer concentration

4.2.4 Homopolymer Adsorption Isotherms

Adsorption isotherms of the poly(amino acids) were measured using the depletion method. A stock solution of polymer in water was made and stirred overnight. This solution was then filtered with a 0.45 μm Nalgene Surfactant-Free Cellulose Acetate (SFCA) filter. The stock solution was diluted to the initial concentration with a total volume of 12 ml in a centrifuge tube with a screw cap with 0.1 M NaCl and at pH 7, adjusted using either 0.1 M NaOH or 0.1 M HCl. For initial concentration measurements, 2 mls of each sample were removed and analyzed with a Hitachi U-2000 spectrophotometer at a wavelength of 220 nm. Next, 1 g of Al_2O_3 was added to the solution and shaken overnight (longer than 16 hours). The sample was then centrifuged for 15 min. at 10,000 rpm (a g-force of 15,000 in a Marathon 21K Centrifuge) and the supernatant was carefully removed and filtered with a 0.2 μm Whatman Anotop 25 mm

[31] Burchard, W. 'Polymer Characterization - Quasi-Elastic and Elastic Light-Scattering', *Makromol. Chem., Macromol. Symp*. **1988**, *18*, 1-35.

[32] Huglin, M.B. *Light Scattering from Polymer Solutions*, Academic Press: London, 1972.

syringe filter. The supernatant concentration was then measured using the spectrophotometer. The adsorbed amount was then calculated using the following equation:

$$\Gamma = \frac{(C_A - C_S)V_T}{M_P A_S} \qquad \text{Equation 4.4}$$

where: C_A is the initial polymer concentration, C_S is the equilibrium polymer concentration, V_T is the volume of solvent used, M_P is the mass of solid, and A_S is the specific surface area of the solid particles.

In order to study the adsorption of GLU on α-Al_2O_3 as a function of ionic strength an initial polymer concentration of 3 mg/ml was chosen based on previous results, which showed that this concentration is clearly on the adsorption plateau. The adsorption of GLU on SiO_2 in the presence of $CaCl_2$ was also studied. The total ionic strength was kept constant at 0.1 M, with 10 mM $CaCl_2$ and 70 mM NaCl. The GLU concentration was varied over range, similar to the adsorption isotherms discussed above.

4.3 Results

4.3.1 Solution Properties of Poly(Amino Acids)

4.3.1.3 Effect of Molecular Weight and Polymer Type

Table 4.1 summarizes the results for the weight average molecular weight, M_w, and the second virial coefficient, A_2, that were calculated using equations 2 and 3. The second virial coefficient was positive for all polymers except for the PGP copolymer.

Table 4.1: Weight-average molecular weight M_w and second virial coefficient A_2 data from static light scattering experiments at pH 7, 0.1 M NaCl, and 25°C. Values of M_w and A_2 were calculated using equation 2. The standard deviation deviations for each value are shown. The number designation for each polymer corresponds to M_w in kDa.

Polymer	Mw	A_2
	g/mole	$m^3kg^{-2}mol$
PRO (7.6k)	7600 ± 400	0.019 ± 0.006
PRO (18.0k)	18000 ± 800	0.004 ± 0.001
PRO (22.2k)	22200 ± 600	0.003 ± 0.001
PGP (3.3k)	3300 ± 200	-0.014 ± 0.008
HPRO (6.4k)	6400 ± 500	0.013 ± 0.005
GLU (8.1k)	8100 ± 800	0.028 ± 0.001

Before the adsorption data were measured, the aqueous solution properties of the polymers were characterized. DLS measurements were used to analyze the polymer solutions in 0.1 M NaCl and pH 7 at 25°C. For these conditions, the Debye length $\kappa^{-1} \approx 1$ nm. The results from the Dynals algorithm and the regularization algorithm were comparable with both showing only one peak. The measured R_H values from these two algorithms typically agreed to within 2 nm and thus the Regularization results are presented. The results for the hydrodynamic radius were compared with freely jointed chain statistic calculations for chain dimensions, using the following equations for the end-to-end distance, R, and radius of gyration, R_g, respectively:

$$\left\langle R^2 \right\rangle = nl^2 C_\infty \qquad \text{Equation 4.5}$$

$$\left\langle R_g^2 \right\rangle = \frac{\left\langle R^2 \right\rangle}{6} \qquad \text{Equation 4.6}$$

where n is the number of backbone bonds (three times the degree of polymerization for the poly(amino acids)), l is the average length of these bonds, which is 0.143 nm for the peptide bond), and C_∞ is the characteristic ratio (given as 15.8 for HPRO[33] and 13.7 for

[33] Clark, D.S.; Mattice, W.L. 'Hydrodynamic Properties and Unperturbed Dimension of Poly(γ-hydroxy-L-proline) in Aqueous Solution', *Macromolecules* **1977**, *10*, 369-374.

PRO[34] in water at 30°C and 8.8 for GLU in 0.3M sodium phosphate buffer at pH 7.85[35] this value for GLU represents a lower bound for our experiments). These values for C_∞ are equivalent to Kuhn lengths of 2.6 nm, 2.3 nm, and 1.5 nm for HPRO, PRO and GLU, respectively. Given the value of C_∞ for GLU at 0.3 M, the calculated Kuhn length represents a lower bound, since the electrostatic contribution to the Kuhn length increases with decreasing ionic strength, the value of L_k for GLU at 0.1 M should be greater than 1.5 nm. The hydrodynamic radius can then be calculated from the radius of gyration, assuming a non-draining sphere[36], by:

$$R_H = 0.875 R_g \qquad \text{Equation 4.7}$$

Table 4.2 shows the calculated R_H values for various degrees of polymerization for the various PRO samples. DLS results using the regularization algorithm were compared to the calculated values and were found to agree within 1-2 nm.

Table 4.2: Comparison of hydrodynamic radii R_H measurements from dynamic light scattering at pH 7, 0.1 M NaCl, and 25°C with R_H values calculated from a non-draining, freely jointed chain model.

	DP	R [a]	Rg [b]	R_H [c]	R_H [d]
		nm	nm	nm	nm
PRO (7.6k)	75	7.9	3.2	2.8	1.8
PRO (18.0k)	175	12.1	5.0	4.3	4.4
PRO (22.2k)	225	13.8	5.6	4.9	7.8
HPRO (6.4k)	50	7.0	2.8	2.5	1.6
PGP (3.3k)	40	5.8 [e]	2.34 [e]	2.1 [e]	1.5
GLU (12.0k)	75	6.4	2.6	2.3	4.7

a) Values of the end-to-end distance R were calculated from equation 4.6.

[34] Mattice, W.L.; Mandelkern, L. 'Conformational Properties of Poly-L-Proline Form II in Dilute Solution', *Journal of the American Chemical Society* **1971**, *93*, 1769-1777.

[35] Brandup, J.; Immergut, E.H. *Polymer Handbook, 3rd ed.,* John Wiley and Sons: New York, 1989, pg.

[36] Tanford, C. *Physical Chemistry of Macromolecules*, John Wiley and Sons: New York, 1962, pg. 20-13.

b) Values of the radius of gyration R_g were calculated from Equation 4.7.

c) Values of the hydrodynamic radius R_H were calculated from Equation 4.8.

d) Experimentally measured values of R_H were calculated using the Regularization algorithm.[30]

e) C_∞ ratio for PRO used in these calculations.

4.3.1.2 Effect o f Calcium on Hydrodynamic Radius

In order to determine the effect of $CaCl_2$ on the adsorption of GLU on SiO_2, the solution behavior of the polymer must first be studied in order to ensure that the polymer still exists as single chains in solution. Table 4.3 shows the measured hydrodynamic radius for GLU in aqueous solutions with fixed NaCl molarity (0.1 M) and with varying amounts of $CaCl_2$. The Debye length calculated from the effective ionic strength is also shown. The effective ionic strength is defined as:

$$I_{eff} = \frac{1}{2}\sum c_i (z_i)^2 \qquad \text{Equation 4.8}$$

For a mixture of NaCl and $CaCl_2$, this reduces to:

$$I_{eff} = [C_{Na} + 3C_{Ca}] \qquad \text{Equation 4.9}$$

At the GLU concentration of 3 mg/ml, the contribution of the GLU to the effective ionic strength was negligible, less than 1 %. It is important to note in Table 4.3 that the hydrodynamic radius of the GLU doubles when the $CaCl_2$ molarity is increased from 0.001 M to 0.01 M, or when the Debye length was 0.8 nm. The Debye length is defined as one over κ:

$$\kappa^2 = \frac{2e^2 \sum (z^i)^2 n_0^i}{\varepsilon k T} \qquad \text{Equation 4.10}$$

where, n_o is the number concentration of counterions in the equilibrium salt solution, ε is the relative permittivity of the solution , k is the Boltzmann constant, T is the temperature in Kelvin, z is the valence of the ion, and e is the elementary charge. κ^{-1} characterizes the length scale of the electrostatic interactions in the fluid. For water at 25°C:

$$\kappa^{-1} = \frac{0.31}{\left(I_{eff}\right)^{1/2}}$$ Equation 4.11

Table 4.3: Hydrodynamic radii of GLU 12.0 kDa, measured using DLS and calculated using the Regularization algorithm, at a fixed concentration of NaCl, and varying the $CaCl_2$ concentration.

NaCl	$CaCl_2$	R_H	Debye length
M	M	nm	nm
0.1	0	6.4	1.0
0.1	0.001	5.5	0.9
0.1	0.01	11.3	0.8
0.1	0.05	11.9	0.6
0.1	0.1	40.2	0.5

4.3.2 Homopolymer Adsorption

All of the adsorption experiments were done at 0.1 M NaCl and pH 7. Figure 4.2 and Figure 4.3 show the homopolymer adsorption isotherms on alumina. The error bars show the reproducibility found by performing the measurements in duplicate**.** The PRO, HPRO, and PGP polymers show relatively little adsorption on alumina, less than 0.2 mg/m^2, while the GLU shows plateau adsorbed amounts of ~ 0.5 mg/m^2.

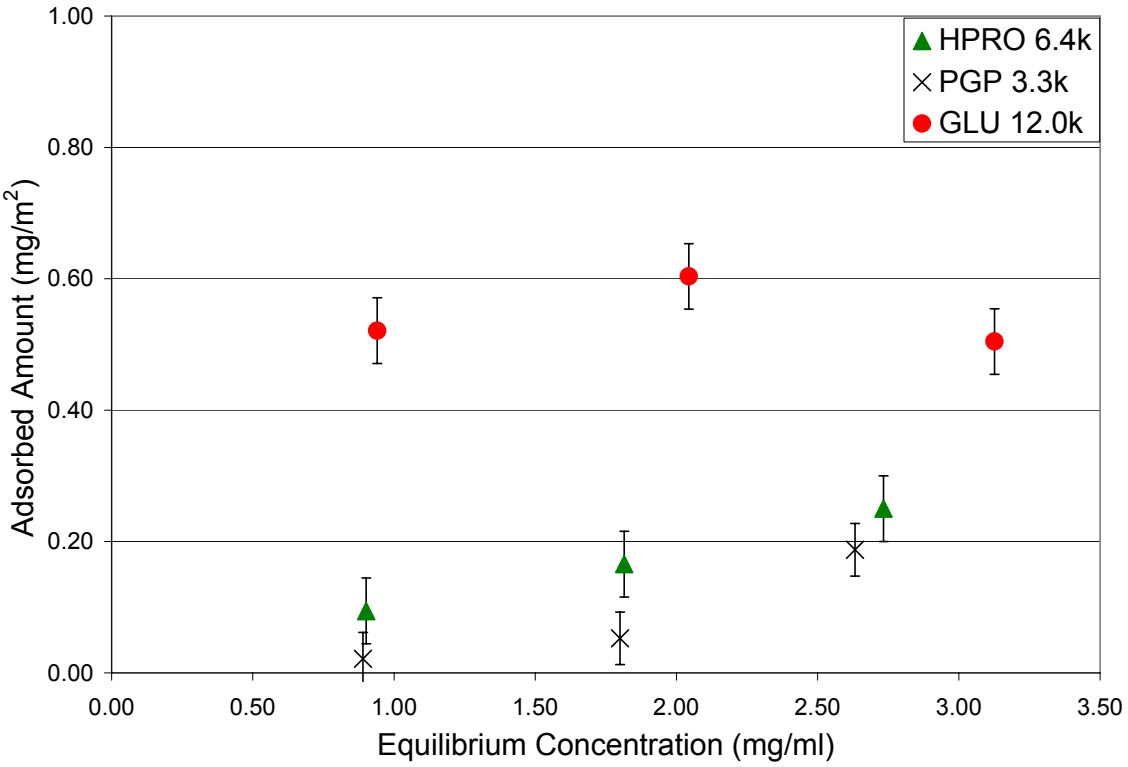

Figure 4.2: Adsorbed amounts of different polymers on alumina at pH 7 and 0.1 M NaCl, calculated using Equation 4.4.

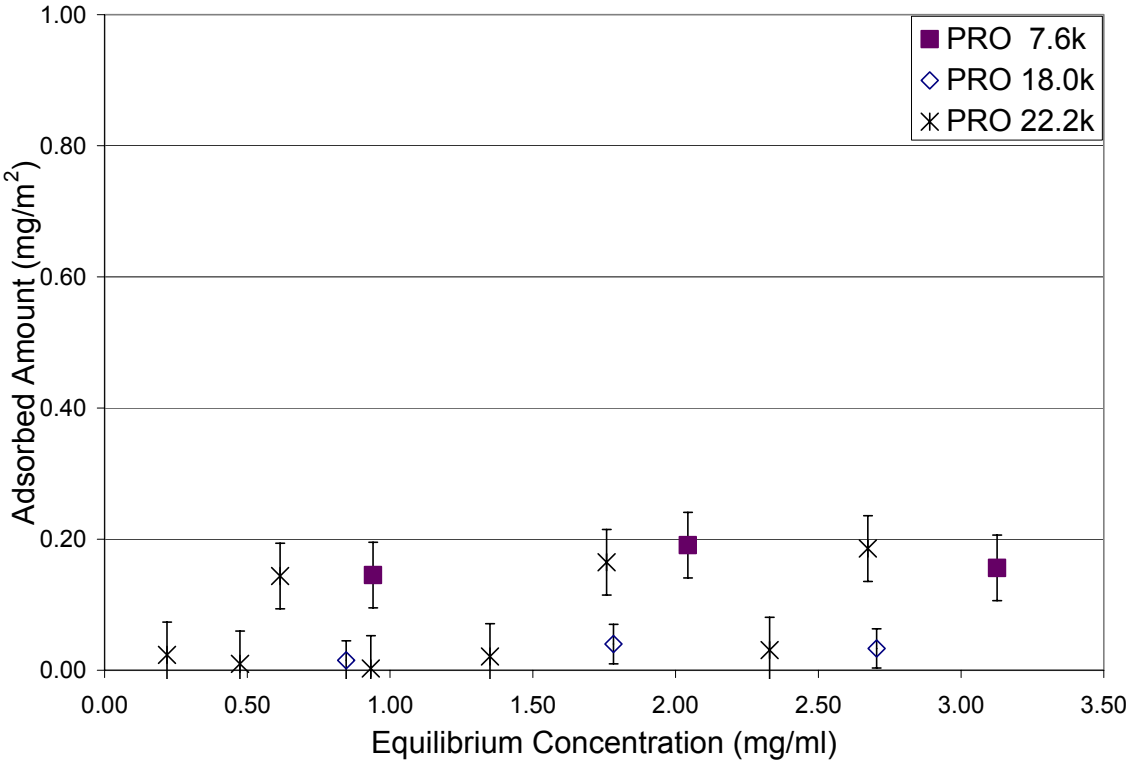

Figure 4.3: Adsorbed amounts of poly-l-proline (PRO) with varying molecular weights on alumina at pH 7 and 0.1 M NaCl, calculated using Equation 4.4.

Figure 4.4 shows the adsorption of two different molecular weight PRO, HPRO and GLU on silica. The two PRO samples do show a significant adsorbed amount on SiO_2, while the GLU did not adsorb onto the silica and the HPRO showed only a slight degree of adsorption.

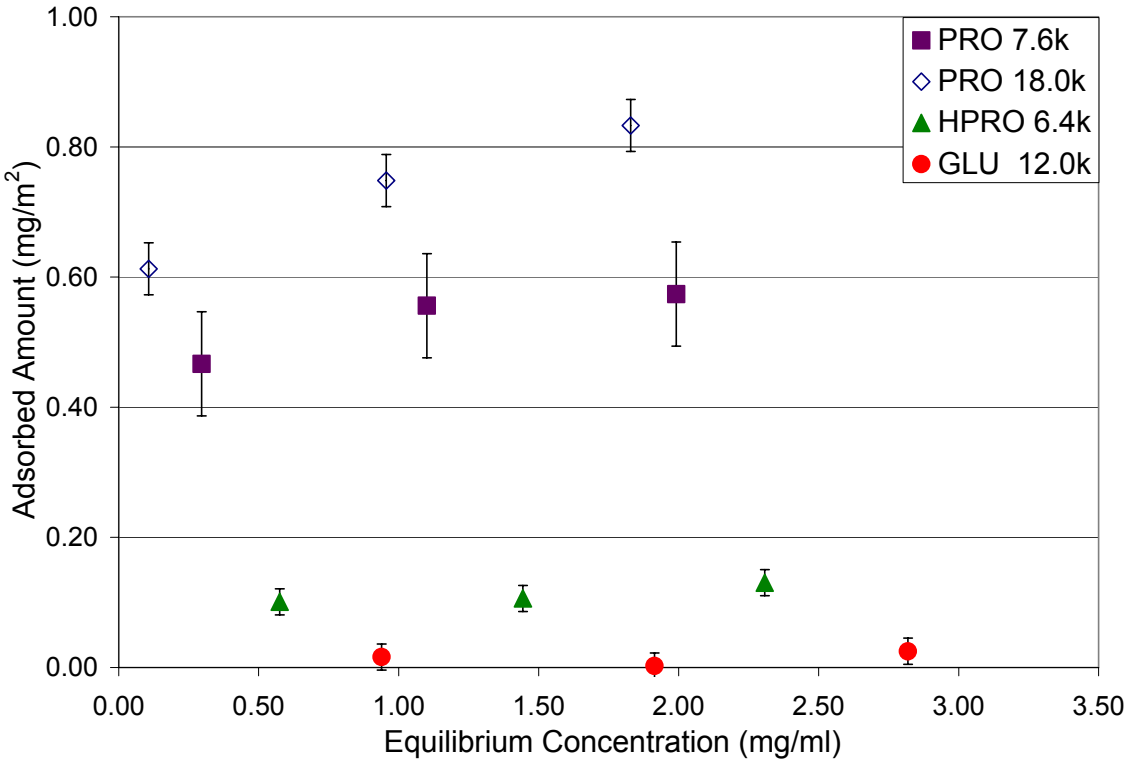

Figure 4.4: Adsorbed amounts of different polymers on silica at pH 7 and 0.1 M NaCl, calculated using Equation 4.4.

The effect of the Debye length (or inverse of the square root of the ionic strength) on GLU adsorption onto Al_2O_3 is shown in Figure 4.5. At the GLU concentration of 3 mg/ml, the contribution of the GLU to the effective ionic strength was negligible. Above a Debye length of 1 nm (below 0.1M NaCl) the adsorbed amount remained effectively constant at 0.55 mg/m^2 while, below a Debye length of 1 nm (above 0.1M NaCl), the adsorbed amount increased to ~ 0.70 mg/m^2.

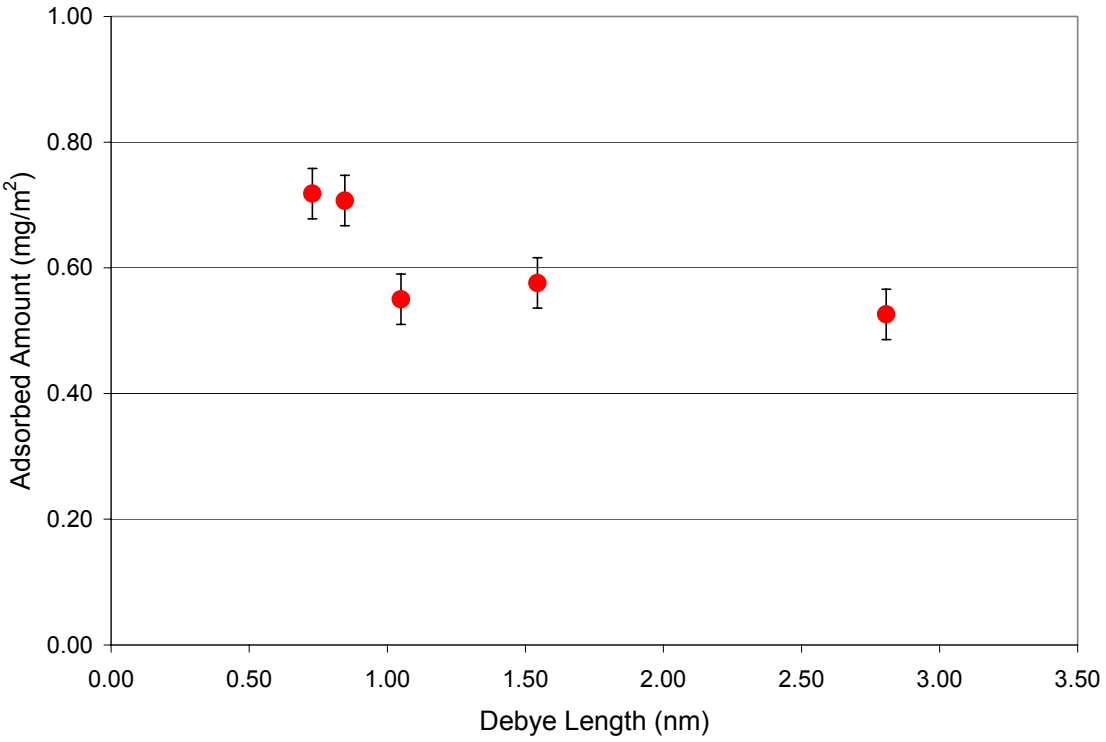

Figure 4.5: Adsorbed amounts of the sodium salt of poly-L-glutamic acid (GLU) 12.0k on alumina in aqueous NaCl solutions as a function of Debye length (ionic strength) at a fixed initial polymer concentration of 3 mg/ml and at pH 7. Calculated using Equation 4.4.

The adsorption of GLU on SiO_2 in the presence of $CaCl_2$ is shown in Figure 4.6. The total ionic strength was kept constant at 0.1 M, the same as in Figure 4.3-4.5. There was very little adsorption of GLU, with $\Gamma < 0.05$ mg/m^2, and essentially no stimulation of adsorption due to the presence of calcium ions.

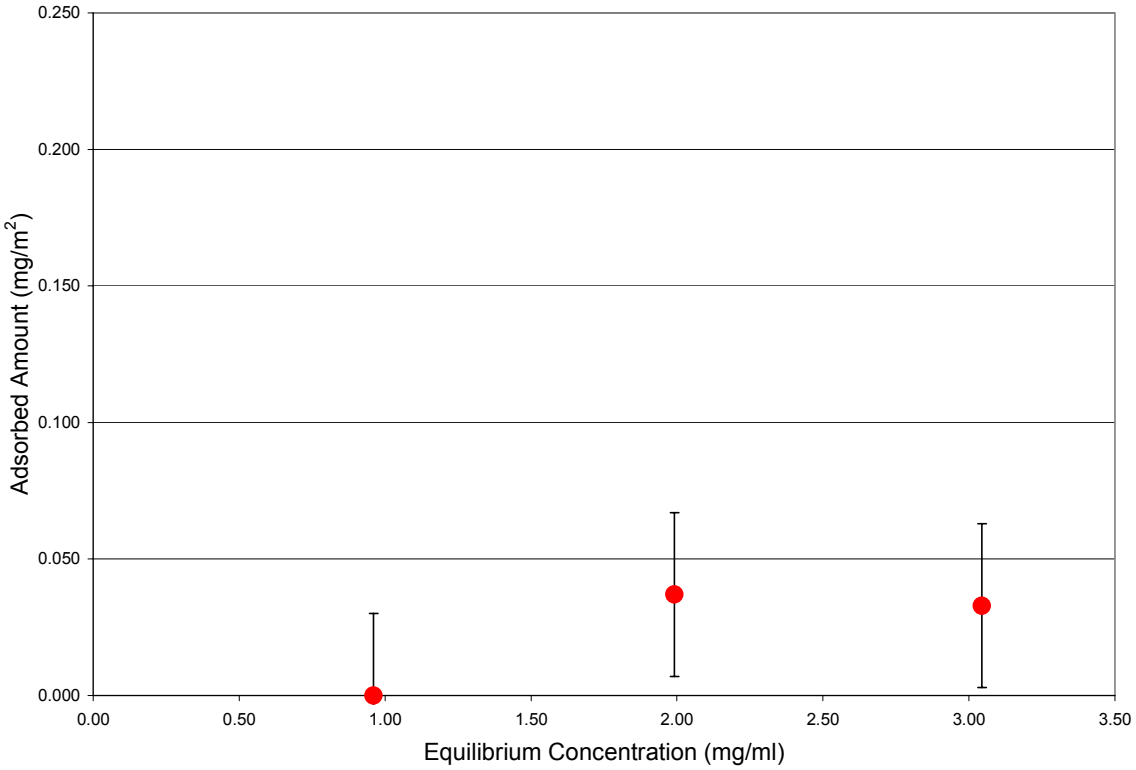

Figure 4.6: Adsorption of GLU 12.0k on SiO_2 at 10mM $CaCl_2$ and 70 mM NaCl at pH 7, with κ^{-1} = 1 nm. calculated using Equation 4.4.

4.4 Discussion

4.4.1 Solution Properties of Poly(Amino Acids)

The agreement between the measured and calculated results in Table 4.2 indicates that all of the polymers are non-aggregated and exist mostly as single chains in NaCl solution. The measurements of weight-average molecular weight M_w and second virial coefficient A_2 summarized in Table 4.1 are then indicative of single chains rather than aggregates even for the PGP sample that has a slightly negative value of A_2. These results for GLU and PRO are consistent with published reports. At pH < 4, GLU forms an α-helix which self-aggregates, and is not soluble in water.[37,38] At pH > 6, the conformation of GLU

[37] Blout, E.R.; Idelson, M. 'Polypeptides. VI. Poly-a-L-Glutamic Acid: Preperation and Helix-Coil Transition', *Journal of the American Chemical Society* **1956**, *78*, 497.

changes to a charged random coil, which is soluble in water.[39] At intermediate pHs, a combination of helical and random coil conformations exists. The PRO and HPRO chains are always helical,[40,41] both existing in the form II left-handed helix,[42] although the solubility of the HPRO is higher than the PRO in water, as evidenced by a higher A_2.[33] Of particular interest is the effect of polymer molecular weight and structure on A_2. A_2 increases as the polymer becomes more soluble.[43] Shorter chains are typically more soluble and thus have a larger A_2. This is seen in Table 1 for PRO where A_2 increased by more than a factor of 5 when M_w decreased from 22.2 kDa to 7.6kDa. The HPRO sample with M_w = 6.4 kDa has a second virial coefficient that is indistinguishable from that of the PRO sample with M_w = 7.6 kDa. Based on the Kuhn length values previously mentioned, 2.6 nm for HPRO and 2.3 nm for PRO, it is expected that the HPRO is more stiff than the PRO, which would tend to decrease the solubility. However, the addition of the hydroxyl on the HPRO would tend to increase solubility. These two factors may effectively cancel each other, explaining why the A_2 values for the two polymers are very similar. It was hypothesized that the presumed increase in flexibility afforded by the GLY residues would increase solubility compared to pure PRO and thus a PGP chain might be a more effective stabilizing tail block. However, the glycine in the PGP copolymer appears to significantly decrease the solubility of the chain compared to pure PRO as indicated by the PGP's slightly negative A_2 even though the molecular weight was only 3.3kDa. This was expected because the amino acid GLY is more hydrophobic

---

[38] Fasman, G.D.; Lindblow, C.; Bodenheimer, E. *Biochemistry* **1964**, *3*, 155.

[39] Nakajima, A.; Shinoda, K.; Hayashi, T.; Sata, H., 'Interactions Between Oppositely Charged Polypeptides', *Polymer Journal* **1975**, *7*, 550-557.

[40] Steinberg, I.Z.; Harrington, W.F.; Berger, A.; Sera, M.; Katchalski, E. 'The Configurational Changes of Poly-L-proline in Solution', *Journal of the American Chemical Society* **1960**, *82*, 5263.

[41] Smith, M.; Walton, A.G.; Koenig, J.L. *Biopolymers* **1969**, *8*, 173.

[42] Williamson, M.P. 'The Structure and Function of Proline-Rich Regions in Proteins', *Biochem J.* **1994**, *297*, 249-260.

[43] Young, R.J.; Lovell, P.A. *Introduction to Polymers*, 2nd Ed., Chapman and Hall: London, 1991.

(solubility in water is 0.25 g/g water) than the PRO (solubility in water is 1.81 g/g water) and polyglycine is insoluble in water.[44] However, it is important to note that there was no aggregation of the PGP, as shown by the hydrodynamic radius from DLS results shown in Table 4.2.

The hydrodynamic data shown in Table 4.3 is important for understanding the effect of additional $CaCl_2$ on the aggregation of GLU 12.0 kDa. At 0.1 M $CaCl_2$ there is a large increase in the hydrodynamic radius, signifying the onset of aggregation. When further $CaCl_2$ was added the solutions became visibly cloudy. Based on these results, an adsorption experiment was designed using 70 mM NaCl and 10 mM $CaCl_2$, which results in a total effective ionic strength of 0.1 M, at which the GLU exists as single chains in solution.

4.4.2 Homopolymer Adsorption

The results from the adsorption on alumina showed that only the GLU adsorbed. This is consistent with results from the previous chapter, which showed strong GLU adsorption, but relatively little PRO adsorption on α-Al_2O_3. These results can also be compared to the work by Cesareno et. al.,[28] who studied the adsorption of the sodium salt of poly(methacrylic acid) (PMMA), with a molecular weight of 15,000 in 0.1 M NaCl, on the same grade of alumina used in this study. Their work showed that the negatively charged PMMA exhibited stronger adsorption on α-Al_2O_3 at pH < IEP (at pH 7.5 $\Gamma_{plateau}$ = 0.5 mg/m^2), but still adsorbed at pH > IEP (at pH 9.2 $\Gamma_{plateau}$ = 0.3 mg/m^2). The adsorbed amount of 0.5 mg GLU/m^2 is equivalent to ~ 0.43 nm^2 of surface per amino acid residue estimated from molecular models.[23] This suggests that the GLU adsorbs mainly in a train conformation on the surface and also explains why the values for the adsorbed amounts were fairly low. In contrast to the high adsorption on alumina, no adsorption of GLU occurred on the silica at 0.1 M NaCl (Figure 4.4) because, at pH 7, both the GLU and the silica surface are negatively charged.

---

[44] Lin, Y.; Bolen, D.W. 'The Peptide Backbone Plays a Dominate Role inProtein Stabilization by Naturally Occurring Osmolytes', *Biochemistry* **1995**, *34*, 12884-12891.

The very low PRO adsorption on alumina shown in Figure 4.3 is also consistent with previous adsorption experiments done by Gibson[45] with PEOX and Mathur and Moudgil[46] with PEO, which showed very little adsorption for those polymers on alumina. PEOX is a synthetic, nonionic, water-soluble polyamide (with a Kuhn length of 0.77nm) and thus is somewhat comparable to PRO. The adsorbed amounts for HPRO 6.4k were comparable to those for all 3 PRO samples, particularly for the PRO 7.6k sample. It was thought that the pendent hydroxyl groups on the HPRO might provide additional hydrogen bonding sites with the alumina surface and thus enhance adsorption compared to PRO but this was not the case

PGP was studied to see how the addition of glycine (GLY), which promotes flexibility in a polypeptide,[29] would affect the solubility and the adsorption of a potential tail block for alumina. It is interesting to note that, even in a poor to theta solvent, the PGP does not show a strong affinity for the surface as seen in Figure 4.2. Polymer adsorption is affected by the degree of polymerization (DP) and also by a complex interplay of polymer-surface-solvent interactions, embodied by the χ^s parameter, and the polymer-solvent interactions, embodied by the Flory χ parameter.[4] In general, the adsorbed amount increases with DP, χ^s (increasing polymer-surface interaction energy), and χ (decreasing solubility). Changing the composition of a polymer can affect both interaction parameters. It is possible that the relatively low adsorbed amount for PGP is due to its low degree of polymerization (~ 40), a low value of χ^s, or some combination of both. Regardless of the precise reasons, the results show that a PGP tail block would probably not be as effective in forming a brush on alumina compared to a PRO block.

---

[45] Gibson, F.W. Stabilization of Submicron Metal Oxide Particles in Aqueous Media, Virginia Tech, 1998.

[46] Mathur, S.; Moudgil, B.M. 'Adsorption Mechanism(s) of Poly(ethylene oxide) on Negatively and Positively Charged Polystyrene Latex' *Journal of Colloid and Interface Science* **1997**, *196*, 92-98.

The PGP exhibits low adsorption, which is desirable for a tail block, but is marginally soluble which is generally not desirable for a tail block.

On silica, the adsorption results for PRO were very different from those on alumina. The two PRO samples now show adsorbed amounts ranging from ~ 0.5-0.8 mg/m^2. This is comparable to the adsorbed amounts of PEO on silica obtained by Dijt et. al.,[47] who showed that PEO adsorbs on silica at isotherm plateau amounts between 0.4-0.6 mg/m^2 for the molecular weight range studied here. For the adsorption of PEOX on SiO_2, plateau adsorbed amounts between 0.5-0.6 mg/m^2 were found in this molecular weight range.[48]

For all three polymers, the adsorption is probably dominated by hydrogen bonding between the Lewis basic polymers and the Lewis acidic silica. Figure 4.4 also shows that the adsorbed amount increases with increasing PRO molecular weight, which is expected for high affinity adsorption of nonionic polymers, as is seen with PEO on silica[47] and for PEOX on silica.[48] As the molecular weight increases, the adsorbed chain conformations include more loops and tails, leading to higher adsorbed amounts.

The relatively low adsorbed amount for HPRO on SiO_2, ~ 0.1 mg/m^2, is interesting because the HPRO showed similar low adsorption on the alumina. It was anticipated that the additional hydroxyl group on the HPRO repeat unit might enhance adsorption onto silica and alumina by providing additional sites on the chain for hydrogen bonding with the surface. The low adsorbed amounts of HPRO on both surfaces and the similar second virial coefficients for PRO and HPRO samples with similar degrees of polymerization suggest that the segmental adsorption energy χ^s parameter for HPRO on both alumina

[47] Dijt, J.C.; Cohen Stuart, M.A.; Hofman, J.E.; Fleer, G.J. 'Kinetics of Polymer Adsorption in Stagnation Point Flow', *Colloids and Surfaces* **1990**, *51*, 141-158.

[48] Chen, C.H.; Wilson, J.E.; Davis, R.M.; Chen, W.; Riffle, J.S. 'Measurement of the Segmental Adsorption Energy of Poly(2-ethyl-2-oxazoline) on Silica in Water and Ethanol', *Macromolecules* **1994**, *27*, 6376-6382.

and silica is close to the critical value $(\chi^s)_{crit}$ needed for adsorption to occur, which is typically in the range from 0.3-1 kT.[4] Polymers with $\chi^s < (\chi^s)_{crit}$ do not adsorb since the net attractive segmental energy of adsorption will not overcome the entropic penalty the polymer must pay for adsorption to occur. By contrast, the adsorption results for PRO on silica show that the χ^s parameter must be somewhat larger than (χ^s)

Figure 4.5 shows that the plateau adsorbed amounts of GLU on alumina increased with ionic strength I. This corresponds to the screening-enhanced adsorption regime in which the repulsive interactions between GLU repeat units both within the chain and between chains are increasingly screened with increasing I, thus allowing higher packing of chains on the surface. This type of behavior has been seen experimentally[49] and theoretically.[50] A scaling theory for polyelectrolyte adsorption takes into account the charge density and molecular weight of the polyelectrolyte, surface charge density, and the ionic strength of the solution.[51] In this model, adsorption occurs in different regimes, depending on the specific conditions of surface charge density σ_o, polymer charge density, degree of polymerization, and ionic strength. For the GLU 12k and alumina used in the present experiments, the values of the parameters are: 6 $\mu C/cm^2$ for the surface charge density σ_o, 1/3 for the fraction of polymer charged, 80 for the degree of polymerization, and a ionic strength range from 0.02 M to 0.2 M NaCl. According to the scaling theory, these conditions correspond to the semidilute high salt 2-D Wigner liquid regime in which the plateau adsorbed amount Γ is proportional to the square root of the salt concentration or, equivalently, $\Gamma \sim 1/\kappa^{-1}$. The reason for the deviation from this theory, especially at low salt where the chain is very stiff, could be due to the relatively low molecular weight of

[49] Blaakmeer, J.; Bohmer, M.R; Cohen Stuart, M.A.; Fleer, G.J. 'Adsorption of Weak Polyelectrolyte on Highly Charged Surfaces. Poly(acrylic acid) on Polystyrene Latex with Strong Cationic Groups', *Macromolecules* **1990**, *23*, 2301-2309.

[50] van de Steeg, H.G.M.; Cohen Stuart, M.A.; de Keizer, A.; Bijsterbosch, B.H., 'Polyelectrolyte Adsorption: A Subtle Balance of Forces', *Langmuir* **1992**, *8*, 2538-2546.

[51] Dobrynin, A.V.; Deshkovski, A.; Rubinstein, M. 'Adsorption of Polyelectrolytes at Oppositely Charged Surfaces', *Macromolecules* **2001**, *34*, 3421-3436.

the polymer, and thus the limited number of Kuhn segments, ranging from 6 Kuhn segments at the lowest ionic strength to 20 Kuhn segments at the highest ionic strength. In this rod-like limit the theory fails.

The effect of the addition of $CaCl_2$ on the adsorption of GLU on SiO_2 was also studied. Based on previous experiments it was expected that the addition of the multi-valent Ca^{+2} ions would facilitate the adsorption by forming a link between the GLU and the silica surface.[27] The results shown in Figure 4.6 show that the addition of $CaCl_2$, while maintaining a constant ionic strength of 0.1 M, did not lead to any significant increase in the GLU adsorption compared to measurements done in pure NaCl. It is possible that a higher concentration of Ca^{+2} ions is necessary to cause the onset of GLU adsorption on SiO_2. However, DLS data showed that aggregation of the GLU occurred when the $CaCl_2$ concentration was substantially increased above 0.01 M when the NaCl concentration was 0.1 M.

4.5 Conclusions and Future Work

The effect of substrate on polypeptide adsorption was clearly seen in this study. On alumina, GLU adsorbed strongly and would make a good anchor block, while the PRO showed very little adsorption and thus would be a good tail to sterically stabilize Al_2O_3 particles. This supports the earlier findings from Chapter 3. Conversely, on silica the PRO showed high affinity adsorption and would make a good anchor block, while the GLU did not adsorb and could act as a tail block that could electro-sterically stabilize SiO_2 particles.

The effect of hydroxylation was shown by comparing the PRO to HPRO adsorption data. Neither polypeptide adsorbed strongly on alumina, and only the PRO showed adsorption on silica. It is still unclear why the HPRO did not adsorb on either surface. This could be useful in designing tail blocks with other nonionic, hydroxylated amino acids such as threonine and serine. Also, the incorporation of GLY into the PRO backbone had the

effect of lowering the solubility, but not inducing adsorption on alumina. It would be important in future work to check the helicity of PGP to see if the PGP has a high helix content. This is important information that can be used in the future biosynthesis of high molecular weight tail blocks for Al_2O_3 particles, by allowing for the addition of other monomers.

The adsorption of GLU on alumina was also studied as a function of ionic strength and ion type. In NaCl solutions, the adsorbed amount increased with ionic strength, a result similar to those found for other polyelectrolyte adsorption, indicating that unstructured proteins behave like classical synthetic polymers. The addition of $CaCl_2$ to NaCl solutions of GLU caused aggregation at high $CaCl_2$ molarities, but did not promote the adsorption of GLU on silica from a non-aggregated solution. Larger molarities of Ca^{+2} are probably required to bind the GLU to the SiO_2 surface, but the GLU solubility then becomes an issue.

Based on these results there are many possibilities for the synthesis of a block copolymer via biosynthetic techniques. A first generation diblock consisting of a GLU anchor and a PRO tail is in the process of being purified. For future generations GLY could be incorporated into the tail block in order to achieve higher molecular weights.

4.6 Acknowledgments

The authors gratefully acknowledge the Center for Adhesive and Sealant Science at Virginia Tech and the Adhesive and Sealant Council Education Foundation for fellowship support for Jody Krsmanovic. This work was funded by the National Science Foundation Grant # BES-0086875.

5 Ellipsometric Study of the Adsorption of Poly(Amino Acids) on Silica and Alumina Surfaces

Abstract

The adsorption of two homopolymer polypeptides on optically smooth surfaces was studied via in situ ellipsometry. The adsorption of Poly-L-proline (PRO) and Poly-L-(glutamic acid) (GLU) from aqueous solutions of KNO_3 onto alumina and silica surfaces was studied to investigate the interactions due to the effect of peptide type and surface chemistry. The PRO was found to adsorb on the SiO_2 at levels of 0.41 mg/m^2, while not adsorbing at all on Al_2O_3. Conversely, the GLU showed minimal adsorption on silica (< 0.15 mg/m^2), but adsorbed on alumina at quantities approaching a monolayer (0.35 mg/m^2). An important finding in this work is that these unstructured polypeptides have adsorption behavior that is similar to synthetic polymers.

Keywords: Poly-L-proline, poly-L-(glutamic acid), alumina, silica, ellipsometry, adsorption.

5.1 Introduction

The study of the adsorption of polymers and proteins at solid interfaces is important for understanding a number of different applications, including particle stabilization, adhesion, and biocompatibility for artificial organs. For these reasons a significant amount of attention has been given to measuring the adsorption and conformation of adsorbed polymers and proteins. Ellipsometry is a very powerful technique for measuring adsorbed amounts without the destruction of the sample or the need for labeling.[1] It is also capable of measuring thin film thickness under certain circumstances.

[1] Elwing, H. *Biomaterials* **1998**, *19*, 397.

Ellipsometry has the advantage over other optical techniques which require specific surfaces or surface properties.[1] Many different substrates can be used, including metals, polymer coated metals, silicon, and modified gold.[1] Ellipsometry is also very useful when the films are very thin, on the order of a nanometer, or are very complicated, such as when voids are present.[2] It is very sensitive to changes in surface concentration and thickness and is more reliable for fitting adsorbed layers to thickness models than other optical techniques such as scanning angle reflectometry or surface plasmon resonance.[3]

Surface plasmon resonance (SPR) is an optical technique which has found many applications in the biotechnology field, including biosensors and immunosensors.[4] One of the main disadvantages with SPR is in the choice of substrate. In order to obtain excellent optical properties, a metal, typically gold or silver, must be deposited in a thin film on a prism.[5] Optical waveguide lightmode spectroscopy (OWLS) is another optical technique which has been used particularly in protein-membrane interactions, protein arrays, biosensors, and biocompatibility.[6] One of the limitations of OWLS is that it requires a grating coupler with lines on the order of a micron. This technique also has limitations in the substrate, in that it must be transparent and have very well-defined optical properties.[7] Scanning angle reflectometry (SAR) is very similar to ellipsometry. The main difference is in the polarization of the light used for the measurements, SAR only uses p-polarized light, whereas ellipsometry uses both p- and s-polarized light. The first drawback of SAR is that it needs more calibration than ellipsometry, because it is

---

[2] McArthur, L.; Chalmers, S. *Vacuum Technology and Coating* **2000**, *Oct*., 35.

[3] van Duijvenbode, R.C.; Koper, G.J.M. *Journal of Physical Chemistry B* **2000**, *104*, 9878.

[4] Homola, J.; Yee, S.S.; Gauglitz, G. *Sensors and Actuators B* **1999**, *54*, 3.

[5] Silin, V.; Plant, A. *Trends in Biotechnology* **1997**, *15*, 353.

[6] Ramsden, J.J. *Chimia* **1999**, *53*, 67.

[7] Kurrat, R.; Walivaara, B.; Marti, A.; Textor, M.; Tengvall, P.; Ramsden, J.J.; Spencer, N.D. *Colloids and Surfaces B: Biointerfaces* **1998**, *11*, 187.

using only half as much data.[8] Another disadvantage of this method is that a highly reflective surface, such as silicon, is needed in order to get high sensitivity.[9]

In recent years, numerous studies have been done that utilize the ellipsometric technique to measure the adsorption of polymers and proteins at the solid-liquid interface. Malmsten studied the adsorption of several model proteins - human serum albumin, immunoglobulin, fibrinogen and lysozyme - on thermally oxidized silicon wafers in aqueous solutions.[10] In another study involving lysozyme in water, Buijs et. al. measured the protein adsorption on silica and gallium arsenide surfaces.[11]

There has been a wealth of biologically important protein adsorption studies on various surfaces.[12,13,14] One of the features often examined is the spreading of the protein on to the surface after the initial adsorption.[15,16] This occurs because typical proteins have a

---

[8] van Duijvenbode, R.C.; Koper, G.J.M. *Journal of Physical Chemistry B* **2000**, *104*, 9878.

[9] Gast, A.P. in Sanchez, I.C. "Physics of Polymer Surfaces and Interfaces"; Butterwork-Heinemann: Boston; 1992, ch. 11.

[10] Malmsten, M. 'Ellipsomety studies of Porotein Layers Adsorbed at Hydrophobic Surfaces', *Journal of Colloid and Interface Science* **1994**, *166*, 333-342.

[11] Buijs, J.; Speidel, M.' Oscarsson, S. *Journal of Colloid and Interface Science* **2000**, *226*, 237-245.

[12] Oscarsson, S. 'Factors Affecting Protein Interaction at Sorbent Interfaces', *Journal of Chromatography B* **1997**, *699*, 117-131.

[13] Norde, W. 'Adsorption of Proteins from Solution at the Solid-Liquid Interface', *Advances in Colloid and Interface Science* **1986**, *25*, 267-340.

[14] Wahlgren, M.; Arnebrant, T. 'Protein Adsorption to Solid Surfaces', *Tibtech* **1991**, *9*, 201-208.

[15] Wertz, C.F.; Santore, M.M., 'Effect of Surface Hydrophobicity on Adsorption and Relaxation Kinetics of Albumin and Fibrinogen: Single-Species and Competitive Behavior', *Langmuir* **2001**, *17*, 3006-3016.

tertiary structure, which can rearrange on the surface. This is not the case for many homopolymer poly(amino acids), which have no tertiary structure and thus there is no rearrangement and spreading during adsorption.

While there has been extensive adsorption studies of proteins of biological importance exhibiting teriary and quaternary structure on materials used in bioimplants,[17,18] relatively little work has been reported on the adsorption of homopolymer polypeptides, particularly with well-defined surfaces, such as with ellipsometry. The adsorption of GLU on hydrophilic and hydrophobic silica particles has been studied.[19] There was greater adsorption on the hydrophobic surface than on the hydrophilic surface, but there was very little adsorption on either surface above pH 8. Adsorption work on positively and negatively charged polystyrene latex has also been done using a random copolymer consisting of 60 %mole GLU and 40 %mole lysine (PLL) and a tetramer of (LYS-GLU-GLY)4.[20] The results for both polymers showed that adsorption was greater on the negative surface at all pHs than on the positive latex. This adsorption has also been studied with synthetic polymers, in particular poly(ethylene oxide) (PEO) and poly(ethyl

---

[16] Wertz, C.F.; Santore, M.M., 'Adsorption and Relaxation Kinetics of Albumin and Fibrinogen on Hydrophobic Surfaces: Single-Species and Competitive Behavior', *Langmuir* **1999**, *15*, 8884-8894.

[17] Kasemo, B., 'Biological Surface Science', *Surface Science* **2002**, *500*, 656-677.

[18] MacDonald, D.E.; Deo, N.; Markovic, B.; Stranick, M.; Somasundaran, P., 'Adsorption and Dissolution Behavior of Human Plasma Fibronectin on Thermally and Chemically Modified Titanium Dioxide Particles', *Biomaterials* **2002**, *23*, 1269-1279.

[19] Killmann, E.; Reiner, M. 'Adsorption of Poly-L-Lysine and Poly-L-(glutamic acid) on Silica Surfaces', *Tenside, Surface, Detergent* **1996**, *33*, 220.

[20] Blaakmeer, J.; Cohen Stuart, M.A.; Fleer, G.J. 'The Adsorption of Polyampholytes on Negatively and Positively Charged Polystyrene Latex', *Journal of Colloid and Interface Science*, **1990**, *140*, 314-325.

oxazoline) (PEOX). Both PEO[21] and PEOX[22], which are Lewis bases, were found to adsorb much more strongly on SiO_2 (a Lewis acid), than on Al_2O_3 (a Lewis base).

There have been several studies of the cationic polypeptide, poly-L-lysine on mica, as studied by atomic force microscopy (AFM).[23,24] In these studies the researchers found that the PLL behaved like a synthetic polyelectrolyte, namely showing flat train-like conformations at low ionic strengths, and an increase in adsorption with increasing ionic strength. Similar results were found for this polypeptide on SiO_2 surfaces using SAR.[25]

These studies show that unstructured protein adsorption is similar to that of synthetic polymers. The goal of this work is to further understand this as part of a program to develop block copolymers that form self assembled brushes and that could provide steric stabilization of aqueous colloidal suspensions. Steric stabilization using mostly homopolymers is used in adhesives, ceramic processing and personal care products. The most promising steric stabilizers are block copolymers[26,27,28] that consist of a strongly

---

[21] Mathur, S.; Moudgil, B.M. 'Adsorption Mechanism(s) of Poly(ethylene oxide) on Oxide Surfaces', *Journal of Colloid and Interface Science*, **1997**, *196*, 92-98.

[22] Gibson, F.W. "Stabilization of Submicron Metal Oxide Particles in Aqueous Media", Virginia Tech, 1998.

[23] Afshar-Rad, R.; Bailey, A.I.; Luckham, L.K.; Macnaughtan, W.; Chapman, D., 'Forces Between Poly-L-Lysine of Molecular Weight Range 4,000-75,000 Adsorbed on Mica Surfaces', *Colloids and Surfaces* **1987**, *25*, 263-277.

[24] Afshar-Rad, T.; Bailey, A.I.; Luckham, P.F.; Macnaughtan, N.; Chapman, D., 'Forces Between Model Polypeptides and Proteins Adsorbed on Mica Surfaces', *Colloids and Surfaces* **1988**, *31*, 125-146.

[25] Furst, E. M.; Pagac, E.S.; Tilton, R.D. 'Coadsorption of Polylysine and the Cationic Surfactant Cetyltrimethylammonium Bromide on Silica', *Ind. Eng. Chem. Res.* **1996**, *35*, 1566-1574.

[26] DeLaat, A.W.M.; Schoo, H.F.M. 'Novel Poly(vinyl ether) Block Copolymers: Synthesis and Colloidal Stabilization of α-Fe_2O_3 in Water and Organic Solvents', *Colloid and Polymer Science* **1998**, *176*, 176-185.

adsorbing anchor block and a weakly or non-adsorbing, soluble, nonionic tail block. When designed properly, these copolymers form self-assembled layers on a surface, with brush-like tails extending from the surface into solution that generate repulsive steric forces.[29,30,31,32] To properly design block copolymers for this, detailed understanding of what influences homopolymer peptide adsorption on model surfaces is needed. Specifically, this study will examine the effects on adsorption of: peptide type, surface chemistry, and ionic strength.

In previous work, Chapter 3, it was demonstrated that at pH 7 and 9 in 0.1 M NaCl that GLU adsorbs on α-Al_2O_3 particles that were positively charged and nearly neutral while PRO showed very little adsorption. It was concluded that the GLU adsorbed onto the aluminum oxide surface due mostly to electrostatic attraction. In Chapter 4, it was further demonstrated that on SiO_2 in 0.1 M NaCl at pH 7, PRO showed high affinity adsorption characteristics while the GLU did not adsorb. In this study, the adsorption of PRO and GLU will be examined on alumina and silica at pH 6.

---

[27] DeLaat, A.W.M.; Schoo, H.F.M. 'Novel Poly(vinyl ether) Block Copolymers: Adsorption from Aqueous Solutions on α-Fe_2O_3 (Hematite) and the Mechanism of Colloidal Stabilization', *Colloid and Interface Science* **1997**, *191*, 416-423.

[28] DeLaat, A.W.M.; Schoo, H.F.M. 'Reversible Thermal Flocculation of Aqueous α-Fe_2O_3 Dispersions Stabilized with Novel Poly(vinyl ether) Block Copolymers', *Colloid and Interface Science* **1998**, *200*, 228-234.

[29] Fleer, G.J; Cohen Stuart, M.A.; Scheutjens, J.M.H.M.; Cosgrove, T.; Vincent, B. *Polymers at Interfaces*, Chapman and Hall: London, 1993.

[30] Guzonas, D.; Hair, M.L. Cosgrove, T. 'Adsorption of Block Copolymers from Nonselective Solvents', *Macromoecules* **1992**, *25*, 2777-2779.

[31] Halperin A.; Tirrell M.; Lodge T.P. 'Macromolecules: Synthesis, Order and Advanced Properties', *Advances in Polymer Science* **1992**, *100*, 31-71.

[32] Gast, A. 'Structure, Interactions, and Dynamics in Tethered chain Systems', *Langmuir* **1996**, *12*, 4060-4067.

As previously mentioned the effect of surface chemistry is also important. Comparing the adsorption of homopolymer polypeptides on Al_2O_3 and SiO_2 is critical for a general understanding of their adsorption behavior. The focus of this study will be at pH 6, at which the Al_2O_3 is positively charged and the SiO_2 is negatively charged. GLU is a negatively charged random coil at pH 6.[33] In Chapter 4, it was clearly demonstrated that PRO and GLU exhibited very different adsorption characteristics on these two surfaces. This effect of substrate has also been found for the adsorption of PEO on these surfaces, namely that PEO adsorbs strongly on SiO_2, but did not adsorb on Al_2O_3.[21] Similar results have been found for the adsorption of poly(ethyl oxazoline) PEOX on these surfaces.[22]

It was also desirable to study the effect of salt concentration and different salt types on adsorption. This has both scientific and practical benefits in that it is often difficult to control the background electrolyte in a processing situation. In Chapter 4, it was shown that the adsorbed amount of GLU on Al_2O_3 increased slightly with ionic strength due to increased screening of electrostatic repulsion between adsorbed chains, allowing a greater packing density on the surface. Similar behavior has been found both experimentally[34] and theoretically[35,36] for synthetic polymers.

The goal of this work is to study the adsorption of two poly(amino acids), poly-L-(glutamic acid) (GLU) and poly-L-proline (PRO) on two surfaces, silicon dioxide and aluminum oxide, using in-situ ellipsometry. Two ionic strengths were studied, 0.01 M and 0.1 M $NaNO_3$, both at pH 6. All of the previous work done with these polypeptides

---

[33] Tropp, B.E. *Biochemistry: Concepts and Applications*, Brooks/Cole Publishing Company: Pacific Grove, CA, 1997, p. 111.

[34] Blaakmeer, J.; Bohmer, M.R; Cohen Stuart, M.A.; Fleer, G.J. 'Adsorption of Weak Polyelectrolyte on Highly Charged Surfaces. Poly(acrylic acid) on Polystyrene Latex with Strong Cationic Groups', *Macromolecules* **1990**, *23*, 2301-2309.

[35] van de Steeg, H.G.M.; Cohen Stuart, M.A.; de Keizer, A.; Bijsterbosch, B.H., 'Polyelectrolyte Adsorption: A Subtle Balance of Forces', *Langmuir* **1992**, *8*, 2538-2546.

[36] Dobrynin, A.V.; Deshkovski, A.; Rubinstein, M. 'Adsorption of Polyelectrolytes at Oppositely Charged Surfaces', *Macromolecules* **2001**, *34*, 3421-3436.

and these surfaces has been on colloidal particles. This study focuses on surfaces that are smooth and well-defined enough for atomic force microscopy (AMF) studies that can probe surface forces generated by an adsorbed layer. For a brush forming block copolymer, AFM is an ideal probe of the surface forces generated by the attached brush structure. This chapter is one part of a two-part study, the second of which will focus on AFM measurements.

5.2 Experimental

5.2.1 Materials

The polypeptides used were all purchased from Sigma and used as received. The structures of the polymers are shown in Figure 5.1. The poly-L-proline used had a lot number of 020K5901 and the poly-L-(glutamic acid) had a lot number 108H1167. The PEO standard was purchased from Polymer Laboratories (batch number 20835-8) and had a weight average molecular weight of 114,000 g/mole with a polydispersity of 1.02. Deionized (DI) water, purified using a NANOpure II ion exchanger from Barnstead with a specific resistance above 17 MΩ·cm, was used for all experiments. ACS Reagent grade sodium nitrate, sodium hydroxide and nitric acid from Fisher were used for ionic strength and pH adjustment.

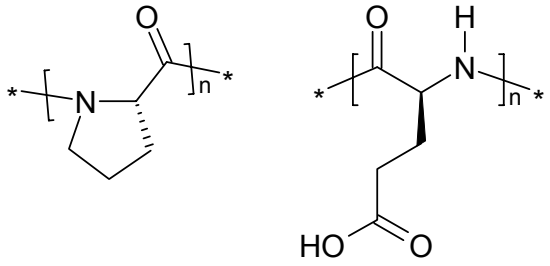

(a) (b)

Figure 5.1: Structures of Poly(amino acids) a) poly-L-proline, b) poly-L-(glutamic acid).

The silicon wafers used in these experiments were calibration standard wafers with a thermally grown SiO_2 layer. Prior to use the wafers were cut into 1 inch by 1 inch

squares and cleaned using a mixture of NH_4OH, H_2O_2, H_2O (0.5:1:5 by volume) at 70°C for 20 minutes, followed by a mixture of HCl, H_2O_2, H_2O (0.5:1:5 by volume) at room temperature for 20 minutes[37]. The wafers were rinsed well after each cleaning with deionized water. They were then dried in a 130°C oven for at least one hour. This procedure results in clean, hydrophilic surfaces. Care was taken to keep the wafers clean prior to use.

Alumina was sputter coated onto a native silicon surface using physical vapor deposition by Dr. Peter Martin at Pacific Northwest National Laboratory in Richland, WA. The resulting amorphous alumina coatings were approximately 30-40 nm in thickness. The surface roughness was measured using atomic force microscopy (Molecular Imagining, Phoenix, AZ) with a silicon cantilever (Park Scientific, CA) having a nominal spring constant of 0.26 N/m. The alumina coated wafers had a root-mean-square roughness of 1 nm. This is very close to values measured for single crystal sapphire surfaces (Commercial Crystal Laboratories Inc., Naples, FL),which had a rms roughness of 1 Å. The alumina coatings were also tested for composition using XPS (Perkin Elmer 5400 x-ray photoelectron spectrometer), and had 60% aluminum and 40% oxygen, with less than 0.5% impurities. The wafers were cleaned using a water plasma treatment, and kept clean prior to use.

A flow loop was set up to measure the adsorption of the polypeptides by ellipsometry in situ. A Masterflex L/S pump with a rigid PTFE –tubing pump head (Cole-Parmer) was used to pump the liquid from a small PTFE flask, where mixing occurred, to the cell and back. Teflon tubing was used in order to eliminate possible contamination sources. The pump was run at a flow rate of 15 ml/min, which was the equivalent of a four minute residence time. In order to increase the polymer concentration in the liquid cell, a concentrated solution of the polymer was added to the mixing flask, in the appropriate

[37] Itano, M.; Kern, F.W.; Miuashita, M.; Ohmi, T. 'Particle Removal from Silicon Wafer Surface in Wet Cleaning Processs', *IEEE Transactions on Semiconductor Manufacturing*, **1993**, *6*, 258.

amount. The concentration was then allowed at least half an hour to equilibrate, or about 7 residence times.

5.2.2 Ellipsometry

Ellipsometry measures the change in polarization of light due to the reflection from a surface. The data obtained are reported as two angles, ψ (measuring the amplitude) and Δ (measuring the phase shift). These angles are related to the ratio of the Fresnel reflection coefficients (R_p and R_s) for (p) and (s) polarized light by the following expression:

$$R_p / R_s = \tan\Psi \exp(i\Delta) \qquad \text{Equation 5.1}$$

where:

$$R_p = \frac{r_{12}^p + r_{23}^p \exp(-i2\beta)}{1 + r_{12}^p r_{23}^p \exp(-i2\beta)} \qquad \text{Equation 5.2}$$

$$R_s = \frac{r_{12}^s + r_{23}^s \exp(-i2\beta)}{1 + r_{12}^s r_{23}^s \exp(-i2\beta)} \qquad \text{Equation 5.3}$$

and

$$\beta = 2\pi\left(\frac{d}{\lambda}\right) N_2 \cos\phi_2 \qquad \text{Equation 5.4}$$

and the complex reflection coefficients at the interface between two arbitrary layers 1 and 2 are:

$$r_{12}^p = \frac{N_2 \cos\phi_1 - N_1 \cos\phi_2}{N_2 \cos\phi_1 + N_1 \cos\phi_2} \qquad \text{Equation 5.5}$$

$$r_{12}^s = \frac{N_1 \cos\phi_1 - N_2 \cos\phi_2}{N_1 \cos\phi_1 + N_2 \cos\phi_2} \qquad \text{Equation 5.6}$$

where ϕ_1 and ϕ_2 are the angles of incidence at each layer and N_1 and N_2 are the complex refractive indices for each layer, and are related to the real (n) and imaginary (k) components by:

$$N = n - ik \qquad \text{Equation 5.7}$$

The measured data can then be fit to an appropriate model to measure the adsorbed amount of a polymer, and in some cases, the layer thickness. Further details on the principle of ellipsometry can be found elsewhere[38,39].

Ellipsometric measurements were taken using a variable angle spectroscopic ellipsometer (VB-200 from J.A. Woollam Co.). In situ measurements were obtained by using a flow cell designed by J.A. Woollam Co. that operates at a fixed angle of 70°, which is near the Brewster angle for silicon, 74°. Measurements were taken over a range of wavelengths, 400-700 nm, in order to obtain a good fit of the data from the model used. A series of measurements were taken in order to construct a suitable model to fit the ellipsometric data as shown in Figure 5.2.[40] First, the thickness of the SiO_2 layer, d_2, on the dry silicon wafer was determined using a model consisting of the silicon substrate, and interfacial layer between the silica and the silicon, and the SiO_2 layer. The thickness of the interfacial layer, d_1, was kept constant at 1 nm and the optical parameters used for these layers can be found in Herzinger et. al.[40] Typically a 20 nm thick oxide layer was used in these experiments. Previous authors have found that the sensitivity of the optical technique is optimized at thicknesses near 20 nm.[41,42]

---

[38] Azzam, R.M.A.; Bashara, N.M. "Ellipsometry and Polarized Light", Elsevier: Amsterdam, 1977.

[39] Tompkins, H.G.; McGahan, W.A. "Spectroscopic Ellipsometry and Reflectrometry", John Wiley and Sons, Inc.: New York, 1999.

[40] Herzinger, C.M.; Johs, B.; McGahan, W.A.; Woollam, J.A.; Paulson, W. *Journal of Applied Physics*, **1998**, *83*, 3323.

[41] Tiberg, F.; Ederth, T. 'Interfacial Properties of Nonionic Surfacts and Decane-Surfactant Microemulsions at the Silica-Water Interface. An Ellipsometry and Surface Force Study', *Journal of Physical Chemistry* B **2000**, *104*, 9689-9695.

[42] Dijt, J.C.; Cohen Stuart, M.A.; Hofman, J.E.; Fleer, G.J. 'Kinetics of Polymer Adsorption in Stagnation Point Flow', *Colloids and Surfaces* **1990**, *51*, 141.

Next, the liquid was pumped through the cell at 25°C ± 2°C, at the appropriate ionic strength and pH for the given experiment. The Cauchy model was used to describe the wavelength dependence of the refractive index of the new ambient aqueous layer:

$$n = A + B/\lambda^2 \ldots \qquad \text{Equation 5.8}$$

This model works well for transparent media ($k = 0$).[39] The A and B parameters were fit to the ellipsometric data. The thickness of the SiO_2 layer measured in air did not vary from that measured with the aqueous medium.

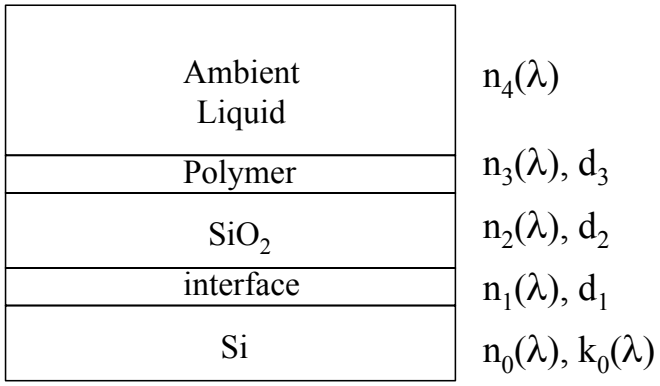

Figure 5.2: Structure of the model used for ellipsometric analysis of adsorbed polymers onto silica.

Finally, a layer was added on top of the SiO_2 layer using the Cauchy model, to account for the adsorbed polymer layer. For this layer, the B parameter in the Cauchy model was kept constant at the value obtained from fitting the aqueous layer, this is reasonable because the polymer layer is approximately 90% water and there is little wavelength dependence in this range.[43] The adsorbed amount of polymer on the SiO_2 was calculated using the following equation:

[43] Filippova, N.L. 'Adsorption of Polyelectrolytes on Planar Surfaces', *Chemical Engineering Communications* **1998**, *167*, 181-203.

$$\Gamma = \frac{d_3(n_3 - n_4)}{dn_3/dc} \qquad \text{Equation 5.9}$$

where d_3 and n_3 are the thickness and refractive index for the polymer layer, n_4 is the refractive index for the aqueous layer, and dn_3/dc is the refractive index increment, given as 0.186 cm^3/g for the polypeptide.[10] Due to the very thin layer formed by the adsorbed polymers used in this study, a unique solution could not be determined for both the thickness and the refractive index. However, the product $d_3(n_3-n_4)$ was constant over a reasonable range of refractive indices for the hydrated polymer layer (i.e. 1.34-1.37). Thus, the A parameter was systematically varied over this range and the different thickness were recorded. It was found that the adsorbed amount calculated was constant over this range of refractive indices, varying by less than 5%. Different polymer concentrations were measured by incremental additions of a concentrated stock solution. The system was allowed to equilibrate for at least 30 minutes after each addition, before measuring with the ellipsometer. For each measurement made the software generates a mean square error (MSE), which was used to determine the "goodness of fit" for each run. A typical value for the MSE was one, which was an indication of a good run. The results presented here are the average values from two or three separate experiments. The error bars represent the uncertainty in the measurements which is 0.07 mg/m^2, and is greater than the reproducibility of the experiments.

5.2.3 Dynamic Light Scattering

Dynamic light scattering (DLS) measurements were performed at 836.4 nm with a DynaPro-801 TC from Protein Solutions Inc. All experiments were done at 25°C and controlled to ± 0.2°C and all samples were filtered with a 0.02 μm Whatman Anotop syringe filter. At the start of each experiment, the sample chamber was flushed with 1-2 ml of DI water. Bovine serum albumin (BSA) standard (from Pierce at 2 mg/ml) was used periodically to check the optical alignment. Approximately 0.5 ml of the sample was injected into the sample chamber, making sure there were no air bubbles in the syringe prior to injection. Initially, a stable intensity count rate was established before measurements were taken. Typically 15 measurements were taken to get an accurate

average. Size distribution analyses were conducted using two algorithms in the Dynamics software.[44] The first is the Regularization algorithm, which calculates up to three peaks and gives the relative scattering percentages for each. The second algorithm, Dynals, can report more than three peaks, and gives relative scattering percentages for each. The hydrodynamic radius is determined using the Stokes-Einstein equation:

$$R_H = \frac{k_b T}{6\pi\eta D_T} \qquad \text{Equation 5.10}$$

where k_b is Boltzman's constant, T is temperature, η is the solvent viscosity, and D_T is the translational diffusion coefficient which is comes from the autocorrelation function. Measurements were taken at polymer concentrations ranging from 1-4 mg/ml. The radius did not vary with concentration, confirming that this is in the dilute range.

5.2.4 Static Light Scattering

The DynaPro 801 was also used for static scattering to measure the weight average molecular weight and the second viral coefficient, A_2. In order to calculate these values, scattering intensity was measured at different polymer concentrations. From scattering theory:

$$\frac{Kc}{R_\theta} = \frac{1}{M_w} + 2A_2 c \qquad \text{Equation 5.11}$$

where, R_θ is the Rayleigh ratio, or the reduced relative scattering intensity, c is the concentration of polymer K is an optical constant defined as:

[44] Ivanova, M.A.; Arutyunyan, A.V.; Lomakin, A.V.; Noskin, V.A., 'Study of DNA Internal Dynamics by Quasi-Elastic Light Scattering' *Applied Optics* **1997**, *36*, 7657-7663.

$$K = \frac{2\pi^2 n_o^2 \left(dn/dc\right)^2}{N_A \lambda^4}$$ Equation 5.12

where n_o is the refractive index of the solvent, (dn/dc) is the refractive index increment, and and λ is the wavelength of light used in the experiment.[45] The dn/dc value used for the solutions was 0.186 ml/g, a typical value for proteins at wavelengths greater than approximately 730 nm.[46] The other instrumental parameter required was the scattering intensity of toluene, I(toluene), which was calculated using a standard. Lysozme, from Sigma (Lot number 57H7045) which has a known molecular weight of 14,400 g/mol, was run before every series of static measurements at pH 7 with 0.1 M NaCl, and the I(toluene) parameter was adjusted to obtain the known molecular weight. Once calibrated, the scattering intensities were used to calculate the weight-average molecular weight, Mw, and the second virial coefficient, A_2, from equations 5 and 6, for the polymer solutions using an Excel program to calculate the standard deviations for A_2 and Mw. A typical experiment consisted of measurements taken at seven different polymer concentrations, ranging from 1 to 4 mg/ml.

5.3 Results and Discussion

5.3.1 Solution Properties

Table 5.1 shows the results for the dynamic and static light scattering experiments for the GLU and PRO at two ionic strengths, 0.01 and 0.1 M $NaNO_3$. The sodium nitrate was chosen because it is an indifferent electrolyte for SiO_2 and Al_2O_3.[47] The hydrodynamic radii was independent of ionic strength and the results are essentially the same as those measured in sodium chloride in Chapter 4, within 10%. The values for the hydrodynamic radii reported in Table 1 are the average of two measurements at both ionic strengths, and

[45] Burchard, W. 'Polymer Characterization – Quasi-Elastic and Elastic Light-Scattering', *Makromol. Chem., Macromol. Symp*. **1988**, *18*, 1.

[46] Huglin, M.B. "Light Scattering from Polymer Solutions", Academic Press: London, 1972.

[47] Hunter, R.J. "Zeta Potential in Colloid Science", Academic Press: London, 1981.

were calculated using the Regularization algorithm. The calculated values for the molecular weight are comparable to values measured in different salts, within the standard deviation of the measurement as shown in Chapter 4. This is to be expected because the molecular weight is not a function of the solvent. The solvent on the other hand affects the second virial coefficient. The results show a slight decrease in A_2 for the PRO with increasing-salt molarity, while the GLU shows the opposite trend. In both cases the change is small, and on the order of the error of the experiment. The most important information from this table is that the second virial coefficient for both polymers is positive, indicating that they are both in a solvent that is better than theta.

Table 5.1: Static light scattering results for PRO and GLU at pH 6 and two ionic strengths.

	0.01 M $NaNO_3$		0.1 M $NaNO_3$		
Polymer	Mw	A_2	Mw	A_2	R_H
	g/mole	$m^3kg^{-2}mol$	g/mole	$m^3kg^{-2}mol$	nm
Proline (18.0k)	18000 ± 2000	0.010 ± 0.001	15300 ± 900	0.008 ± 0.001	4.3
Glutamic Acid (8.1k)	9200 ± 1800	0.015 ± 0.005	9300 ± 1200	0.019 ± 0.002	2.2

The GLU has carboxylate side groups with a pKa of 4.07 and is therefore negatively charged at pH 6.[33] At pH < 4, GLU forms an α-helix which self-aggregates, and is not soluble in water.[48,49] At pH > 6, the conformation of GLU changes to a charged random coil, which is soluble in water.[50] At intermediate pH a combination of helical and random coil conformations exists. The PRO chain exists in its form II state in aqueous

[48] Blout, E.R.; Idelson, M. 'Polypeptides. VI. Poly-a-L-Glutamic Acid: Preparation and Helix-Coil Conversions', *Journal of the American Chemical Society* **1956**, *78*, 497.

[49] Fasman, G.D.; Lindblow, C.; Bodenheimer, E. *Biochemistry* **1964**, *3*, 155.

[50] Nakajima, A.; Shinoda, K.; Hayashi, T.; Sata, H. *Polymer Journal* **1975**, *7*, 550.

solution, which is the left-handed helical form with the peptide bonds in the trans configuration.[51,52]

5.3.2 Ellipsometry

5.3.2.1 PEO on Silica

The in situ ellipsometry set-up was tested by first measuring the adsorption of PEO on SiO_2, for which there are reliable data in the literature from another optical technique, scanning angle reflectrometry.[42] To show that the adsorbed amount was constant over a reasonable range of refractive indices, measurements from two different days were compared. The values for n_4 were calculated for each run using the polymer free solvent measurements. Table 5.2 shows that over the range of refractive indices used, the adsorbed amount varies less than 0.02 mg/m^2, and is essentially constant.

Table 5.2: Raw and calculated data for the adsorption of 114 kDa PEO in DI water at 25 ± 2^{o}C on SiO_2 from two different data sets.

	Run A, n_4 = 1.3223		Run B, n_4 = 1.3214	
n_3	d_3	Γ	d_3	Γ
	nm	mg/m^2	nm	mg/m^2
1.33	10.852	0.614	10.054	0.636
1.34	4.6227	0.602	4.5540	0.623
1.35	2.9617	0.603	2.9679	0.624
1.36	2.1927	0.608	2.2150	0.629
1.37	1.7494	0.614	1.7754	0.634

Figure 5.3 shows the adsorption results for a 114k PEO sample on SiO_2 from three different days. The results show good reproducibility from day to day, within the

[51] Steinberg, I.Z.; Harrington, W.F.; Berger, A.; Sera, M.; Katchalski, E. 'The Configurational Changes of Poly-L-Proline in Solution', *Journal of the American Chemical Society* **1960**, *82*, 5263.

[52] Smith, M.; Walton, A.G.; Koenig, J.L. 'Raman Spectroscopy of Poly-L-Proline Form II in Solution', *Biopolymers* **1969**, *8*, 173.

uncertainty of the measurement. The plateau values measured in this study, ~0.64 mg/m^2 were very close to 0.67 mg/m^2, measured by Dijt et al. for a 105k PEO sample on SiO_2. These results are a clear indication that the assumptions used in designing the model for ellipsometry are correct.

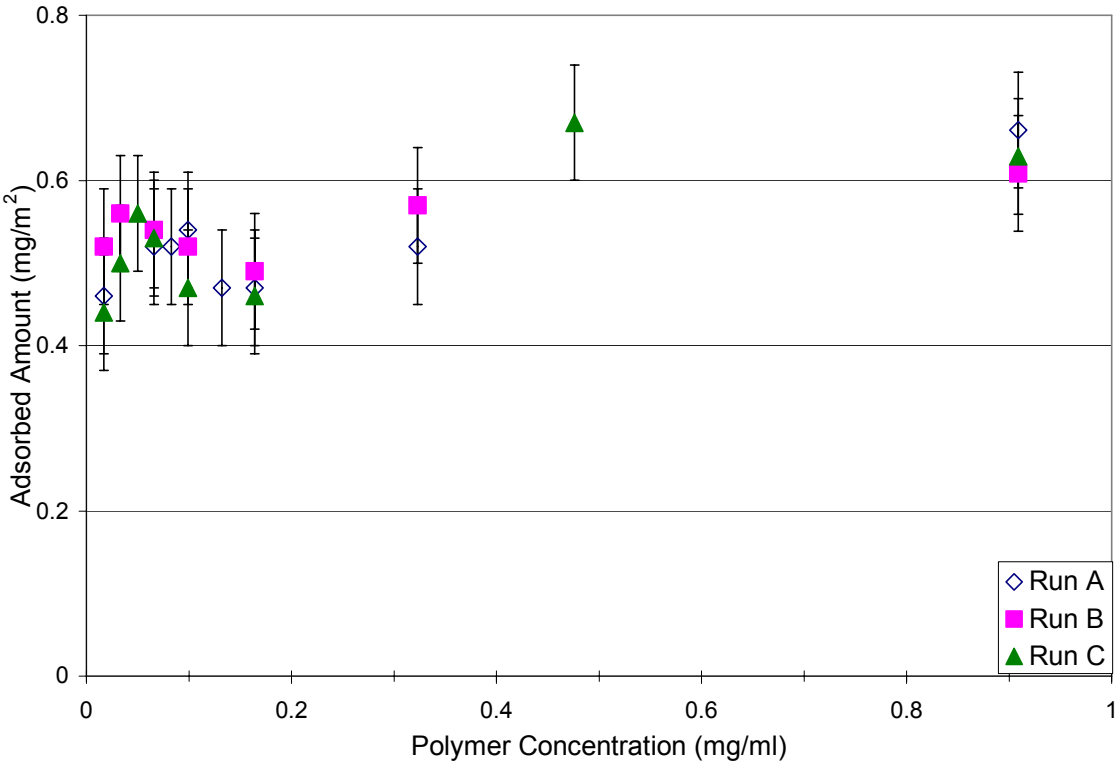

Figure 5.3: Adsorption of 114k PEO on SiO_2, measured on three different days. The error bars represent the uncertainty in the measurement and is ± 0.07 mg/m^2.

5.3.2.2 PRO and GLU on Silica

The results for the adsorption of the PRO 18.0 k and the GLU 8.1 k onto the silicon dioxide surface at pH 6 and at two ionic strengths are shown in Figure 5.4, and the plateau vales for the adsorbed amounts are tabulated in Table 5.3. The results are consistent with those for the particle adsorption in Chapter 4, namely that the PRO shows good adsorption while the GLU shows a lower adsorbed amount. The results for PRO can be compared to the work by Dijt et. al.,[42] who studied the adsorption of PEO on silica using optical, reflectometry. For a PEO sample with a DP of 180, or 7100 g/mole, the

adsorbed amount was measured to be 0.43 mg/m^2, very close to our plateau value of 0.41 mg/m^2. The decrease in the adsorbed amounts of PRO with increasing ionic strength is due to a displacing of the polymer on the surface by the presence of the salt. This effect is commonly observed for the adsorption of nonionic water soluble polymers, and is due to a competition between the salt and the polymer for the surface sites.[29]

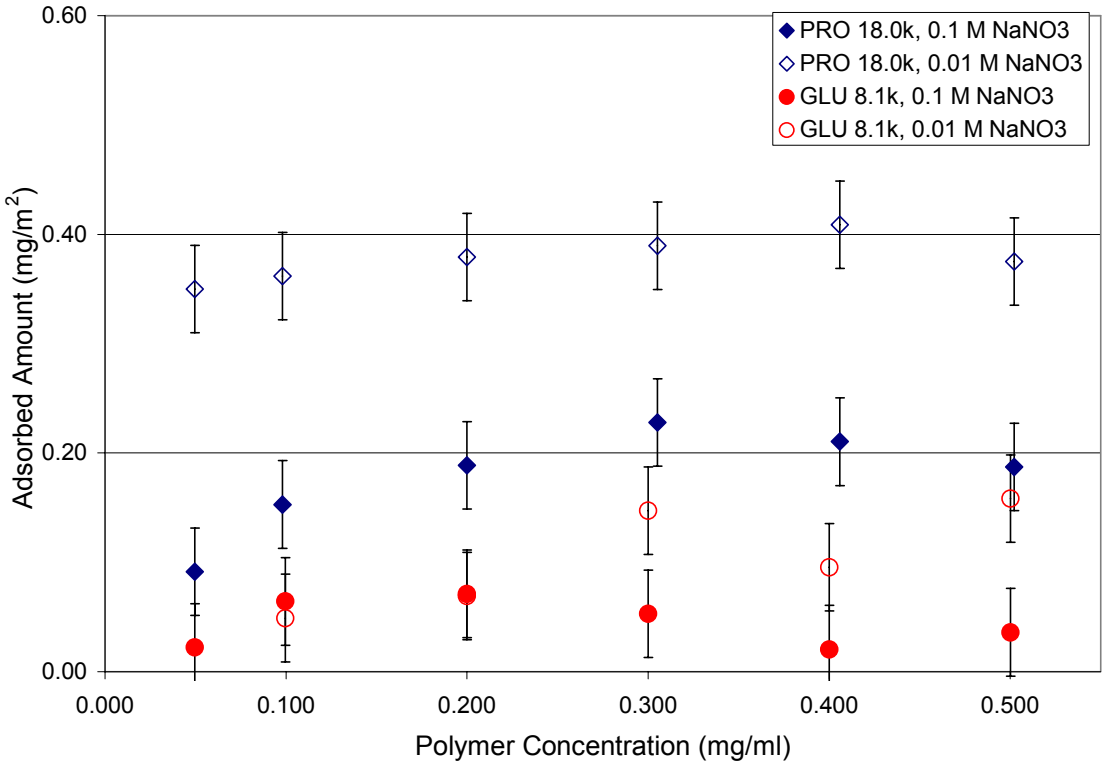

Figure 5.4: Adsorbed amount of PRO 18.0k and GLU 8.1k on silicon dioxide at pH 6.

Table 5.3: Summary of adsorption experiments.

		Plateau Adsorbed Amount (mg/m^2)	
Surface	Polymer	0.01 M $NaNO_3$	0.1 M $NaNO_3$
SiO_2	PRO 18.0k	0.41 ± 0.07	0.26 ± 0.07
	GLU 8.1k	0.14 ± 0.07	0.09 ± 0.07
Al_2O_3	PRO 18.0k	0.06 ± 0.07	0.00 ± 0.07
	GLU 8.1k	0.31 ± 0.07	0.35 ± 0.07

The adsorbed amounts for the GLU on the silica surface are significantly larger than that seen on the Cab-o-sil particles in Chapter 4, where no adsorption occurred. This is most likely due to a difference in the surface chemistries of these silicas, such as the silanol site density. Although it is not clear why the GLU plateau adsorbed amount increased slightly with decreasing ionic strength, the difference is small, less than the uncertainty of the measurement. At high salt concentrations the charges between the surface and the polymer will be screened, lessening the repulsions between the two. This difference is small, less than the uncertainty of the measurement.

5.3.2.3 PRO and GLU on Alumina

The adsorbed amounts of the PRO 18.0 k and the GLU 8.1 k onto the alumina coated wafer at pH 6 are shown in Figure 5.5. The GLU showed fairly strong adsorption at both ionic strengths (0.31 – 0.35 mg/m^2), with values slightly less than those found for the particle adsorption (0.50 mg/m^2) in Chapters 3 and 4. It is not expected that the adsorbed amounts would be identical since the alumina surface were different – the AKP-30 used in the previous two chapters consists of α-Al_2O_3 that is polycrystalline with a possible amorphous hydrated oxide surface.

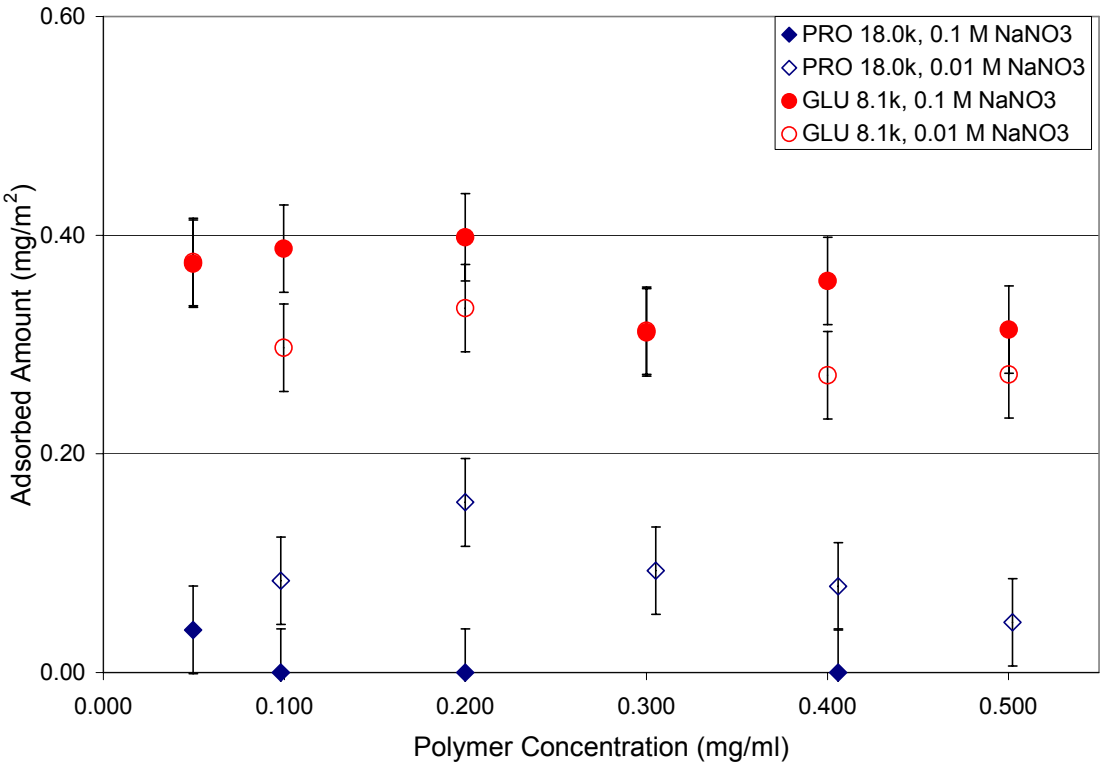

Figure 5.5: Adsorbed amount of PRO 18.0k and GLU 8.1k on an alumina coated wafer at pH 6.

The adsorbed amount of the GLU was slightly greater at the higher ionic strength, although within the uncertainty of the experiment. This increase is expected due to the screening of the charges on the polymer by the salt, which decreases the intermolecular repulsions between the chains, thus allowing for higher packing of the polymer on the surface and an increase in adsorbed amount. An increase in adsorbed amount with increasing ionic strength has also been proposed theoretically.[35,36] A similar result was found for GLU adsorption on α-AL_2O_3 particles in Chapter 4. An adsorbed amount of 0.5 mg GLU/m^2 would be the equivalent of 0.43 nm^2 of surface per amino acid residue estimated from molecular models.[34] This suggests that the GLU adsorbs mainly in a train-like conformation with less than a monolayer on the surface and also explains why the values for the adsorbed amounts were fairly low.

The PRO showed very weak adsorption at 0.01 M $NaNO_3$ and negligible adsorption at 0.1 M $NaNO_3$ on the alumina. This is very similar to the adsorption found on the Cab-o-sil particles in Chapter 4, where the adsorbed amount of PRO 18.0k was measured at less than 0.05 mg/m^2. The very low PRO adsorption on alumina is also consistent with previous adsorption experiments done by Gibson with PEOX and Mathur and Moudgil[21] with PEO, which showed very little adsorption for those polymers on alumina. PEOX is a synthetic, nonionic, water-soluble polyamide and thus is somewhat comparable to PRO. These results also agree in terms of acid-base interactions. PRO, PEO and PEOX are all Lewis basic, while silica is a Lewis acid and alumina is a Lewis base, so it is expected that there would be a positive interaction between these polymers and silica, and a repulsive interaction between these polymers and alumina.

5.4 Conclusions

This work is one of very few studies to measure the adsorption of homopolymer polypeptides on well-defined surfaces using in-situ ellipsometry. The results showed that the adsorption behavior of GLU and PRO, two unstructured homopolymer polypeptides closely resembles that of synthetic polymers. The effect of the surface chemistry greatly affected the resulting adsorption. The GLU was found to adsorb on the oppositely charged Al_2O_3 while the uncharged PRO adsorbed strongly on SiO_2. There was a small effect of ionic strength on the adsorption of GLU on alumina, typical of polyelectrolyte adsorption. The results represent the first in a series of two studies of polypeptides on smooth surfaces. The follow-up paper will consist of AFM measurements for the same systems studied here.

5.5 Acknowledgements

The authors gratefully acknowledge the Center for Adhesive and Sealant Science at Virginia Tech and the Adhesive and Sealant Council Education Foundation for

fellowship support for Jody Krsmanovic. This work was funded by the National Science Foundation Grant # BES-0086875.

6 Stimulation of PEO Adsorption on Al_2O_3 with Polypeptide Cofactor

Abstract

The complexation between a random copolymer of two amino acids, glutamic acid and tyrosine, and poly(ethylene oxide) (PEO) was studied using an in-situ adsorption experiment. First, the adsorption of the copolymer on an alumina surface in a flow cell was measured using ellipsometry. Next, the adsorption of PEO on top of the compolymer was measured. The experiment was performed at two different ionic strengths and two different PEO molecular weights. It was found that both the conformation of the copolymer on the surface, controlled by the ionic strength, and the conformation of the adsorbed PEO, controlled by the PEO molecular weight, affected the molar complexation ratio between the PEO and the tyrosine repeat units.

Keywords: polypeptide, poly(ethylene oxide), alumina, ellipsometry, adsorption, cofactor

6.1 Introduction

Polymer flocculants are typically used for solid-liquid separations including: manufacturing in the papermaking industry to help in the retention of filler particles, flotation processes for ore separations, and for waste water clarification. The most common of these flocculants is high molecular weight poly(ethylene oxide), PEO. For many systems a second component, a low molecular weight cofactor, is required to facilitate the flocculation because the PEO does not adsorb on the filler particles. These cofactors are water-soluble and adsorb onto the filler particles typically be electrostatic interactions. They are typically phenolic, and it is believed that they hydrogen bond with the PEO, causing bridging flocculation to occur.[1]

[1] Pelton, R.H.; Allen, L.H.; Nugent, H.M. *Svensk Papperstidning* **1980**, *83*, 251.

In recent years, a number of new synthetic cofactors have been designed in order to study the physical chemistry of flocculation.[2,3,4] This was required because cofactors currently used in industrial processes typically have broad molecular weight distributions and structures. Most of the cofactors studied were either poly(4-vinyl phenol) or copolymers of vinyl phenol with a charged monomer, which are typically sulfonated for solubility. These types of cofactors have been shown to facilitate flocculation of calcium carbonate, clay, wood pulps, titanium dioxide, and polystyrene latex through hydrogen bond complexation with PEO.[4,5,6,7]

In a recent study by Lu et. al. polypeptide cofactors were used to flocculate precipitated calcium carbonate (PCC) and PCC coated with dextran sulfate.[8] The results showed that those polypeptides, which contained a sufficiently high content of tyrosine (a phenolic

---

[2] Pelton, R.; Xiao, H.; Brook, M.A.; Hamielec, A. 'Flocculation of Polystyrene Latex with Mixtures of Poly(p-vinylphenol) and Poly(ethylene oxide)', *Langmuir* **1996**, *12*, 5756-5762.

[3] Goto, S.; Pelton, R. 'The Influence of Phenolic Cofactors on the Properties of Calcium Carbonate Flocs Formed with PEO', *Colloids and Surfaces A: Physicochemical and Engineering Aspects* **1999**, *155*, 231-239.

[4] Goto, S.; Pelton, R. 'Novel Cofactors/PEO Flocculation Systems for Colloidal Suspensions', *Nordic Pulp and Paper Research Journal* **2000**, *15*, 395-399.

[5] Xiao, H.; Gibbons, s.; Ovenden, C.; Wiseman, N., 'Clay Retention Induced by Poly(ethylene oxide) with Various Cofactors', *Appita Journal* **1999**, *52*, 114-120.

[6] Carignan, A.; Garnier, G.; Van de Van, T.G.M., 'The Flocculation of Fines by PEO/Cofactor Retention Aid Systems', *Journal of Pulp and Paper Science* **1998**, *24*, 94-99.

[7] Lindstron, T.; Glad-Nordmark, G., 'Selective Adsorption, Flocculation, and Fractionation of Wood Pulps with Polyelethyleneoxide', *Journal of Colloid and Interface Science* **1983**, *94*, 404-411.

[8] Lu, C.; Pelton, R.; Valliant, J.' Bothwell, S.' Stephenson, K. 'Colloidal Flocculation with Poly(ethylene oxide)/Polypeptide Complexes', *Langmuir*, **2002**, *18*, 4536-4538.

amino acid) and a sufficiently high enough molecular weight, were able to complex with PEO and flocculate the colloidal particles.

The use of polypeptides as the cofactor has a number of advantages over typical synthetic materials. Using a biosynthetic route, it is possible to exactly control both the structure and molecular weight of a polypeptide sequence. Another advantage is the large number of chemistries available in naturally occurring amino acids, which gives the researcher limitless options in the composition of the polypeptide.

To date there have been no studies of PEO adsorption stimulated by cofactors on well-defined surfaces. Prior work in this area has focused on flocculation studies to determine the effect of various cofactors on PEO adsorption.

In this work, the effect of copolymers containing glutamic acid (GLU) and tyrosine (TYR) on the stimulation of the adsorption of PEO on aluminum oxide were studied using in-situ ellipsometry. Two copolymers were used, which contain different ratios of GLU:TYR, namely 4:1 and 1:1, to study the effect of composition. There has also been little work to study the effect of molecular weight of the PEO on complexation with the cofactors and thus, two different molecular weight PEO samples were used to probe the interactions between the ethylene oxide repeat units and TYR repeat units. Finally, the effect of ionic strength on cofactor and PEO adsorption was studied. This type of study is not possible with a flocculation study, because although the polymer adsorption can be changed by adjusting the ionic strength, the colloidal interactions will also be affected, making it difficult to separate the effects of ionic strength on polymer adsorption from flocculation rate.

6.2 Experimental

6.2.1 Materials

The copolypeptides used were both random copolymers and were purchased from Sigma and used as received. The structures of the two monomers used are shown in Figure 6.1.

The 4:1 molar ratio GLU:TYR used had a lot number of 060K5100, with a reported M_w of 32,700, the 1:1 GLU:TYR used had a lot number of 076H5525, with a reported M_w of 24,500. The PEO standards were purchased from Polymer Laboratories and the details are given in Table 6.1. Deionized (DI) water, purified using a NANOpure II ion exchanger from Barnstead with a specific resistance above 17 MΩ·cm, was used for all experiments. ACS Reagent grade sodium chloride, sodium hydroxide and hydrochloric acid from Fisher were used for ionic strength and pH adjustment.

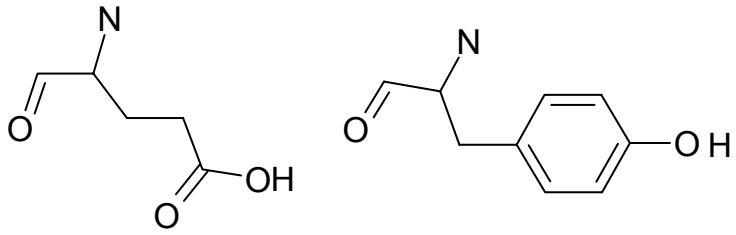

(a) (b)

Figure 6.1: Structure of monomers used in the random copolymers 4:1 GLU:TYR and 1:1 GLU:TYR, (a) Glutamic Acid (GLU) and (b) Tyrosine (TYR).

Table 6.1: Molecular weight information provided by the supplier for the PEO samples used.

Sample	Batch Number	M_n	M_w/M_n
PEO 6.2k	20708-3	6,190	1.02
PEO 921k	20841-13	921,000	1.08

Alumina was sputter coated onto a native silicon surface using physical vapor deposition by Dr. Peter Martin at Pacific Northwest National Laboratory in Richland, WA. The resulting amorphous alumina coatings were approximately 30-40 nm in thickness. The surface roughness was measured using atomic force microscopy (Molecular Imagining, Phoenix, AZ) with a silicon cantilever (Park Scientific, CA) having a nominal spring constant of 0.26 N/m. The alumina coated wafers had a root-mean-square roughness of 1 nm. This is close to values measured for single crystal sapphire surfaces, which had a rms roughness of 1 Å. The alumina coatings were also tested for composition using XPS

(Perkin Elmer 5400 x-ray photoelectron spectrometer), and had 60% aluminum and 40% oxygen, with less than 0.5% impurities. The wafers were cleaned using a water plasma treatment, and kept clean prior to use.

A flow loop was set up to measure the adsorption of the polypeptides by ellipsometry in situ. A Masterflex L/S pump with a rigid PTFE –tubing pump head (Cole-Parmer) was used to pump the liquid from a small PTFE flask, where mixing occurred, to the cell and back. Teflon tubing was used in order to eliminate possible contamination sources. The pump was run at a flow rate of 15 ml/min, which was the equivalent of a four minute residence time. In order to increase the polymer concentration in the liquid cell, a concentrated solution of the polymer was added to the mixing flask, in the appropriate amount. The concentration was then allowed at least half an hour to equilibrate, or about 7 residence times.

6.2.2 Ellipsometry

Ellipsometry measures the change in polarization of light due to the reflection from a surface. The data obtained are reported as two angles, ψ (measuring the amplitude) and Δ (measuring the phase shift). These angles are related to the ratio of the Fresnel reflection coefficients (R_p and R_s) for (p) and (s) polarized light by the following expression:

$$R_p \Big/ R_s = \tan\Psi \exp(i\Delta) \qquad \text{Equation 6.1}$$

where:

$$R_p = \frac{r_{12}^p + r_{23}^p \exp(-i2\beta)}{1 + r_{12}^p r_{23}^p \exp(-i2\beta)} \qquad \text{Equation 6.2}$$

$$R_s = \frac{r_{12}^s + r_{23}^s \exp(-i2\beta)}{1 + r_{12}^s r_{23}^s \exp(-i2\beta)} \qquad \text{Equation 6.3}$$

and

$$\beta = 2\pi\left(\frac{d}{\lambda}\right)N_2 \cos\phi_2 \qquad \text{Equation 6.4}$$

and the complex reflection coefficients at the interface between two arbitrary layers 1 and 2 are:

$$r_{12}^{p} = \frac{N_2 \cos\phi_1 - N_1 \cos\phi_2}{N_2 \cos\phi_1 + N_1 \cos\phi_2} \qquad \text{Equation 6.5}$$

$$r_{12}^{s} = \frac{N_1 \cos\phi_1 - N_2 \cos\phi_2}{N_1 \cos\phi_1 + N_2 \cos\phi_2} \qquad \text{Equation 6.6}$$

where ϕ_1 and ϕ_2 are the angles of incidence at each layer and N_1 and N_2 are the complex refractive indices for each layer, and are related to the real (n) and imaginary (k) components by:

$$N = n - ik \qquad \text{Equation 6.7}$$

The measured data can then be fit to an appropriate model to measure the adsorbed amount of a polymer, and in some cases, the layer thickness. Further details on the principle of ellipsometry can be found elsewhere.[9,10]

Ellipsometric measurements were taken using a variable angle spectroscopic ellipsometer (VB-200 from J.A. Woollam Co.). In situ measurements were obtained by using a flow cell designed by J.A. Woollam Co. that operates at a fixed angle of 70°, which is near the Brewster angle for silicon, 74°. Measurements were taken over a range of wavelengths, 400-700 nm, in order to obtain a good fit with the data to the model used. A series of measurements were taken in order to construct a suitable model to fit the ellipsometric data as shown in Figure 6.2.[11] First, the thickness of the Al_2O_3 layer, d_2, on the dry silicon wafer was determined using a model consisting of the silicon substrate, the native

[9] Azzam, R.M.A.; Bashara, N.M. Ellipsometry and Polarized Light, Elsevier: Amsterdam, 1977.

[10] Tompkins, H.G.; McGahan, W.A. Spectroscopic Ellipsometry and Reflectrometry, John Wiley and Sons, Inc.: New York, 1999.

[11] Herzinger, C.M.; Johs, B.; McGahan, W.A.; Woollam, J.A.; Paulson, W. *Journal of Applied Physics*, **1998**, *83*, 3323.

silicon dioxide layer, and the Al_2O_3 layer. The thickness of the SiO_2 layer, d_1, was kept constant at 1 nm and the optical parameters used for these layers can be found in Herzinger et al.[11] Typically an oxide layer of 20 nm thick was used in these experiments. Previous authors have found that the sensitivity of the optical technique is optimized at thicknesses near 20 nm.[12,13]

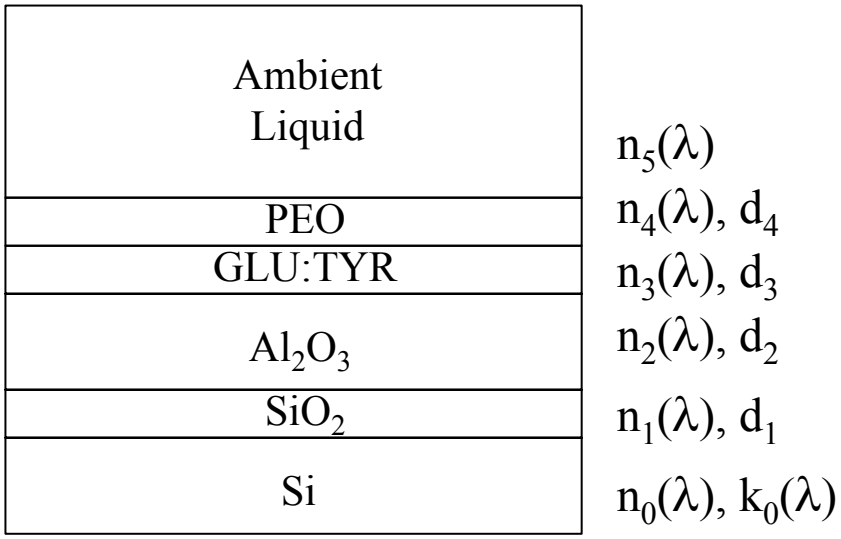

Figure 6.2: Structure of the model used for ellipsometric analysis of adsorbed polymers on to amorphous alumina.

Next, the liquid was pumped through the cell at 25°C ± 2°C, at the ionic strength and pH for the given experiment. The Cauchy model was used to describe the wavelength dependence of the refractive index of the new ambient aqueous layer:

[12] Tiberg, F.; Ederth, T. 'Interfacial Properties of Nonionic Surfacts and Decane-Surfactant Microemulsions at the Silica-Water Interface. An Ellipsometry and Surface Force Study', *Journal of Physical Chemistry* B **2000**, *104*, 9689-9695.

[13] Dijt, J.C.; Cohen Stuart, M.A.; Hofman, J.E.; Fleer, G.J. 'Kinetics of Polymer Adsorption in Stagnation Point Flow', *Colloids and Surfaces* **1990**, *51*, 141.

$$n = A + B/\lambda^2 \ldots \qquad \text{Equation 6.8}$$

This model works well for transparent media ($k = 0$).[10] The A and B parameters were fit to the ellipsometric data.

Finally, a layer was added on top of the Al_2O_3 layer using the Cauchy model, to account for the adsorbed GLU:TYR layer. For this layer the B parameter in the Cauchy model was kept constant, at the value obtained from fitting the aqueous layer, this is reasonable because the polymer layer is approximately 90% water.[14] The adsorbed amount of GLU:TYR on the Al_2O_3 was calculated using the following equation:

$$\Gamma = \frac{d_3(n_3 - n_5)}{dn_3/dc} \qquad \text{Equation 6.9}$$

where d_3 and n_3 are the thickness and refractive index for the GLU:TYR layer, n_5 is the refractive index for the aqueous layer, and dn_3/dc is the refractive index increment, given as 0.186 cm^3/g for the polypeptide.[15] Due to the very thin layer formed by the adsorbed polymers, used in this study a unique solution could not be determined for both the thickness and the refractive index. However, the product $d(n_3\text{-}n_5)$ is constant over a reasonable range of refractive indices for the hydrated polymer layer (i.e. 1.34-1.37), as was shown in Chapter 5. Thus, the A parameter was systematically varied over this range and the different thickness were recorded. It was found that the adsorbed amount calculated was constant over this range of refractive indices, varying by less than 5%. Different polymer concentrations were measured by incremental additions of a concentrated stock solution. The system was allowed to equilibrate for at least 30 minutes after each addition, before measuring with the ellipsometer. Finally, the PEO layer was added on top of the GLU:TYR with thickness, d_4, refractive index n_4 and

[14] Filippova, N.L. 'Adsorption of Polyelectrolytes on Planar Surfaces', *Chemical Engineering Communications* **1998**, *167*, 181-203.

[15] Malmsten, M. 'Ellipsomety studies of Porotein Layers Adsorbed at Hydrophobic Surfaces', *Journal of Colloid and Interface Science* **1994**, *166*, 333-342.

refractive index increment 0.136 ml/g.[16] The adsorbed amount was calculated using the same equations as for the GLU:TYR. For each measurement made the software generates a mean square error (MSE), which was used to determine the "goodness of fit" for each run. A typical value for the MSE was one, which was an indication of a good run. The results presented here are the average values from two or three separate experiments. And the error bars represent the uncertainty in the measurements, which is 0.07 mg/m^2, and was greater than the reproducibility of the experiments.

6.2.3 Dynamic Light Scattering

Dynamic light scattering (DLS) measurements were performed at 836.4 nm with a DynaPro-801 TC from Protein Solutions Inc. All experiments were done at 25^{o}C and controlled to ± 0.2^{o}C and all samples were filtered with a 0.02 μm Whatman Anotop syringe filter. At the start of each experiment, the sample chamber was flushed with 1-2 ml of DI water. Bovine serum albumin (BSA) standard (from Pierce at 2 mg/ml) was used periodically to check the optical alignment. Approximately 0.5 ml of the sample was injected into the sample chamber, making sure there were no air bubbles in the syringe prior to injection. Initially, a stable intensity count rate was established before measurements were taken. Typically 15 measurements were taken to get an accurate average. Size distribution analyses were conducted using two algorithms in the Dynamics software.[17] The first is the Regularization algorithm, which calculates up to three peaks and gives the relative scattering percentages for each. The second algorithm, Dynals, can report more than three peaks, and gives relative scattering percentages for each. The hydrodynamic radius was determined using the Stokes-Einstein equation:

---

[16] Molyneux, P. *Water-Soluble Synthetic Polymers: Properties and Behavior Vol. 1*, CRC Press: Boca Raton, FL, 1983, p. 39.

[17] Ivanova, M.A.; Arutyunyan, A.V.; Lomakin, A.V.; Noskin, V.A., 'Study of DNA Internal Dynamics by Quasi-Elastic Light Scattering' *Applied Optics* **1997**, *36*, 7657-7663.

$$R_H = \frac{k_b T}{6\pi\eta D_T} \qquad \text{Equation 6.10}$$

where k_b is Boltzman's constant, T is temperature, η is the solvent viscosity, and D_T is the translational diffusion coefficient which comes from the autocorrelation function. As discussed below, measurements were only taken for the 4:1 copolymer, and these were done at polymer concentrations ranging from 1 to 4 mg/ml. The radius did not vary with concentration and only one peak was observed, confirming that this is in the dilute range. Results from the two different algorithms were identical, verifying the data.

6.2.4 Static Light Scattering

The DynaPro 801 was also used for static scattering to measure the weight average molecular weight and the second viral coefficient, A_2. In order to calculate these values, scattering intensity was measured at different polymer concentrations. From scattering theory:

$$\frac{Kc}{R_\theta} = \frac{1}{M_w} + 2A_2 c \qquad \text{Equation 6.11}$$

where, R_θ is the Rayleigh ratio, or the reduced relative scattering intensity, c is the concentration of polymer K is an optical constant defined as:

$$K = \frac{2\pi^2 n_o^2 \left(dn/dc\right)^2}{N_A \lambda^4} \qquad \text{Equation 6.12}$$

where n_o is the refractive index of the solvent, (dn/dc) is the refractive index increment, and and λ is the wavelength of light used in the experiment.[18] The dn/dc value used for the solutions was 0.186 mg/ml, a typical value for proteins at wavelengths greater than approximately 730 nm.[19] The other instrumental parameter required was the scattering

[18] Burchard, W. 'Polymer Characterization – Quasi-Elastic and Elastic Light-Scattering', *Makromol. Chem., Macromol. Symp*. **1988**, *18*, 1.

[19] Huglin, M.B. *Light Scattering from Polymer Solutions*, Academic Press: London, 1972.

intensity of toluene, *I*(toluene), which was calculated using a standard. Lysozme, from Sigma (Lot number 57H7045) which has a known molecular weight of 14,400 g/mol, was run before every series of static measurements at pH 7 with 0.1 M NaCl, and the *I*(toluene) parameter was adjusted to obtain the known molecular weight. Once calibrated, the scattering intensities were used to calculate the molecular weight M_w and the second virial coefficient A_2 from Equations 5 and 6 for the polymer solutions using an Excel program to calculate standard deviations for A_2 and M_w. A typical experiment consisted of measurements taken at seven different polymer concentrations, ranging from 1 to 4 mg/ml.

6.3 Results and Discussion

6.3.1 PEO Adsorption

The adsorption of the two molecular PEO samples was first measured on Al_2O_3 in the absence of GLU:TYR. Figure 1 shows that the PEO 6.2k did not adsorb at all on the alumina surface, and the adsorption of the PEO 921k was low, ~ 0.2 mg/m^2. These results are consistent with previous adsorption experiments done by Mathur and Moudgil[20] for PEO adsorption on alumina.

[20] Mathur, S.; Moudgil, B.M. 'Adsorption Mechanism(s) of Poly(ethylene oxide) on Oxide Surfaces', *Journal of Colloid and Interface Science*, **1997**, *196*, 92-98.

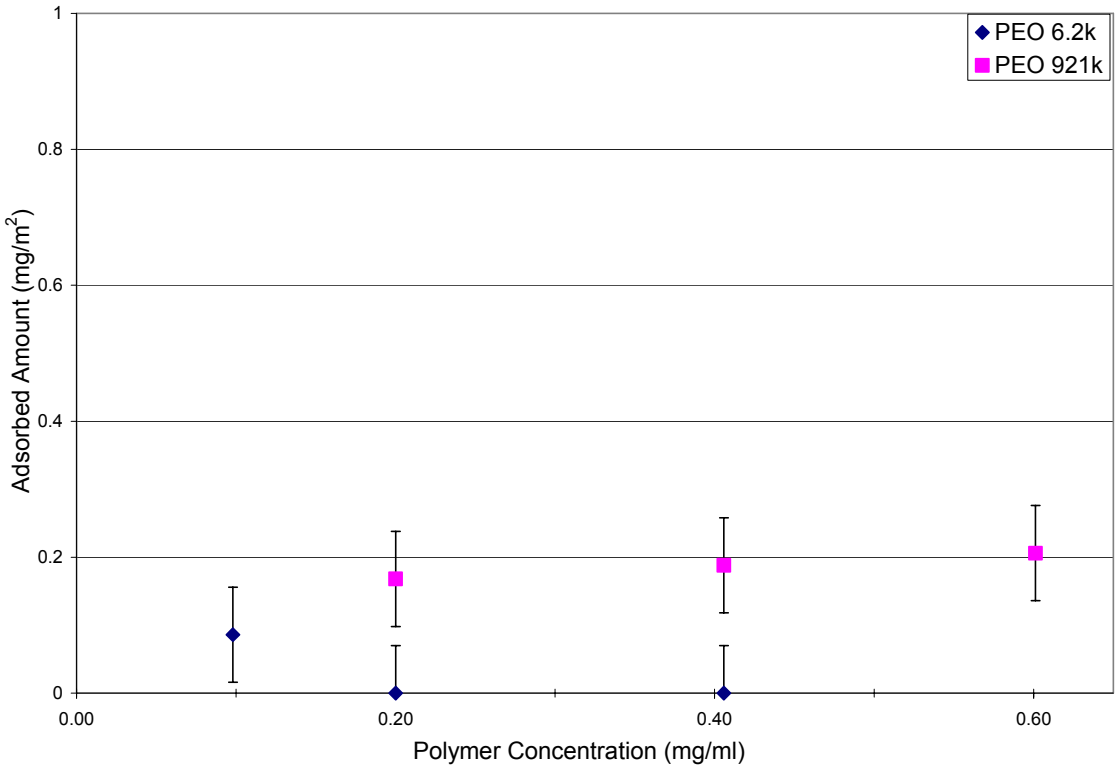

Figure 6.3: Adsorbed amounts for two molecular weight PEO samples on Al_2O_3 at 0.1 M NaCl, pH 6.

6.3.2 GLU:TYR 4:1 Adsorption

The solution properties of the GLU:TYR 4:1 were characterized by dynamic and static light scattering. The results shown in Table 6.2 confirm the molecular weight data provided by the supplier. The second virial coefficient, A_2, of the polymer was positive indicating good solubility in water. The measured hydrodynamic radius of 4.9 nm, obtained with the Regularization algorithm, indicates that individual chains are present in solution, which is consistent with the positive A_2 value. A hydrodynamic radius of 4.9 nm is close to the value calculated using chain statistics for pure GLU, 4.6 nm.

Table 6.2: Dynamic and static light scattering results for GLU:TYR 4:1 in 0.1M NaCl at pH 7 and 25°C.

Polymer	Mw*	A_2*	R_H
	g/mole	$m^3kg^{-2}mol$	nm
GLU:TYR 4:1	31400 ± 2200	0.009 ± 0.002	4.9

* ± one standard deviation

Figure 6.4 shows the adsorption data obtained using ellipsometry for the GLU:TYR 4:1 at two ionic strengths. The first three data points represent successive additions of GLU:TYR 4:1 concentrations that established the plateau adsorbed amount. The fourth point was obtained by first removing all of the GLU:TYR 4:1 solution from the cell and then rinsing with the appropriate buffer solution for at least 30 minutes. Within experimental error, there was no significant desorption of the polymer during this rinse cycle. Finally, the PEO was added in three successive increments, as indicated by the remaining three data points. The values for the PEO adsorbed amount are on top of the already present GLU:TYR, and it would not be expected that the PEO would displace any of the GLU:TYR from the surface, due to the low affinity for PEO for Al_2O_3.

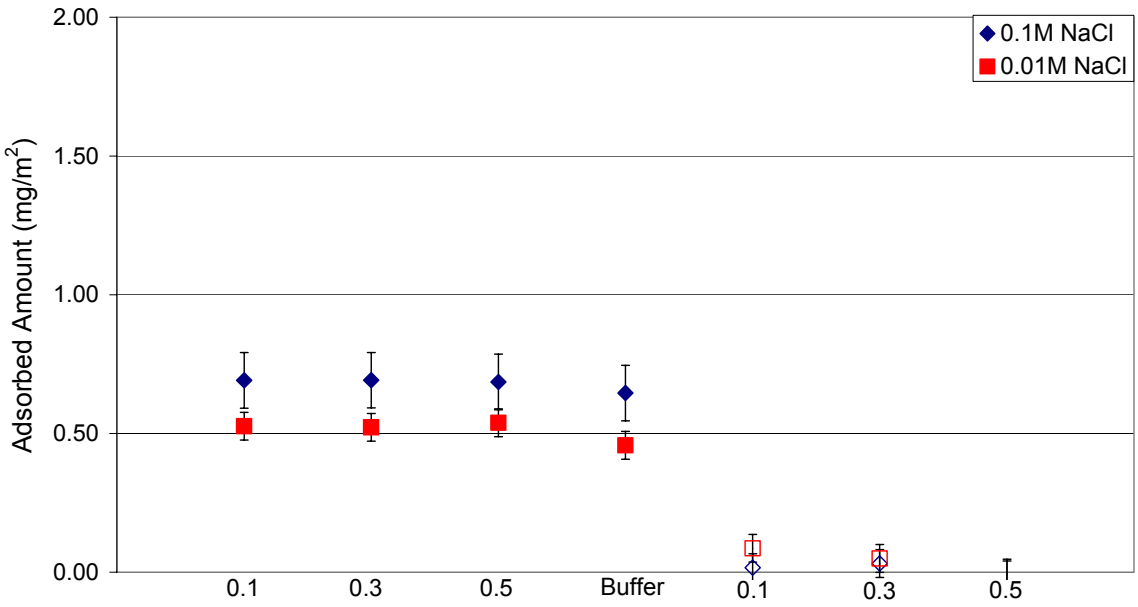

Figure 6.4: Adsorbed amounts of GLU:TYR 4:1 on alumina at pH 6 and two ionic strengths, followed by adsorption of PEO 921k.

The results for the GLU:TYR adsorption show that there is an increase in adsorbed amount with increasing ionic strength. This is due to the screening of the charged GLU units within and between chains, allowing for higher packing on the surface.[21] By comparison, pure GLU with a molecular weight of 8.1 kDa showed a plateau adsorbed amount of 0.35 mg/m^2 at 0.1 M $NaNO_3$ on alumina. Higher adsorbed amounts for GLU:TYR could be due to either the higher molecular weight of the GLU:TYR, or that the TYR component reduces solubility, thus driving adsorption. The result of 0.5 mg/m^2 for the 0.01 M NaCl case is consistent with a mostly train-like conformation of polypeptides on the surface.[22]

[21] van de Steeg, H.G.M.; Cohen Stuart, M.A.; de Keizer, A.; Bijsterbosch, B.H., 'Polyelectrolyte Adsorption: A Subtle Balance of Forces', *Langmuir* **1992**, *8*, 2538-2546.

[22] Blaakmeer, J.; Cohen Stuart, M.A.; Fleer, G.J. 'The Adsorption of Polyampholytes on Negatively and Positively Charged Polystyrene Latex', *Journal of Colloid and Interface Science*, **1990**, *140*, 314-325.

When the cell was rinsed with buffer and the adsorbed amount of the GLU:TYR measured, there was only a slight drop in adsorbed amount, less than the typical reproducibility of the measurement. This is typical behavior of high affinity adsorption that does not desorb readily due to dilution alone. When the PEO 921k was added, there was no additional adsorption on the surface. This is consistent with work done by Lu et. al., who showed no complexation between PEO and GLU:TYR 4:1 as measured using on isothermal calorimetric titration.[8] This result is also consistent with work in Chapter 3 in which it was shown that PRO and GLU have a repulsive potential, which prevents their complexation. Work in Chapter 4 and 5 showed that the adsorption of PRO on Al_2O_3 and SiO_2 is remarkably similar to that of PEO. Thus, it is not surprising PEO and GLU would also exhibit a repulsive potential. It is important to note here that the adsorption of the GLU:TYR 4:1 was at pH 6, while the GLU:TYR 1:1 work, which will be discussed next, was at pH 7.8. It is not expected that the solubility or the adsorption of the GLU:TYR 4:1 would be greatly affected at all if measured at pH 7.8. The solubility of the 4:1 material would only be greater at the higher pH, which could lead to a slight decrease in adsorbed amount. There is no indication that this would promote PEO adsorption.

6.3.3 GLU:TYR 1:1 Adsorption

The GLU:TYR 1:1 copolymer formed aggregates in water larger than 200 nm as evidenced by the clogging of a 200 nm filter used prior to scattering. Thus, no light scattering measurements were possible with the GLU:TYR 1:1 copolymer. It was also necessary to measure the adsorption of the GLU:TYR 1:1 at pH 7.8, because the polypeptide was insoluble for pH $\leq$ 7.

The adsorption of the GLU:TYR 1:1 copolymer on the Al_2O_3 surface was much greater than that measured with the 4:1 copolymer at the same ionic strength. This could be due to adsorption of aggregates of the 1:1 copolymer or adsorption of single chains with loop and tail conformations. The increase in adsorbed amount with ionic strength is even more pronounced with this polymer than with the GLU:TYR 4:1 copolymer. This may

be an indication of single chain adsorption, because the 1:1 copolymer at 0.01 M NaCl adsorbed with an amount comparable to the 4:1 materials (~ 0.5 mg/m^2), which displays single chain adsorption. The effect of ionic strength on the adsorption of the 1:1 copolymer is more pronounced than with the 4:1 copolymer. The reproducibility of the measurement of the GLU:TYR 1:1 materials was not as good as that for the 4:1 samples due to the near insolubility of the 1:1 polypeptide, in which a slight change in pH can lead to significant differences in the adsorbed amount. It was observed that, at pH values just below 7.8, a visible precipitate formed. Just as with the 4:1 copolymer, there was no significant desorption of the 1:1 copolymer during the 30 minute buffer rinsing step.

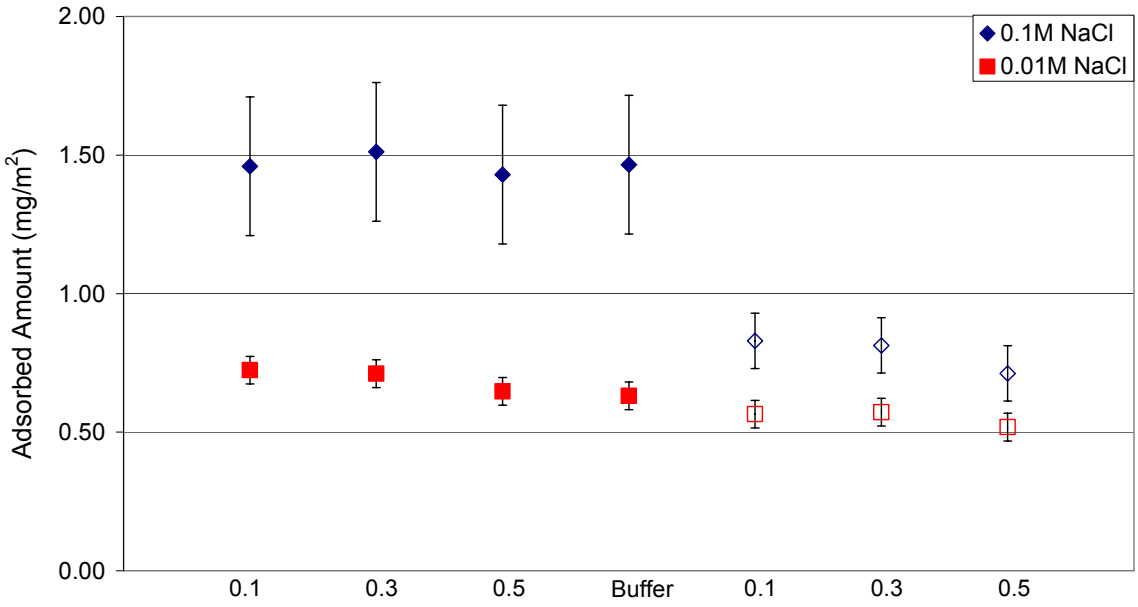

Figure 6.5: Adsorbed amounts of GLU:TYR 1:1 on alumina at pH 7.8 at two ionic strengths, followed by adsorption of PEO 921k.

When the PEO 921k was added to the rinsed cell, there was significant adsorption on the GLU:TYR 1:1 layer. The PEO adsorption was much higher than that found for pure adsorption of the PEO on bare alumina, which was approximately 0.20 mg/m^2. These results are also consistent with the work mentioned earlier by Lu et. al.,[8] who showed by microcalorimetry that complexation between PEO and GLU:TYR 1:1 occurred. Figure 6.5 shows that the PEO adsorbed amount increased with the adsorbed amount of the 1:1

copolymer, although this increase is not directly proportional to the GLU:TYR 1:1 adsorption increase.

Figure 6.6 again shows the results of first adsorbing the GLU:TYR 1:1, but then adsorbing a much lower molecular weight PEO on top of this layer. Although the adsorbed amount of the PEO 6.2k is small, 0.15 mg/m^2, there was no adsorption found for this PEO sample in the absence of the GLU:TYR 1:1. The drop in adsorbed amount compared to the 921k PEO material was expected because the higher molecular weight PEO can adsorb with more loops and tails than the 6.2k PEO.

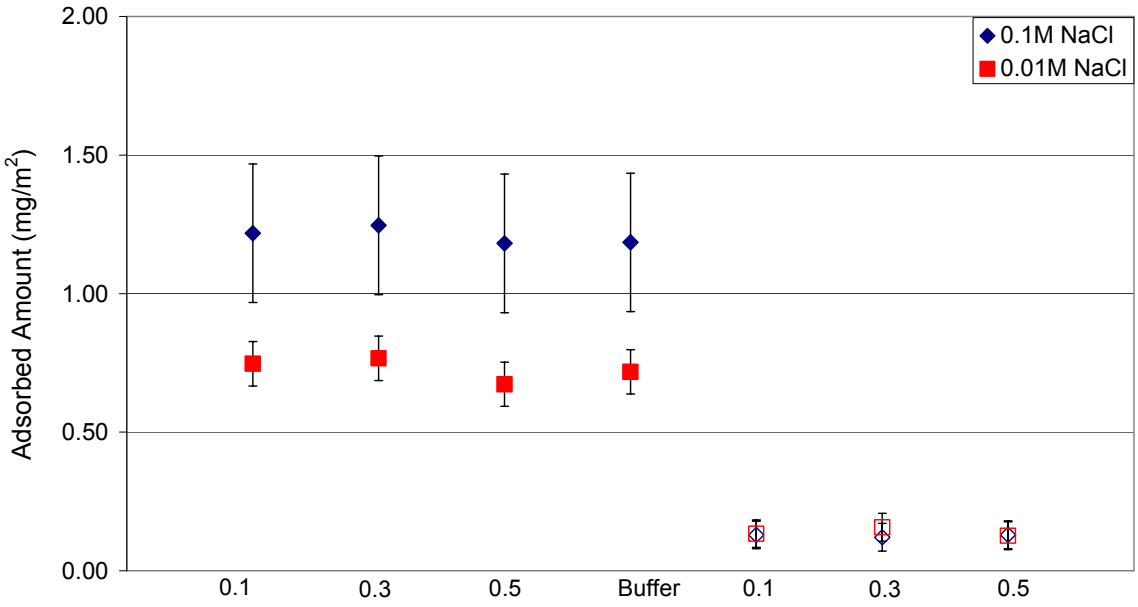

Figure 6.6: Adsorbed amounts of GLU:TYR 1:1 on alumina at pH 7.8 at two ionic strengths, followed by adsorption of PEO 6.2k.

In Table 6.3 the results from the GLU:TYR 1:1 experiments are summarized. The table shows the calculated value for the moles of PEO adsorbed per mole of GLU:TYR 1:1 for each case of ionic strength and PEO molecular weight. This ratio can be useful in discussing the results and in interpreting the possible conformations of the polymers on the surface. It is this ratio that is most important for discussing the results, not the absolute values for PEO adsorbed amount from each experiment.

Table 6.3: Summary of results for the adsorption of GLU:TYR 1:1 (GT 1:1) on alumina at pH 7.8, at two ionic strengths, followed by the adsorption of two different molecular weight PEO samples. The last column represents the value for the moles of PEO adsorbed per mole of GLU:TYR adsorbed, calculated from the two adsorbed amount values.

Salt	Polymer	Adsorbed Amount GT 1:1 (mg/m^2)	Adsorbed Amount PEO (mg/m^2)	[EO]/[TYR]*
0.01M NaCl	PEO 921k	0.65	0.52	5.7
	PEO 6.2k	0.68	0.13	1.4
0.1M NaCl	PEO 921k	1.4	0.71	3.6
	PEO 6.2k	1.2	0.13	0.78

* moles of adsorbed EO repeat unit per mole of adsorbed TYR functionality

From Table 6.3 the molar complexation ratio, [EO]/[TYR], increases with PEO molecular weight. It is also evident that the lower ionic strength samples had a higher molar complexation ratio than their corresponding high ionic strength results.

The possible conformations of the GLU:TYR 1:1 adsorption on alumina followed by PEO adsorption are shown in Figure 6.7. At low ionic strength and low molecular weight PEO, Figure 6.7(a), it is likely both the GLU:TYR 1:1 and the PEO adsorb in a relatively flat train-like conformation and the complexation ratio between PEO to GLU:TYR is close to 1. At low ionic strength and high molecular weight PEO, Figure 6.7(b), the GLU:TYR again shows the train like conformation, but the PEO now adsorbs with more loops and tails because of the high molecular weight, thus increasing the complexation ratio.

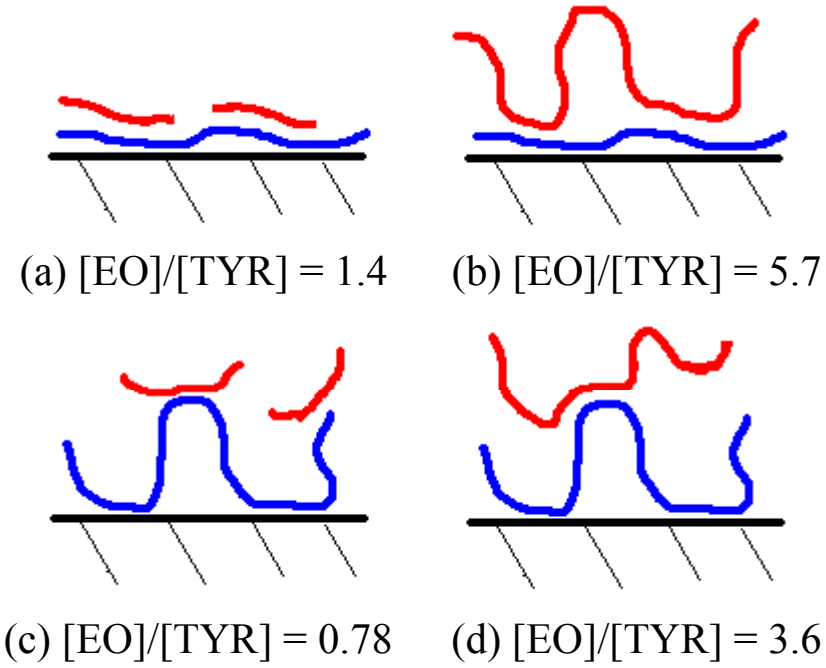

Figure 6.7: Schematic of possible adsorption conformations for different conditions with the GLU:TYR 1:1: (a) Low ionic strength and low molecular weight PEO; (b) Low ionic strength and high molecular weight PEO; (c) High ionic strength with low molecular weight PEO; (d) High ionic strength and high molecular weight PEO.

Figure 6.7(c) shows a schematic for the adsorption at high ionic strength with low molecular weight PEO. Now, the GLU:TYR has more loops and tails, which although gives rise to a greater adsorbed amount than for the low ionic strength case, (a), there are not as many moles of PEO per mole of GLU:TYR, due to steric effects. At high ionic strength and high molecular weight PEO, Figure 6.7(d), the results are similar to (c), namely that there is an increasing in PEO adsorption compared to (b), but the molar ratio [EO]/[TYR] decreased due to the increased fraction of the GLU:TYR in loops and tails. This is a very interesting effect, because in solution it has been found that the higher the PEO molecular weight the stronger the complexation,[23] so any decrease in efficiency

[23] Tsuchida, E.; Takeoka, S. in *Macromolecular Complexes in Chemistry and Biology* Eds. Dubin, P.; Bock, J.; Davis, R.M.; Schulz, D. N.; Thies, C.; Springer-Verlag: Berlin, 1994.

with increasing molecular weight must be due to the presence of the surface, which hinders complexation.

At each ionic strength, the ratio, [EO]/[TYR], between the for PEO 921k to that for PEO 6.2k is approximately 4.3, i.e. the increase in complexation due to increasing the PEO molecular weight was the same. This is an indication that salt effects do not affect hydrogen bonding but only indirectly affect the PEO adsorption by affecting the adsorption of the GLU:TYR copolymer.

Another observation from Table 6.3 is that at each PEO molecular weight the ratio between the (mol EO/mol TYR) for I = 0.01 M NaCl to that for I = 0.1 M NaCl is approximately 1.6, or the decrease in complexation with increasing ionic strength is independent of PEO molecular weight. The increase in GLU:TYR 1:1 adsorption with increasing ionic strength is believed to be due to the increase screening of GLU electrostatic repulsions between GLU segments, which then leads to a higher adsorbed amount. Thus, the increased fraction of segments in loops and tails for the GLU:TYR 1:1 at high ionic strengths creates a steric barrier for the subsequent adsorption of the PEO and thus there is a lower ratio [EO]/[TYR] at higher ionic strengths.

6.4 Conclusions and Future Work

This study illustrates how complexation of a cofactor, GLU:TYR 1:1, is affected by the both the liquid phase conditions, i.e. ionic strength and the PEO molecular weight. As the ionic strength is increased, the GLU:TYR adsorbs in a conformation with more loops and tails, leading to a lower molar complexation ratio, [EO]/[TYR]. Molar complexation ratios close to one were obtained for PEO with low molecular weight under conditions that promote adsorption in train-like conformation. Conversely, molar complexation ratios significantly greater than one were obtained for a high molecular weight PEO that tended to adsorb more in loops and tail conformation. No complexation with PEO

occurred with the GLU:TYR 4:1 materials, due to the low fraction of hydrogen bonding sites, needed for complexation to occur.

The design of a biosynthetically based cofactor to specifically recognize certain surfaces is the next step for this work. One approach would be to design copolymers with a random sequence, as was studied here, where the hydrodygen bonding rich monomer, TYR, are randomly mixed with strongly adsorbing monomer units. Alternatively, a block copolymer approach could also be investigated, that would consist of TYR rich segments coupled to anchor block segments.

The nature of the anchor block units can be tailored for a specific surface. For example, GLU and ASP monomers would be good choices for cationic surfaces, while LYS and ARG would work well for anionic surfaces. Another option would be to take advantage of know specific interactions between amino acids and surfaces, such as that between hystidine and copper. An alternative approach would be to perform a combinatorial library search to identify sequences of amino acids that strongly bind to specific surfaces.

The nature of the binding unit can also be modified to aid in the complexation with the polymer flocculant. From this study it was found that TYR binds well with PEO, as long as there is enough of the phenolic group present. Using a combinatorial library search, it would be possible to find short peptide sequences that bind with other polymer flocculants, such as polyacrylamides, which are often used in industrial separation techniques.

6.5 Acknowledgments

The authors would like to thank Dr. Robert Pelton for kindly providing a preprint on a related study performed by his laboratory.

7 Adsorption of Novel PEO Triblock Materials on Alumina and Silica Surfaces Using Ellipsometry

Abstract

The adsorption of two novel triblock copolymers, with poly(ethylene oxide) (PEO) tails and anionic hydrophobic center blocks, was studied on alumina and silica surfaces. On silica the adsorption was due to the PEO tails, resulting in low adsorbed amounts. The adsorption was much greater on alumina, indicating either brush formation on the surface or the adsorption of micelles, which are present in solution. The effect of adsorbed polymer on the steric stabilization of alumina particles was studied using sedimentation and electrophoretic mobility experiments. These results do not show conclusively that brush formation is occurring on the surface.

Keywords: Polymer Adsorption, Triblock Copolymer, Poly(ethylene oxide), Alumina, Silica, Micelles, Ellipsometry, Steric Stabilization

7.1 Introduction

Brush forming block copolymers are among the most effective colloidal stabilizers because of the repulsive forces that arise from densely packed, extended tail blocks that are anchored to a surface. The specific polymer used here are triblock copolymers have the structure BAB, where is B is the nonadsorbing buoy or tail blocks and A is the adsorbing anchor block. Triblock copolymers have the advantage over diblock copolymers in that at constant tail block lengths, the triblock copolymer layer on the surface will be denser than the diblock, leading to better stabilization due to shorter, but steeper, range repulsion. These types of polymers have been used as detergents, stabilizers and flocculants in the chemical and pharmaceutical industries for many

years.[1,2] Compared to diblocks, there are relatively few studies of the adsorption of well-defined triblocks onto model surfaces and the subsequent effect of the triblocks on colloidal stability.

A series of triblock copolymers containing sodium methacrylate (MANa) with either 4-vinylpyridine, (dimethylamino)ethyl methacrylate, or aminoalkyl methacrylate were studied for their stabilization effect on TiO_2 particles in water.[3,4] When the charged MANa was the center block of a triblock system, the stabilization of the particles was similar to or poorer than that seen by diblocks of the same monomers, depending on the end block choice. This behavior was attributed to the adsorption of the tails, either both tails adsorbed on one particle, which would result in flat conformation, or the two tails adsorbing on different particles, which causes bridging flocculation to occur between particles. This was to be expected because the tails were positively charged and the anchor was negatively charged.

The most commonly studied triblocks are the Pluronics and Meroxapol systems. The Pluronics polymer is a triblock, consisting of two PEO blocks surrounding a PPO block in the middle, while the Meroxapols has the PEO block in between two PPO blocks.

---

[1] Shar, J.A.; Obey, T.M.; Cosgrove, T. Adsorption Studies of Polyethers Part 1. Adsorption onto Hydrophobic Surfaces', *Colloids and Surfaces A: Physicochemical and Engineering Aspects* **1998**, *136*, 21-33.

[2] Green, R.J.; Tasker, S.; Davies, J.; Davies, M.C.; Roberts, C.J.; Tendler, S.J.B. 'Adsorption of PEO-PPO-PEO Triblock Copolymers a the Solid/Liquid Interface: A Surface Plasmon Resonance Study', *Langmuir* **1997**, *13*, 6510-6515.

[3] Cretz, S.; Jerome, R.,' Effectiveness of Poly(vinylpyridine) Block Copolymers as Stabilizers of Aqueous Titanium Dioxide Dispersions of a High Solid Content', *Langmuir* **1999**, *15*, 7145-7156.

[4] Creutz, S.; Jerome, R., 'Effectiveness of Block Copolymers as Stabilizers for Aqueous Titanium Dioxide Dispersions of a High Solid Content', *Progress in Organic Coatings* **2000**, *40*, 21-29.

Their adsorption behavior has been studied on polystyrene latex (PSL) in water[5]. Dynamic light scattering (DLS) was used to determine the hydrodynamic layer thickness of the adsorbed polymers. The Pluronics had a very thick layer with the PEO chains extending into solution, as expected because the PPO adsorbs on PSL due to poor solubility in water and due to the hydrophobic nature of PSL. In another paper, the layer thickness of the Pluronics adsorbed onto PSL was found to be proportional to the molecular weight by: $M_{PEO}^{0.55}$.[6] It is uncertain whether these triblocks would make good stabilizers because theoretically it has been found that linear relationship between the layer thickness and the tail block molecular weight is required for strong stretching of the tail block chains. The Meroxapols showed similar trends in layer thickness, but had about half the value obtained for the Pluronics. This was attributed to the PPO blocks adsorbing on the hydrophobic surface while the PEO was trapped between the two PPO end blocks as loops and trains.

The adsorption of Pluronics has also been studied on hydrophilic silica in water[7]. An interesting effect here is that PEO adsorbs on this surface while PPO does not. The adsorption was characterized using the solution depletion method, ellipsometry, and dynamic light scattering (DLS). The experimental results were compared to the adsorption behavior of PEO and PPO homopolymers, and to model calculations. The results showed very low adsorbed amounts for the copolymer, similar to values obtained for the homopolymer PEO, and the layer thickness was also very small. This confirms that the two PEO blocks are adsorbing on the surface, while the PPO is confined at both ends and so does not extend out far into the solution. A final observation was, that upon

---

[5] Baker, J.A.; Berg, J.C. Investigation of the Adsorption Configuration of Poly(ethylene oxide) and Its Copolymers with Poly(propylene oxide) on Model Polystyrene Latex Dispersions', *Langmuir* **1988**, *4*, 1055-1061.

[6] Killmann, E.; Maier, H.; Baker, J.A., 'Hydrodynamic Layer Thicknesses of Various Adsorbed Polymers on Precipitated Silica and Polystyrene Latex', *Colloids and Surfaces* **1988**, *31*, 51-71.

[7] Malmsten, M.; Linse, P.; Cosgrove, T. 'Adsorption of PEO-PPO-PEO Block Copolymers at Silica', *Macromolecules* **1992**, *25*, 2474-2481.

micellization the adsorbed amounts increased significantly while the layer thickness remained small. This dependence on micelles was not seen on hydrophobic surfaces, which have high values of adsorbed amounts and layer thicknesses, due to brush formation.

It is well known that these types of copolymers can form micelles in water, particularly if the center block is not very soluble.[8] The micellization behavior is typically dependent on polymer concentration, temperature, and salt content. For the Pluronics materials, it has been found that the PPO forms a hydrophobic core, while the PEO chains exist in a highly hydrated state in the shell.[9] It has also been found the addition of salt causes the PEO chains to move from the shell to the core, due to dehydration. This leads to an increase in core radius, while the micelle radius remains constant.

The presence of micelles can greatly affect the adsorption kinetics and the adsorbed layer conformation. For Pluronics materials, it has been found that the plateau adsorbed amount is typically reached at polymer concentrations slightly greater than the cmc, when adsorbing in a brush-like conformation on PSL.[5] On silica surfaces, it has been shown with ellipsometry, that the plateau adsorbed amount was reached prior to micelle formation.[10] This effect has also been studied for the adsorption on silica and titania of a diblock copolymer containing a hydrophobic block of poly(dimethyl siloxane) (PDMS) and a hydrophilic block of poly(2-ethyl-2-oxazoline) (PEOX), a polymer that behaves

---

[8] Alexandridis, P.; Hatton, T.A. 'Poly(ethylene oxide)-Poly(propylene oxide)-Poly(ethylene oxide) Block Copolymer Surfactants in Aqueous Solution and at Interfaces: Thermodynamics, Structure, Dynamics and Modeling', *Colloids and Surfaces A: Physicochemical and Engineering Asp*ects **1995**, *96*, 1-46.

[9] Jain, N.J.; Aswal, V.K.; Goyal, P.S.; Bahadur, P. 'Salt Induced Micellization and Micelle Structure of PEO/PPO/PEO Block Copolymers in Aqueous Solution', *Colloids and Surfaces A: Physicochemical and Engineering Asp*ects **2000**, *173*, 85-94.

[10] Tiberg, F.; Malmsten, M.; Linse, P.; Lindman, B. "Kinetic And Equilibrium Aspects Of Block Copolymer Adsorption", *Langmuir* **1991**, *7*, 2723-2730.

similar to PEO.[11] It was found that the initial rate of adsorption was dependent on molecular weight. For the smaller chains the rate was dependent on the diffusion of the micelles to the surface, while for the longer chains the rate was determined by the exchange rate of unimers between the micelle and the solution. Very large adsorbed amounts were found on both surfaces with the copolymer adsorbing more strongly on the silica than on titania. For both surfaces though, a brush layer was formed with the PDMS acting as the anchor block and PEOX as the tail block.

This work concerns a novel triblock system consisting of PEO tails and a negatively charged, hydrophobic center block. The adsorbed amount was studied for two triblocks with two different compositions on two surfaces, SiO_2 and Al_2O_3, as a function of concentration and ionic strength. The solubility and micellization of the copolymers in aqueous solutions was studied using dynamic light scattering, surface tension measurements, sedimentation, and electrophoretic mobility.

It was hypothesized that, on silica, the PEO tails would adsorb,[12,24] while the negatively charged center block might interact only weakly if at all, with the negatively charged substrate. On the alumina surfaces, it was expected that the oppositely charged center block would adsorb, while PEO has been previously found to be only weakly to non-adsorbing.[12,13] It was hypothesized that the PEO tails might form a brush layer or that there could be micelle adsorption on the surface. The addition of salt was expected to reduce the charge repulsion between two center blocks and possibly lead to greater micellization.

---

[11] Bijsterbosch, H.D.; Cohen Stuart, M.A.; Fleer, G.J. 'Adsorption Kinetics of Diblock Copolymer from a Micellar Solution on Silica and Titania', *Macromolecules* **1998**, *31*, 9281-9294.

[12] Mathur, S.; Moudgil, B.M. 'Adsorption Mechanism(s) of Poly(ethylene oxide) on Oxide Surfaces', *Journal of Colloid and Interface Science* **1997**, *196*, 92.

[13] Gibson, F.W. *Stabilization of Submicron Metal Oxide Particles in Aqueous Media*, Virginia Tech, 1998.

7.2 Experimental

7.2.1 Materials

The PEO triblocks were synthesized and provided by Dr. Judy Riffle in the Department of Chemistry at Virginia Tech. The general structure of the triblock copolymers is shown in Figure 7.1, with the specific details of the molecular weights of each block described in Table 7.1.[14] Deionized (DI) water, purified using a NANOpure II ion exchanger from Barnstead with a specific resistance above 17 MΩ·cm, was used for all experiments. ACS Reagent grade sodium chloride, sodium hydroxide and hydrochloric acid from Fisher were used for ionic strength and pH adjustment.

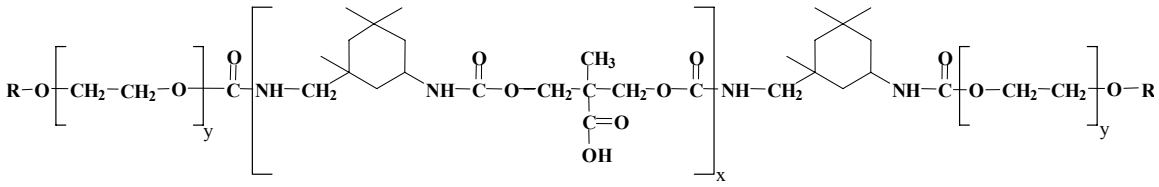

Figure 7.1: Structure of the triblock copolymer.

Table 7.1: Molecular weight values for the two PEO triblocks studied.

Polymer	PEO tail M_n (g/mole)	DP of PEO tail blocks	Ave. # of COOH/mole*	Center M_n (g/mole)	Total M_n (g/mole)
2k-**3**-2k	1930	44	3.1	1300	5160
5k-**5**-5k	4845	110	4.7	1850	11540

* Calculated from ^{13}C NMR data. Due to the condensation mechanism used for the polymerization of the center block, M_w/M_n for center block is about 2.

The silicon wafers used in these experiments were calibration standard wafers (100 crystal face) with a thermally grown SiO_2 layer. Prior to use the wafers were cut into 1

[14] Harris, L.A.; Goff, J.D.; Carmichael, A.Y.; Riffle, J.S.; Harburn, J.J.; St. Pierre, T.G.; Saunders, M., 'Magnetite Nanoparticle Dispersions Stabilized with Triblockk Copolymers', to be submitted.

inch by 1 inch squares and cleaned using a mixture of NH_4OH, H_2O_2, H_2O (0.5:1:5 by volume) at 70°C for 20 minutes, followed by a mixture of HCl, H_2O_2, H_2O (0.5:1:5 by volume) at room temperature for 20 minutes[15]. The wafers were rinsed well after each cleaning with deionized water. They were then dried in a 130°C oven for at least one hour. This procedure results in clean, hydrophilic surfaces. Care was taken to keep the wafers clean prior to use.

Alumina was sputter coated onto a native silicon surface using physical vapor deposition by Dr. Peter Martin at Pacific Northwest National Laboratory in Richland, WA. The resulting amorphous alumina coatings were approximately 30-40 nm in thickness. The surface roughness was measured using atomic force microscopy (Molecular Imagining, Phoenix, AZ) with a silicon cantilever (Park Scientific, CA) having a nominal spring constant of 0.26 N/m. The alumina coated wafers had a root-mean-square roughness of 1 nm. This is close to values measured for single crystal sapphire surfaces (Commercial Crystal Laboratories Inc. Naples, FL),which had a rms roughness of 1 Å. The alumina coatings were also tested for composition using XPS (Perkin Elmer 5400 x-ray photoelectron spectrometer), and had 60% aluminum and 40% oxygen, with less than 0.5% impurities. The wafers were cleaned using a water plasma treatment, and kept clean prior to use.

The alumina particles for the sedimentation and electrophoretic mobility experiments were NanoTek Aluminum Oxide, Lot # AABG1001, from Nanophase, Burr Ridge, IL. The particles had an average diameter 39 nm and a specific surface area of 42 m^2/g.

A flow loop was set up to measure the adsorption of the polypeptides by ellipsometry in situ. A Masterflex L/S pump with a rigid PTFE –tubing pump head (Cole-Parmer) was used to pump the liquid from a small PTFE flask, where mixing occurred, to the cell and back. Teflon tubing was used in order to eliminate possible contamination sources. The

[15] Itano, M.; Kern, F.W.; Miuashita, M.; Ohmi, T. 'Particle Removal from Silicon Wafer Surface in Wet Cleaning Processs', *IEEE Transactions on Semiconductor Manufacturing*, **1993**, *6*, 258.

pump was run at a flow rate of 15 ml/min, which was the equivalent of a four minute residence time for the entire flow loop. In order to increase the polymer concentration in the liquid cell, a concentrated solution of the polymer was added to the mixing flask, in the appropriate amount. The concentration was then allowed at least half an hour to equilibrate, or about 7 residence times.

7.2.2 Ellipsometry

Ellipsometry is a powerful optical technique which can be used to study very thin films. The ellipsometric theory will be described briefly here, and is discussed in more detail in Chapter 5. It measures the change in polarization of light due to the reflection from a surface. The data obtained are reported as two angles, ψ (measuring the amplitude) and Δ (measuring the phase shift). These angles are related to the ratio of the Fresnel reflection coefficients (R_p and R_s)for –p and –s polarized light by the following expression:

$$R_p / R_s = \tan\Psi \exp(i\Delta) \qquad \text{Equation 7.1}$$

The measured data can then be fit to an appropriate model for the system studied. Further details on the principle of ellipsometry can be found elsewhere[16].

Ellipsometric measurements were taken using a variable angle spectroscopic ellipsometer (VB-200 from J.A. Woollam Co.). In situ measurements were obtained by using a flow cell designed by J.A. Woollam Co. that operates at a fixed angle of 70°. Measurements were taken over a range of wavelengths, 400-700 nm, in order to obtain a good fit with the data to the model used. A series of measurements were taken in order to construct a suitable model to fit the ellipsometric data as shown in Figure 7.2. First, the thickness of the SiO_2 layer, d_2, on the dry silicon wafer was determined using a model consisting of the silicon substrate, and interfacial layer between the silica and the silicon, and the SiO_2 layer. The thickness of the interfacial layer, d_1, was kept constant at 1 nm and the optical

[16] Azzam, R.M.A.; Bashara, N.M. Ellipsometry and Polarized Light, Elsevier: Amsterdam, 1977.

parameters used for these layers can be found in Herzinger et. al[17]. Next, the liquid was pumped through the cell at 25°C ± 2°C, at the ionic strength and pH for the given experiment. The Cauchy model was used to describe the wavelength dependence of *n* for this new ambient aqueous layer:

$$n = A + B/\lambda^2 \ldots \qquad \text{Equation 7.2}$$

This model works well for transparent media ($k = 0$). The A and B parameters were fit to the ellipsometric data.

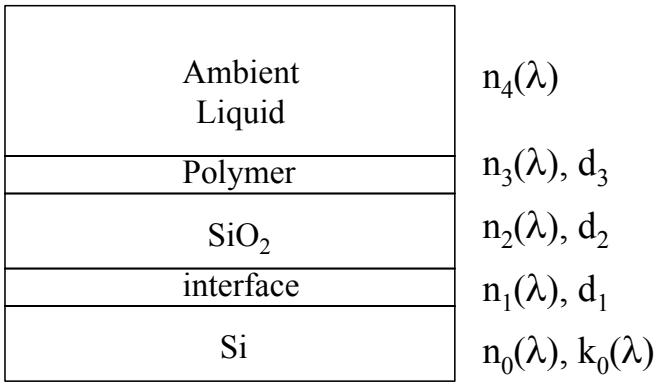

Figure 7.2: Structure of the model used for ellipsometric analysis of adsorbed polymers on to silica.

Finally, a layer was added on top of the SiO_2 layer using the Cauchy model, to account for the adsorbed polymer layer. For this layer, the B parameter in the Cauchy model was kept constant at the value obtained from fitting the aqueous layer. The adsorbed amount of polymer on the SiO_2 was calculated using the following equation:

$$\Gamma = \frac{d_3(n_3 - n_4)}{dn_3/dc} \qquad \text{Equation 7.3}$$

where, d_3 and n_3 are the thickness and refractive index for the polymer layer, n_4 is the refractive index for the aqueous layer, and dn_3/dc is the refractive index increment, given

[17] Herzinger, C.M.; Johs, B.; McGahan, W.A.; Woollam, J.A.; Paulson, W. *Journal of Applied Physics*, **1998**, *83*, 3323.

as 0.136 cm^3/g for PEO homopolymer.[18] Due to the very thin layer formed by the adsorbed polymer, a unique solution can not be determined for both the thickness and the refractive index. However, the product $d(n-n_o)$ is constant over a reasonable range of refractive indices for the hydrated polymer layer (i.e. 1.34-1.37). Thus, the A parameter was varied over this range and the different thicknesses were calculated. It was found that the adsorbed amount calculated was effectively constant over this range of refractive indices, varying by less than 5%. Different polymer concentrations were measured by incremental additions of a concentrated stock solution. The system was allowed to equilibrate for at least 30 minutes after each addition, before measuring with the ellipsometer. For each measurement made the software generates a mean square error (MSE), which was used to determine the "goodness of fit" for each run. A typical value for the MSE was one, which was an indication of a good run. The results presented here are the average values from three separate experiments. And the error bars represent the standard deviation from three measurements.

7.2.3 Dynamic Light Scattering

Dynamic light scattering (DLS) measurements were performed at 836.4 nm with a DynaPro-801 TC from Protein Solutions Inc. All experiments were done at 25°C and controlled to ± 0.2°C and all samples were filtered with a 0.1 μm Whatman Anotop syringe filter. At the start of each experiment, the sample chamber was flushed with 1-2 ml of DI water. Bovine serum albumin (BSA) standard (from Pierce at 2 mg/ml) was used periodically to check the optical alignment. Approximately 0.5 ml of the sample was injected into the sample chamber, making sure there were no air bubbles in the syringe prior to injection. Initially, a stable intensity count rate was established before measurements were taken. Typically 15 measurements were taken to get an accurate average. Size distribution analyses were conducted using two algorithms in the Dynamics software.[19] The first is the Regularization algorithm, which calculates up to

[18] Molyneux, P. *Water-Soluble Synthetic Polymers: Properties and Behavior Vol. 1*, CRC Press: Boca Raton, FL, 1983, p. 39.

[19] www.protein-solutions.com

three peaks and gives the relative scattering percentages for each. The second algorithm, Dynals, can report more than three peaks, and gives relative scattering percentages for each. The hydrodynamic radius is determined using the Stokes-Einstein equation:

$$R_H = \frac{k_b T}{6\pi\eta D_T} \qquad \text{Equation 7.4}$$

where, k_b is Boltzman's constant, T is temperature, η is the solvent viscosity and D_T is the diffusion coefficient which is comes from the autocorrelation function. Measurements were taken at polymer concentrations ranging from 0.125-4 mg/ml.

7.2.4 Surface Tension Measurements

The surface tension of the two polymers in water was measured by lowering a small metal cylindrical mass, attached to an analytical balance, into a large bath of the polymer solution, just until contact was made. The liquid reservoir was then slowly lowered from the cylinder, while the force attributed to this was monitored. The surface tension was measured at the maximum force on the rod and was calculated using the procedure described by Padday et. at.[20] The volume, V, of the meniscus above liquid level is given by the maximum measured force divided by ρg, where ρ is the density difference between the liquid and the air and g is the gravitational acceleration. The volume, V, and the cylinder radius, R, are related to the meniscus coefficient, k, by the equation:

$$R/k = a_0 + a_1\left(R^3/V\right) + a_2\left(R^3/V\right)^2 + a_3\left(R^3/V\right)^3 \qquad \text{Equation 7.5}$$

Where a_0, a_1, a_2, and a_3,are coefficients listed in Reference 20 and he surface tension, γ, is given by:

[20] Padday, J.F.; Pitt, A.R.; Pahley, R.M. "Menisci at a Free Liquid Surface: Surface Tension from the Maximum Pull on a Rod", *Faraday Transactions 1* **1975**, *71*, 1919-1931.

$$\gamma = k^2 g\rho \qquad \text{Equation 7.6}$$

For a given polymer at a given ionic strength a series of solutions were run at different polymer concentrations. The cmc was obtained by finding the concentration where there was a change in the slope of the surface tension data.

7.2.5 Sedimentation

The effect of polymer adsorption on the stability of colloidal alumina particles was measured with a sedimentation experiment. The alumina was kept constant at 2 vol.% and the polymer concentration was varied from 0 to 0.6 Wt.% polymer on the dry weight basis of the alumina, or 0 to 0.5 mg/ml. For a typical experiment, 1.63 grams of alumina powder was mixed with an aqueous polymer solution resulting in a final volume of 20.4 ml. For both polymers, a series of polymer concentrations were run at each ionic strength. The suspensions were shaken for thirty minutes and then transferred to a graduated cylinder. The sediment height was monitored until no further change occurred.

After the sediment height had stabilized, after approximately one month, the suspensions were centrifuged and the supernatant, with a small amount of the solids, was used for zeta potential measurements. The zeta potential of the Al_2O_3 particles was measured with a ZetaSizer 3000 from Malvern Instruments, Ltd. In the limit of a thin double layer, $a/\kappa^{-1} >> 1$, the zeta potential, ζ, is related to the electrophoretic mobility, u, by the following equation:

$$u = \frac{\zeta\varepsilon}{\eta} \qquad \text{Equation 7.7}$$

where ε is the electric permitivity of the liquid, η is the viscosity.[21] This approximation can be corrected for the fact that a/κ^{-1} is close to 1, because at the lowest ionic strength, 0.002 M NaCl, $\kappa^{-1} = 7$ nm and so $a/\kappa^{-1} \approx 2$, while for I = 0.05 M NaCl, $\kappa^{-1} \approx 1.4$ nm and

[21] Hunter, R.J. *Zeta Potential in Colloid Science: Principles and Applications*, Academic Press: London, 1981.

$a/\kappa^{-1} \approx 10$. The corrected zeta potential uses the value obtained from the ZetaSizer and a correction factor given by:[21]

$$\zeta_{corrected} = \frac{\zeta_{measured}}{2/3\, f_1(a\kappa)} \qquad \text{Equation 7.8}$$

where, $f_1(a\kappa)$ is a correction factor, which is calculated using the following equation:

$$f_1(a\kappa) = \frac{3}{2} - \frac{9}{2a\kappa} + \frac{75}{2a^2\kappa^2} - \frac{330}{a^3\kappa^3} \qquad \text{Equation 7.9}$$

All of the values for zeta potential show here were corrected using this approximation.

7.3 Results and Discussion

7.3.1 Dynamic Light Scattering

DLS measurements were taken for each block copolymer as a function of concentration. Figure 7.3 and Figure 7.4 show a typical results for the scattering intensity as a function of polymer concentration for the 2k-3-2k material and 5k-5-5k material, respectively. The critical micelle concentration (cmc) can be approximately located by determining the concentration where the scattering intensity dropped to an unmeasurably low value. For both polymers studied this occurred near 0.125 mg/ml. The same transitions were seen for these polymers at the other ionic strengths studied.

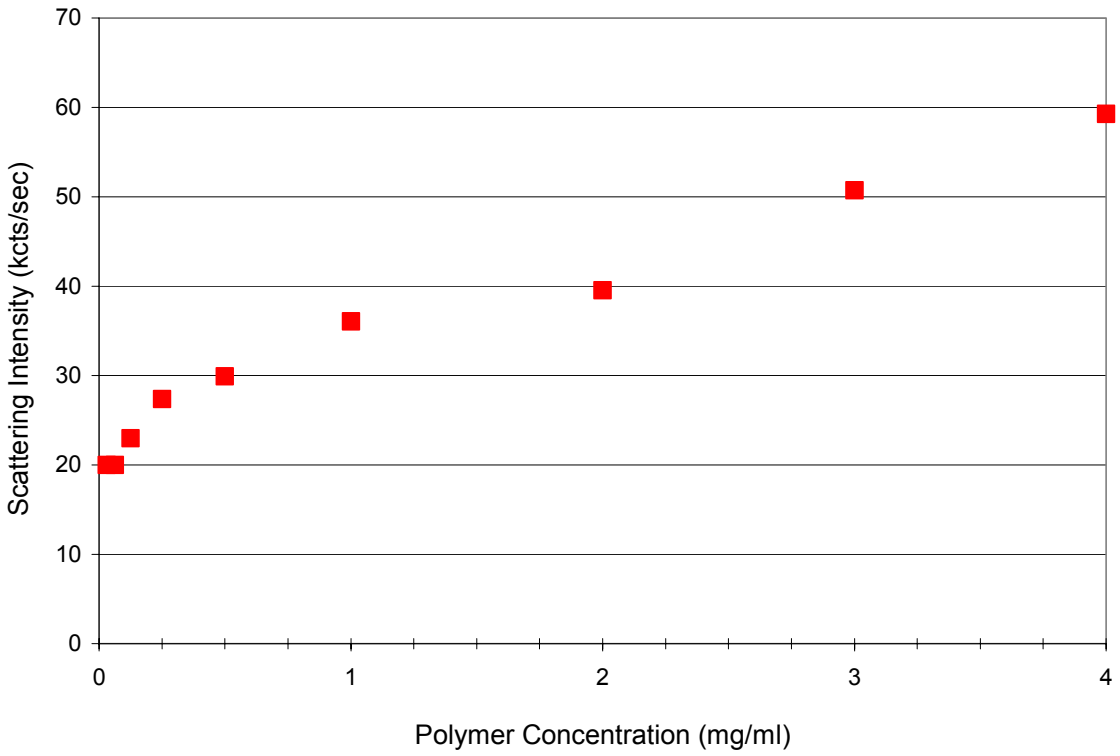

Figure 7.3: Scattering intensity versus polymer concentration for 2k-3-2k at 0.05 M NaCl, pH 6, and 25^{o}C. The apparent cmc occurred at 0.125 mg/ml.

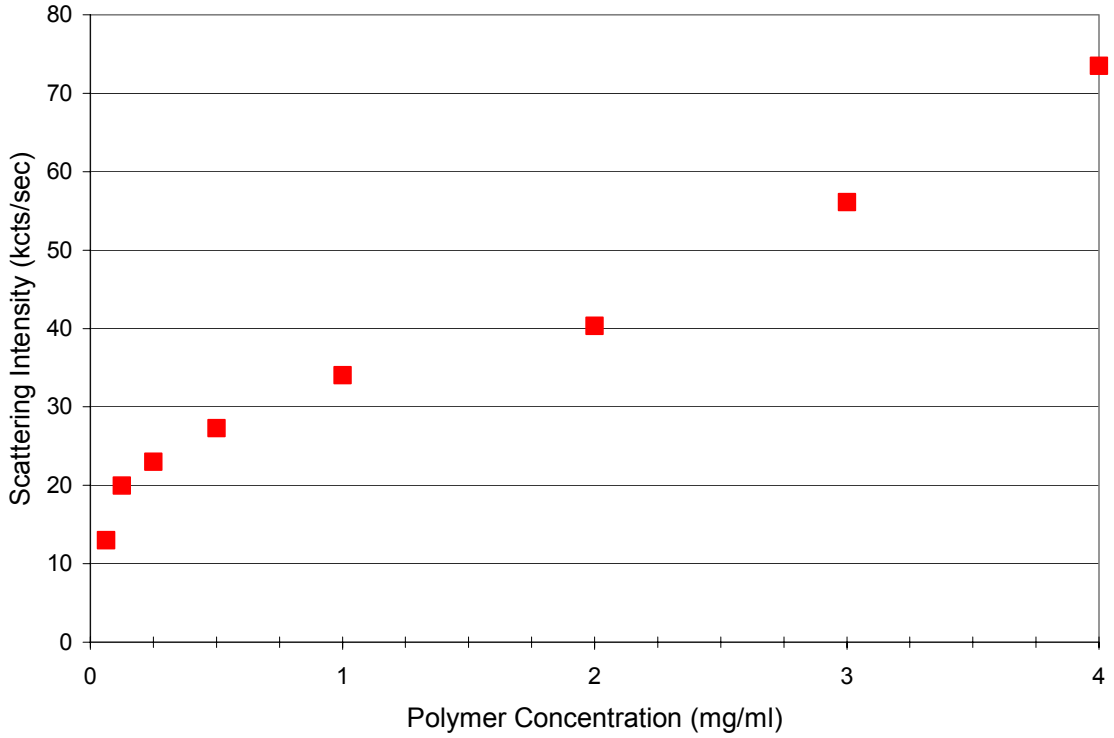

Figure 7.4: Scattering intensity versus polymer concentration for 5k-5-5k at 0.05 M NaCl, pH 6, and 25°C. The apparent cmc occurred at 0.125 mg/ml.

DLS was also used to measure the hydrodynamic radius of the polymers. Above the cmc there were consistently two peaks present for all polymers. At 0.125 mg/ml and below there was no usable peak found with the DLS. The average of five measurements, above the cmc, were used to compare the results as a function of ionic strength and polymer. Figure 7.5 shows two representative plots for the hydrodynamic radius as a function of polymer concentration, above the cmc. There was no discernible effect of concentration on the radius for any ionic strength. The results for 2k-3-2k are shown in Table 7.2 at three ionic strengths. It is clear from these results that there is micellization above 0.125 mg/ml. There were consistent results between the two algorithms used in the software, within ± 0.5 nm, and the data from the Regularization algorithm is presented here. The hydrodynamic radius of a PEO chain has been experimentally found to vary with

molecular weight via the following power law at 30°C[22]:

$$R_H = 0.0145 M_w^{0.571} \quad \text{(nm)} \qquad \text{Equation 7.10}$$

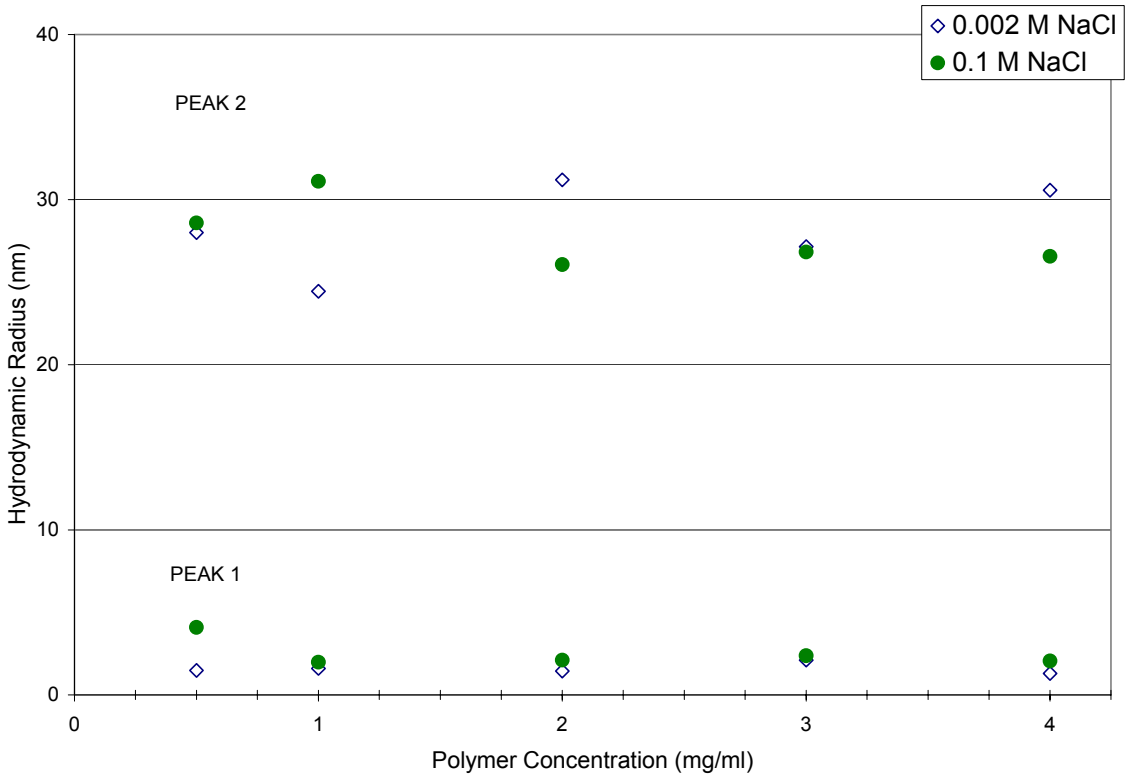

Figure 7.5: Hydrodynamic radius for 2k-3-2k polymer at two ionic strengths as a function of polymer concentration above the cmc.

[22] Devanand, K.; Selser, J.C. "Asymptotic-Behavior And Long-Range Interactions In Aqueous-Solutions Of Poly(Ethylene Oxide)", *Macromolecules* **1991**, *24*, 5943-5947.

Table 7.2: Hydrodynamic radius measurements for 2k-3-2k, averaged over five concentrations above the cmc (0.125 mg/ml) at pH 6, and 25°C. "Percentage of Peak 1" is the percentage of the total peak area attributed to Peak 1.

Ionic Strength	Peak 1	Percentage	Peak 2
M	R_H* (nm)	of Peak 1	R_H* (nm)
0.002	1.59 ± 0.31	24 ± 7	26.1 ± 5.79
0.05	2.16 ± 0.32	27 ± 1	30.9 ± 6.14
0.1	2.52 ± 0.89	36 ± 12	27.8 ± 2.07

* Calculated from Equation 7.4 using the Regularization algorithm.

The small peak is on the order of the hydrodynamic radius of two PEO chains, R_H = 2.2 nm from Equation 7.8, while the bigger peak is clearly a large polymer micelle. There was only a slight increase in the hydrodynamic radius of the small peak at the two higher ionic strengths. The percentage of the total peak area attributed to peak 1 also showed a slight increase with ionic strength. There was no discernible effect of ionic strength on the larger peak, which had an average value of 28 nm.

The DLS results for the 5k-5-5k material are shown in Figure 7.6 and Table 7.3. Again, there is a slight increase in the small peak at the two higher ionic strengths, which is on the order of two PEO chains of molecular weight 5000 g/mole each in solution, R_H = 3.8 nm. There are some significant difference between the results for the two polymers. The small peak for the 5k-5-5k material was larger than that for the 2k-3-2k, which was reasonable because two 5k PEO chains in solution are larger than two 2k PEO chains. There was also a much higher percentage of the chains present in micelles for the 2k-3-2k polymer. The larger peak, conversely, was very similar for both polymers, indicating that the micelle size did not change appreciably. The micelles seen here are much larger than micelles seen with comparable molecular weight Pluronics triblocks, $(PEO)_{100}$–$(PPO)_{40}$–$(PEO)_{100}$, where the hydrodynamic radius is about 7 nm.[8] Micelles of similar size were seen with another Pluronics material which had a much lower molecular weight, $(PEO)_{19}$-$(PPO)_{39}$-$(PEO)_{19}$.[9] Spherical micelles around 7 nm in radius were found, and the radius was independent of salt concentration.

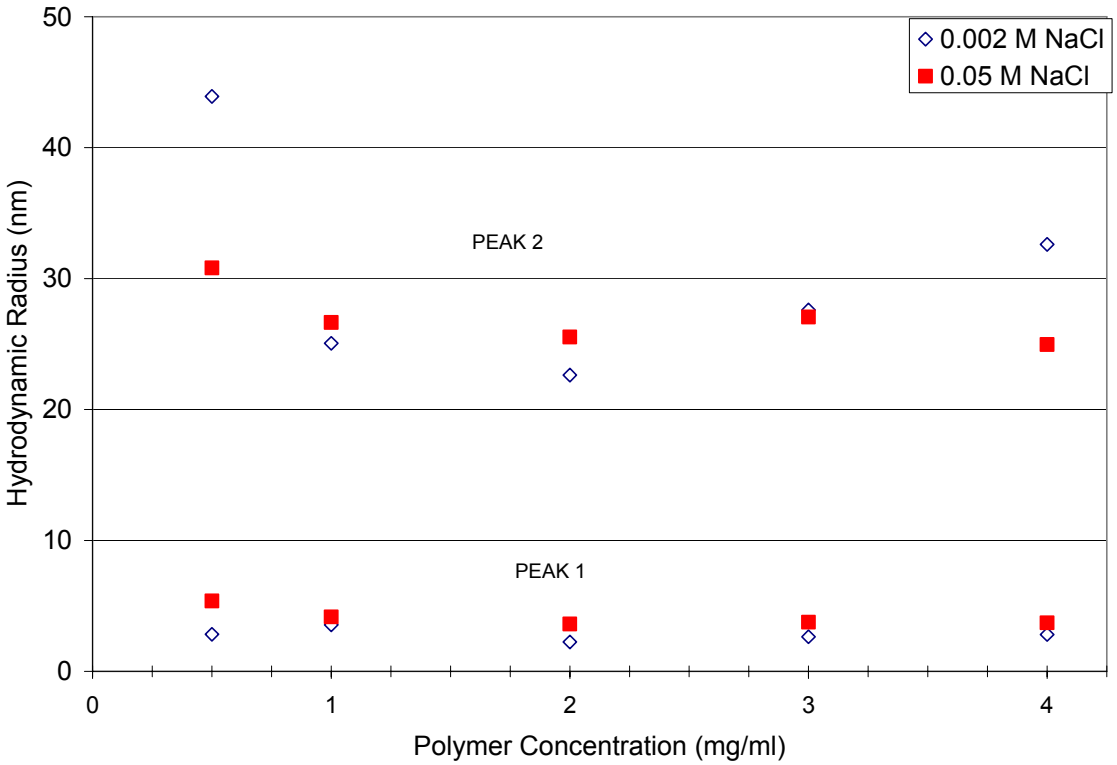

Figure 7.6: Hydrodynamic radius for 5k-5-5k polymer at two ionic strengths as a function of polymer concentration above the cmc.

Table 7.3: Hydrodynamic radius measurements for 5k-5-5k, averaged over five concentrations above the cmc (0.125 mg/ml) at pH 6, and 25°C. "Percentage of Peak 1" is the percentage of the total peak area attributed to Peak 1.

Ionic Strength M	Peak 1 R_H* (nm)	Percentage of Peak 1	Peak 2 R_H* (nm)
0.002	2.81 ± 0.47	63 ± 10	30.4 ± 8.43
0.05	4.12 ± 0.73	68 ± 2	27.0 ± 2.29
0.1	4.37 ± 0.34	72 ± 7	43.0 ± 19.9

* Calculated from Equation 7.4, using the Regularization algorithm.

There are several possible explanations for the large size of the second peak seen with DLS. If the PEO end blocks are fully extended in the corona of the micelle, this could lead to a large micelle, the contour length of a 2k PEO chain is 20 nm and that of a 5k PEO chain is 50 nm. However, given that the center blocks are charged this does not

seem likely. Another possibility is that the charged center blocks cause the core to become swollen with water, leading to a large micelle. If this were the case, it would be expected that the micelle size would vary with ionic strength, which is not seen here. The aggregation of micelles is another possibility. It is unclear at this time why this would occur, given the high solubility of the PEO tail blocks. A fourth possible reason for the large second peak could be the formation of non-spherical micelles. Such micelles would result in a large apparent spherical radius. A scattering technique, such as small angle neutron scattering or small angle x-ray scattering could be used to answer this question.

7.3.2 Surface Tension

To confirm the results obtained by DLS for the critical micelle concentration, surface tension measurements were made for both polymers at the three ionic strengths as a function of polymer concentration. Figure 7.7 and Figure 7.8 show the results for the 2k-3-2k material and the 5k-5-5k material, respectively. The cmc can be estimated by finding the concentration where the slope changes. Due to the polydispersity of these polymers, it is not expected that the determination of the cmc will be as accurate as that for monodisperse surfactant materials. In fact, for Pluronics materials there has been much debate over surface tension results, because of the presence of two changes in slope typically seen for these materials.[8] An author cited a value for the cmc for Pluronics F127 ($(PEO)_{100}$-$(PPO)_{70}$-$(PEO)_{100}$) at 1.3 mg/ml, well above the results found for the triblocks studied here.[23]

[23] Vasilescu, M.; Caragheorgheopol, A.; Caldararu, H., "Aggregation Numbers and Microstructure Characterization of Self-Assembled Aggregates of Poly(ethylene oxide) Surfactants and Related Block-Copolymers, Studied by Spectroscopic Methods", *Advances in Colloid and Interface Science* **2001**, *89-90*, 169-194.

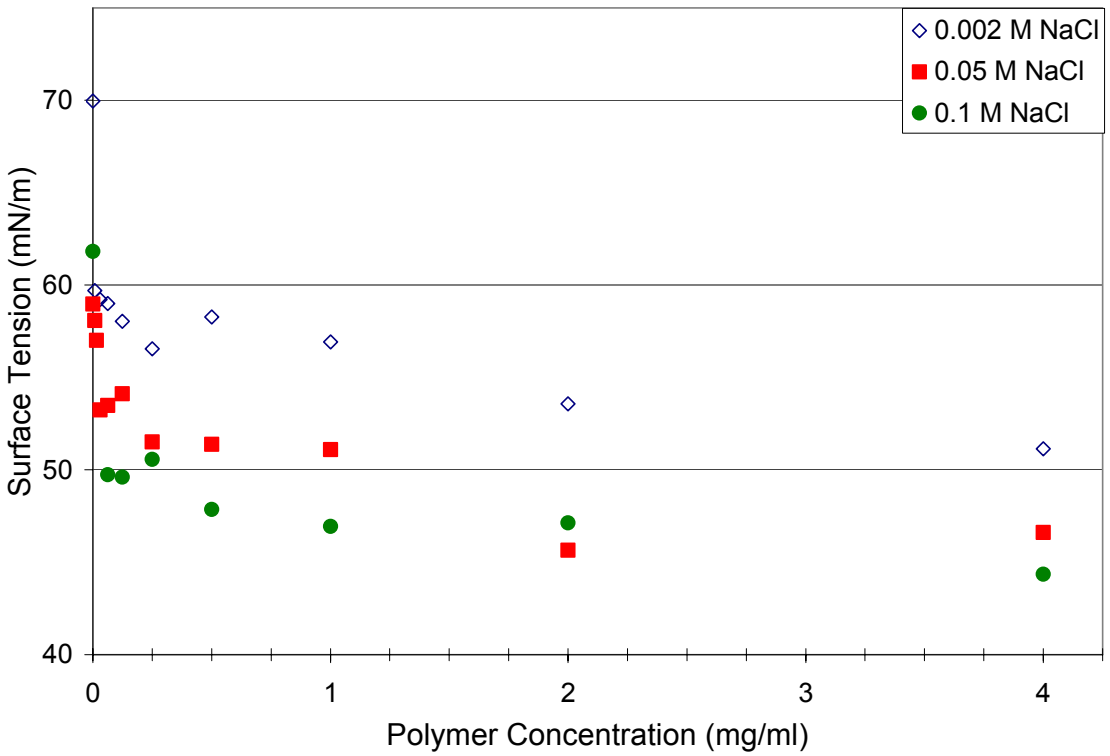

Figure 7.7: Surface tension as a function of 2k-3-2k polymer concentration, for three ionic strengths.

For both polymers, at all ionic strengths, the change in slope can visually be determined to be around 0.125 mg/ml, which was the value determined from DLS. A more analytical approach would be to divide the data into two parts, one above the visual change, and one below. A line can be fit to both parts of the data, and concentration where the change in slope occurs can be obtained from the intercept of the two resulting linear fits. The results calculated using this method are shown in Table 7.4. It is expected that there would be fairly large uncertainty in these values, due to the method used to obtain the data. However, the cmc values obtained here are very close to 0.125 mg/ml determined from DLS, and there appears to be no strong effect of polymer type or ionic strength.

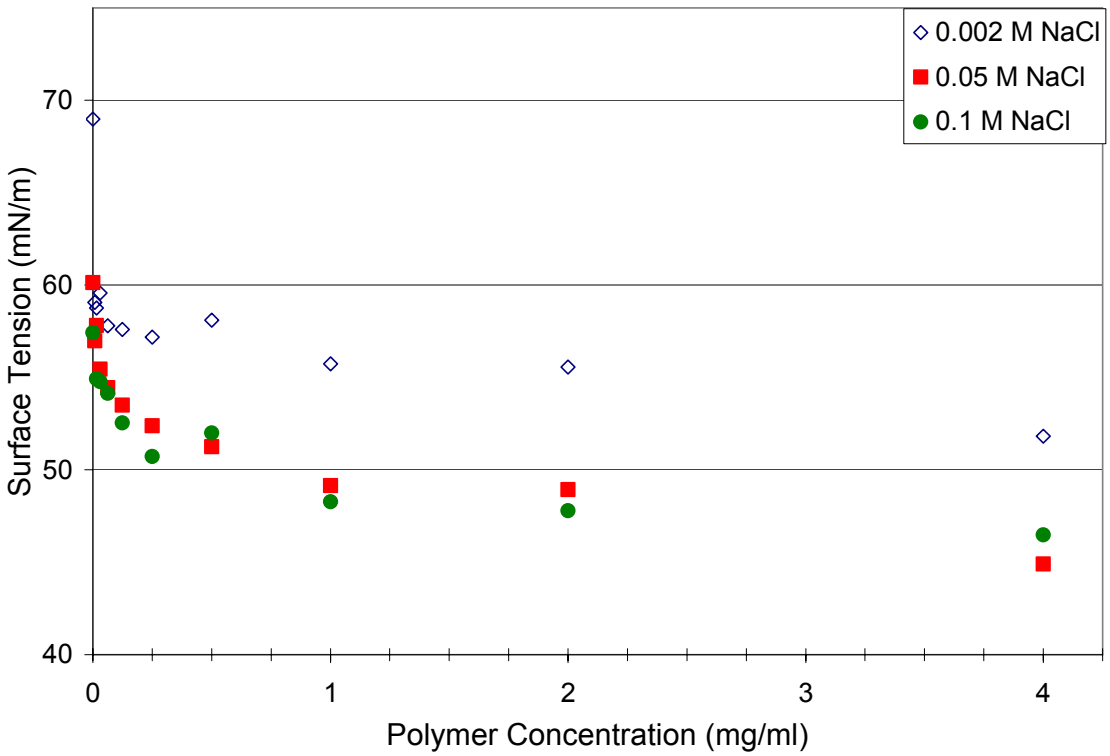

Figure 7.8: Surface tension as a function of 5k-5-5k polymer concentration, for three ionic strengths.

Table 7.4: Calculated critical micelle concentration for the two triblock copolymers at three ionic strengths, determined from surface tension measurements, using Equations 7.5 and 7.6.

Ionic Strength	cmc (mg/ml)	
M NaCl	2k-3-2k	5k-5-5k
0.002	0.10	0.09
0.05	0.14	0.13
0.1	0.11	0.15

To summarize, the cmc is essentially unaffected by ionic strength, polymer concentration and composition or molecular weight for the two polymers studied.

7.3.3 Adsorption on SiO_2

The adsorption of the 2k-3-2k polymer on SiO_2 was measured at three ionic strengths and the results are shown in Figure 7.9. Prior work by Dijt et. al.[24] studied the adsorption of PEO homopolymer on silica in DI water, and found for a 4 kDa PEO the adsorbed amount was 0.40 mg/m^2. This is close to the values measured for the triblocks on silica. It was expected that the center block would not adsorb on the surface, due to electrostatic repulsion. The data suggests that the PEO endblocks are adsorbing in a train like conformation on the surface and the center block has little effect on adsorption. It is also apparent that there is no significant effect of ionic strength on the adsorption. Even though increasing the ionic strength reduces the repulsion between the center block and the surface, there is no effect on the adsorbed amount, and thus, adsorption is dominated by the interactions between the PEO and the silica. Similar results for Pluronics adsorption on hydrophilic silica have been found, namely that the adsorption is comparable to that of PEO homopolymer of similar molecular weight and the center block has little effect on adsorption.[7] It is also important to note that there is no significant difference, or increase, in the adsorbed amounts measured below and above the cmc (0.125 mg/ml). This was seen for all cases of polymer adsorption. This has also been observed for Pluronics adsorbing onto silica.[8]

[24] Dijt, J.C.; Cohen Stuart, M.A.; Hofman, J. E.; Fleer, G.J. "Kinetics of polymer adsorption in stagnation point flow" *Colloids and Surfaces* **1990**, *51*, 141-158.

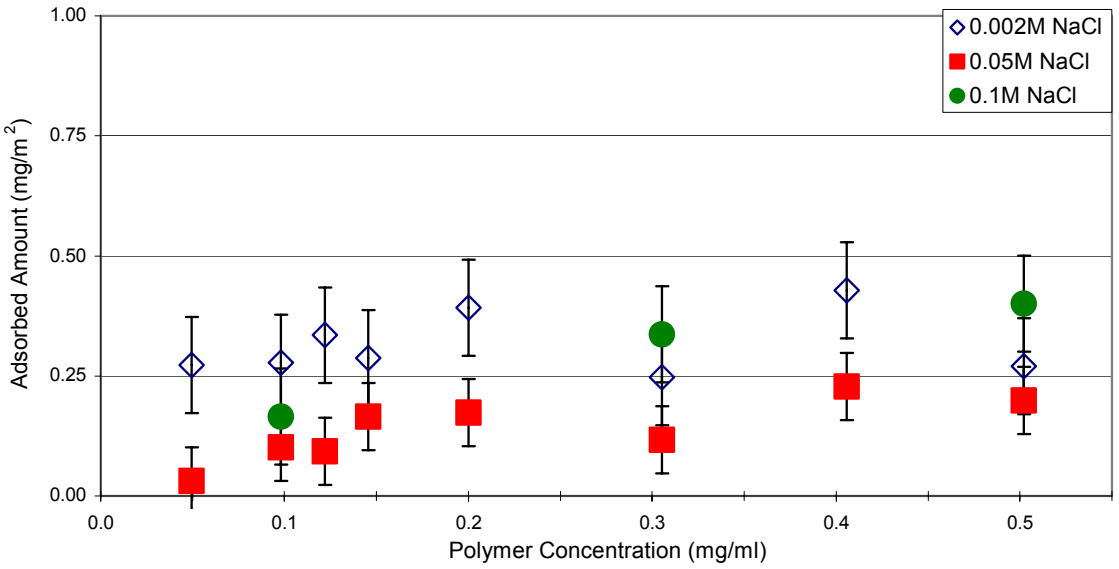

Figure 7.9: Adsorbed amount for of 2k-3-2k on SiO_2 at pH 6 for three different ionic strengths. The error bars represent the standard deviation from three measurements.

The adsorption results for the 5k-5-5k triblock on silica are shown in Figure 7.10. For this polymer there is a small but significant effect of salt on the adsorbed amount, namely that the adsorbed amount increases with increasing ionic strength. As the ionic strength increases the repulsive forces between the center block and the surface and also between two adjacent, adsorbed center blocks are increasingly screened. This results in a higher adsorbed amount. The adsorbed amount for the 0.1 M NaCl case is similar to the value measured for homopolymer 10 kDa PEO by Dijt et. al., 0.48 mg/m^2.[24] It seems that the center block has little effect on adsorption at higher ionic strengths, and so the interactions between the PEO and the surface dominate. At lower ionic strengths, the charged center block suppresses adsorption. The effect of salt seen for the 5k-5-5k is stronger than that seen for the 2k-3-2k. It is possible that the three repeat units in the 2k-3-2k triblock are effectively screened from the surface by the PEO tail blocks, while the five repeat units in the 5k-5-5k triblock are not as effectively screened by the 5k PEO tail blocks.

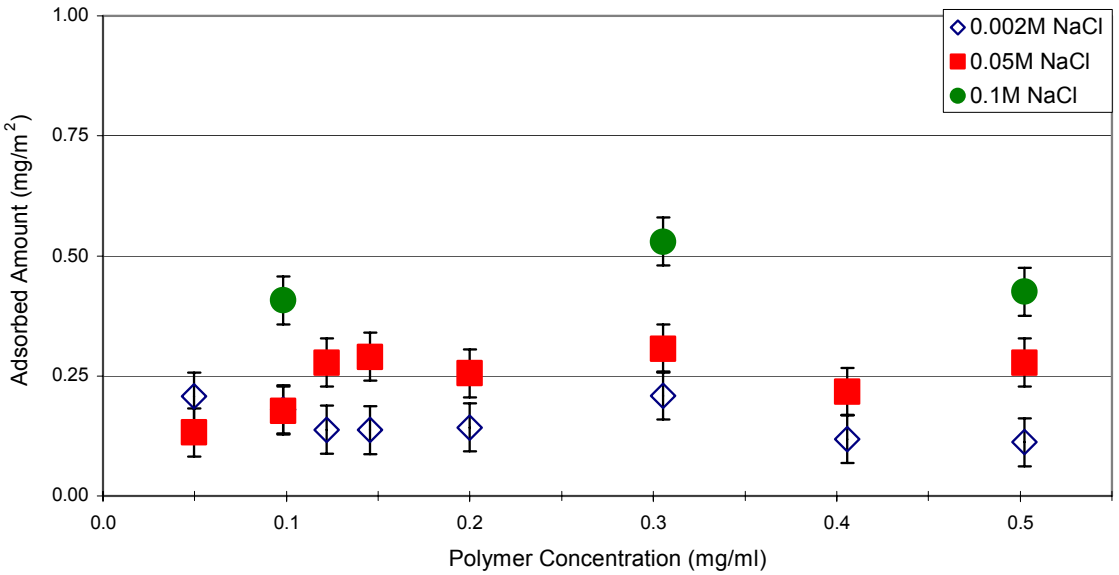

Figure 7.10: Adsorbed amounts for 5k-5-5k on SiO_2 at pH 6 and three different ionic strengths. The error bars represent the standard deviation from three measurements.

7.3.4 Adsorption on Al_2O_3

The adsorption of 2k-3-2k on alumina was very different from that on silica, as shown in Figure 7.11. The adsorbed amount at low ionic strength is much higher than that on SiO_2. There is also a significant increase in the adsorbed amount when going from 0.002 M NaCl to 0.05 M NaCl. This could be attributed to one of two different adsorption conformations on the surface. First, for the 0.002 M NaCl case, the polymer may adsorb as brushes extending away from the surface, as is typically depicted for block copolymers. When the salt is added, the charge interactions between the center blocks are screened and thus the polymer can achieve higher packing density on the surface, resulting in an increase in adsorbed amount. This interpretation is confirmed by chain statistic calculations for the PEO tails compared to the area occupied by an adsorbed triblock calculated from the adsorption data, as shown in Table 7.5. The area occupied per triblock molecule for the low ionic strength case is comparable to the predicted area for two 2 kDa PEO chains. The radius of gyration was used to calculate the areas for the

PEO homopolymer chains, using Equation 7.8 and the relationship assuming a non-draining sphere[25]:

$$R_H = 0.875 R_g \qquad \text{Equation 7.11}$$

The radius of gyration was also calculated using the wormlike chain theory:[26]

$$R_{go}^2 = L^2 \left\{ \frac{1}{6N_k} - \frac{1}{4N_k^2} + \frac{1}{4N_k^3} - \frac{1 - e^{-2N_k}}{8N_k^4} \right\} \qquad \text{Equation 7.12}$$

where, L is the contour length, and Nk is the number of Kuhn segments. Calculations using this equation showed agreement with those calculated using chain statistics within ± 0.2 nm. At higher ionic strengths, the area per molecule is greatly diminished, indicating higher packing on the surface and PEO brush extension. The values calculated here are quite similar to those found for a Pluronics with a similar molecular weight, $(PEO)_{42}$–$(PPO)_{16}$–$(PEO)_{42}$, adsorbing on PSL with an area per triblock of 6.5 nm^2/chain.[27]

[25] Tanford, C. *Physical Chemistry of Macromolecules*, John Wiley and Sons: New York, 1962, pg. 20-13.

[26] Davis, R.M., "Analysis of Dilute Solutionsof (Carboxymethyl) cellulose with the Electrostatic Wormlike Chain Theory", *Macromolecules* **1991**, *24*, 1149-1155.

[27] Kayes, J.B.; Rawlins, D.A. *Colloid and Polymer Science* **1979**, *257*, 622.

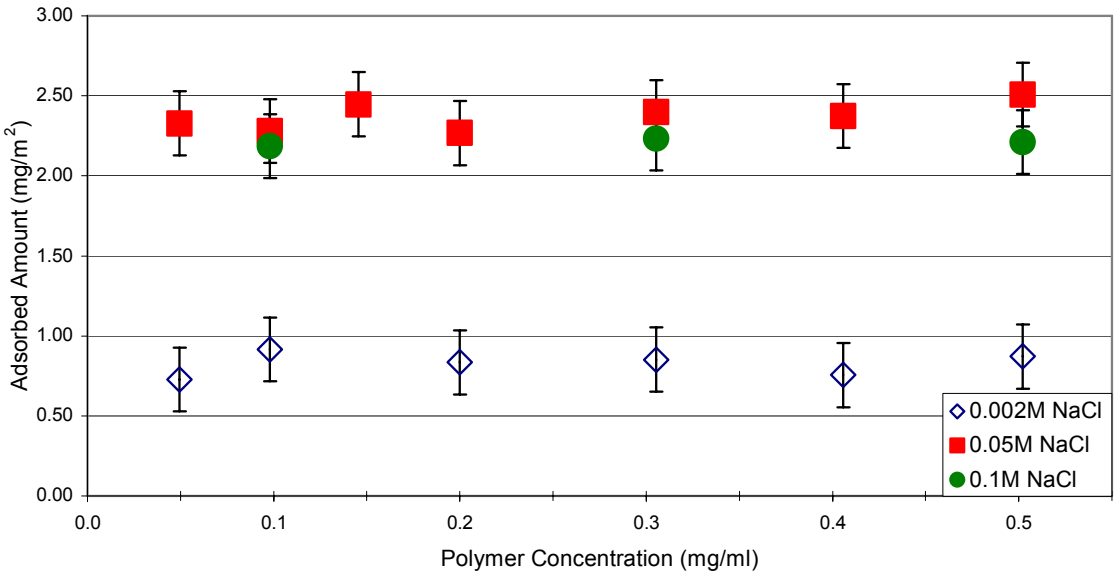

Figure 7.11: Adsorbed amounts for 2k-3-2k on alumina at pH 6 for three different ionic strengths. The error bars represent the standard deviation from three measurements.

Table 7.5: Calculated values from the adsorption data for the area occupied per 2k-3-2k triblock molecule on Al_2O_3 at three ionic strengths, and the random walk chain statistic calculations (Equations 7.8 and 7.9) for the area occupied by two PEO chains with a molecular weight of 2000 g/mole each.

Ionic Strength	M_n	Adsorbed Amount	triblocks/area	area/triblock
M	g/mole	mg/m^2	$1/nm^2$	nm^2
0.002	5160	0.94	0.11	9.1
0.050	5160	2.39	0.28	3.6
0.100	5160	2.22	0.26	3.9
PEO	2-2000		0.10*	10*

* Not a triblock

The second possibility for the conformation of the triblock on the surface is micelle adsorption. Assuming the same initial conformation for the 0.002 M NaCl case, when salt is added, the polymer may adsorb in micelles on the surface, with the center blocks

associating in the center of the micelle. This would result in an abnormally high adsorbed amount, compared to monolayer coverage, although there is no general rule to predict the plateau adsorbed amount for adsorbed micelles. This is a distinct possibility due to the presence of micelles in solution as shown with DLS. However, there was no discernible effect of ionic strength on micelle formation in solution, and so it is unclear why the adsorbed amount would increase so greatly with increasing ionic strength.

The results for the adsorption of the 5k-5-5k triblock on alumina are shown in Figure 7.12. A similar effect of ionic strength is seen for the 5k-5-5k as was for the 2k-3-2k, although the effect is not as dramatic. The adsorbed amount for the 0.002 M NaCl case with the 5k-5-5k is much greater than was found for 2k-3-2k at the same ionic strength. This difference could be due to the greater amount of charged groups on the 5k-5-5k material, the higher molecular weight tails of the 5k-5-5k, or due to higher packing on the surface as will be discussed.

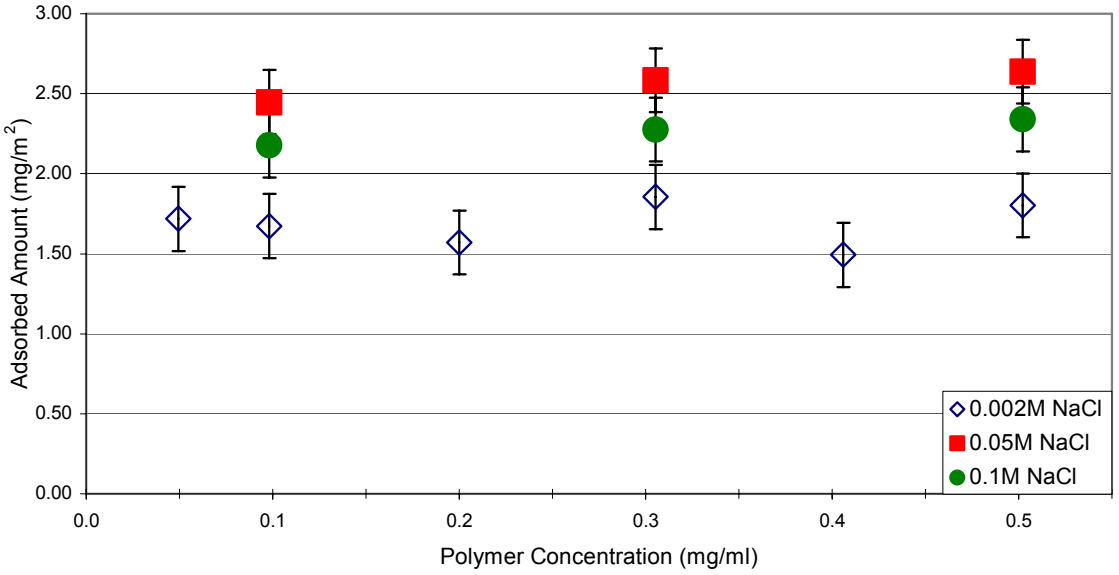

Figure 7.12: Adsorbed amounts for 5k-5-5k on alumina at pH 6 and three different ionic strengths. The error bars represent the standard deviation from three measurements.

As the ionic strength is increased the differences in adsorbed plateau amounts between the two different triblocks diminishes. This could be due to one of two possible reasons. If there is a brush-like structure on the surface, it is expected from the Pluronics literature that the 5k-5-5k would have a higher adsorbed amount than the 2k-3-2k material, due to the longer tails. However, the 5k-5-5k material may not be able to pack as tightly on the surface as the 2k-3-2k material because of the larger center block and possibly because of the stronger repulsions between the larger PEO tails block, which could account for the similarities in adsorbed amounts. This hypothesis is given credence by the calculations given in Table 7.6 for the area occupied by the polymers. Also, the values calculated here are somewhat less than that found for a Pluronics with a similar molecular weight, $(PEO)_{100}$–$(PPO)_{40}$–$(PEO)_{100}$, adsorbing on PSL with an area/triblock of 17.5 nm^2/chain.[27] The main difference in Table 7.6, as compared to Table 7.5, is that the calculated area occupied for each triblock, as determined from the adsorption data, is in all cases less than that for two PEO chains with a molecular weight of 5000. Also, at high ionic strengths the area per triblock is greater than that found at the same ionic strengths for the 2k-3-2k, indicating that the 5k-5-5k material can not pack as tightly on the surface as the 2k-3-2k material.

Table 7.6: Calculated values from the adsorption data for the area occupied per 5k-5-5k triblock molecule on Al_2O_3 at three ionic strengths, and the random walk chain statistic calculations (Equations 7.8 and 7.9) for the area occupied by two PEO chains with a molecular weight of 5000 g/mole each.

Ionic Strength	M_n	Adsorbed Amount	triblocks/area	area/triblock
M	g/mole	mg/m^2	$1/nm^2$	nm^2
0.002	11540	1.61	0.08	12
0.050	11540	2.64	0.14	7.3
0.100	11540	2.34	0.12	8.2
PEO	2-5000		0.03*	29*

* Not a triblock

The second case would be to assume that there is a micellar like structure on the surface. In this case the adsorbed amount could be similar for both polymer systems, because the micelles for the two polymers may be similar in size, as was shown by DLS experiments.

Figure 7.13 shows a schematic for the possible adsorption conformations of the PEO triblocks on alumina and silica. Figure 7.13(a) represents the flat train like conformation of the triblocks on silica at all ionic strengths, where the PEO endblocks are the adsorbing moiety. In Figure 7.13(b) a schematic for the brush-like structure of the triblocks on alumina at low and possibly high ionic strengths is shown. Figure 7.13(c) shows the possible micellar-like structure of the triblocks on alumina at high ionic strengths. In Figure 7.13(d) another possibility, agglomerated micelle adsorption is shown.

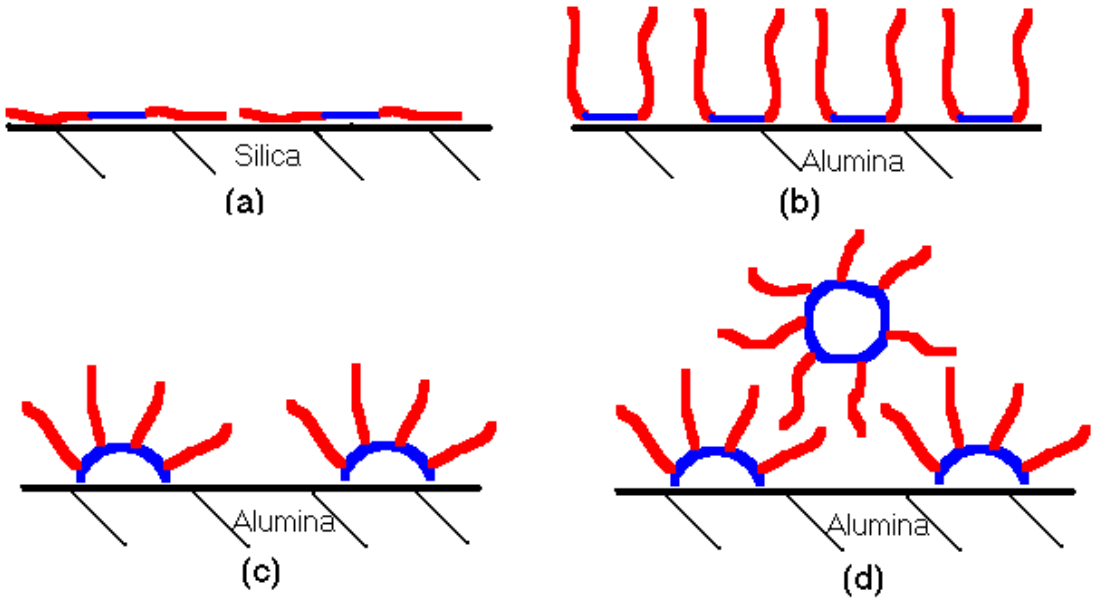

Figure 7.13: Schematic showing the possible adsorption conformations of the PEO triblocks on alumina and silica: (a) flat train-like conformation of triblocks on silica at all ionic strengths; (b) brush-like structure of triblocks on alumina at low and possibly high ionic strengths; (c) micellar-like structure of triblocks on alumina at high ionic strengths; (d) agglomerated micelles on alumina at high ionic strengths.

7.3.5 Sedimentation on Al_2O_3

Figure 7.14 and Figure 7.15 show for the 2k-3-2k material the relative sediment volume and the resulting zeta potential as a function of polymer concentration, respectively. The relative sediment volume is the volume of the final sediment divided by the total initial volume of the liquid. If a suspension is flocculated, the particles will form aggregates that will settle into a thick, fluffy layer. For a stabilized suspension, the particles will eventually over time settle due to gravity, even for these small particles. For this case a thin, dense sediment will form at the bottom. At pH 6 the alumina particles would have a net positive charge, and thus be electrostatically stabilized in the absence of polymer and at low ionic strength. This stabilization is apparent from the 0.0 wt.% polymer data points. In Figure 7.14, the 0.002M and 0.05M NaCl results show a thin sediment, with a relative sediment volume (RSV) around 0.05, and the zeta potential is a large positive number, greater than 25 mV. For the 0.1 M NaCl case the sediment is much thicker, with an RSV of 0.2, due to screening of the electrostatic charges on the particles and flocculation.

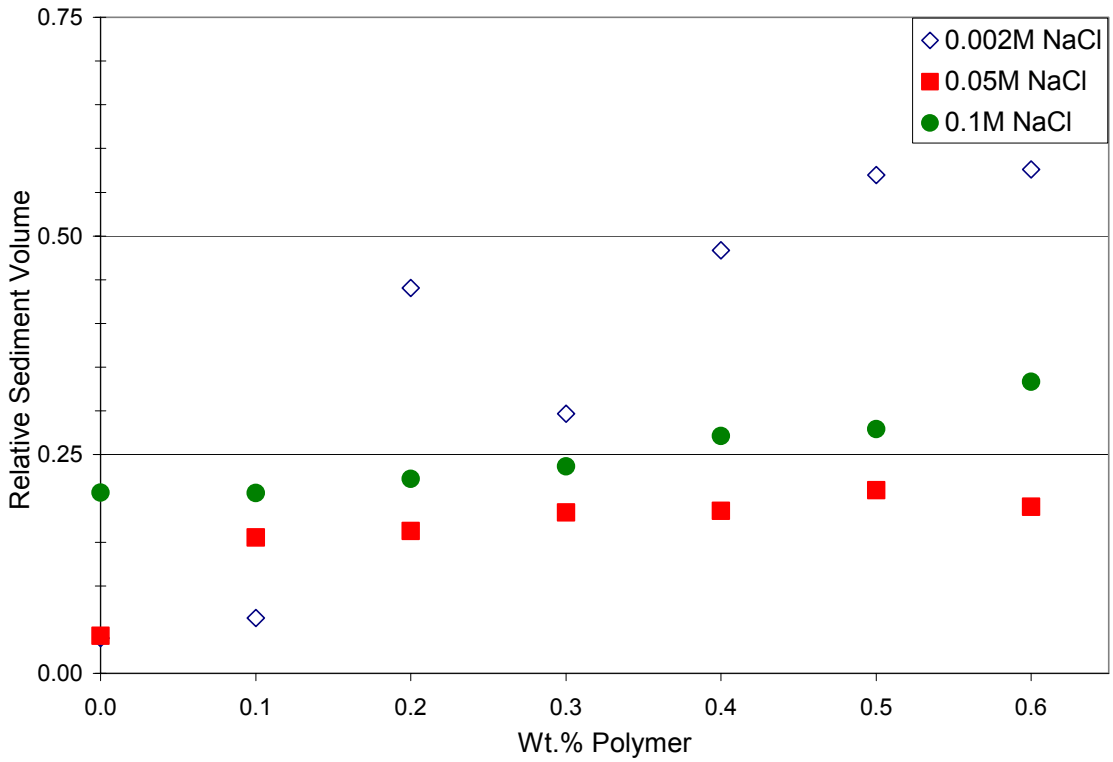

Figure 7.14: Sediment volume for 30 nm alumina particles, as a function of 2k-3-2k polymer weight percent on the dry weight basis, for three ionic strengths, at pH 6.

The results for the 2k-3-2k material, in Figure 7.14, show the effect of the adsorbed polymer on the stabilization of the particles. It is important to note that even at the highest polymer content the surface is not fully covered with a monolayer of chains. This was calculated by balancing the mass of polymer in the supernatant, C_S, to the total input, C_T, subtracted from that adsorbed onto the particles:

$$C_S = C_T - \frac{\Gamma A_S m_p}{V_S} \qquad \text{Equation 7.13}$$

where Γ is the adsorbed amount measured using ellipsometry, A_S is the surface area of the particles, m_p is the mass of particles, and V_S is the total volume of the system. By setting the supernatant concentration to zero, a minimum value for the total initial polymer concentration can be calculated, where full coverage will occur. Based on adsorbed amount measurements found previously, even at 0.6 Wt.% polymer, this system is still well below saturation.

There is no evidence that the adsorbed polymer is sterically stabilizing the particles, due to the lack of full coverage on the particles. From the adsorption results in Figure 7.11, it is obvious that there is great deal of adsorption occurring for this case. The lack of stabilization could be a strong indication that there is no brush formation on the particle surfaces. At the two lower ionic strengths, the effect of polymer adsorption is similar to each other, although the response is more dramatic for the 0.002 M NaCl case. As more polymer is added the system becomes more flocculated. This is most likely due to charge neutralization on the surface from the adsorption of the charged center blocks, which leads to a deeper secondary minimum in the potential energy curve. Zeta potential results in Figure 7.15 show that with the addition of polymer the zeta potential drops to values near zero, which supports this hypothesis. It is clear from these results that there is no steric stabilization of the particles due to the adsorption of the polymer. However, at higher polymer concentrations, when the surface is saturated, stabilization may occur. The minimum adsorbed layer thickness for these polymers, assuming an end-attached PEO chain, can be determined by calculating the end-to-end distance for the PEO chains. For the PEO 2000 this would be 3.1 nm, and for the PEO 5000 the minimum adsorbed layer thickness would be 5.3 nm. These thicknesses should be sufficient to sterically stabilize these small particles, by decreasing the depth of the secondary minimum in the potential energy curve. For the 0.1 M NaCl case, all of the suspensions are flocculated, and charge neutralization is seen with the zeta potential results. This is consistent with the observation that the addition of polymer did not improve the stability of the particles at these polymer levels.

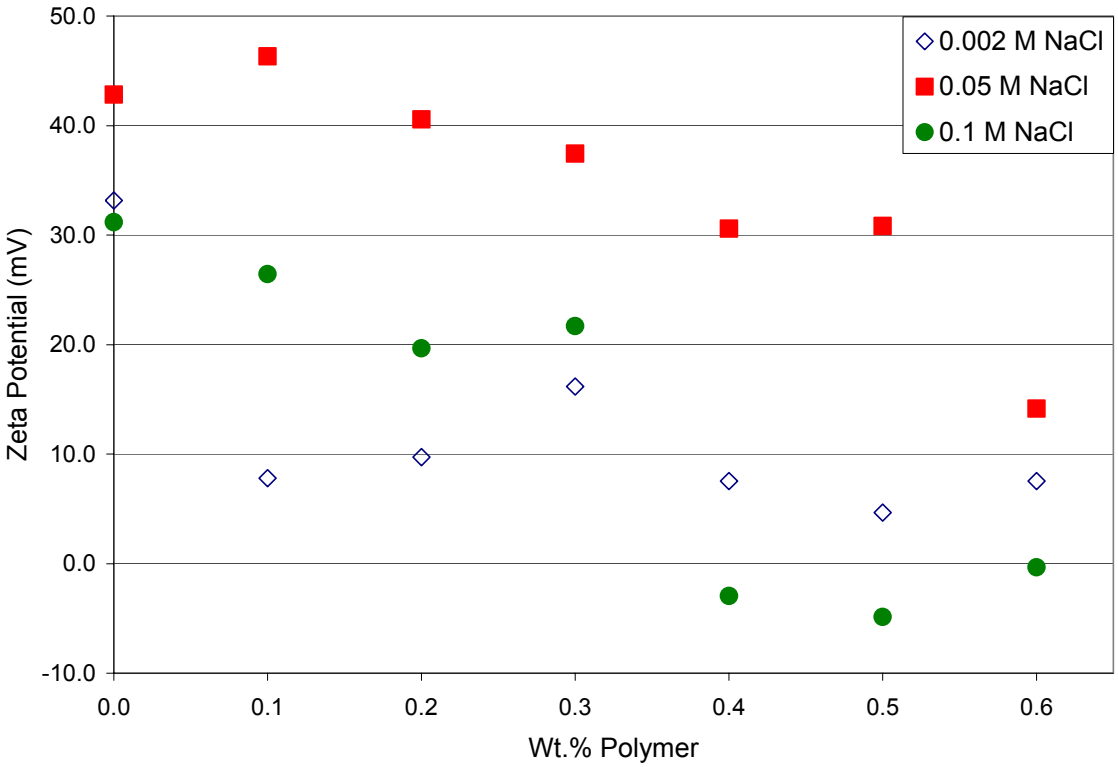

Figure 7.15: Zeta potential of 30 nm alumina particles as a function of 2k-3-2k polymer weight percent on the dry weight basis, at three ionic strengths, at pH 6.

The results for the 5k-5-5k material are shown in Figure 7.16 and Figure 7.17. For the 0.1 M NaCl case the results are very similar to the results for the 2k-3-2k material for the 0.1 M NaCl ionic strength. Again, there is no effect of polymer adsorption on the stabilization of the particles, which remain flocculated at all polymer concentrations studied. The result at 0.002 M and 0.05 M NaCl both show no change in the sediment volume with increasing polymer concentrations. From the zeta potential results, there is some evidence of charge neutralization with increasing polymer concentration. However, even at the highest polymer concentration the zeta potential is a large positive number, and thus electrostatically stabilized. The lack of complete charge neutralization is most likely due to submonolayer coverage on the surface. The differences seen for the two polymers at the two lower ionic strengths may be due to molecular weight effects. From Table 7.5 and Table 7.6, the plateau adsorbed amounts for the two polymers are comparable. Thus, there would have to be a greater number of 2k-3-2k chains adsorbed

on the surface for this to occur. The increased number of chains adsorbed would be closer to fully covering the surface, and the higher ratio of charged groups may be enough for charge neutralization to occur, even though there are two fewer charged groups on the 2k-3-2k copolymer.

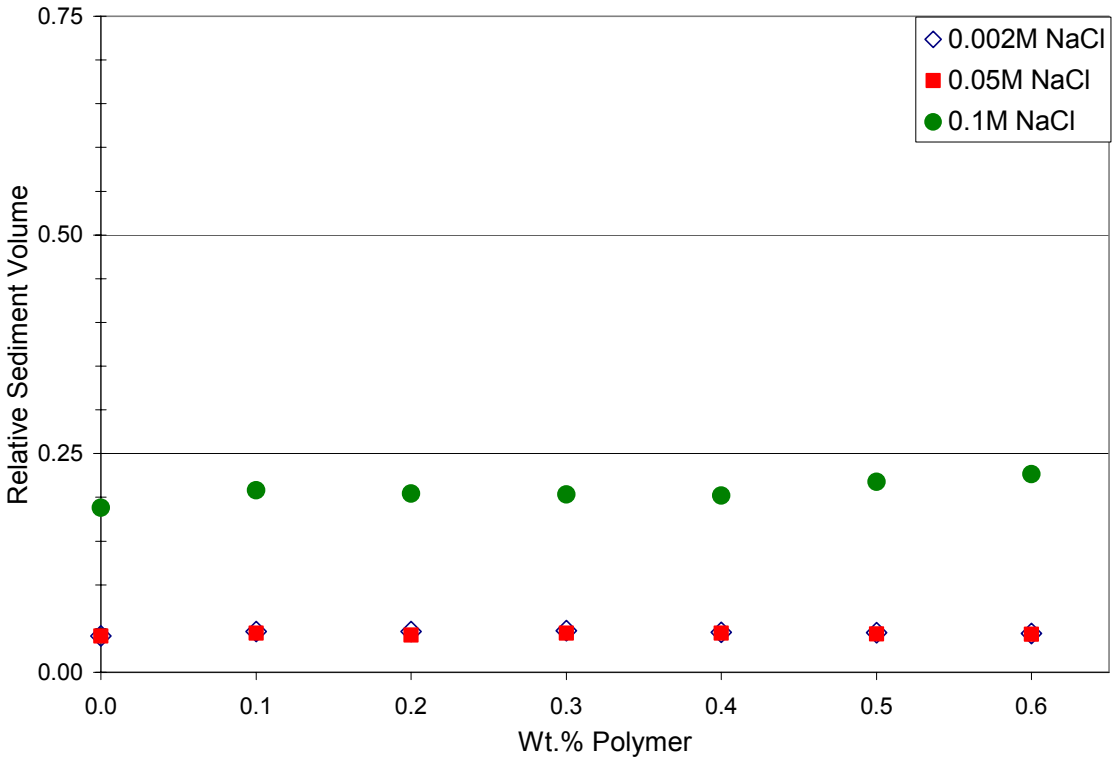

Figure 7.16: Sediment volume for 30 nm alumina particles, as a function of 5k-5-5k polymer weight percent on the dry weight basis, for three ionic strengths, at pH 6.

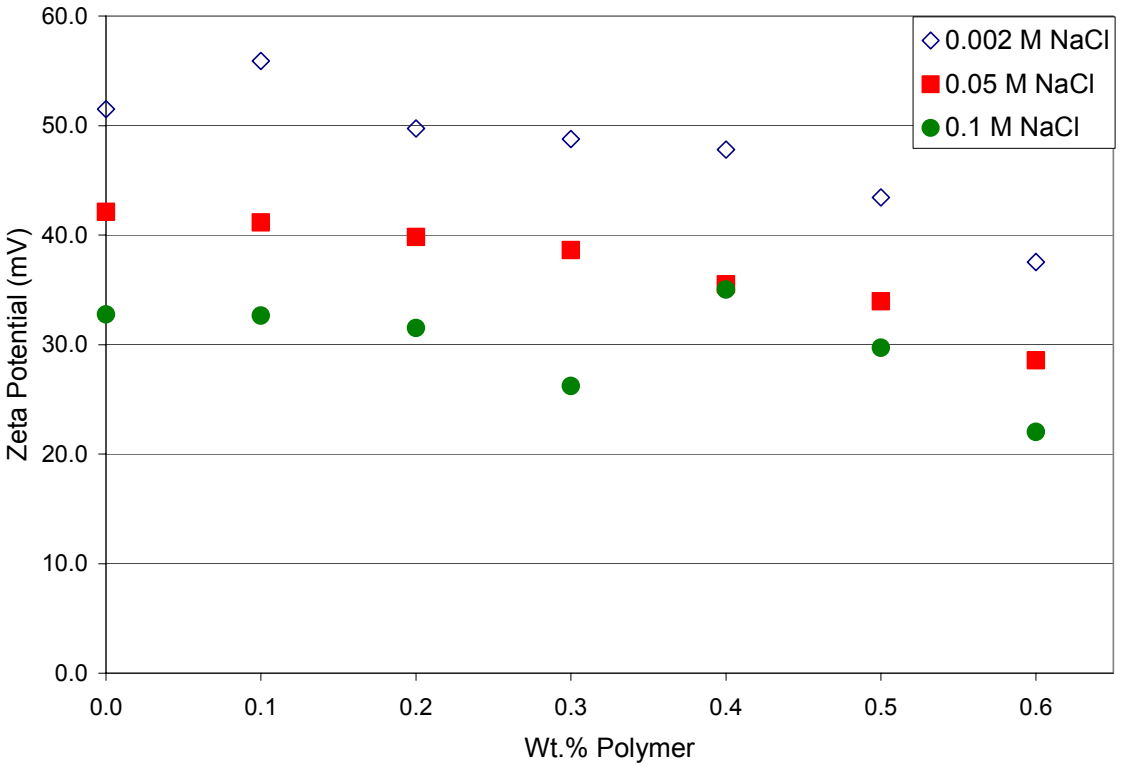

Figure 7.17: Zeta potential of 30 nm alumina particles as a function of 5k-5-5k polymer weight percent on the dry weight basis, for three ionic strengths, at pH 6.

7.4 Conclusions and Future Work

In conclusion, the adsorption behavior of two novel triblocks, each consisting of two PEO tail blocks and a charged center block, has been studied on silica and alumina. On SiO_2 the PEO tails dominate the adsorption and the resulting adsorbed amounts are comparable to similar molecular weight PEO samples on silica. The adsorbed layer conformation for both triblocks is flat trains, with the center block constrained by the adsorbed tails.

In contrast the adsorption on Al_2O_3 was very different. The adsorbed amounts were much greater, indicating either brush formation or micellar adsorption. There was a strong dependence on ionic strength for both polymers. As the salt concentration was

increased the repulsions between neighboring center blocks was reduced, which allowed for higher packing on the surface and a larger adsorbed amount.

The work done here is only the beginning of a much more extensive study of these types of copolymers. Dr. Riffle in the Department of Chemistry has synthesized a number of PEO triblocks, similar in structure, but varying in PEO molecular weight and center block length. A detailed study of the remaining polymers in this series will be done in order to understand their solution behavior and their behavior at interfaces.

A number of solution phase experiments could be done to determine the structure of the large objects seen via DLS. Are they micelles, aggregated micelles, larger vesicles, or some other type of structure? Scattering experiments such as small angle x-ray scattering or small angle neutron scattering or other techniques such as fast-freeze cryo transmission electron microscopy, might help in answer this question.

Adsorption experiments using ellipsometry with the other triblocks on alumina and silica and other surfaces such as polymeric and hydrophobic silica would also be done. In order to elucidate the adsorbed layer structure on these surfaces, atomic force microscopy and neutron reflectivity will be used. These techniques offer the greatest potential for studying the interactions between the polymer and the surface at the nanometer scale.

The colloidal stability of the copolymers on alumina particles can also be studied. One method that will be used to measure stability is a sedimentation experiment, in which the amount or volume of sediment will be monitored as a function of time. This technique will be used in conjunction with electrophoretic mobility as qualitative measure of the stability of the system due to the adsorption of the triblock copolymer, and the results will be compared to those obtained when no polymer is added.

8 Conclusions and Future Work

8.1 Conclusions

Throughout this research the principal focus has been on studying the adsorption of polymers made from amino acid monomers on metal oxide surfaces from aqueous media. This approach is the first step to understanding how these simple proteins interact and adsorb on non-biological surfaces. There is great potential for synthetic proteins for applications where the control of surface activity is important, because there is a wide range of possible protein chemistries. The results of this work can be used by future researchers to synthesize monodisperse, well-defined proteins from genetically engineered *E. coli* that have the desired features for a specific system. A second focus of this work was to study the solution and interfacial behavior of a novel triblock copolymer developed by Professor Judy Riffle in the Chemistry Department at Virginia Tech.

In **Chapter 3**, homopolymer adsorption isotherms showed that both poly-L-(glutamic acid) (GLU) and poly-L-(aspartic acid) (ASP) adsorb onto alumina at reasonably high surface concentrations, $\Gamma = 0.5$ mg/m^2 consistent with adsorption in flat trains. Poly-L-proline (PRO), on the other hand, showed relatively little adsorption, even at high polymer concentrations. Competitive adsorption experiments were done to determine which polymer, PRO or GLU, would selectively adsorb when both were present. The results showed that the PRO adsorption was very small, compared to that for the GLU, even though the initial concentration of PRO was three times that of GLU. These results show that either GLU and very likely ASP would make a good adsorbing anchor block, while PRO would make a good non-adsorbing tail block for a brush forming copolymer on alumina that would sterically stabilize Al_2O_3 particles in aqueous solutions.

The effect of metal oxide substrate chemistry was clearly seen in **Chapter 4**. On silica the PRO showed high affinity adsorption and would likely make a good anchor block,

while the GLU did not adsorb and could act as a tail block that could electro-sterically stabilize SiO_2 particles.

The effect of hydroxylation was shown by comparing the PRO to HPRO adsorption data. Neither polypeptide adsorbed strongly on alumina, and only the PRO showed adsorption on silica. It is still unclear why the HPRO did not adsorb on either surface. Also, the incorporation of GLY into the PRO backbone in the form of the PRO-GLY-PRO copolymer had the effect of lowering the solubility, but not inducing adsorption on alumina. This is important information that can be used in the future biosynthesis of high molecular weight tail blocks for Al_2O_3 particles. The incorporation of GLY units in the anchor or tails can also increase the flexibility of these chains. This could be very important for a tail block, in order to allow for extension of the tail upon brush formation.

The adsorption of GLU on alumina was also studied as a function of ionic strength. Greater adsorbed amounts were obtained at higher ionic strengths indicating that screening of repulsions between adjacent chains led to greater packing on the surface. This result is similar to those found for other polyelectrolyte adsorption, indicating that unstructured proteins behave like classical synthetic polymers. The addition of $CaCl_2$ did not promote the adsorption of GLU on silica. Larger molarities of Ca^{+2} are probably required to bind the GLU to the SiO_2 surface, but the GLU solubility then becomes an issue.

The work in **Chapter 5** is one of very few studies to measure the adsorption of homopolymer polypeptides on well-defined surfaces using in-situ ellipsometry. The results showed that the adsorption behavior of GLU and PRO, two unstructured homopolymer polypeptides, closely resembles that of synthetic polymers. The effect of the surface chemistry greatly affected the resulting adsorption. The GLU was found to adsorb on the oppositely charged Al_2O_3, while the uncharged PRO adsorbed strongly on SiO_2. There was a small effect of ionic strength on the adsorption of GLU on alumina, typical of polyelectrolyte adsorption. The results represent the first in a series of two studies of polypeptides on smooth surfaces. The follow-up study will consist of AFM

measurements for the same systems studied here to characterize the surface forces caused by the adsorbed layers.

In **Chapter 6**, it was determined that a copolymer consisting of GLU and TYR can be used to stimulate adsorption of PEO on alumina surfaces. The copolymer GLU:TYR 4:1 is soluble in water, and adsorbs on alumina, but there was no complexation between it and PEO with M_w = 921 kDa. The copolymer GLU:TYR 1:1 forms aggregates in water and absorbs more strongly than the 4:1, especially at high ionic strength, possibly due to a large number of loops and tails in the adsorbed conformation. PEO adsorption was stimulated by the presence of preadsorbed GLU:TYR 1:1, and the adsorbed amount of PEO increased with its molecular weight. The NaCl concentration did not affect the hydrogen bonding between the GLU:TYR 1:1 and the PEO but it did affect the conformation of the adsorbed GLU:TYR 1:1, which then dictated the PEO adsorption. The efficiency of complexation between the GLU:TYR 1:1 and the PEO was not as great at high ionic strengths, due to steric effects.

In **Chapter 7**, the adsorption behavior of two novel triblocks, each consisting of two PEO tail blocks and a charged but hydrophobic center block, was studied on silica and alumina. On SiO_2, the PEO tails dominated the adsorption and the resulting adsorbed amounts were comparable to those of PEO homopolymers with similar molecular weight. The adsorbed layer conformation for both triblocks was mostly flat trains, with the center block constrained by the adsorbed tails.

By contrast, the adsorption on Al_2O_3 was very different. The adsorbed amounts were much greater, indicating either brush formation or micellar adsorption. There was a strong dependence on ionic strength for both polymers. As the salt concentration was increased, the repulsions between neighboring center blocks was reduced, which allowed for higher packing on the surface and a larger adsorbed amount.

8.2 Future Work

1. Characterization of first generation diblock copolymer – PRO_{26}-GLU_{10}

The primary goal of this work is to design a biological block copolymer in order to form brush layers on metal oxide surfaces. As a result of work reported in Chapter 3, a diblock consisting of PRO_{26}-GLU_{10} has been synthesized. Once it is purified in sufficient amounts, the first step will be to characterize the solution behavior of the polypeptide block copolymer using DLS, as was done with the homopolymers. Specifically, by comparing the measured hydrodynamic radius to that from chain statistic calculations, the state of aggregation of the polymer can be inferred. Both of the blocks are soluble in water, so it is expected that the block copolymer will not form micelles in solution. Although the presence of micelles is undesirable for efficient steric stabilization, if the copolymer does form micelles a scientifically valuable study of micellization would be done because of the novelty of this system. If the PRO_{26}-GLU_{10} diblock readily formed micelles, a detailed analysis of the solution behavior would be done as a function of pH, ionic strength, and polymer concentration.

If there is no aggregation of the block copolymer, then static light scattering (SLS) can also be used to calculate the weight average molecular weight and the second virial coefficient of the polymer, as described in Chapter 3. These data will be used as another verification that the polymer synthesized conforms to the original design targets.

After the solution behavior of the block copolymer has been fully characterized, the adsorption isotherms of the polymer on alumina can be measured. The adsorption onto α-Al_2O_3 particles will be studied using the solution depletion method, as described in Chapter 3. Capillary zone electrophoresis or UV-Vis spectrophotometry will be used to quantify the concentration of polymer in solution. It is expected that the adsorbed amounts will be fairly high, even considering the low molecular weight of the copolymer, due to the compact adsorption of the GLU anchor on the surface and the expected brush

formation. From scaling theory it can be calculated that this diblock copolymer will occupy 1.5 nm^2 per molecule on the surface.[1]

The adsorption can be measured on an alumina coated wafer using ellipsometry. From the homopolymer adsorption data (in Section 3.3.3), it is expected that the GLU will act as the anchor block and the PRO will act as the tail block. More advanced modeling calculations will be performed, that will better help to understand how the diblock copolymer adsorbs on the surface, specifically the brush model developed by Ploehn and Russel.[2,3]

2. AFM experiments with GLU and PRO on alumina and silica

Professor Ducker's group in the Department of Chemistry at Virginia Tech will measure the interaction potential of adsorbed polymer using atomic force microscopy (AFM). These results will then be compared to model DLVO calculations for the pair interaction potential, as discussed in Section 2.2. Another experiment that can be performed in conjunction with this work would be to measure the depletion flocculation caused by nonadsorbing PRO on alumina. These data could then be compared to model calculations, discussed in Section 2.2.4.

3. Combinatorial search for a strongly adsorbing block for target surfaces such as alumina

A combinatorial library search of amino acid sequences can be screened to determine which sequences preferentially adsorb on a specific surface, such as the (100) crystal face of alumina. This technique involves using a combinatorial library of different random

---

[1] Marques, C.M.; Joanny, J.F.,' Block Copolymer Adsorption in a Nonselective Solvent', *Macromolecules* **1989**, *22*, 1454-1458.

[2] Ploehn, H.J., Ph.D. Thesis, Princeton University, Princeton, New Jersey, 1988.

[3] Russel, W.B.; Saville, D.A.; Schowlter, W.R. "Colloidal Dispersions"; Cambridge University Press: New York, 1989.

peptides of a certain length, each with a different sequence. Thus, tens of millions of different peptides can be tested simultaneously. For example, the dodecapeptide sequences are expressed on the flagella of genetically engineered *E. Coli* and are exposed to the solvent. Thus, when the cells are contacted with a surface, only those containing peptide sequences that bind to the surface will adhere, and the others will be eluted away. The bound *E. Coli* are then removed by shearing and incubated to grow new cells. This process, called biopanning, can be repeated several times under different conditions in order to find those peptides that show the highest affinity for the surface. The DNA sequence is then determined from those cells which showed strong binding and the amino acids in the peptides are identified.[4,5] A sequence found through this technique could then be used as an anchor block in future iterations of a brush-forming diblock copolymer.

4. Synthesis and characterization of a zwitterion for possible universal nonadsorbing tail block

A zwitterion, or charged polymer that has local charges but an overall neutral charge, is highly water soluble and would make a good choice as a possible tail block. A zwitterion made from amino acids is currently being synthesized though genetically engineered E. Coli. This is a relatively short sequence of amino acids, a 26-mer, that can be repeated many times in order to produce a long tail block. Once it is purified in significant quantities, the polypeptide can be characterized by MALDI-TOF, and for its solution properties using DLS. The adsorption, or lack thereof, would be measured on various surfaces using ellipsometry and AFM.

[4] www.invitrogen.com

[5] Westerlund-Wikstrom, B. *International Journal of Medical Microbiology* **2000**, *290*, 223.

5. Development of a second generation diblock

A second generation diblock will be synthesized via the biosynthetic technique that would have a zwitterion for the universal tail block and an anionic anchor block consisting of GLU and ASP. The charged anchor block would adsorb strongly onto Al_2O_3, and the zwitterion previously discussed can be synthesized with a high enough molecular weight in order to stabilize alumina particles of a specified size. The characterization of this copolymer will follow closely what was outlined for the first generation diblock. This will include characterizing the solution behavior by DLS, the adsorption on an alumina surface using ellipsometry, measuring the surface by AFM, and determining the colloidal stabilization imparted by the adsorption of the block copolymer by sedimentation experiments and by electrophoresis.

6. Development of a third generation diblock

For the third generation diblock for alumina, it is proposed to combine the zwitterion tail, used in the second generation, with a combinatorially derived anchor block, discussed above. This would be a very advanced material and could work as an excellent "smart" dispersant for a surface such as alumina. This means that it would be a dispersant designed for a specific particle. Alternatively, a general purpose dispersant could be designed that would stabilize mixtures of particles, with multiple isoelectric points. This generation will be characterized as discussed for the previous two versions.

7. Search for Novel Polypeptide Cofactors and Selective Flocculants

A combinatorial library search of amino acid sequences can be screened as a selective flocculant or cofactor for a specific surface such as alumina. For a cofactor in a PEO flocculation experiment this polypeptide must adsorb on the surface and hydrogen bond with the PEO. It is also possible to find sequences that adsorb with one surface and not another, so that selective flocculation of a mixture of particles can be achieved. This would be characterized for its solution behavior, by DLS, as well measuring the

adsorption on alumina, by ellipsometry, the subsequent adsorption of PEO, and finally by flocculation experiments.

8. Continue to Study the PEO Triblock Series

Dr. Riffle in the Department of Chemistry at Virginia Tech has synthesized a number of PEO triblocks, similar in structure, but varying in PEO molecular weight and center block length. A detailed study of the remaining polymers in this series could be done in order to understand the solution behavior and the adsorption on alumina and silica. The colloidal stability of the copolymers on alumina particles can also be studied. One method that will be used to measure stability is a sedimentation experiment, in which the amount or volume of sediment will be monitored as a function of time. When the particles are dense, as they are in this system, then they will settle due to gravity, even if they are stabilized. A stabilized system will form a thin, dense layer of sediment on the bottom, due to a lack of the secondary minimum in the interaction potential curve, as discussed in Section 2.3.3. A flocculated system will form a thick, low density layer over time. This technique will be used as qualitative measure of the stability of the system due to the adsorption of the diblock copolymer, and the results will be compared to those obtained when no polymer is added.

The stability of the colloidal suspensions will also be characterized by rheological testing. As discussed in Section 2.3.2, the steady shear and dynamic viscoelastic properties of colloidal suspension will be dramatically affected by the stability. If the system is well dispersed and stabilized, it will have a low zero-shear viscosity, and will exhibit little to no shear thinning. The flocculated system on the other hand will show a high zero-shear viscosity due to the onset of a yield stress, it will also show a high degree of shear thinning.

Vita

Jody Lynn Krsmanovic

1526 Maine Circle
Sanford, NC 27332
Home: (919) 498-0142
jkrsmano@vt.edu

Education

Ph.D. Chemical Engineering (January 2003)
Virginia Tech, Blacksburg, VA
Topic: Novel Biologically Derived Block Copolymers for Steric Stabilization of Colloidal Particles in Aqueous Environments
Advisor: Dr. R.M. Davis
GPA: 3.7/4.0

M.Eng. Chemical Engineering (May 2001)
Virginia Tech, Blacksburg, VA
Advisor: Dr. R.M. Davis

B.S. Chemical Engineering (June 1997)
University of Minnesota, Minneapolis, MN

Polymer related course work:
Colloid and Surface Science, Polymer Morphology, Rheo-Optics of Polymers, Organic Chemistry of Polymers, Polymer Physical Chemistry, Non-Newtonian Fluid Mechanics, Adhesion Science

Research Experience

1/99 to Present –Virginia Tech Blacksburg, VA
Graduate Research Assistant

- Performed dynamic and static light scattering experiments to characterize polymers in solution
- Developed experiments for measuring protein adsorption onto metal oxide particles that facilitated in the design of novel protein-based polymers
- Implemented a liquid cell attachment to an ellipsometer for in-situ measurements of polymer adsorption
- Conducted experiments utilizing capillary zone electrophoresis, dynamic oscillatory rheometry, UV-Vis spectroscopy, electrophoretic light scattering, and scanning electron microscopy
- Analyzed copolymer composition and molecular weight using H-NMR spectra and GPC data

11/94 to 8/97 – 3M St. Paul, MN
Technical Aide, Dental Products Division

- Assisted in specification of process conditions for polymer synthesis
- Characterized polymers using static and oscillatory rheometry and FTIR
- Analyzed polymers using H-NMR spectra, GPC data, and GC results
- Worked with statistical analysis methods, including factorial and mixture designs

Honors

- Adhesive and Sealant Council Education Foundation Graduate Fellowship (1/00 to present)

Papers and Presentations

"Characterization and Adsorption of Homopolymer Polypeptides on Colloidal α-Al_2O_3 for Potential Use as a Brush Forming Block Copolymer", J.L. Krsmanovic, D. Henderson, M. Lindsay, K.E. Van Cott, R.M. Davis, C. Russell, (to be submitted)

"Novel Biologically Derived Block Copolymers for Steric Stabilization of Colloidal Particles in Aqueous Adhesives", J.L. Krsmanovic, D.Henderson, M. Lindsay, K.E. Van Cott, and R.M. Davis, Adhesion Society Meeting, Orlando, FL; February 10-15, 2002.

"Novel Biologically Derived Block Copolymers for Steric Stabilization of Colloidal Particles in Aqueous Adhesives", J.L. Krsmanovic, D.Henderson, M. Lindsay, K.E. Van Cott, and R.M. Davis, Adhesive & Sealant Council Fall Convention, New Orleans, LA, November 18-21, 2001.

"Peptide-Based Polymeric Surfactants", J.L. Streeter, D.Henderson, M. Lindsay, K.E. Van Cott, R.M. Davis, W. Ducker, C. Russell, American Chemical Society 75th Colloid and Surface Science Symposium, Pittsburgh , PA, June 23-26, 2001.

"Novel Block Copolymers for the Steric Stabilization of Waterborne Adhesives", J.L. Streeter, D.Henderson, M. Lindsay, K.E. Van Cott, and R.M. Davis, Adhesive & Sealant Council Spring Convention, Orlando, FL, March 18-19, 2001.

"Novel Block Copolymers for the Steric Stabilization of Waterborne Adhesives", J.L. Streeter, D.Henderson, M. Lindsay, K.E. Van Cott, and R.M. Davis, Adhesion Society Meeting, Williamsburg, VA; February 28-29, 2001.

"Synthesis and Characterization of Novel Block Copolymers for the Stabilization of Metal Oxides in Aqueous Systems", J.L. Streeter, K.E. Van Cott, and R.M. Davis, Adhesion Society Meeting, Myrtle Beach, SC; February 20-23, 2000.

Teaching Experience

Graduate Teaching Assistant, Virginia Tech
Chemical Engineering Mass and Energy Balances (8/97 to 5/98)

Chemical Engineering Unit Operations Laboratory (5/98 to 7/98)

Chemical Engineering Thermodynamics (8/98 to 12/98)

Chemical Engineering Simulations (1/99 to 5/99)